Universidade Federal do Rio de Janeiro

Instituto de Bioquímica Médica

Vitor Hugo Pomin

FUCANAS E GALACTANAS SULFATADAS:

ESTRUTURA, BIOLOGIA E FILOGENIA

Rio de Janeiro

2008.

Livros Grátis

http://www.livrosgratis.com.br

Milhares de livros grátis para download.

Vitor Hugo Pomin

Fucanas e galactanas sulfatadas: estrutura, biologia e filogenia

Tese de doutorado apresentada ao Programa de Pós-graduação em Química Biológica, Instituto de Bioquímica Médica, da Universidade Federal do Rio de Janeiro, como parte dos requisitos necessários à obtenção do título de Doutor em Química Biológica.

Orientador: Paulo Antônio de Souza Mourão, Professor Titular - UFRJ

Universidade Federal do Rio de Janeiro
Instituto de Bioquímica Médica
2008

Pomin, Vitor Hugo

Fucanas e galactanas sulfatadas: estrutura, biologia e filogenia / Vitor Hugo Pomin. Rio de Janeiro: UFRJ, IBqM, 2008.

XIII, 231 p.

Orientador: Paulo Antônio de Souza Mourão.

Tese (doutorado) – UFRJ / Instituto de Bioquímica Médica/Programa de pós-graduação em Química Biológica.

Referências bibliográficas: 188-197.

1. Polissacarídeos sulfatados. 2. Organismos Marinhos. 3. Ressonância Magnética Nuclear. 4. Relação filogenética. I Mourão, Paulo Antônio de Souza. II. Universidade Federal do Rio de Janeiro, Instituto de Bioquímica Médica, Programa de Pós-graduação em Química Biológica.III. Fucanas e galactanas sulfatadas: estrutura, biologia e filogenia.

Folha de aprovação

Vitor Hugo Pomin

Fucanas e galactanas sulfatadas: estrutura, biologia e filogenia

Orientador: Paulo Antônio de Souza Mourão, Prof. Titular, Instituto de Bioquímica Médica, UFRJ

Banca Examinadora:

Prof. Norton Heise
Prof. Adjunto do Instituto de Biofísica Carlos Chagas Filho, Centro de Ciências da Saúde, UFRJ

Prof. Marcio Lourenço Rodrigues
Prof. Adjunto do Instituto de Microbiologia Professor Paulo de Góes, Centro de Ciências da Saúde, UFRJ

Prof. Marcius da Silva Almeida
Prof. Adjunto do Instituto de Bioquímica Médica, Centro de Ciências da Saúde, UFRJ

Revisor:

Prof. Mauro S. G. Pavão
Prof. Associado do Instituto de Bioquímica Médica, Centro de Ciências da Saúde, UFRJ

Suplente externo: Prof[a]. Eliana Barreto Bergter, Professora Titular do Instituto de Microbiologia Professor Paulo de Góes, Centro de Ciências da Saúde, UFRJ

APRESENTAÇÃO DA TESE

Este trabalho foi realizado no Laboratório de Tecido Conjuntivo, durante o curso de Doutorado (e Mestrado) do Programa de Pós-graduação em Química Biológica do Instituto de Bioquímica Médica da Universidade Federal do Rio de Janeiro, com apoio financeiro do Conselho Nacional de Desenvolvimento Científico e Tecnológico (CNPq) e sob a orientação do Prof. Paulo Antônio de Souza Mourão.

Esta tese é apresentada na forma de 5 capítulos e 3 anexos finais: 1) uma introdução a respeito dos polissacarídeos sulfatados de organismos marinhos, suas estruturas e ações biológicas (um artigo correlato a este capítulo); 2) uma descrição dos principais resultados sobre a hidrólise ácida branda de fucanas sulfatadas (resultados obtidos durante o mestrado neste mesmo programa de pós-graduação, e incorporados a esta tese devido à defesa da dissertação ter ocorrido em 18 meses) (dois artigos correlatos a este capítulo); 3) estudo estrutural de uma β-galactana sulfatada de uma espécie de alga verde (um artigo correlato a este capítulo); 4) estudo estrutural de uma β-galactana sulfatada de uma espécie de ouriço-do-mar (um manuscrito correlato a este capítulo), e 5) uma descrição taxonômica e estrutural da ocorrência de resíduos 3-β-D-Gal*p*-1 nos polissacarídeos sulfatados de organismos marinhos.

Artigos correlatos:

I. Pomin, V.H., Mourão, P.A. (2008) Structure, biology, evolution and medical importance of sulfated –fucans and -galactans. ***Glycobiology*** (em impressão).

II. Pomin, V;H., Pereira, M.S., Valente, A.P., Tollefsen, D.M., Pavão, M.G. e Mourão, P.A.S. (2005a). Selective cleavage and anticoagulant activity of a sulfated fucan: stereospecific removal of a 2-sulfate ester from the polysaccharide by mild acid hydrolysis, preparation of oligosaccharides, and heparin cofactor II-dependent anticoagulant activity. ***Glycobiology*** 15(4), 369-381.

III. Pomin, V.H., Valente, A.P., Pereira, M.S. e Mourão, P.A.S. (2005b). Mild acid hydrolysis of sulfated fucans: a selective 2-desulfation reaction and an alternative approach for preparing tailored sulfated oligosaccharides. ***Glycobiology*** 15(12),1376-1385.

IV. Farias, E.H. e Pomin, V.H., Valente, A.P., Nader, H.B., Rocha, H.A., Mourão, P.A. (2008) A preponderantly 4-sulfated, 3-linked galactan from the green alga Codium isthmocladum. ***Glycobiology*** 18(3), 250-259.

V. Castro, M.O., Pomin, V.H., Santos, L.L., Vilela-Silva, A.-C.E.S. Hirohashi, N., Pol-Fachin, L., Verli, H., e Mourão, P.A.S. (2008) A unique 2-sulfated β-galactan from the egg jelly of the sea urchin *Glyptocidaris crenularis*: conformation flexibility *versus* induction of the sperm acrosome reaction (manuscrito em revisão).

Anexos:

I. Vitor H. Pomin e Paulo A.S. Mourão (2006) Carboidratos: de adoçantes a medicamentos. ***Ciência Hoje*****.** 39:24-31.

II. de Barros, C.M., Andrade, L.R., Allodi, S., Viskov, C., Mourier, P.A., Cavalcante, M.C., Straus, A.H., Takahashi, H.K., Pomin, V.H., Carvalho, V.F., Martins, M.A., Pavão, M.S. (2007) The Hemolymph of the ascidian *Styela plicata* (Chordata-Tunicata) contains heparin inside basophil-like cells and a unique sulfated galactoglucan in the plasma. ***J Biol Chem.*** 282(3),1615-1626.

III. Santos, A.M., Pomin, V.H., Stelling, M.P., Guimarães, M.A., Cardoso, L.R., Mourão, P.A. (2007) The renal clearance of dextran sulfate decreases in puromycin aminonucleoside-induced glomerulosclerosis: a puzzle observation. ***Clin. Chim. Acta.*** 383(1-2),116-125.

"O estudo, a busca da verdade e da beleza são domínios em que nos é consentido sermos crianças por toda a vida."

"A coisa mais bela que podemos experimentar é o mistério. Essa é a fonte de toda a arte e ciências verdadeiras."

"A imaginação é mais importante do que o conhecimento."

"A ciência sem a religião é paralítica. A religião sem a ciência é cega."

"A mente que se abre a uma nova idéia jamais voltará ao seu tamanho original."

"Não existe nenhum caminho lógico para a descoberta das leis do Universo - o único caminho é o da intuição."

"Há duas coisas infinitas: o Universo e a tolice dos homens."

Frases Famosas de Albert Einstein (*1879-†1955)

Dedico esta tese a minha mãe, Marli Couto,
e ao meu amor, Fátima de Carvalho.

AGRADECIMENTOS

Agradeço à minha mãe, Marli Couto (*in Memoriam*) pela grande educação que recebi, me permitindo caminhar sabidamente, mesmo na sua ausência.

À minha noiva Fátima de Carvalho pelo apoio, incentivo, companheirismo, mas principalmente por acreditar incondicionalmente.

Ao meu orientador, o Prof. Titular Paulo Antonio de Souza Mourão, por sua excepcional orientação, associada ao seu equilíbrio emocional exemplar. Ao seu apoio e conselhos de grande experiência que certamente contribuem para uma ótima formação acadêmica e profissional.

À Prof[a]. Ana Paula Valente pelo convite, no ínicio do doutorado, aos seminários semanais de seu laboratório, curso de RMN, congresso de Biofísica na Argentina (me sugerindo o Prof. Prestegard como orientador para pós-doc) e aprendizado prático e teórico de RMN, juntamente com o Prof. Fábio Almeida. A este, pela enorme empenho e disposição em lecionar o curso de mecânica quântica aplicada ao RMN, que foi um dos meus maiores incentivos para esta área da ciência.

Ao Prof. Eminent Scholar Jim Prestegard, por ter me recebido tão nobremente em seu laboratório na Universidade da Geórgia, EUA, durante os seis meses de doutorado-sanduíche. Pelo convite ao curso de Biomolecular NMR, oportunidade de trabalho e orientação, e também ao apoio financeiro. Mas, acima de tudo, ao convite de estágio de Pós-doutorado.

A todos do laboratório de Tecido Conjuntivo por formarem um ótimo grupo de pesquisa, de bom convívio de trabalho, mas, em especial à Prof[a]. Mariana Sá Pereira e ao aluno Bruno Cunha Vairo, pelo companheirismo.

Ao meu irmão, Julio Cesar Pomin e a minha cunhada, Cyntia Lopes pela grande ajuda e apoio pessoal durante minha formação.

Ao Eros, meu filhote que me ensina muito, além de ser um grande companheiro.

ÍNDICE

Lista de abreviaturas.....1
Resumo.....2
Abstract.....3
CAPÍTULO 1: FUCANAS E GALACTANAS SULFATADAS.....4
1.1 Os polissacarídeos sulfatados apresentam grande variedade estrutural.....4
1.2 Estrutura das fucanas sulfatadas.....5
1.2.1 As fucanas sulfatadas de algas pardas são heterogêneas e complexas.5
1.2.2 As fucanas sulfatadas de equinodermas possuem estruturas regulares e repetitivas.....6
1.3 Estrutura das galactanas sulfatadas.....9
1.3.1 Galactanas de algas vermelhas e angiospermas marinhas.....9
1.3.2 Galactanas de algas verdes.....11
1.3.3 Galactanas de invertebrados marinhos (ouriços-do-mar e ascídias).....12
1.4 Estrutura *versus* atividades biológicas de fucanas e galactanas sulfatadas.....12
1.4.1 Papéis fisiológicos e atividades biológicas.....12
1.4.1.1 Requisitos estruturais para a indução da reação acrossômica.16
1.4.1.2 A atividade anticoagulante depende de componentes estruturais específicos: polissacarídeos de algas *versus* de equinodermas.....17
1.5 Conclusões gerais.....19
1.6 Artigo I.....21
CAPÍTULO 2: FRAGMENTAÇÃO DE FUCANAS SULFATADAS.....60
2.1 A importância da preparação de oligossacarídeos por hidrólise ácida branda....60
2.2 Objetivos.....62
2.3 Materiais e Métodos.....62
2.3.1 Extração e purificação de fucanas sulfatadas.....62
2.3.2 Hidrólise ácida branda de fucanas sulfatadas.....62
2.3.3 Eletroforese em gel de poliacarilamida (PAGE).....62
2.3.4 Espectros unidimensionais de ^{1}H-Ressonância Magnética Nuclear (RMN) 63
2.4 Resultados e discussão.....63
2.4.1 Hidrólise ácida branda de fucanas sulfatadas: dependência da estrutura do polissacarídeo 63

2.4.2 Modificações estruturais das fucanas de *S. pallidus* e *L. variegatus* durante a reação de hidrólise ácida branda.....65
2.5 Conclusões gerais sobre a hidrólise ácida branda de fucanas sulfatadas.....70
2.6.1 Artigo II.....75
2.6.2 Artigo III.....89
CAPÍTULO 3: β-GALACTANA SULFATADA DE ALGA VERDE.....100
3.1 Objetivos.....100
3.2 Materiais e Métodos.....100
3.2.1 Extração da galactana sulfatada da alga verde *C. isthmocladum*.....100
3.2.2 Análise química dos precipitados obtidos com diferentes volumes de acetona.....100
3.2.3 Purificação da galactana sulfatada da alga verde *C. isthmocladum*....101
3.2.4 Eletroforeses em géis de agarose e poliacrilamida.....102
3.2.5 Reações químicas de dessulfatação e metilação.....103
3.2.6 Experimentos de RMN.....103
3.3 Resultados e discussão.....104
3.3.1 Purificação da galactana sulfatada da alga verde.....104
3.3.2 Presença de 4- e 6-sulfatação nas galactanas sulfatadas da alga verde.....110
3.3.3 Preponderância de resíduos de β-D-galactopiranose 4-sulfatado e 3-ligado nas galactanas sulfatadas da alga verde.....110
3.3.4 Ocorrência de resíduos 3,4-*O*-(1´carboxi)-etilideno nas galactanas sulfatadas.....118
3.4 Principais conclusões sobre os componentes estruturais da galactana sulfatada e piruvatada da alga verde *C. isthmoclaium*.....121
3.5 Artigo IV.....124
CAPÍTULO 4: β-GALACTANA SULFATADA EM OURIÇO-DO-MAR.....135
4.1 Objetivos.....135
4.2 Materiais e Métodos.....135
4.2.1 Extração e purificação.....135
4.2.2 Eletroforeses e dessulfatação do polissacarídeo.....136
4.2.3 Experimentos de RMN.....136
4.2.4 Dinâmica molecular (DM).....136
4.3 Resultados e discussão.....137

4.3.1 O gel do óvulo do ouriço-do-mar *G. crenularis* comtém uma D-galactana sulfatada.....137
4.3.2 A galactana sulfatada de *G. crenularis* contém uma unidade dissacarídica regular composta por resíduos de β-galactopiranose 3-ligada, alternando 2-sulfatação e não-sulfatação.....139
4.3.3 As constantes de acopamento $^{3}J_{H-H}$ e $^{1}J_{C-H}$ das α- e β-galactanas sulfatadas de ouriços-do-mar indicam conformações distintas.....146
4.3.4 Diferentes estados conformacionais das α- e β-galactanas sulfatadas são observados pela dinâmica molecular.....147
4.4 Conclusões gerais.....150
4.5 Artigo V.....152
CAPÍTULO 5: OCORRÊNCIA DE UNIDADE 3-β-D-Gal*p*-1 NOS ORGANISMOS MARINHOS ATRAVÉS DA EVOLUÇÃO.....185
REFERÊNCIAS BIBLIOGRÁFICAS.....188
ANEXOS.....198
Anexo I.....199
Anexo II.....208
Anexo III.....219

ÍNDICE DE FIGURAS

Figura 1. Estruturas químicas das unidades repetitivas das fucanas sulfatadas de equinodermas (pepino-do-mar e ouriços-do-mar).....7
Figura 2. Estruturas químicas das unidades repetitivas das galactanas sulfatadas de algas vermelhas e angiosperma marinha.....10
Figura 3. Estruturas das galactanas sulfatadas das espécies de ouriço-do-mar *E. lucunter* e das ascídias *H. monus* e *S. plicata*.....13
Figura 4. PAGE das fucanas sulfatadas intactas e submetidas à hidrólise ácida branda.....64
Figura 5. Cinética de hidrólise ácida branda das fucanas sulfatadas de *S. pallidus* e *L. variegatus* analisada por PAGE.....66
Figura 6. Cinética de hidrólise ácida branda das fucanas sulfatadas de *S. pallidus*, *L. variegatus* e *S. franciscanus* analisada por espectroscopia 1D ^{1}H-RMN.....67
Figura 7. Esquema resumido das etapas de hidrólise ácida branda das fucanas sulfatadas de *S. pallidus*, *L. variegatus* e *S. franciscanus*.....71
Figura 8. Perfil de purificação das frações de galactanas sulfatadas da alga verde *C. isthmocladum* em cromatografia de troca-iônica.....107
Figura 9. Análise dos polissacarídeos da alga *C. isthmocladum* por gel de agarose.....108
Figura 10. Análise dos polissacarídeos da alga *C. isthmocladum* por PAGE.....109
Figura 11. Espectros 1D de ^{1}H-RMN em 400 MHz da Galactana Sulfatada (GS) 1 nativa, da GS 2 nativa da alga verde *C. isthmocladum* e seus respectivos derivados dessulfatados.....112
Figura 12. Espectros ^{1}H/^{13}C DEPT-HSQC da GS 2 nativa e seu derivado dessulfatado.....114
Figura 13. Regiões anoméricas dos espectros 2D COSY, TOCSY e NOESY da galactana 2 dessulfatada e nativa de *C. isthmocladum*.....115
Figura 14. Espectros heteronucleares ^{1}H/^{13}C HSQC e HMBC da região correspondente ao sinal metil do grupamento piruvato da molécula da GS 2 nativa.....119
Figura 15. Principais componentes estruturais encontrados na galactana sulfatada da alga verde *C. isthmocladum*.....122

Figura 16. Purificação da galactana sulfatada de *G. crenularis* em coluna de Mono-Q, análises por eletroforese em gel de agarose e PAGE.....138

Figura 17. Espectros 1D de ^{1}H-RMN em 400 MHz (de ~ 5.5 a ~ 3.0 ppm) da galactana sulfatada nativa do ouriço-do-mar *G. crenularis* e seu derivado dessulfatado.....140

Figura 18. Espectros de ^{1}H/^{13}C HSQC da galactana sulfatada do ouriço-do-mar *G. crenularis* e seu derivado dessulfatado.....141

Figura 19. Regiões anoméricas dos espectros COSY, TOCSY e NOESY da galactana sulfatada do ouriço-do-mar *G. crenularis* e seu derivado dessulfatado..142

Figura 20. Unidade dissacarídica repetitiva da galactana sulfatada do ouriço-do-mar *G. crenularis*.....145

Figura 21. Mapas de conformação (ângulos diedros *versus* energia) para os dissacarídeos constituintes das α- e β-galactanas sulfatadas e dessulfatadas de ouriços-do-mar.....148

Figura 22. Árvore filogenética esquemática mostrando a relação entre polissacarídeos sulfatados compostos de unidades beta(1-3)galactose com organismos marinhos pertencentes a diferentes filos taxonômicos.....187

ÍNDICE DE TABELAS

Tabela I. Estruturas escritas das fucanas sulfatadas de equinodermas.....8

Tabela II. Dosagem de açúcar nas frações precipitadas em diferentes volumes de acetone, conteúdo de sulfato e massa molecular das galactanas sulfatadas da alga verde *C. isthmocladum*.....105

Tabela III. Análise dos produtos metilados das GS nativas e de seus respectivos derivados dessulfatados obtidos da alga verde *C. isthmocladum.*.....111

Tabela IV. Deslocamento químico (ppm) dos ^{1}H-prótons e ^{13}C-carbonos para as estruturas propostas da GS 2 da alga verde *C. isthmocladum*, seu respectivo derivado dessulfatado e, para comparação, da galactana sulfatada nativa da alga verde *C. yezoense* e seu respectivo derivado dessulfatado.....116

Tabela V. Deslocamento químico (ppm) dos picos de correlação - δ_H/δ_C – (ppm) obtidos nos espectros de ^{1}H/^{13}C HMBC do piruvato em quetal ciclíco da galactopiranose do terminal não-redutor da SG 2 e da galactana sulfatada nas algas verdes *C. isthmocladum* e *C. yezoense*[b] respectivamente.....120

Tabela VI. Deslocamentos químicos de ^{1}H e ^{13}C (ppm), $^{3}J_{H\text{-}H}$ e $^{1}J_{C\text{-}H}$ dos espectros de RMN das α-L- e β-D-galactanas sulfatadas dos ouriços-do-mar *E. lucunter* e *G. crenularis*, respectivamente.....144

LISTA DE ABREVIATURAS

AT	Antitrombina
COSY	do inglês “Correlation spectroscopy”
C4S	Condroitim 4-sulfato
C6S	Condroitim 6-sulfato
DEPT	do inglês “Distortionless enhancement by polarization transfer”
DxS	Dextram sulfato
DM	Dinâmica molecular
FPLC	do inglês “Fast protein liquid-chromatography”
GAGs	Glicosaminoglicanos
Gal*N*Ac	*N*-acetil Galactosamina
GS	Galactana sulfatada
HCII	do inglês “Heparin cofactor II”
HMBC	do inglês “Heteronuclear multiple bound correlation”
HMQC	do inglês “Heteronuclear multiple quantum coherence”
IdoA	Ácido Idurônico
LMWH	do inglês “Low-molecular-weight heparin”
NOESY	do inglês “Nuclear Overhauser enhancement spectroscopy”
PAGE	do inglês “Polyacrylamide gel electrophoresis”
RMN	Ressonância magnética nuclear
TOCSY	do inglês “Total correlation spectroscopy”
UFH	do inglês “Unfractionaed heparin”

RESUMO

Pomin, Vitor Hugo. Fucanas e galactanas sulfatadas: estrutura, biologia e filogenia. Rio de Janeiro, 2008. Tese de Doutorado, Instituto de Bioquímica Médica, Universidade Federal do Rio de Janeiro, Rio de Janeiro, 2008.

As fucanas e galactanas sulfatadas são os polissacarídeos sulfatados mais abundantes do ambiente marinho. Esses polímeros ocorrem principalmente em algas e equinodermas. Para preparar derivados de baixo peso molecular de fucanas sulfatadas para estudos mais detalhados de suas ações biológicas, empregamos uma metodologia de depolimerização baseada na hidrólise ácida branda. Por análises de Ressonância Magnética Nuclear (RMN), foi visto que os oligossacarídeos de estrutura e peso moleculares bem definidos são formados a partir de uma 2-dessulfatação seletiva de um resíduo ligado a uma unidade 4-sulfatada, seguido da clivagem específica daquele resíduo dessulfatado. Também por RMN, caracterizamos duas novas β-galactanas sulfatadas: uma da alga verde *Codium isthmocladium*, piruvatada e formada pela unidade predominante de 3-D-Gal*p*-1 altamente 4-sulfatada; e outra, da espécie de ouriço-do-mar *Gliptocidaris crenularis*, constituída pela unidade repetitiva [→3)-β-D-Gal*p*-2(SO_4)-(1→3)-β-D-Gal*p*-(1→]$_n$. Resultados de Dinâmica Molecular, assim como valores de constante de acoplamento escalar, mostraram que α- e β-galactanas de ouriços-do-mar apresentam diferentes estados conformacionais, ocasionando efeitos diferentes na indução da reação acrossômica. A ocorrência de duas β-galactanas sulfatadas constituídas de unidades β(1-3)-Gal*p*, permitiu inferir que as galactosiltransferases são altamente conservadas nos diversos filos; enquanto, sulfotransferases são altamente diversificadas, porém, com certa tendência de ocorrência (4-sulfatação em plantas, 2-sulfatação em animais e aleatoriedade na 6-sulfatação).

Palavras-chave: fucoidam / algas marinhas / equinodermas / filogenia / anticoagulante / reação acrossômica.

ABSTRACT

Pomin, Vitor Hugo. Fucanas e galactanas sulfatadas: estrutura, biologia e filogenia. Rio de Janeiro, 2008. Tese de Doutorado, Instituto de Bioquímica Médica, Universidade Federal do Rio de Janeiro, Rio de Janeiro, 2008.

Sulfated fucans and galactans are the most abundant sulfated polysaccharides in the marine environment. These polymers occur mainly in algae and echinoderms. To prepare low-molecular-weight derivatives of sulfated fucans for more detailed studies of their biological actions, we employed a methodology for depolymerization based on mild acid hydrolysis. Through Nuclear Magnetic Resonance analysis (NMR), it was seen that the well-defined -structures and -molecular-weights oligosaccharides are yielded by a selective 2-desulfation of a unit linked to a 4-sulfated unit, followed by specific cleavage of that desulfated residue. Again, with NMR experiments, we have characterized two novel sulfated β-galactans: one from the green alga *Codium isthmocladium*, pyruvilated and composed of the predominant unit 3-D-Gal*p*-1 highly 4-sulfated; and another, from the sea-urchin *Gliptocidaris crenularis*, composed of the repetitive unit: [→3)-β-D-Gal*p*-2(SO_4)-(1→3)-β-D-Gal*p*-(1→]$_n$. Results of Molecular Dynamics, as well as scalar coupling values, showed that sea-urchin α- and β-galactans revealed different conformational states, leading to different effects as inducers of the acrosome reaction. The occurrence of two sulfated β-galactans composed of units β(1-3)-Gal*p*, allow us to determine that galactosyltransferases are highly conserved throughout different phyla; while, sulfotransferases are highly diverse, however, with a certain tendency of occurrence (4-sulfatation in plants, 2-sulfatation in animals and random distribution of 6-sulfation).

Keywords: fucoidan / seaweed / echinoderms / phylogeny / anticoagulant / acrosome reaction.

CAPÍTULO 1: FUCANAS E GALACTANAS SULFATADAS

1.1 Os polissacarídeos sulfatados apresentam grande variedade estrutural

Os polissacarídeos sulfatados formam um grupo de macromoléculas amplamente distribuído entre os seres vivos. Estes compostos apresentam grande variedade estrutural e alta densidade de carga negativa devido à presença de ésteres de sulfato e/ou grupamentos carboxila. A enorme variedade estrutural decorre da existência de diferentes tipos de açúcar (ex.: glucose, fucose, galactose, etc.) em homopolímeros ou heteropolímeros, diferentes formas enantioméricas (L ou D), diferentes configurações (α ou β) e posições das ligações glicosídicas (2, 3, 4 ou 6), e ainda, da presença ou ausência de ramificações, e das diferentes posições dos grupamentos sulfatos.

Os polissacarídeos sulfatados estão amplamente distribuídos nos tecidos de vertebrados, principalmente nos mamíferos (Mathews, 1975) e também em alguns invertebrados, onde ocorrem sob a forma de glicosaminoglicanos (GAGs). Estes compostos formam um grupo particular, fundamentalmente definido por uma estrutura repetitiva, com unidades alternadas de um açúcar aminado e outro açúcar não-aminado, que em geral é um ácido hexurônico (Nelson e Cox, 2004). Os GAGs não ocorrem nos tecidos como polissacarídeos livres, mas covalentemente ligados às proteínas, formando moléculas denominadas de proteoglicanos. Os principais exemplos de GAGs em vertebrados são condroitim sulfato, dermatam sulfato, heparam sulfato e heparina. Em invertebrados marinhos, estes compostos podem ocorrer como: heparam ou heparina e dermatam sulfato nas ascídias (Tunicata, Chordata) com padrões de sulfatação distintos do seu correspondente em vertebrados (Pavão *et al.*, 1998; Cavalcante *et al*., 1999; 2002), como condroitim sulfato-fucosilado em pepino-do-mar (Echinodermata, Holothuroidea) (Vieira e Mourão, 1988) ou como dermatam sulfato em ouriço-do-mar (Echinodermata, Echinoidea) (Vilela-Silva *et al*., 2001).

Em organismos marinhos (invertebrados e algas marinhas), os polissacarídeos sulfatados são encontrados majoritariamente como fucanas sulfatadas e galactanas sulfatadas. As fucanas sulfatadas são polímeros constituídos principalmente por resíduos de α-L-fucopiranose, mas as estruturas variam de espécie para espécie, em relação ao tipo de ligação glicosídica, ao padrão de sulfatação e a presença de ramificação (Berteau e Mulloy, 2003; Mourão, 2004; 2007). A fonte mais comum de fucanas sulfatadas é a parede celular das algas pardas (Phaeophyta) (Pereira *et al*., 1999; Rocha *et al*., 2005). No entanto, estes polissacarídeos sulfatados também podem ser encontrados na camada gelatinosa que recobre os óvulos dos ouriços-do-mar (Mulloy *et al*., 1994; Alves *et al*., 1997) ou na parede do corpo de pepinos-do-mar (Ribeiro *et al*., 1994).

As galactanas sulfatadas (polímeros de galactopiranose sulfatada) também podem ser isoladas da camada externa dos óvulos dos ouriços-do-mar (Alves *et al*., 1997), ou extraídas de outras classes de invertebrados, como as ascídias (Pavão *et al*., 1989; Albano *et al*., 1990; Santos *et al*., 1992) e bivalves (Mollusca, Bivalvia) (Amornrut *et al*., 1999). Recentemente, novas galactanas sulfatadas também foram descritas na grama marinha (Plantae, Liliopsida) (Aquino *et al*., 2005) e em algas verdes (Bryopsidales, Chorophyta) (Love e Percival, 1964). Assim como os polissacarídeos sulfatados de vertebrados (principalmente GAGs) as fucanas e galactanas sulfatadas são encontradas nas matrizes extracelulares dos organismos marinhos

1.2 Estrutura das fucanas sulfatadas

1.2.1 As fucanas sulfatadas de algas pardas são heterogêneas e complexas

As fucanas sulfatadas podem ser consideradas os polissacarídeos sulfatados mais abundantes da natureza, pois as algas pardas, que são a maior fonte das fucanas sulfatadas, dominam o ambiente marinho, tanto em número de espécies (1.500-2.000) quanto em biomassa (gigantes florestas de alta profundidade). As fucanas sulfatadas de algas marrons, também conhecidas como

fucoidanas, apresentam uma grande complexidade estrutural, sendo geralmente polímeros ramificados e de alto peso molecular (Berteau e Mulloy, 2003; Pereira *et al.* 1999). Existem algumas contradições relacionadas à estrutura das fucanas sulfatadas de certas espécies de algas pardas, devido às dificuldades tanto para a purificação quanto para a análise estrutural destes polímeros (Percival e Ross, 1950; Chevolot *et al*. 1999; Pereira *et al*. 1999). A estrutura das fucanas sulfatadas de algas pardas apresenta extrema complexidade, devido à presença e posições aleatórias de ramificações, posições aleatórias de sulfatação, além de ser em polímeros muitas vezes heterogêneos (com presença de outros açúcares como galactose, glicose, manose e xilose) (Rocha *et al*. 2005) e, ocasionalmente, com outros grupamentos químicos como acetil, metil e piruvato (Chizhov *et al*. 1999; Bilan *et al*. 2007). Em geral, esta alta complexidade estrutural impossibilita o desenho preciso de uma molécula de fucana sulfatada das espécies de algas marrons. Além disso, é muito difícil elaborar um estudo de relação *versus* atividade anticoagulante desses polissacarídeos devido à dificuldade para determinar, precisamente, sua estrutura desses polímeros de alga (Pereira et al. 1999; Mourão e Pereira, 1999).

1.2.2 As fucanas sulfatadas de equinodermas possuem estruturas regulares e repetitivas

As fucanas sulfatadas dos equinodermos apresentam certas vantagens estruturais para o estudo das atividades biológicas. Isso porque esses polissacarídeos possuem estruturas simples, lineares e compostas de unidades repetitivas de oligossacarídeos (mono, tri, ou tetrassacarídeos), que diferem de espécie para espécie no padrão de sulfatação e/ou no tipo de ligação glicosídica (Figura 1, Tabela 1).

Por exemplo, a fucana sulfatada isolada da parede do corpo do pepino-do-mar *Ludwigothurea grisea* é constituída por unidades tetrassacarídicas repetitivas, unidas por ligação do tipo $\alpha(1\rightarrow3)$, variando apenas nas sulfatações nas posições 2 e 4 (Mourão e Bastos, 1987; Mulloy *et al*. 1994) (Figura 1A, Tabela 1).

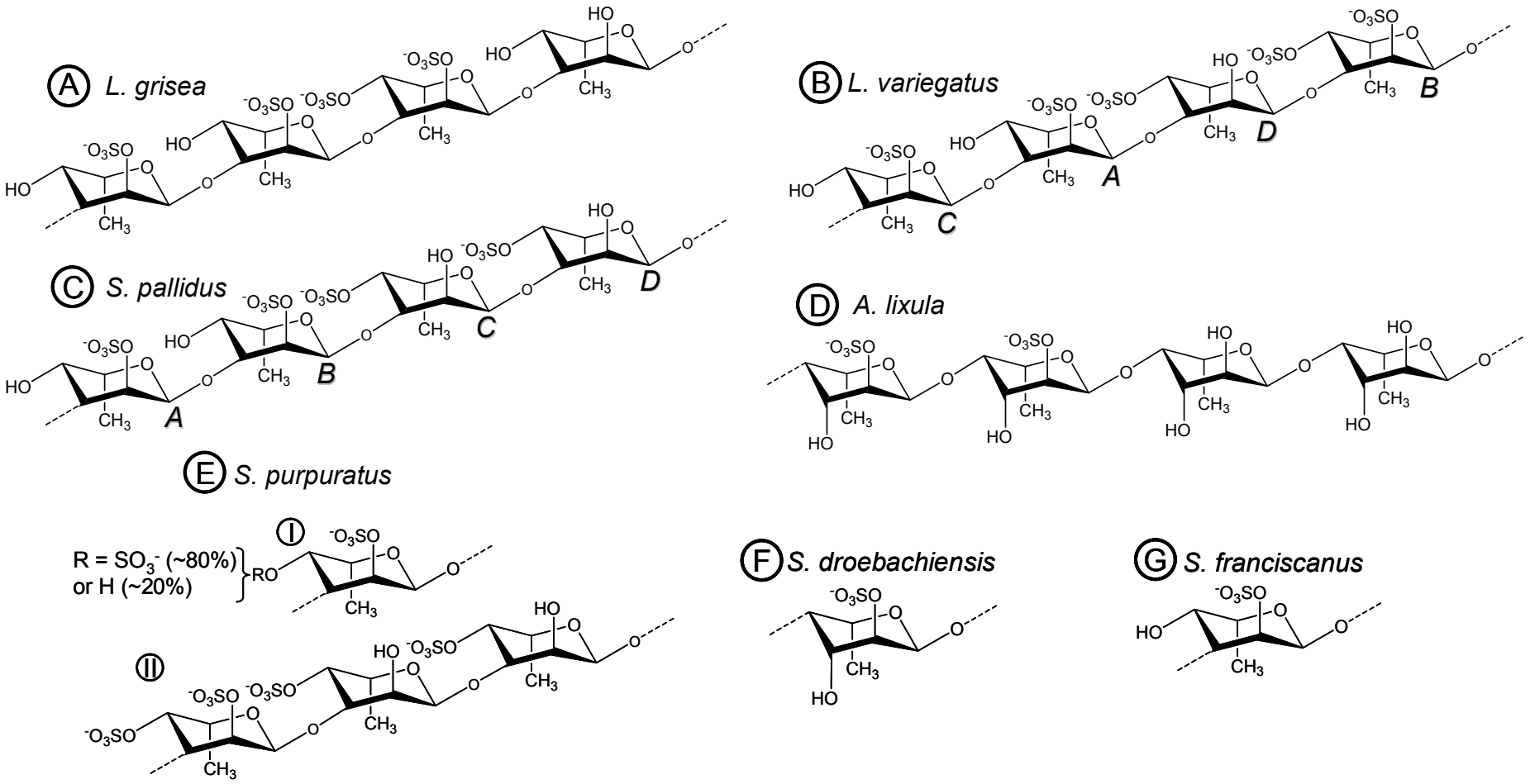

Figura 1. Estruturas químicas das unidades oligossacarídicas repetitivas das α-L-fucanas sulfatadas da parede do corpo do pepino-do-mar (A) e dos envoltórios gelatinosos que recobrem os óvulos dos ouriços-do-mar (B-G). As estruturas espécie-específicas variam no padrão de sulfatação (mas, exclusivamente nas posições 2-*O*- e/ou 4-*O*-), nas ligações glicosídicas $\alpha(1\rightarrow3)$ (A-C, E e G) ou $\alpha(1\rightarrow4)$ (D e F) e no número de resíduos contidos nas unidades repetitivas: tetrassacarídeos (A-D), trissacarídeos (E-II) e monossacarídeos (E-I, F e G), mas todos compostos lineares. Os quatro tipos de unidades anoméricas das fucanas de *L. variegatus* (B) e *S. pallidus* (C) estão identificados pelas letras A-D para correspondente assinalamento nos espectros de ^{1}H-RMN.

Tabela I. Unidades repetitivas das α-L-fucanas sulfatadas das espécies de pepino-do-mar (*L. grisea)* e ouriços-do-mar (*L. variegatus*, *S. pallidus*, *A. lixula*, *S. purpuratus*, *S. droebachiensis* e *S. franciscanus*). A espécie *S. purpuratus* expressa duas fucanas sulfatadas.

Espécies	Estruturas das α-L-fucanas sulfatadas	Referência.
L. grisea	[→3)-α-L-Fuc*p*-2,4(OSO_4)-(1→3)-α-L-Fuc*p*-(1→3)-α-L-Fuc*p*-2(OSO_4)-(1→3)-α-L-Fuc*p*-2(OSO_4)-(1→]$_n$	Mulloy *et al*. 1994
L. variegatus	[→3)-α-L-Fuc*p*-2(OSO_4)-(1→3)-α-L-Fuc*p*-2(OSO_4)-(1→3)-α-L-Fuc*p*-4(OSO_4)-(1→3)-α-L-Fuc*p*-2,4(OSO_4)-(1→]$_n$	Mulloy *et al*. 1994
S. pallidus	[→3)-α-L-Fuc*p*-2(OSO_4)-(1→3)-α-L-Fuc*p*-2(OSO_4)-(1→3)-α-L-Fuc*p*-(1→3)-α-L-Fuc*p*-(1→]$_n$	Vilela-Silva *et al*. 2002
A. lixula	[→4)-α-L-Fuc*p*-2(OSO_4)-(1→4)-α-L-Fuc*p*-2(OSO_4)-(1→4)-α-L-Fuc*p*-(1→4)-α-L-Fuc*p*-(1→]$_n$	Alves *et al*. 1997
S. purpuratus I	~80% [→3)-α-L-Fuc*p*-2,4(OSO_4)-(1→]$_n$ and ~20% [→3)-α-L-Fuc*p*-2(OSO_4)-(1→]$_n$	Alves *et al*. 1998
S. purpuratus II	[→3)-α-L-Fuc*p*-2,4(OSO_4)-(1→3)-α-L-Fuc*p*-4(OSO_4)-(1→3)-α-L-Fuc*p*-4(OSO_4)-(1→]$_n$	Alves *et al*. 1998
S. droebachiensis	[→4)-α-L-Fuc*p*-2(OSO_4)-(1→] $_n$	Vilela-Silva *et al*. 2002
S. franciscanus	[3)-α-L-Fuc*p*-2(OSO_4)-(1→] $_n$	Vilela-Silva *et al*. 1999

O tecido conjuntivo deste invertebrado também apresenta grandes quantidades de outro polissacarídeo, semelhante ao glicosaminoglicano condroitim sulfato de vertebrados, porém com ramificações de fucose sulfatada (Vieira e Mourão, 1988).

No caso dos ouriços-do-mar, os polissacarídeos sulfatados, formados por unidades repetitivas regulares são isolados do envoltório gelatinoso dos óvulos. A grande maioria desses polissacarídeos são constituídos de resíduos de α-L-fucopiranose, com ligações glicosídicas do tipo α(1→3) ou α(1→4) e com sulfatação nas posições 2 e/ou 4 (Figura 1B-G, Tabela 1).

1.3 Estrutura das galactanas sulfatadas

1.3.1 Galactanas de algas vermelhas e angiospermas marinhas

As galactanas sulfatadas de rodófitas apresentam uma estrututa quase regular, composta por unidades dissacarídicas repetitivas, com padrão variável de sulfatação (Farias *et al*., 2000; Pereira *et al*., 2005), similar aos GAGs de animais. Esses polissacarídeos apresentam uma cadeia glicosídica composta por unidades alternadas de resíduos de β-D-galactopiranose 3-ligados e resíduos de α-galactopiranose 4-ligados. Os resíduos de β-galactose sempre são o enantiômero-D, enquanto que os resíduos de α-galactose podem ocorrer como isômeros -L ou -D (Usov, 1998). O padrão de sulfatação varia de espécie para espécie e também pode mudar em amostras da mesma espécie, coletadas em diferentes ambientes ou em diferentes estações do ano (Pereira *et al*., 2005).

A distribuição de sulfato no polímero de galactose é heterogênea na maioria das espécies, mas seu conteúdo é nitidamente diferenciado entre elas. Por exemplo, as galactanas sulfatadas das algas vermelhas *Botriocladia occidentalis* e *Gelidium crinali* diferem apenas no conteúdo de sulfatação (Figura 2A) (Farias *et al*., 2000; Pereira *et al*., 2005). Esta simples diferença resulta em mudanças dramáticas em sua atividade anticoagulante e antitrombótica (veja Pereira *et al*., 2005 e Fonseca *et al*., 2008).

Contudo, há um grupo pequeno de espécies de rodófitas que expressa galactanas sulfatadas com alto grau de homogeneidade e regularidade. Esses po-

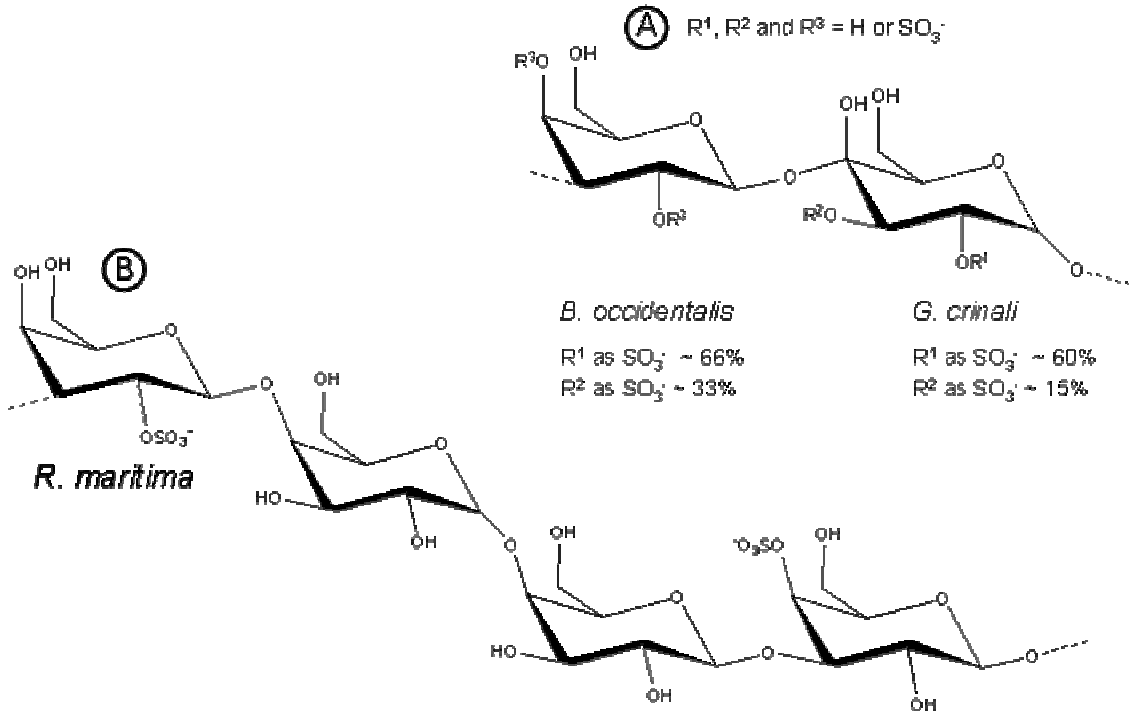

Figura 2. Estruturas de galactanas sulfatadas de algas vermelhas e angiosperma marinha, constituídas por unidades repetitivas. As espécies de algas vermelhas (**A**) *B. occidentalis* e *G. crinali* expressam galactanas sulfatadas compostas por unidades dissacarídicas repetitivas de [3-β-D-Gal*p*-1→4-α-L-Gal*p*-1]$_n$ cujos teores de sulfatação variam entre as espécies (Farias *et al*., 2000; Pereira *et al*., 2005). A grama marinha (**B**) *R. maritima* sintetiza uma galactana sulfatada com unidades tetrassacarídicas repetitivas (Aquino *et al*., 2005).

límeros são chamados de carragenanas e agaranas, onde os resíduos de α-galactose são D ou L, respectivamente. Algumas vezes, estes polímeros também podem apresentar resíduos de 3,6-anhydro-α-D-galactopiranose (Usov, 1998; Lahaye, 2001; van de Velde *et al*., 2004).

Recentemente, outra galactana sulfata, também com estrutura regular, linear e repetitiva, foi descrita na espécie de grama marinha *Rupia Maritima*. A grama marinha é um grupo particular de plantas vasculares (angiospermas), que habita regiões extremamente salinas (Aquino *et al*., 2005). Esta galactana sulfatada tem sua estrutura constituída pela unidade tetrassacarídica repetitiva [→3-β-D-Gal*p*-2(OSO_4)-1→4-α-D-Gal*p*-1→4-α-D-Gal*p*-1→3-β-D-Gal*p*-4(OSO_4)-1→]$_n$ (Figura 2B).

1.3.2 Galactanas de algas verdes

As algas verdes, particularmente do gênero *Codium* (Bryopsidales, Chorophyta) (Matsubara *et al*., 2001; Bilan *et al.,* 2007) também são fontes de galactanas sulfatadas do ambiente marinho. Poucas estruturas de galactanas sulfatadas foram determinadas nas clorófitas, quando comparado com a grande quantidade de estruturas descritas nas galactanas sulfatadas de algas vermelhas.

Dentro do gênero *Codium*, as espécies apresentam grande variedade estrutural, com diferentes graus de heterogeneidade. *Bilan* e colaboradores (2007) isolaram uma galactana sulfatada da espécie *C. yezoense*. Esse polissacarídeo é composto essencialmente por uma cadeia de β-D-galactopiranose 3-ligada, com alguns resíduos ramificados no carbono-6 e é, ainda, altamente piruvatado. Grupamentos sulfatos estão presentes principalmente no carbono-4 e em pequenas quantidades no carbono-6. Alguns grupamentos piruvato (25% do total de resíduos) formam resíduos de β-D-galactopiranose 3,4-*O*-(1´-carboxi)-etilideno, localizados nos terminais não-redutores da cadeia de galactose.

As galactanas sulfatadas de *C. fragile* e *C. cylindricum* são polímeros altamente heterogêneos. Além da predominância dos resíduos de galactose, o polissacarídeo de *C. fragile* também contém arabinose, portanto, trata-se de uma

arabinogalactana (Love *et al*., 1964). O polissacarídeo de *C. cylindricum* contém além de resíduos de galactose, resíduos de glucose (glucogalactana) (Matsubara *et al*., 2001).

1.3.3 Galactanas de invertebrados marinhos (ouriços-do-mar e ascídias)

As galactanas sulfatadas de ouriços-do-mar apresentam um padrão estrutural claro, regular e bem definido, similar às fucanas sulfatadas de ouriços-do-mar (Alves *et al*., 1997). Esta regularidade estrutural está relacionada com a interação entre os gametas durante a fertilização desses animais (Mourão, 2007). Esse evento biológico depende da especificidade estrutural das galactanas (padrão de sulfatação e tipo de ligação glicosídica), que servem como um "código" de reconhecimento, com a finalidade de evitar a fertilização cruzada (interespecífica). Cada espécie possui uma estrutura específica de polissacarídeo sulfatado. Por exemplo, a espécie de ouriço-do-mar *Echinometra lucunter* sintetiza uma galactana sulfatada composta apenas pela unidade monossacarídica repetitiva: $[\rightarrow 3)$-α-L-Gal*p*-2(OSO_4)-$(1\rightarrow]_n$ (Figura 3A).

Outro tipo de invertebrado que sintetiza galactanas sulfatadas é as ascídias, também conhecidas como tunicatos. A espécie *Herdmania monus* contém um polissacarídeo composto por unidades de α-L-galactopiranose 4-ligada e 3-sulfatada (Figura 3B), enquanto que a espécie *Styela plicata* expressa uma galactana sulfatada com a mesma unidade glicosídica na cadeia principal, mas com ramificações ligadas no carbono 2 da hexose (Figura 3C).

1.4 Estrutura *versus* atividades biológicas de fucanas e galactanas sulfatadas

1.4.1 Papéis fisiológicos e atividades biológicas

As fucanas sulfatadas de algas marrons e as galactanas sulfatadas de algas verdes e vermelhas estão envolvidas na constituição e organização da parede celular dessas macroalgas (Andrade *et al*. 2004; Usov, 1998). No caso das

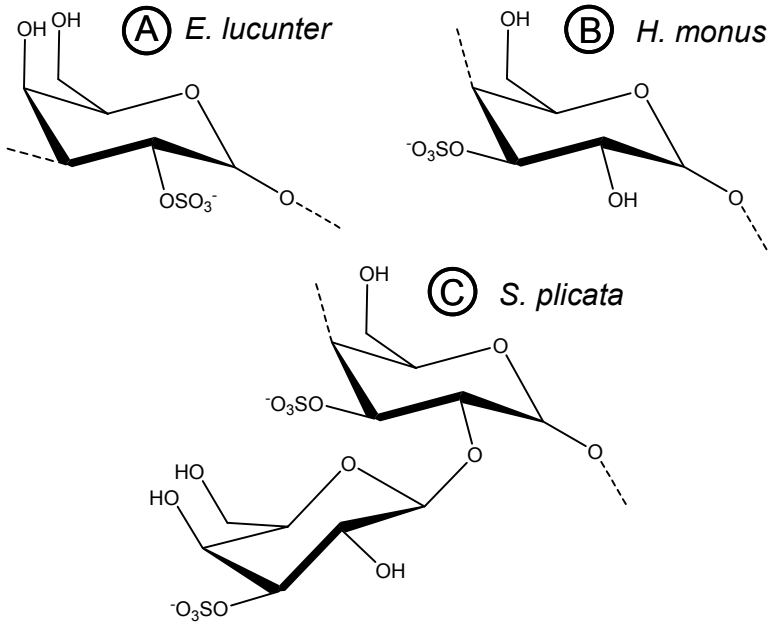

Figura 3. Estruturas das galactanas sulfatadas das espécies de ouriço-do-mar *E. lucunter* (**A**) e das ascídias *H. monus* (**B**) e *S. plicata* (**C**). A galactana sulfatada isolada da camada gelatinosa do óvulo do ouriço-do-mar é composta pela unidade $[3\text{-}\alpha\text{-L-Gal}p\text{-}2(SO_4)\text{-}1]_n$ (**A**) (Alves *et al*., 1997), enquanto que as galactanas isoladas das túnicas das ascídias são constituídas pelas unidades $[4\text{-}\alpha\text{-L-Gal}p\text{-}3(SO_4)\text{-}1]_n$ (**B**) (Santos *et al*. 1992) e $\{4\text{-}\alpha\text{-L-Gal}p\text{-}3(SO_4)\text{-}2[\rightarrow 1)\text{-}\alpha\text{-L-Gal}p\text{-}3(SO_4)]\text{-}1\}_n$ (**C**) (Albano e Mourão, 1986).

fucanas sulfatadas de feófitas, essas moléculas perfazem mais de 40% da massa da parede celular. Em contrapartida, as fucanas e galactanas sulfatadas dos ouriços-do-mar possuem um papel fisiológico específico para a fertilização externa desses animais, apesar de também estarem localizadas no espaço extracelular. Esses polissacarídeos sulfatados são encontrados no envoltório gelatinoso que recobre os óvulos dos ouriços-do-mar. Outras moléculas encontradas neste gel são sialoproteínas, glicoproteínas e peptídeos (Suzuki, 1990; Bonnell *et al.*, 1994). Uma das funções desse envoltório é proteger o gameta durante a sua liberação da gônada feminina (Thomas *et al.*, 2001). Além da função estrutural, os polissacarídeos sulfatados encontrados nessa matriz são imprescindíveis para a reação acrossômica, que é um evento obrigatório para a fertilização espécie-específica dos ouriços-do-mar (SeGall e Lennarz, 1979; 1981; Alves *et al.*, 1997, Mourão 2007).

A reação acrossômica é um evento que possibilita a interação do espermatozóide com o gameta feminino (Trimmer e Vacquier, 1986; Foltz e Lennarz, 1993). Este evento se inicia após o contato de um receptor protéico (suREJ) na superfície do espermatozóide com a fucana sulfatada do óvulo (Moy *et al.*, 1996; Vacquier e Moy, 1997). Esse contato promove a ativação de dois canais de cálcio no espermatozóide (Guerreiro e Darzon, 1989; Gonzales-Martinez *et al.*, 2001). Assim, o aumento do cálcio intracelular induz a fusão da vesícula acrossomal à membrana do espermatozóide, liberando proteases capazes de digerir o envoltório do óvulo (Levine *et al*., 1978). Além disso, há um aumento do pH intracelular que, por conseguinte, induz uma polimerização de actina, desencadeado pela atuação dos polissacarídeos sulfatados e pela ação sinérgica dos sialo-glicoconjugados, ambos os polissacarídeos encontrados na camada gelatinosa dos óvulos (Hirohashi e Vacquier, 2002a). Esta polimerização forma uma ponta afunilada na extremidade do espermatozóide (Dan, 1954; Tilney *et al.*, 1973) que, além de exercer uma pressão na membrana do óvulo, expõe uma proteína denominada bindina, que prende eficazmente os dois gametas via um receptor na superfície do óvulo (Trimmer e Vacquier, 1986; Foltz e Lennarz, 1993).

Em síntese, as fucanas sulfatadas encontradas no envoltório do gel do óvulo são responsáveis pela indução da reação acrossômica (Mulloy *et al.*, 1994; Alves *et al.*,1998; Vacquier e Moy, 1997, Mourão 2007). Esses polissacarídeos sulfatados agem como indutores espécie-específicos da fertilização em ouriços-do-mar (Mourão, 2007) e representam um exemplo importante de interação carboidrato-proteína (Miller e Ax, 1990).

As fucanas e galactanas sulfatadas de algas marinhas apresentam diversas atividades biológicas em mamíferos. Como exemplos, podemos mencionar: inibição da proliferação de músculo liso, ativação do sistema imunológico, ação antiinflamatória (Berteau and Mulloy 2003; Cumashi *et al*. 2007), anticoagulante e antitrombótica (Berteau e Mulloy, 2003; Pereira *et al*. 1999; Mourão 2004), antiangiogênica, anticâncer, antiparasitária (Berteau e Mulloy, 2003) e antiviral (Harrop *et al*. 1992). Porém, existem poucos dados sobre as atividades biológicas de fucanas e galactanas sulfatadas de ouriços-do-mar. Isso decorre, provavelmente, da pequena disponibilidade desses compostos e/ou da sua descoberta ainda recente. Naturalmente, essas ações estão distantes do papel fisiológico como indutores espécie-específicos da reação acrossômica.

Certamente a ação anticoagulante dos polissacarídeos sulfatados (principalmente as fucanas e galactanas sulfatadas) de organismos marinhos é a atividade biológica mais estudada (Pereira *et al.*, 2002; Mourão, 2004). Essa linha de pesquisa tem crescido devido à necesidade de novos anticoagulantes em consequência do aumento da ocorrência das doenças tromboembólicas. Por exemplo, 12 milhões de mortes no mundo a cada ano são decorrentes de doenças cardiovasculares. Nesses casos patológicos, a heparina, um glicosaminoglicano com ação anticoagulante, é uma das drogas mais utilizadas. Porém, clinicamente ela possui uma série de efeitos adversos como: trombocitopenia (Warkentin, 1999; Visentin, 1999), ação hemorrágica, efeito dose-resposta muito variável (Kelton e Hirsh, 1980; Kakkar e Hedges, 1989) e risco de contaminantes patológicos, como vírus e príons. Logo, a busca de alternativas para a heparina aumentou o interesse pelo estudo de novas moléculas anticoagulantes, como os

polissacarídeos sulfatados de organismos marinhos. Similar à heparina, o mecanismo anticoagulante das fucanas e galactanas sulfatadas reside na capacidade de potencializar a inibição da trombina (em alguns casos, também do fator Xa) mediada por inibidores plasmáticos naturais, como as serpinas (AT e HCII) (Mourão e Pereira, 1999; Pereira *et al.*, 2002; Mourão, 2004).

1.4.1.1 Requisitos estruturais para a indução da reação acrossômica

As atividades biológicas desempenhadas pelas fucanas e galactanas sulfatadas extraídas de ouriços-do-mar dependem da sua estrutura (Mourão e Pereira, 1999; Berteau e Mulloy, 2003; Mourão, 2004, 2007), em especial o tipo de ligação glicosídica (Hirohashi *et al.*, 2002) e da posição de sulfatação (Vilela-Silva *et al.*, 1999; Pereira *et al.*, 2002).

O estudo de Biermann *et al*. (2004) mostrou que a posição da ligação glicosídica é fundamental na indução da reação acrossômica em espermatozóides do gênero *Strongylocentrotus*. Surpreendentemente, outro trabalho mostrou que a galactana sulfatada de *E. lucunter* (Figura 2A) é capaz de induzir a reação acrossômica em espermatozóides da espécie *Strongylocentrotus franciscanus* (Figura 1G), com a mesma potência que a fucana sulfatada. Claramente o tipo de monossacarídeo não influencia na indução da reação acrossômica, porque os polissacarídeos destas duas espécies diferem apenas no tipo de resíduo constituinte - fucose no *S. franciscanus* e galactose no *E. lucunter* (Figura 1G e 2A).

A proporção de 2-*O*- ou 4-*O*-sulfatação, também é um requisito estrutural para a indução da reação acrossômica. Por exemplo, a fucana sulfatada de *Lytechinus variegatus* (Figura 1B) induz a reação acrossômica em espermatozóides de *S. franciscanus* com a mesma potência que a fucana homóloga (Figura 1G). Estas duas fucanas sulfatadas têm estruturas similares, enriquecidas em 2-sulfatação. Em contraste, as fucanas sulfatadas de *Strongylocentrotus purpuratus* (Figura 1E-I e II) tem uma potência significativamente mais reduzida na indução da reação acrossômica em

espermatozóides de *S. franciscanus* em decorrência da sua preponderância de 4-O-sulfatação (Vilela-Silva *et al*., 1999).

1.4.1.2 A atividade anticoagulante depende de componentes estruturais específicos: polissacarídeos de algas *versus* de equinodermas

A atividade anticoagulante das fucanas sulfatadas depende do grau e da posição da sulfatação (Pereira *et al.* 2002). A comparação da atividade anticoagulante de diferentes fucanas sulfatadas, todas com ligação glicosídica $\alpha(1\rightarrow3)$, mas com diferentes graus e sítios de sulfatação, permitiu demonstrar que a 2,4-di-sulfatação, presente nas fucanas de *S. purpuratus* (Figura 1E-I e II) e *L. variegatus* (Figura 1B) têm um efeito amplificador da ação inibidora das fucanas sulfatadas sobre a trombina mediada pela antitrombina. Por outro lado, a 2-*O*-sulfatação, presente na fucana de *S. franciscanus* (Figura 1G), exibiu um efeito atenuador sobre essa ação inibitória. Quando a antitrombina é substituída pelo HCII, a presença da 2-O-sulfatação também apresentou um efeito deletério na inibição da trombina. Particularmente, no caso desta serpina, o aumento do conteúdo de 4-sulfatação (e redução de 2-sulfatação) incrementa o efeito inibidor das fucanas sulfatadas sobre a trombina. Em conseqüência, a ação anticoagulante das fucanas de *S. purpuratus* (ricas em 4-sulfatação) é elevada, mas diminui significativamente no caso da fucana sulfatada de *Strongylocentrotus pallidus* (~50 % 2-sulfatada e ~50 % 4-sulfatada, Figura 1C). A fucana sulfatada de *Arbacia lixula* (~50 % 2-sulfatada e ~50 % não-sulfatada, Figura 1D) apresentou uma atividade ~50 vezes menor do que o polissacarídeo de *S. pallidus*. Portanto, as interações desses polissacarídeos sulfatados com os cofatores e proteases da coagulação dependem de características estruturais específicas e não decorre apenas da densidade de cargas negativas da molécula (Pereira *et al.* 2002; Mourão, 2004).

O tipo de monossacarídeo constituinte dos polissacarídeos sulfatados influencia significativamente a ação anticoagulante. Essa observação decorre

principalmente da observação de que a galactana sulfatada de *E lucunter* (Figura 3A) tem uma ação anticoagulante muito mais potente do que a fucana de *S. franciscanus* (Figura 1G). Esses dois polissacarídeos estão sulfatados na posição 2, unidos por ligações glicosídicas $\alpha(1\rightarrow3)$ e diferem apenas no tipo de monossacarídeo constituinte (Pereira *et al*., 2002).

Os estudos sobre as influências das características estruturais (posição da ligação glicosídica, sítio de sulfatação e tipo de açúcar constituinte) das fucanas e galactanas na atividade anticoagulante ficam mais claros quando se utiliza polissacarídeos homogêneos e regulares dos equinodermos nos ensaios de coagulação (Pereira e Mourão, 1999; Mourão, 2004).

Em contrapartida, as fucanas sulfatadas de algas pardas não são bons modelos de estudo de estrutura *versus* atividade biológica devido à ausência de uma estrutura clara, num padrão repetitivo e definido. Mesmo quando estas moléculas apresentam potente efeito anticoagulante é difícil estudar seu efeito ao nível molecular.

As galactanas sulfatadas de rodófitas apresentam estruturas com unidades repetitivas mais definidas quando comparadas com as fucanas sulfatadas de feófitas. Fonseca e colaboradores (2008), demostraram, recentemente, que as galactanas sulfatadas de *G. crinali* e *B. occidentalis* (Figura 2A), compostas da mesma unidade repetitiva e com discretas diferenças no padrão de sulfatação, apresentam atividades antitrombóticas e anticoagulantes bem distintas. A galactana sulfatada de *G. crinali* apresenta efeito pró-coagulante e pró-trombótico *in vivo* em baixas doses (até 1,0 mg/Kg de peso de rato) e atividade antitrombótica venosa e arterial em doses acima de 1,0 mg/Kg de peso de rato. Em contrapartida, a galactana sulfatada de *B. occidentalis* apresenta uma potente atividade anticoagulante e atenua a trombose venosa na dose de 0,5 mg/Kg. No entanto, estes efeitos são revertidos em doses mais altas. Acima da dose de 1,0 mg/Kg, a galactana de *B. occidentalis* inibe o trombo arterial. Os efeitos de potencialização das serpinas na inibição de trombina também são diferentes para esses dois polissacarídeos de algas vermelhas (Fonseca *et al*. 2008). Em síntese,

pequenas diferenças no teor de sulfatação influenciam significativamente os níveis e os efeitos biológicos destes carboidratos.

1.5 Conclusões gerais

As fucanas e galactanas sulfatadas são os polissacarídeos sulfatados mais abundantes do ambiente marinho e também os mais estudados quanto às suas aplicações farmacológicas. A estrutura desses polissacarídeos varia de espécie para espécie, mas apresentam características peculiares em cada filo. As fucanas sulfatadas de algas pardas são geralmente complexas e heterogêneas, enquanto que as galactanas sulfatadas de algas vermelhas são formadas de unidades dissacarídicas repetitivas à semelhança dos GAGs de mamíferos. Porém, com um padrão complexo de sulfatação, além da substituição com grupamentos metil, etil, piruvato e a formação de 3,6-anidro açúcares. As algas verdes também apresentam galactanas sulfatadas, porém, mais heterogêneas que as de algas vermelhas, mas com unidades estruturais mais evidentes do que as fucanas sulfatadas de algas marrons.

Em contrapartida, as fucanas e galactanas sulfatadas de invertebrados marinhos, particularmente de equinodermas e de alguns tunicatos (ascídias), e da angiosperma marinha, apresentam estruturas com unidades regulares e repetitivas. Os ouriços-do-mar e pepinos-do-mar sintetizam polissacarídeos sulfatados que variam de maneira espécie-específica no tipo de açúcar (galactose ou fucose), no padrão de sulfatação (2 e/ou 4), na ligação glicosídica (1-3) ou (1-4) ou no número de unidades repetitivas (1, 3 ou 4 resíduos de açúcar).

Os polissacarídeos de algas, das ascídias e dos pepinos-do-mar são constituintes de matrizes extracelulares. Os polissacarídeos sulfatados de ouriços-do-mar ocorrem no envoltório gelatinoso que recobre os óvulos e participam diretamente da indução da reação acrossômica nos espermatozóides. Este evento é fundamental para o reconhecimento de gametas, que participa da fertilização desses animais.

Os polissacarídeos sulfatados de organismos marinhos possuem, portanto, ação anticoagulante e antitrombótica, embora essas ações estejam distantes do papel fisiológico desses compostos. Esses polissacarídeos potencializam a ação dos inibidores plasmáticos (AT e HCII) sobre as proteases da coagulação, à semelhança do efeito da heparina. Potencialmente, esses resultados podem levar ao desenvolvimento de novos agentes anticoagulantes e antitrombóticos. As moléculas obtidas de algas marinhas apresentam efeitos mais potentes. Porém, os compostos de invertebrados marinhos são mais apropriados por revelar os mecanismos moleculares da ação biológica devido as suas estruturas regulares e repetitivas.

1.6 Artigo I

Glycobiology

(aceito em 04 de setembro de 2008)

"Structure, biology, evolution and medical importance of sulfated –fucans and -galactans"

Vitor H. Pomin e Paulo A.S. Mourão

Os comentários que compôem este capítulo de introdução estão discutidos detalhadamente neste manuscrito em anexo.

Structure, biology, evolution and medical importance of sulfated -fucans and -galactans

Vitor H. Pomin[1,2] and Paulo A.S. Mourão[2]

[2]Laboratório de Tecido Conjuntivo, Hospital Universitário Clementino Fraga Filho and Programa de Glicobiologia, Instituto de Bioquímica Médica, Centro de Ciências da Saúde, Universidade Federal do Rio de Janeiro, Caixa Postal 68041, Rio de Janeiro, RJ, 21941–590, Brazil.

[1]To whom correspondence should be addressed; e-mail: vhpomin@gmail.com, Tel/Fax +55-21-2562-2090.

Summary:

Sulfated fucans and galactans are strongly anionic polysaccharides found in marine organisms. Their structures vary among species, but their major features are conserved among phyla. Sulfated fucans are found in marine brown algae and echinoderms, whereas sulfated galactans occur in red and green algae, marine angiosperms, tunicates (ascidians) and sea urchins. Polysaccharides with 3-linked, β-galactose units are highly conserved in some taxonomic groups of marine organisms and show a strong tendency toward 4-sulfation in algae and marine angiosperms, and 2-sulfation in invertebrates. Marine algae mainly express sulfated polysaccharides with complex, heterogeneous structures, whereas marine invertebrates synthesize sulfated fucans and sulfated galactans with regular repetitive structures. These polysaccharides are structural components of the extracellular matrix. Sulfated fucans and galactans are involved in sea urchin fertilization acting as species-specific inducers of the sperm acrosome reaction. Because of this function the structural evolution of sulfated fucans could be a component in the speciation process. The algal and invertebrate polysaccharides are also potent anticoagulant agents of mammalian blood and represent a potential source of compounds for antithrombotic therapies.

Keywords: fucoidan / carrageenans / algae / marine invertebrate / anticoagulant / sea urchin fertilization / acrosome reaction / species-specificity / sulfated polysaccharides / sperm-egg recognition.

Running title: *Sulfated -fucans and -galactans.*

Introduction

With the exception of some mammalian polysaccharides, the sulfated fucans and galactans of algae and marine invertebrates are the most well-studied sulfated polysaccharides. In terms of total biomass, they are more abundant than glycosaminoglycans. As we will discuss below, these compounds exhibit a wide structural diversity and have intriguing biological functions.

In this review, we describe the main structural features of sulfated fucans and galactans isolated from marine organisms. The structures of the algal polysaccharides are complex and heterogeneous (Pereira et al. 1999; Berteau and Mulloy 2003). In contrast, polysaccharides from marine angiosperms and invertebrates have simpler, more homogeneous structures. They are composed of repeating units, which vary in a species-specific manner (Mourão 2004; Aquino et al. 2005; Mourão 2007). Here, we also discuss the evolutionary implications of these marine sulfated polysaccharides and their biological effects, focusing on the description of their natural role in echinoderm fertilization. Finally, we also describe the inhibition by these polysaccharides of mammalian blood coagulation, with emphasis on developing new therapeutic agents.

Heterogeneous sulfated fucans from algae

The first isolation of a sulfated fucan (originally denoted fucoidan) from marine brown algae (Phaeophyta) was reported by Killing in 1913. These sulfated polysaccharides can be extracted from algal cell walls with hot water (Percival and Ross 1950), acid solutions (Black 1954) or protease digestion (Martinez-Rumayor and Januzzi 2006; Leite et al. 1998). They can account for >40% of the dry weight of algal cell walls (Kloareg 1984). Sulfated fucans have been extensively studied in brown algae, and are present in all brown algae thus far investigated (Patankar et al. 1993; Nishino et al. 1995; Chevolot et al. 1999; Chizhov et al. 1999; Chevolot et al. 2001; Pereira et al. 1999; Bilan et al. 2002; Yoon et al. 2007). The composition of these molecules may vary according to the species (Percival and Ross 1950; Mian and Percival 1973), the extraction procedure (Mabeau et al. 1990), the season and climatic conditions (Black 1954; Von Holdt et al. 1955; Wort

1955; Honya et al. 1999). These polysaccharides are absent, or occur only in minor amounts in green algae (Chlorophyta), red algae (Rhodophyta), and golden algae (Xanthophyta). Brown algal sulfated fucans are among the most abundant marine sulfated polysaccharides, since these algae dominate the near-shore environment in both number of species (1,500-2,000) and biomass.

The initial structural study of a sulfated fucan was that obtained from the common brown alga *Fucus vesiculosus*. Early on, Percival and Ross (1950) suggested a polysaccharide composed of α-L-fucopyranose, mainly bound by 1→2 glycosidic linkages and sulfation at 4-position (Figure 1A). The simplicity of this structure was contested by Patankar and co-workers in 1993. Based on methylation analysis, these authors proposed that this sulfated fucan has a central core, composed of 4-sulfated or non-sulfated, 3-linked α-L-fucopyranose units, with branches of non-sulfated fucose linked to the central core at position 2 or 4 (Figure 1B). Recently, studies based on high field NMR, revealed that the sulfated fucans from this and other brown algal species are composed equally of alternating units of 2,3-disulfated, 4-linked and 2-sulfated, 3-linked α-L-fucopyranosyl units (Figure 1C). The heterogeneity of this polysaccharide results mainly from the occurrence of branches of non-sulfated fucose residues (Chevolot et al. 1999; Pereira et al. 1999). More recently, NMR analysis of sulfated fucans from other species of brown algae revealed unique structures (Figure 1D and E). In particular, occurrence of *O*-acetylation is also commonly present (Chizhov et al. 1999). Contradictions related to the structures of brown algal sulfated fucans arise from the difficulties in purifying these molecules as well as their highly complex structures due to presence of branching, random distribution of sulfation, different types of glycosidic linkages, and also the presence of other heterogeneities like acetylation, methylation and pyruvilation (Figure 1) (Chizhov et al. 1999; Bilan et al. 2007).

Homogeneous, repetitive sulfated fucans of echinoderms

In addition to brown algae, sulfated fucans are found in marine invertebrates. The first evidence showing sulfated fucans in sea urchins (Echinodermata, Echinoidea) was published ~60 years ago (Vasseur 1948), but no structural study was performed at this time. Since 1994, our laboratory has been performing a systematic structural analysis of

the sulfated fucans from different species of sea urchins. Most of our work is on these molecules isolated from the jelly coats surrounding sea urchin eggs.

In contrast to the algal polysaccharides, sulfated fucans from sea urchins and sea cucumbers (Echinodermata, Holothuroidea) are easily purified and possess simple, unique structures of linear chains of α-L-fucose in well-defined repetitive patterns. Their specific sulfation patterns and the positioning of glycosidic bonds vary with the species (Figure 2).

The simplest sea urchin sulfated fucan, which is composed of $[3\text{-}\alpha\text{-L-Fuc-2}(OSO_3)\text{-}1]_n$, is found in the egg jelly of *Strongylocentrotus franciscanus* (Vilela-Silva et al. 1999). Other sea urchins so far studied possess sulfated fucans with different numbers of residues in the repeating units, which vary among the different species according to the position of the glycosidic linkages [α(1→3) or α(1→4)], and the sulfation sites (2-*O*- and/or 4-*O*-positions) (Figure 2).

Sulfated galactans: the heterogeneity arises mostly due to complex sulfation patterns

Marine sulfated galactans are widely abundant in red algae. Carrageenans and agarans are the most common sulfated galactans from macroalgae. The origin of the name carrageenan derived from a small village, Carragheen, on the Irish coast, where the carrageenan-bearing seaweed *Chondrus crispus* or “Irish moss” grows (Bixler 1994). The word agaran (name proposed by Kuntsen et al. 1994, see also Lahaye 2001) originally derived from the word “agar”, which that means jelly in the Malay language (agar-agar). Both of these red algal polysaccharides usually have a linear backbone made of alternating 3-linked β-D-galactopyranose and 4-linked α-galactopyranose residues (Figure 3A), showing a ‘masked repeat’ unit of disaccharides similar to the animal glycosaminoglycans. The β-galactoses are always D-enantiomers, whereas the α-galactose residues may be present in the D- or L-configuration (Usov 1998). A substantial portion may also exist in the form of 3,6-anhydro derivatives (Figure 3A). Like sulfated fucans from brown algae, considerable structural variation in the red alga sulfated galactans occurs among different species and in samples collected at different environments, or in different seasons of the year (Pereira et al. 2005). Furthermore, various hydroxyl groups may be substituted by a sulfate ester, a methyl group or pyruvic acid (Usov 1998). The major structural variation in these polysaccharides is the sulfation

pattern. The sulfate distribution along the galactose-backbone is quite heterogeneous as in animal glycosaminoglycans and the sulfate contents are markedly different between different species (Pereira et al. 2005).

Although the majority of red algal species express sulfated galactan with some heterogeneities, a minor number express homogeneous galactans, classically named as carrageenans and agarans. Carrageenans are traditionally classified by a Greek prefix according to the sulfation pattern and the presence of 3,6-anhydro bridge (carrageenose) on the 4-linked α-D-galactose (van de Velde et al. 2004) (Figure 3A). We will not discuss variations in the structures of this class of polysaccharide since this topic has been extensively covered in several other reviews (Usov 1998, Lahaye 2001, van de Velde et al. 2004).

The carrageenans and agarans are extensively exploited due to their industrial applications. The wide uses of these sulfated polysaccharides are based on their unique properties to form strong aqueous gels. These molecules are the major hydrocolloids used as texturing agents for food. A small change from α-D-galactopyranoses in carrageenans to α-L-galactopyranoses in agaran is enough to promote great changes in the physical-properties of these molecules (Lahaye 2001). Other modifications in the backbone of the sulfated galactans can greatly change their physicochemical properties and, consequently, in industrial applications and biological activities. For example, high levels of 3,6-anhydro-α-L-galactopyranosyl units in agar group polysaccharides (also known as agarose) and low sulfate contents are the major structural requirements for gelling (Lahaye 2001). Several types of these gels are widely exploited by industries in their attempt to obtain the best and specific gel formation under different conditions (regulated by temperature and the combination of ingredients) (Lahaye 2001).

Recently, sulfated galactans have also been characterized in green algal species, particularly those from the genus *Codium* (Matsubara et al. 2001; Bilan et al. 2007; Farias et al. 2008). In contrast to the repetitive disaccharides found in the sulfated galactans from red algae, the polysaccharides from green algae exhibit a backbone composed preponderantly of 4-sulfated, 3-linked β-D-galactopyranose units (Figure 3B). These green algal sulfated galactans can be highly pyruvilated at their non-reducing terminal residues, forming cyclic ketals such as 3,4-*O*-(1´carboxi)-ethylidene-β-D-Gal*p*-1 (Bilan et al. 2007; Farias et al. 2008). Although they are more complex than those from red alga, evidence

indicates the existence of a predominant structure and less structural variation as compared to those found in brown algal sulfated fucans (Figure 1).

Sulfated polysaccharides have not been described in vascular plants (angiosperm) until a recent report of a novel sulfated galactan isolated from the marine sea-grass, *Rupia maritima* (Angiospermae, Spermatophyta) (Aquino et al. 2005). The sea-grass is a group of vascular flowering plants, which grow in highly saline marine environments. The structure of the sea-grass sulfated D-galactan is composed of regular tetrasaccharide repeating units (Figure 3C). Like red algae, the marine angiosperm polysaccharide contains both α- and β-D-galactose residues; however, these units are not distributed in an alternating order as found in red algal sulfated galactans.

In the marine environment, the sulfated galactans were also described in some species of invertebrates. In ascidians (also known as sea squirts or tunicates) (Urochordata, Ascidiacea), these polysaccharides contain a central core composed of 3-sulfated, 4-linked α-L-galactopyranosyl units (Figure 3D). Heterogeneity and variation among different ascidian sulfated galactans species arise from the occurrence of non-sulfated L-galactose or D-glucose branches (Mourão and Perlin 1987; Pavão et al. 1989; Santos et al. 1992). The discovery of sulfated galactans in tunicates was the first report of the existence of a polysaccharide composed exclusively of L-galactose residues (Mourão and Perlin 1987). Curiously, some biology textbooks refer to ascidians as the only animal possessing cellulose (Barnes 1980). The sulfated L-galactans, which are poorly soluble in water when highly branched, could possibly have been mistaken for cellulose in these studies performed several decades ago. Recent studies described genes responsible for cellulose synthesis in ascidians (Nakashima et al 2004). A functional cellulose synthase was also reported in the invertebrate epidermis (Matthysse et al 2004). The enzyme catalyzes synthesis of 4-linked β-D-glucopyranose units. However, this enzyme may in fact be involved in the biosynthesis of sulfated α-L-galactans. The D-glucose is the best precursor of α-L-galactose units in ascidian polysaccharides (Mourão, 1991; Pavão et al 1994). Possibly, biosynthesis of the sulfated L-galactans involves incorporation of 4-linked β-D-glucopyranose followed by epimerization to α-L-galactopyranose units on the polysaccharide chain (Mourão and Assreuy 1995).

Sulfated galactans were also found in two species of sea urchins. One species (*Echinometra lucunter*) contains an egg jelly sulfated galactan composed of α-L-galactopyranosyl units, similar to those found in the ascidian polysaccharides. However, it is more homogeneous and clearly composed of linear chains of 2-sulfated, 3-linked repetitive units (Figure 3E) (Alves et al. 1997), instead of 3-sulfated and 4-linked residues. Another sea urchin species (*Glyptocidaris crenularis*) synthesizes a galactan composed of 3-linked galactopyranose units in the β-D-enantiomeric form, similar to those observed in galactans from green algae. However, this sea urchin polysaccharide is very homogeneous, composed of alternating 2-sulfated and non-sulfated galactopyranose residues (Figure 3E) (our unpublished data).

How has the 3-linked, β-galactose unit occurred in marine organisms throughout the course of evolution?

A comparison among sulfated galactans from different organisms indicates that polysaccharides with the glycosidic linkage β(1→3) are strongly conserved in some taxonomic groups of eukaryotes (rhodophytes, chlorophytes, angiosperms, echinoderms and mollusks). The sulfated galactans found among these phyla differ mainly in sulfation sites, with a strong tendency towards 4-sulfation in algae and marine angiosperms, and 2-sulfation in invertebrates. The 6-sulfation is dispersed in minor amounts throughout phylogeny. Similar distribution of sulfation pattern is not observed for the sulfated fucans. These observations provide grounds for speculation about the evolutionary history of sulfated polysaccharides.

The occurrence of the 3-β-D-Gal*p*-1 unit in the sulfated galactan from the sea-urchin *Glyptocidaris crenularis* and its presence in sulfated galactans from green algae (Bilan et al. 2007; Farias et al. 2008) and from sea-grass (Aquino et al. 2005) (Figure 3) stimulated us to review the distribution of this structure in animal and plant kingdoms (Whittaker 1969) in order to propose a phylogenetic relationship of this unit (Figure 4). Although this comparison is based only on structural components of the sulfated galactans, which are products of action of several genes and biosynthetic enzymes, this

taxonomic comparison might allow us to ask whether there is a relationship among the marine organisms that express sulfated 3-β-D-Gal*p*-1.

Thus, the hypothetical cladogram (Figure 4) shows that the sulfated 3-β-D-Gal*p*-1 units are preserved among species of specific phyla that inhabit the marine environment, including green algae, red seaweeds, marine sea-grass (Angiospermae, Spermatophyta), invertebrates (sea urchins, clams and tunicates) and vertebrates such as fishes that express keratan sulfate (Scudder et al. 1986).

Although the 3-β-D-Gal*p*-1 unit has been preserved in the major phyla during evolution (with the only exception being brown algae), the preferential sulfation site on this structure varies in a tendency toward 2-sulfation for animals, 4-sulfation for algae and marine angiosperms, and a dispersive distribution of 6-sulfation.

These observations raise the hypothesis that the galactosyltransferases responsible for the incorporation of 3-β-D-Gal*p*-1 units in the biosynthesis of sulfated galactans have been maintained during evolution in specific phyla of marine organisms, but was allowed to vary in the distribution of sulfotransferases types. In favor of this hypothesis is the evidence that the basic backbones are the same, but with a variable position of sulfation that differs from species to species and from tissue to tissue. To some extent, these results are analogous to the biosynthesis of the glycosaminoglycans from vertebrates, where the glycosidic chains vary relatively little among polymers constructed in different tissues, organs and species. Modifications on the glycosidic core occur mostly after chain elongation, when the principal modification is the sulfation at different sites. Unfortunately, the biosynthesis of the sulfated galactans from marine organisms is virtually unknown and therefore it is not yet possible to compare the expression of these molecules. The alternative, and just as likely hypothesis, is that the presence of these sulfated galactans in such distantly related organisms is an example of independent, convergent evolution of biosynthetic pathways. This hypothesis is not based on gene sequence, not even on the sequence of proteins, and requires future work to propose a firm theory.

Biological relevance of marine invertebrate sulfated fucans and galactans

In the case of the invertebrates, these sulfated polysaccharides are components of the extracellular matrix. For example, the ascidians contain high concentrations of sulfated

galactan as a component of the outer tunic, a protective layer enveloping the organism (Albano et al. 1990; Santos et al. 1992). Similarly, sulfated fucans from sea cucumbers also form part of the body wall (Mulloy et al. 1994; Ribeiro et al. 1994). In all of these cases, sulfated galactans or sulfated fucans occur in high concentrations in the extracellular matrix, which resemble the amount of glycosaminoglycans in proteoglycans found in the extracellular matrix of mammalian connective tissue (especially cartilage).

However, marine sulfated fucans and galactans have their own structural particularities. Firstly, they are more sulfated than vertebrate glycosaminoglycans such as chondroitin sulfate and dermatan sulfate, which contain one sulfate group per disaccharide unit. Perhaps, interactions between components of the extracellular matrix in marine organisms occur at higher salt concentrations than in vertebrates, and therefore require polysaccharides with higher charge density. Secondly, glycosaminoglycans from mammalian extracellular matrices have molecular masses only between ~15 and ~60 kDa. The covalent complex of these mammalian chains with the core protein results in a high molecular mass complex (>100 kDa). In contrast, sulfated galactans and sulfated fucans from algae and invertebrates are themselves high molecular weight molecules. The attachment to a protein core still needs to be demonstrated and it is apparently irrelevant for the biological activities of this class of polysaccharide. In sea urchin egg jellies, the sulfated fucans have masses >1 million Da.

In addition to the sulfated polysaccharides found in the extracellular matrices of algae, marine angiosperms, ascidians and sea cucumbers, sulfated polysaccharides from sea urchins are also localized in the hydrated, usually transparent, jelly layer surrounding the eggs. The sea urchin egg jelly sulfated polysaccharides form a complex extracellular matrix containing the sulfated fucan complexed with many unknown proteins of both high and low molecular mass (Vacquier and Moy 1997). As described below, the egg sulfated fucan is intimately involved in gamete recognition (Mulloy et al. 1994; Ribeiro et al. 1994; Alves et al. 1997, 1998; Vilela-Silva et al. 1999, 2002; Hirohashi et al. 2002; Biermann et al. 2004; Mourão 2007).

A necessary event for the sea urchin fertilization is the sperm acrosome reaction (AR). The sea urchin AR involves the calcium-triggered exocytosis of the acrosome vesicle and the pH-induced polymerization of actin to form the ~1 μm long, finger-like, acrosomal process which protrudes from the anterior of the sperm head (Vacquier and Hirohashi 2004). When sperm approach the sea urchin egg, the sulfated fucan binds to sperm

receptors which are homologs of human polycystin, the protein mutated in autosomal dominant polycystic kidney disease (Gunaratne et al. 2007). At least two pharmacologically distinct calcium channels open to allow calcium influx from the seawater (Darszon, Acevedo et al. 2006; Darszon, López-Martínez et al. 2006). The internal pH of the sperm also rises about 0.25 pH units due to sodium/proton exchange (de la Sancha et al. 2007). Both the calcium influx and pH rise are required for AR induction. The AR exposes the protein bindin which coats the acrosome process at the anterior tip of the sperm. The bindin attaches the sperm to the EBR1 receptor on the egg suface. Sperm bindin mediates both the species-specific attachment of sperm to egg and also the fusion of the plasma membranes of the two gametes (Vacquier et al. 1995; Cameron et al. 1996; Glaser et al. 1999; Kamei and Glabe 2003). The sequences of bindins are species-specific and have been shown to be subjected to positive selection (Zigler 2008)

The purified sulfated fucan of egg jelly, devoid of any detectable protein, will by itself induce the sperm AR (Vacquier and Moy 1997). Induction by the sulfated fucan is potentiated by a polysialic acid containing-"sialoglycan" also isolated from egg jelly (Hirohashi and Vacquier 2002a). Large molecular mass sulfated fucan is needed to open both sperm calcium channels and degradation of its mass to ~60-kDa will open one channel, but not the other (Hirohashi and Vacquier 2002b).

A preliminary study indicated that AR was induced by sulfated polysaccharides from the sea urchin egg jellies (Segall and Lennarz 1979). The well-defined chemical structures of the sea urchin egg jelly sulfated fucans, and the observation that each species possesses a polymer with a different structure, suggests that these sulfated polysaccharides are the egg molecules involved in the species-specific induction of the sperm AR (Alves et al. 1997; Vilela-Silva et al. 2002, 2008). Indeed, when they were tested with homo-specific and hetero-specific sperm from species that co-inhabit the same area in Rio de Janeiro (sympatric species) we observed that sulfated polysaccharides are species-specific inducers of the AR (Alves et al. 1997) (Figure 5). This observation was confirmed as the study was extended to other species of the genus *Strongylocentrotus* (Hirohashi et al. 2002). The monosaccharide composition (galactose or fucose), the position of the glycosidic linkage (3- or 4-linked), the pattern of sulfation (at 2- or 4-positions), and the number of fucose moeities per repeting unit are all crucial for inducing the sea urchin sperm AR (Biermann et al. 2004; Mourão 2007). Independent work by Koyota et al. (1997) on starfish corroborates these findings on an additional class of

echinoderms, the asteroids. They characterized an AR inducing substance (ARIS) isolated from a single species of starfish, *A. amurensis*. They showed that ARIS is a polysaccharide composed of 10-11 repetitive units of the pentasaccharide [→4)-β-D-Xyl*p*-(1→3)-α-D-Gal*p*-(1→3)-α-L-Fuc*p*-4(SO_4)-(1→3)-α-L-Fuc*p*-4(SO_4)-(1→4)-α-L-Fuc*p*-(1→]$_n$. (for more details about this biological event in starfish, see the review by Hoshi et al. 1994, and by Matsumoto et al. 2008).

One reason it is important to investigate the molecular details of AR induction by the egg jelly sulfated fucans is because it is very rare for a pure carbohydrate to induce a signal transduction event in animal cells. The demonstration that sulfated fucans induce the sperm AR in a species-specific manner led to additional experimentation with three related sympatric species of *Strongylocentrotus* (Figure 6). Egg jelly induces the AR species specifically in *S. droebachiensis* and *S. pallidus*. There are no other significant barriers to inter-specific fertilization between these two species. However, the AR in the species *S. purpuratus* reacts non-specifically with the egg jellies of these two other species. However, hetero-specific fertilization is still blocked because the bindin protein of *S. purpuratus* does not attach the sperm to the eggs of the other two species (Biermann et al. 2004) (Figure 6).

As shown in the accompanying structural figures, the species-specific recognition of sulfated fucan with the sperm must be based on: the glycosidic linkage, pattern of sulfation, and size of the repeating unit. Small structural changes modulate an entire system of sperm-egg recognition and species-specific fertilization in sea urchins (Vilela-Silva et al. 2008). Thus, in addition to their known function in cell proliferation, coagulation, inflammation, angiogenesis, and viral infection, sulfated polysaccharides also mediate invertebrate fertilization (Figure 7).

Could egg jelly sulfated fucans play a role in sea urchin speciation?

Generally speaking, almost all genes involved in sexual reproduction evolve rapidly and many show that positive selection is involved in their divergence (Swanson and Vacquier 2002). Figure 6 depicts the phylogenetic relation and species divergence times of sea urchins as well as a summary of the structures of their egg jelly polysaccharides (Biermann et al. 2004; Vilela-Silva et al. 2008). Two of the Strongylocentrotid species, *S. purpuratus* and *S. droebachiensis* are very closely related. However, the former synthesizes the egg jelly fucan with a 1 to 3 glycosidic linkage, whereas the latter

synthesizes a 1 to 4 linkage (Alves et al. 1997, 1998; Vilela-Silva et al. 2002). Females of both these species also make two distinct, female-specific, forms of these egg jelly polymers (Alves et al. 1998; Vilela-Silva et al. 2002). These observations suggest that the genes involved in the biosynthesis of these sulfated fucans may differentiate within a short evolutionary time. Thus, these genes have recently undergone a dramatic change during speciation in the *Strongylocentrotid* tree (Biermann et al. 2003; Lee 2003; Smith et al. 2006).

Cross-species fertilization can be prevented by one or more of the five steps those comprise the whole fertilization process: *i*) chemotaxis of the sperm to egg-released peptides (Kaupp et al. 2008), *ii*) induction of the sperm AR by the sulfated fucan, *iii*) binding of the acrosome process coated with bindin to the bindin receptor on the egg surface (Kamei and Glabe 2003), *iv*) penetration of the egg vitelline envelop, and *v*) fusion of the plasma membranes of the two gametes (Vacquier 1998). The synthesis of specific-specific structures of the sulfated fucans AR (Figure 7) could play a role in establishing the pre-zygotic reproductive isolation that gave rise to these species. Phylogeny suggests that *S. droebachiensis* and *S. pallidus* separated from *S. purpuratus* before their divergence from each other. The bindin mechanism may have functioned as an isolation mechanism in the earlier separation of these two sister species from *S. purpuratus*. A later speciation event led to the formation of *S. droebachiensis* and *S. pallidus*, possibly due to incompatibility of the sulfated fucans and AR induction (Figures 6 and 7).

Surprisingly, the egg jelly of *S. droebachiensis* contains a 1 to 4-linked sulfated fucan, which is clearly distinct from those of the two closely related congeneric species. However, *Arbacia lixula,* which diverged from *Strongylocentrotid* species about 200 million years ago, also has a 1 to 4-linked fucan (Figure 6). This similarity in glycosidic bond among fucosyl residues is most probably due to convergent evolution. The occurrence of the same sulfated fucan in these two very distantly related species is not relevant to their cross-fertilization, because the populations of *A. lixula* and *S. droebachiensis* do not overlap geographically. Nevertheless, this observation suggests that the gene for the biosynthesis of 4-linked fucan may have been retained during evolution of *S. droebachiensis*, but remained repressed or non-expressed until a period of strong natural selection. This observation reminds us of a general concept in evolution, which states that "the past of an organism not only determines its future, but also gives an enormous

reserve for a rapid modification, based on little genetic changes" (Gould 1984). Of course we cannot exclude that similar carbohydrate structure (as 4-linked sulfated fucans) may be synthesized by different genes.

The hypothesis that changes in the polysaccharide structure drive speciation of sea urchins, as a result of fertilization incompatibility, requires future investigation, especially at the genotype level, in order to propose a firm theory.

Anticoagulant and antithrombotic activities

Sulfated galactans and sulfated fucans exhibit potential pharmacological actions in mammalian-systems. These include antiviral (Harrop et al. 1992), antimetastatic (Coombe et al. 1987), antiangiogenic (Cumashi et al. 2007), antiinflammatory (Berteau and Mulloy 2003; Cumashi et al. 2007), antiadhesive (Berteau and Mulloy 2003; Cumashi et al. 2007), anticoagulant (Pereira et al. 1999, Farias et al. 2000, Pereira, Melo, Mourão 2002, Pereira, Vilela-Silva et al. 2002, Pereira et al. 2005, Mourão 2004; Cumashi et al. 2007) and antithrombotic (Berteau and Mulloy 2003; Mourão and Pereira 1999; Mourão 2004, Fonseca et al. 2008) activities. We will focus this review on the anticoagulant and antithrombotic activities of these sulfated polysaccharides due to the pressing need for new antithrombotic drugs as a consequence of the increasing incidence of thromboembolic diseases - cardiovascular diseases are the leading cause of death (30% of total) in the world.

Heparin preparations are widely used for the treatment and prevention of arterial and venous thrombosis (Fareed et al. 2000). However, this polysaccharide has several limitations due to collateral effects and limited source of material (Mourão 2004). The situation is even more complex recently because of the alarming notification that heparin preparations have been contaminated with oversulfated chondroitin sulfate (Guerrini et al. 2008). This contaminant induces hypotension associated with kallikrein release when administered by intravenous injection (Kishimoto et al. 2008).

Sulfated fucans from brown algae (Berteau and Mulloy 2003) and also sulfated galactans from red algae (Pereira et al. 2005), and green algae (Matsubara et al. 2001) have been known for some time to act as modulators of coagulation. Most of their activities are mediated by both antithrombin and heparin cofactor II, although there is a particular

case of a sulfated galactan from a specific green alga that exhibits a serpin-independent anticoagulant effect, possibly due to inhibition of fibrin polymerization (Matsubara et al. 2001). However, relatively few studies have interpreted the biological activity of sulfated fucans and sulfated galactans in terms of molecular structure.

The attempts to identify in the algal polysaccharide structural features necessary for their anticoagulant activity have been limited by the fact that algal sulfated fucans and sulfated galactans have complex, heterogeneous structures and their repeating sequences are not easily deduced. Only in the case of sulfated galactans isolated from two species of red algae has it been shown that the occurrence of 2,3-di-sulfated α-galactose units is a critical structural motif in promoting the interaction of the polysaccharide with the plasma protease and the serpins (Pereira et al. 2005). Obviously, identification of specific structural requirements in the algal polysaccharides necessary for interaction with coagulation cofactors is an essential step for more rational development anticoagulant drugs from these compounds.

Several authors attempted to overcome this difficulty using either chemical oversulfation (Soeda et al. 1993) or desulfation (Haroun-Bouhedja et al. 2000) of native algal polysaccharides. The activity increases with increasing sulfate content (Boisson-Vidal et al. 2000) and decreases when the native pattern of sulfation is disrupted by partial desulfation (Haroun-Bouhedja et al. 2000). In order to avoid the wide size dispersion observed for native, high-molecular-weight algal polysaccharides, several low-molecular-weight derivatives were prepared. The anticoagulant activity decreases with a decrease in the molecular size of the polysaccharide (Soeda et al. 1993). The main obstacle that continues to persist is that most of the low-molecular-weight derivatives still have complex and heterogeneous structures.

In contrast to most algal sulfated polysaccharides, the invertebrate carbohydrates constitute the most reasonable class of molecules to undergo structure-activity relationship studies. The regular and well-defined units in these compounds reveal clearly which type of sugar, glycosidic bonds and sulfate positions are responsible for the specific interaction with blood coagulation proteins that triggers the anticoagulant process (Mourão and Pereira 1999; Mourão 2004).

The results with the sulfated fucans and sulfated galactans from invertebrates reveal that the anticoagulant activity is not merely a consequence of their charge density and sulfate content. The structural requirement for interaction of these polysaccharides with coagulation cofactors and their target proteases are stereospecific (Pereira, Melo, Mourão 2002). First, the nature of the sugar residue (galactose or fucose) modifies markedly the anticoagulant activity as outlined by comparison between the active 2-sulfated, 3-linked α-L-galactan (Figure 3E) and the almost inactive 2-sulfated, 3-linked α-L-fucan (Figure 2H) (Pereira, Vilela-Silva et al. 2002). Second, the site of sulfation and/or position of the glycosidic linkage affect the activity, as indicated by comparison between the inactive 3-sulfated, 4-linked (Figure 3D) and the active 2-sulfated, 3-linked α-L-galactans (Figure 3E). Third, the occurrence of 2,4-di-sulfated units has an amplifying effect on the antithrombin-mediated anticoagulant activity of 3-linked α-L-fucans (Figure 1B). This is not merely a consequence of increased charge density. The anticoagulant activity increases ~38-fold from a 2-sulfated, 3-linked α-L-fucan (Figure 2H) to a 2,4-disulfated α-L-fucan (Figure 2E), even though their sulfate content increases only ~1.8-fold. Finally, specific sulfation sites are required for interaction with plasma serine-protease inhibitors. Notably, the occurrence of a single 4-sulfated unit in 3-linked α-L-fucan is the structural motif required to enhance inhibition of thrombin by heparin cofactor II, and the presence of exclusively 2-sulfated residues has a deleterious effect (Mourão 2004).

Prolongation of plasma coagulation time achieved by several sulfated polysaccharides is referred to as anticoagulant effect. However, the anticoagulant action of these compounds correlates only weakly with their antithrombotic properties (Björk and Lindahl 1982). Investigation of the antithrombotic activity requires the use of *in vivo* models of thrombosis in experimental animals, which is a laborious methodology. These models mimic different pathological conditions involved in thrombosis, such as decrease in blood flow, hypercoagulability state and lesion of the vascular endothelium.

Few studies report the antithrombotic activity of sulfated fucans and sulfated galactans. A low-molecular-weight fraction of algal sulfated fucan was shown to possess antithrombotic activity when tested on a venous thrombosis model in rabbits after intravenous (Mauray et al. 1995) or subcutaneous administration (Millet et al. 1999). Algal sulfated fucans were also tested on *in vivo* models of arterial surface damage. Intravenous

administration of the polysaccharide prevents formation of microvascular thrombus induced by endothelial damage in arterioles and venules of mice (Thorlacius et al. 2000). The protective effect was attributable to the anticoagulant activity of the algal fucan. Sulfated fucan inhibits adhesion of radioactive labeled platelet and neutrophils to the surface of coronary arteries of pigs injured by angioplasty (Chavet et al. 1999). After perfusion of iliac arteries of rabbits with fluoro-labeled sulfated fucans**,** the labeling is mainly localized on the sites of injury (Deux et al. 2002).

Test of algal sulfated galactans on animal models of venous thrombosis revealed that these polysaccharides have a serpin-dependent anticoagulant activity due to inactivation of thrombin and factor Xa. But, these polysaccharides have also a pro-coagulant effect due to activation of factor XII. This last effect depends on the sulfation pattern of the polysaccharide. As a consequence of their anti- and pro-coagulant actions the algal galactans differ in their venous antithrombotic activities. Slight differences in the proportions and/or distribution of sulfated residues along the galactan chain is critical for the interaction between proteases, inhibitors and activators of the coagulation system, resulting in a distinct pattern in anti- and pro-coagulant activities as well as in the antithrombotic action. It is noteworthy that the algal sulfated galactans have no hemorrhagic effect even when tested at high doses (Fonseca et al. 2008).

The availability of sulfated galactans and sulfated fucans with well-defined structures and the possibility to compare their effects in a variety of *in vivo* models of experimental thrombosis open new perspectives for the development of sulfated galactans and sulfated fucans as therapeutic agents.

Conclusions and perspectives

Sulfated fucans and sulfated galactans are widespread polysaccharides in marine organisms. These carbohydrates vary from species to species, but the major structural features tend to be conserved in each phylum. They have structural function as components of the extracellular matrix of algal and invertebrate tissues. They are also responsible for induction of the acrosome reaction in sea urchin sperm in a species-

specific manner. Through this function, sulfated polysaccharides could play a role in the speciation process which establishes prezygotic reproductive isolation. The algal and invertebrate polysaccharides can also be assayed as alternative anticoagulant agents and represent a potential source of compounds for antithrombotic therapies. Indeed, all these data reveal that the biological actions of sulfated fucans and sufated galactans do not simply depend on their negative charge density, but is also directly influenced by their structural features (sugar type, specific positions of sulfation and glycosidic linkage).

Further characterization of the action of these polysaccharides involves several challenges. A possible route to follow is the characterization of their binding to target proteins. With respect to their anticoagulant activities, the study of the interaction between polysaccharides with well-defined structures and purified proteins from the coagulation system is especially attractive. Computational modeling of the polysaccharide conformation using molecular dynamics may help to clarify these interactions. The action of sulfated polysaccharides as inducers of the sperm AR suggests the occurrence of plasma membrane receptor (Moy et al. 1996; Gunaratne et al. 2007). Experimental evidence suggests that suREJ1 is one receptor in the sea urchin sperm for the sulfated fucans from egg jelly coats (Vacquier and Moy 1997; Moy et al. 1996). Evidence for an egg receptor for sperm bindin has been shown for two species of sea urchin (Kamei and Glabe 2003). Certainly, studies of the specific interaction between the egg sulfated polysaccharide and the sperm receptor will define the regulation of sea urchin fertilization on a more refined molecular basis.

Preparation of oligosaccharides with well-defined chemical structures is always helpful for studies of carbohydrate-protein interaction. In this aspect we already described a procedure to obtain oligosaccharides from the sulfated fucans, which still retain the regular and repetitive structure (Pomin, Valente et al. 2005; Pomin, Pereira et al. 2005).

Possibly, the major challenge at this stage is the identification of the metabolic pathways involved in the biosynthesis of the invertebrate polysaccharides, especially those from sea urchins. This is not only a fascinating challenge in the carbohydrate field, but may also help to define the genetic basis for the sulfated polysaccharide mechanism of species recognition.

Funding

Conselho Nacional de Desenvolvimento Científico e Tecnológico (CNPq) and Fundação de Amparo à Pesquisa do Estado do Rio de Janeiro (FAPERJ).

Acknowledgements

We are grateful to Drs Xu Wang, Mauro Pavão and Victor D. Vacquier with the critical discussions and editing of the manuscript.

Conflict of interest statement

None declared.

References

Albano RM, Pavão MS, Mourão PA, Mulloy B. 1990. Structural studies of a sulfated L-galactan from Styela plicata (Tunicate): analysis of the Smith-degraded polysaccharide. Carbohydr Res. 208:163-174.

Alves A-P, Mulloy B, Diniz JA, Mourão PA. 1997. Sulfated polysaccharides from the egg jelly layer are species-specific inducers of acrosomal reaction in sperms of sea urchins. J Biol Chem. 272:6965-6971.

Alves A-P, Mulloy B, Moy GW, Vacquier VD, Mourão PA. 1998. Females of the sea urchin *Strongylocentrotus purpuratus* differ in the structures of their egg jelly sulfated fucans. Glycobiology. 8:939-946.

Amornrut C, Toida T, Imanari T, Woo E-R, Park H, Linhardt R, Wu SJ, Kim YS. 1999. A new sulfated beta-galactan from clams with anti-HIV activity. Carbohydr Res. 321:121-127.

Aquino RS, Landeira-Fernandez AM, Valente A-P, Andrade LR, Mourão PA.S. 2005. Occurrence of sulfated galactans in marine angiosperms: evolutionary implications. Glycobiology. 15:11-20.

Barnes, RD. 1980. *Invertebrate Zoology.* Philadelphia:WB Saunders Company.

Berteau O and Mulloy B. 2003. Sulfated fucans, fresh perspectives: structures, functions, and biological properties of sulfated fucans and an overview of enzymes active toward this class of polysaccharide. Glycobiology. 13:29R-40R.

Biermann CH, Marks JA, Vilela-Silva A-CES, Castro MO, Mourão PA. 2004. Carbohydrate-based species recognition in sea urchin fertilization: another avenue for speciation? Evolution & Development. 6:353–61.

Biermann CH, Kessing BD, Palumbi SR. 2003. Phylogeny and development of marine model species: strongylocentrotid sea urchins. Evol Dev. 5: 360-371.

Bilan MI, Grachev AA, Ustuzhanina NE, Shashkov AS, Nifantiev NE, Usov AI. 2002. Structure of a fucoidan from the brown seaweed *Fucus evanescens*. Carbohydr Res. 337:719-730.

Bilan MI, Vinogradova EV, Shashkov AS, Usov AI. 2007. Structure of a highly pyruvylated galactan sulfate from the Pacific green alga *Codium yezoense* (Bryopsidales, Chlorophyta). Carbohydr Res. 342:586-596.

Bixler HJ. 1994. The Carrageenan Connection IV. Brit Food J. 96(3):12-17.

Björk I, Lindahl U. 1982. Mechanism of the anticoagulant action of heparin. Mol Cell Biochem. 48: 161-182.

Black WAP. 1954. The seasonal variation in the combined L-fucose content of the common British laminariaceae and fucaceae. J Scien Food Agr. 5:445-448.

Boisson-Vidal C, Chaubet F, Chevolot L, Sinquin C, Theveniaux J, Millet J, et al. 2000. Relationship between antithrombotic activities of fucans and their structure. Drug Develop Res. 51:216-224.

Cameron RA, Walkup TS, Rood K, Moore JG, Davidson EH. 1996. Specific in vitro interaction between recombinant *Strongylocentrotus purpuratus* bindin and a recombinant 45A fragment of the putative bindin receptor. Dev Biol. 180:348-352.

Chavet P, Bienvenu JG, Theoret JF, Latour JG, Merhi Y. 1999. Inhibition of platelet-neutrophil interactions by fucoidan reduces adhesion and vasoconstriction after acute arterial injury by angioplasty in pigs. J Cardiovasc Pharm. 34:597-603.

Chevolot L, Foucault A, Kervarec N, Sinquin C, Fisher AM, Boisson-Vidal C. 1999. Further data on the structure of brown seaweed fucans: relationships with anticoagulant activity. Carbohydr Res. 319:154-165.

Chevolot L, Mulloy B, Ratiskol J, Foucault A, Colliec-Jouault S. 2001. A disaccharide repeat unit is the major structure in fucoidans from two species of brown algae. Carbohydr Res. 330:529-535.

Chizhov AO, Dell A, Morris HR, Haslam SM, McDowell RA, Shashkov AS. 1999. A study of fucoidan from the brown seaweed *Chorda filum*. Carbohydr Res. 320:108-119.

Coombe DR, Parish CR, Ramshaw IA, Snowden JM. 1987. Analysis of the inhibition of tumour metastasis by sulphated polysaccharides. Int J Cancer. 39:82-88.

Cumashi A, Ushakova NA, Preobrazhenskaya ME, D'Incecco A, Piccoli A, Totani L, Tinari N, Morozevich GE, Berman AE, Bilan MI, Usov AI, Ustyuzhanina NE, Grachev AA, Sanderson CJ, Kelly M, Rabinovich GA, Iacobelli S, Nifantiev NE, Consorzio Interuniversitario Nazionale per la Bio-Oncologia, Italy. 2007. A comparative study of the anti-inflammatory, anticoagulant, antiangiogenic, and antiadhesive activities of nine different fucoidans from brown seaweeds. Glycobiology. 17:541-552.

Darszon A, Acevedo JJ, Galindo BE, Hernández-González EO, Nishigaki T, Treviño CL, Wood C, Beltrán C. 2006. Sperm channel diversity and functional multiplicity. Reproduction. 161:977-988.

Darszon A, López-Martínez P, Acevedo JJ, Hernández-Cruz A, Treviño CL. 2006. T-type Ca2+ channels in sperm function.

de la Sancha CU, Martinez-Cadena G, López-Godínez J, Castellano LE, Nishigaki T, Darszon A, García-Soto J. 2007. Rho-kinase (ROCK) in sea urchin sperm: its role in regulating the intracellular pH during the acrosome reaction. Biochem Biophys Res Commun. 364:470-475.

Deux JF, Meddahi-Pelle A, Le Blanche AF, Feldman LJ, ColliecJouault S, Bree F, et al. 2002. Low molecular weight fucoidan prevents neointimal hyperplasia in rabbit iliac artery in stent restenosis model. Arterioscl Throm Vas Biol. 22:1604-1609.

Fareed JW, Hoppensteadt D, Bick RL. 2000. An update of heparins at the beginning of the new millennium. Sem Thromb Haemost. 26:5-21.

Farias WR, Valente A-P, Pereira MS, Mourão PA. 2000. Structure and anticoagulant activity of sulfated galactans. Isolation of a unique sulfated galactan from the red algae Botryocladia occidentalis and comparison of its anticoagulant action with that of sulfated galactans from invertebrates. J Biol Chem. 275:29299-29307.

Farias EH. Pomin VH, Valente A-P, Nader HB, Rocha HA, Mourão PA. 2008. A preponderantly 4-sulfated, 3-linked galactan from the green alga *Codium isthmocladum*. Glycobiology. 18:250-259.

Fonseca, RJC, Oliveira, S-NMCG, Melo FR, Pereira MG, Benevides NMB, Mourão PAS. 2008. Slight differences in sulfation of algal galactans account for differences in their anticoagulant and venous antithrombotic activities. Thromb Haemost. 99:539-545.

Gould, SJ. 1984. Hen´s teeth and house´s toes. Further reflections in natural history. Penguin, London

Glaser RW, Grüne M, Wandelt C, Ulrich AS. 1999. Structure analysis of a fusogenic peptide sequence from the sea urchin fertilization protein bindin. Biochemistry. 38:2560-2569.

Guerrini M,Beccati D, Shriver Z, Naggi A, Viswanathan K, Bisio A, Capila I, Lansing JC, Guglieri S, Fraser B, Al-Hakim A, Gunay NS, Zhang Z, Robinson L, Buhse L, Nasr M, Woodcock J, Langer R, Venkataraman G, Linhardt RJ, Casu B, Torri G & Sasisekharan R 2008. Oversulfated chondroitin sulfate is a contaminant in heparin associated with adverse clinical events. Nat Biotechnol. 10:1-7.

Gunaratne HJ, Moy GW, Kinukawa M, Miyata S, Mash SA, Vacquier VD. 2007. The 10 sea urchin receptor for egg jelly proteins (SpREJ) are members of the polycystic kidney disease-1 (PKD1) family. BMC Genomics. 8:235.

Haroun-Bouhedja F, Ellouali M, Sinquin C, Boisson-Vidal C. 2000. Relationship between sulfate groups and biological activities of fucans. Thromb Res. 100:453-459.

Harrop HA, Rider CC, Coombe DR. 1992. Sulphated polysaccharides exert anti-HIV activity at differing sites. Biochem Soc Trans. 20:163S.

Hirohashi N and Vacquier VD. 2002a. Egg sialoglycans increase intracellular pH and potentiate the acrosome reaction of the sea urchin sperm. J Biol Chem. 277:8041-8047.

Hirohashi N and Vacquier VD. 2002b. High molecular mass egg fucose sulfate polymer is required for opening both Ca2+ channels involved in triggering the sea urchin sperm acrosome reaction. J Biol Chem. 277:1182-1189.

Hirohashi N, Vilela-Silva A-CES, Mourão PA, Vacquier VD. 2002. Structural requirements for species-specific induction of the sperm acrosome reaction by sea urchin egg sulfated fucan. Biochem. Bioph. Res. Commun. 298:403-7.

Honya M, Morim M, Anzai M, Araki Y, Nisizawa K. 1999. Monthly changes in the content of fucans their constituent sugars and sulphate in cultured *Laminaria japonica*. Hydrobiologia. 398:411-416.

Hoshi M, Nishigaki T, Ushiyama A, Okinaga T, Chiba K, Matsumoto M. 1994. Egg-jelly signal molecules for triggering the acrosome reaction in starfish spermatozoa. Int J Dev Biol. 38:167-174.

Kamei N, Glabe CG. 2003. The species-specific egg receptor for sea urchin sperm adhesion is EBR1, a novel ADAMTS protein. Gene Dev. 17:2502-2507.

Kaupp UB, Kashikar ND, Weyand I. 2008. Mechanism of sperm chemotaxis. Annu Rev Physiol. 70:93-117.

Killing H. 1913. Zur biochemie der meersalgen. S Physiol Chem. 83:171-197.

Kishimoto TK, Viswanathan K, Ganguly T, Elankumaran S, Smith S, Pelzer K, Lansing JC, Sriranganathan N, Zhao G, Galcheva-Gargova Z, Al-Hakim A, Bailey GS, Fraser B, Roy S, Rogers-Cotrone T, Buhse L, Whary M, Fox J, Nasr M, Pan GJD, Shriver Z, Langer RS, Venkataraman G, Austen KF, Woodcock J, Sasisekharan R. 2008. New Engl J Med. 358:1-11.

Kloareg B. 1984. Isolation and analysis of cell walls of the brown marine algae *Pelvetia canaliculata* and *Ascophyllum nodosum*. Physiol Vég. 22:47-56.

Knutsen SH, Myslabodski DE, Larsen B, Usov AI. 1994. A modified system of nomenclature for red algal galactans. Bot Mar. 37(2):163-169.

Koyota S, Swarna Wimalasiri KM, Hoshi M. 1997. Structure of the main saccharide chain in the acrosome reaction-inducing substance of the starfish, *Asterias amurensis*. J Biol Chem. 272:10372-10376.

Lahaye M. 2001. Developments on gelling algal galactans, their structure and physico-chemistry. J Appl Phycol. 13:173–184.

Lee YH. 2003. Molecular phylogenies and divergence times of sea urchin species of Strongylocentrotidae, Echinoida. Mol Biol Evol. 20:1211-1221.

Leite EL, Medeiros MGL, Rocha HAD, Farias GGM, da Silva LF, Chavante SF, de Abreu LD. 1998. Structure and pharmacological activities of a sulfated xylofucoglucuronan from the red alga *Spatoglossum shroederi*. Plant Science 132:215-28.

Mabeau S, Kloareg B, Joseleau JP. 1990. Fractionation and analysis of fucans from brown algae. Phytochemistry. 29:2441-2445.

Martinez-Rumayor A, Januzzi JLJr. 2006. Non-ST segment elevation acute coronary syndromes: A comprehensive review. South Med J. 99:1103-1110.

Matsubara K, Matsuura Y, Bacic A, Liao M, Hori K, Miyazawa K. 2001. Anticoagulant properties of a sulfated galactan preparation from a marine green alga, *Codium cylindricum*. Int J Biol Macromol. 28:395-399.

Matsumoto M, Kawase O, Islam S, Naruse M, Watanabe S-n, Ishikawa R, Hoshi M. 2008. Int J Dev Biol. 52:523-526.

Matthysse AG, Deschet K, Williams M, Marry M, White AR, Smith WC. 2004. A functional cellulose synthase from ascidian epidermis. PNAS. 101:986-991.

Mauray S, Sternberg C, Theveniaux J, Millet J, Sinquin C, Tapon-Bretaudière C et al. 1995. Venous antithrombotic and anticoagulant activities of a fucoidan fraction. Thromb Haemost. 74:1280-1285.

Metz EC, Kane RE, Yanagimachi H, Palumbi SR. 1994. Fertilization between closely related sea urchins is blocked by incompatibilities during sperm-egg attachment and early stages of fusion. Biol Bull. 187:23-34.

Mian AJ and Percival E. 1973. Carbohydrate of the brown seaweeds *Himanthalia lorea*, *Bifurcaria bifurcata* and *Padina pavonia*. Carbohydr Res. 26:133-146.

Millet J, Jouault SC, Mauray S, Theveniaux J, Sternberg C, Boisson-Vidal C. 1999. Antithrombotic and anticoagulant activities of a low molecular weight fucoidan by the subcutaneous route. Thromb Haemost. 81:391-395.

Mourão PA and Assreuy AM. 1995. Trehalose as a possible precursor of the sulfated L-galactan in the ascidian tunic. J Biol Chem. 270:3132-3140.

Mourão PA and Perlin AS. 1987. Structural features of sulfated glycans from the tunic of Styela plicata Chordata-Tunicata: a unique occurrence of L-galactose in sulfated polysaccharides. Eur J Biochem. 166:431-436.

Mourão PA and Pereira MS. 1999. Searching for alternatives to heparin: sulfated fucans from marine invertebrates. Trends Cardiovasc Med. 9:225-232.

Mourão PA. 1991. Epimerization of D-glucose to L-galactose durig the biosynthesis of a sulfated L-galactan in the ascidian tunic. Biochemistry. 30:3458-3464.

Mourão PA. 2004. Use os sulfated fucans as anticoagulant and atithrombotic agents: future perspectives. Curr Pharm Design. 10:967-981.

Mourão PA. 2007. A carbohydrate-based mechanism of species recognition in sea urchin fertilization. Braz. J. Med. Biol. Res. 40:5-17.

Moy GW, Mendonza LM, Schulz JR, Swanson WJ, Glabe CG, Vacqueir VD. 1996. The sea urchin sperm receptor for egg jelly is a molecular protein with extensive homology to the human polycystic kidney disease protein, PKD1. J Cell Biol. 133:809-817.

Mulloy B, Ribeiro A-C, Alves AP, Vieira RP, Mourão PA. 1994. Sulfated fucans from echinoderms have a regular tetrasaccharide repeating unit defined by specific patterns of sulfation at the 0-2 and 0-4 positions. J Biol Chem. 269:22113-22123.

Murano E, Toffanin R, Cecere E, Rizzo R, Knutsen SH. 1997. Investigation of the carrageenans extracted from *Solieria filiformis* and *Agardhiella subulata* from Mar Piccolo, Taranto. Mar Chem. 58:319-325.

Nakashima K, Yamada L, Satou Y, Azuma J-I, Satoh N. 2004. The evolutionary origin of animal cellulose synthase. Dev Genes Evol. 214:81-88.

Nishino T and Nagumo T. 1991. Structural characterization of a new anticoagulant fucan sulfate from the brown seaweed *Ecklonia kurome*. Carbohydr Res. 211:77-90.

Nishino T, Ura H, Nagumo T. 1995. The relationship between the sulfate content and the antithrombin activity of an α1→2-fucoidan purified from a commercial fucoidan fraction. Botanica Marina 38:187-193.

Patankar MS, Oehninger S, Barnett T, Williams RL, Clark GF. 1993. A revised structure for fucoidan may explain some of its biological activities. J Biol Chem. 268:21770-21776.

Pavão MSG, Albano RM, Lawsom AM, Mourão PA. 1989. Structural heterogeneity among unique sulfated L-galactans from different species of ascidians (tunicates). J Biol Chem. 264:9972-9979.

Pavão MSG, Rodrigues MA, Mourão PA. 1994. Acidic polysaccharides of the ascidian *Styela plicata*. Biosynthetic studies on the sulfated L-galactans of the tunic, and preliminary characterization of a dermatan sulfate-like polymer in body tissues. Biochim Biophys Acta. 1199:29-237.

Pavão MSG, Mourão PA, Mulloy B. 1990. Structure of a unique sulfated alpha-L-galactofucan from the tunicate Clavelina. Carbohydr Res. 208:153-161.

Percival E and Ross AG. 1950. The isolation and purification of fucoidin from brown seaweeds. J Chem Soc. 717-720.

Pereira MS, Mulloy B, Mourão PA. 1999. Structure and anticoagulant activity of sulfated fucans: comparison between the regular repetitive and linear fucans from

echinoderms with the more heterogeneous and branched polymers from brown algae. J Biol Chem. 274:7656-7667.

Pereira MS, Melo FR, Mourão PA. 2002. Is there a correlation between structure and anticoagulant action of sulfated galactans and sulfated fucans? Glycobiology. 12:573-580.

Pereira MS, Vilela-Silva A-CES, Valente A-P, Mourão PA. 2002. A 2-sulfated, 3-linked alpha-L-galactan is an anticoagulant polysaccharide. Carbohydr Res. 337:2231-2238.

Pereira MG, Benevides NM, Melo MR, Valente AP, Melo FR, Mourão PA. 2005. Structure and anticoagulant activity of a sulfated galactan from the red alga, *Gelidium crinale*. Is there a specific structural requirement for the anticoagulant action? Carbohydr Res. 340:2015-2023.

Pomin VH, Pereira MS, Valente A-P, Tollefsen DM, Pavão MS, Mourão PA. 2005. Selective cleavage and anticoagulant activity of a sulfated fucan: stereospecific removal of a 2-sulfate ester from the polysaccharide by mild acid hydrolysis, preparation of oligosaccharides, and heparin cofactor II-dependent anticoagulant activity. Glycobiology. 15:369-381.

Pomin VH, Valente A-P, Pereira MS, Mourão PA. 2005. Mild acid hydrolysis of sulfated fucans: a selective 2-desulfation reaction and an alternative approach for preparing tailored sulfated oligosaccharides. Glycobiology. 15:1376-1385.

Ribeiro AC, Vieira RP, Mourão PA, Mulloy B. 1994. A sulfated alpha-L-fucan from sea cucumber. Carbohydr Res. 255:225-240.

Santos JA, Mulloy B, Mourão PA. 1992. Structural diversity among sulfated alpha-L-galactans from ascidians (tunicates). Studies on the species *Ciona intestinalis* and *Herdmania monus*. Eur J Biochem. 204:669-677.

Scudder P, Tanq PW, Hounsell EF, Lawson AM, Mehmet H, Feizi T. 1986. Isolation and characterization of sulphated oligosaccharides released from bovine corneal keratin sulphate by the action of endo-beta-galactosidase. Eur J Biochem. 157:365-373.

Segall GK, Lennarz WJ. 1979. Chemical characterization of the component of the jelly coat from sea urchin eggs responsible for induction of the acrosome reaction. Dev Biol. 71:33-48.

Smith AB, Pisani D, Mackenzie-Dodds JÁ, Stockley B, Webster BL, Littlewood DT. 2006. Testing the molecular clock: molecular and paleontological estimates of divergence times in the Echinoidea (Echinodermata). Mol Biol Evol. 23:1832-1851.

Soeda S, Ohmagari Y, Shimeno H, Nagamatsu A. 1993. Preparation of oversulfated fucoidan fragments and evaluation of their antithrombotic activities. Thromb Res. 72:247-256.

Swanson WJ and Vacquier VD. 2002. The rapid evolution of reproductive proteins. Nat Rev Genet. 3:137-1344.

Thorlacius H, Vollmar B, Seyfert UT, Vestweber D, Menger MD. 2000. The polysaccharide fucoidan inhibits microvascular thrombus formation independently from P- and L-selectin function in vivo. Eur J Clin Invest. 30:804-810.

Usov AI. 1998. Structural analysis of red seaweed galactans of agar and carrageenan groups. Food Hydrocolloids. 12:301–308.

van de Velde F, Pereira L, Rollema HS. 2004. The revised NMR chemical shift data of carrageenans. Carbohydr Res. 339:2309–2313.

Vacquier VD. 1998. Evolution of gamete recognition proteins. Science. 281:1995-1998.

Vacquier VD, Hirohashi N. 2004. Sea urchin spermatozoa. Methods Cell Biol. 74:523-544.

Vacquier VD, Moy GW. 1997. The fucose sulfate polymer of egg jelly binds to sperm REJ and is the inducer of the sea urchin sperm acrosome reaction. Dev Biol. 192:125-135.

Vacquier VD, Swanson WJ, Hellberg ME. 1995. What have we learned about sea urchin sperm bindin? Dev Growth Differ. 37:1-10.

Vasseur E. 1948. Chemical studies on the jelly coat of the sea-urchin egg. Acta Chem Acand. 2:900-913.

Vilela-Silva A-CES, Alves AP, Valente A-P, Vacquier VD, Mourão PA. 1999. Structure of the sulfated α-L-fucan from the egg jelly coat of the sea urchin *Strongylocentrotus franciscanus*: patterns of preferential 2-O- and 4-O-sulfation determine sperm cell recognition. Glycobiology. 9:927-233.

Vilela-Silva A-CES, Castro MO, Valente A-P, Biermann CH, Mourão PA. 2002. Sulfated fucans from the egg jellies of the closely related sea urchins *Strongylocentrotus droebachiensis* and *Strongylocentrotus pallidus* ensure species-specific fertilization. J Biol Chem. 277:379-387.

Vilela-Silva A-CES, Hirohashi M. Mourão PAS. 2008. The structure of sulfated polysaccharides ensures a carbohydrate-based mechanism for species recognition during sea urchin fertilization. Int J Dev Biol. 52:551-559.

Von Holdt MM, Ligthelm SP, Nunn JR. 1955. South African seaweeds: seasonal variations in the chemical composition of some phaeophyceae. J Sci Food Agr. 6:193-197.

Whittaker RH. 1969. New concepts of kingdoms of organisms. Science. 163:150-160.

Wort DJ. 1955. The seasonal variation in chemical composition of *Macrocystis integrifolia* and *Neroecystis luetkeana* in British Colombia coastal waters. Can J Bot. 33:323-340.

Yoon SJ, Pyun YR, Hwang JK, Mourão PA. 2007. A sulfated fucan from the brown alga Laminaria cichorioides has mainly heparin cofactor II-dependent anticoagulant activity. Carbohydr Res. 342:2326-2330.

Zigler KS. 2008. The evolution of sea urchin sperm bindin. Int J Dev Biol. 52:791-796.

Legends to figures

Fig. 1. Structures for the most dominant components of sulfated fucans from brown algae proposed during the years. These polysaccharides have very complex and heterogeneous structures and it is often not easy to determine any regular structure, even if they are present. (**A**) The 4-sulfated, 2-linked α-L-fucopyranoses was the first proposition by Percival and Ross (1950) as the major units of the fucoidan (name adopted at this time) from the common alga *Fucus vesiculosus*. In contradiction, after 43 years, Patankar et al (1993) proposed for this same species a more complex structure (**B**) composed of branched pentasaccharide repetitive units of 3-linked α-L-fucopyranose. The currently proposed structure for the sulfated fucan from this species (**C**), and also for *Ascophyllum. nodosum* and *Fucus evanescences* (Chevolot et al. 1999, 2001; Bilan et al. 2002) is a polysaccharide preponderantly composed of 2- and/or 3-sulfated α-L-fucopyranosyl units with alternating 3-and 4-linkages with also occurrence of non-sulfated and branched units. (**D**) The sulfated fucan from *Ecklomia kurome* is a polymer of mostly 4-sulfated, 3-linked α-L-fucopyranosyl units (Nishino and Nagumo 1991). (**E**) The sulfated fucan from *Chorda filum* contains a quasi-regular structure of a repeating branched hexasaccharide unit but, with a variable 2- and 4-sulfation (Chizhov et al. 1999). The irregularities of the sulfated polysaccharides from *E. kurome* and *C. filum* (**D** and **E**) arise from the presence of non-sulfate and/or acetylated α-L-fucopyranosyl residues.

Fig. 2. Structures of the repeating units of the sulfated α-L-fucans from the cell wall of the sea cucumber (**A**) *Ludwigothurea grisea* (Mulloy et al. 1994) and from the egg jelly coat of sea urchins: (**B**) *Lytechinus variegatus* (Mulloy et al. 1994), (**C**) *Strongylocentrotus pallidus* (Vilela-Silva et al. 2002), (**D**) *Arbacia lixula* (Alves et al. 1997), (**E**) *Strongylocentrotus purpuratus* isotype I and (**F**) isotype II (Alves et al. 1998), (**G**) *Strongylocentrotus droebachiensis* (Vilela-Silva et al. 2002) and (**H**) *Strongylocentrotus franciscanus* (Vilela-Silva et al. 1999). The species-specific structures vary in sulfation patterns (but, restricted at 2- and/or 4-positions), in glycosidic linkages: α(1→3) (**A**-**C**, **E,F** and **H**) and α(1→4) (**D** and **G**), and in number of residues of the repetitive units: tetrasaccharides (**A**-**D**), trisaccharide (**F**) and monosaccharides (**E,G** and **G**) however, they are all unbranched, linear polymers.

Fig. 3. Structures of the sulfated galactans from (**A**) red algae (Usov 1998, Lahaye 2001, Farias et al. 2000, Pereira et al. 2005), (**B**) green algae (Matsubara et al. 2001; Bilan et al. 2007; Farias et al. 2008), (**C**) sea grass (marine angiosperm) (Aquino et al. 2005), and marine invertebrates, such as (**D**) ascidians (also known as tunicates) (Mourão and Perlin 1987; Pavão et al. 1989, 1990; Santos et al. 1992; Albano et al. 1990) and (**E**) sea urchins (Alves et al. 1997).

Fig. 4. Schematic phylogenetic tree showing the proposed relationship among sulfated polysaccharides from marine organisms of different phyla. The structure 3-β-D-Gal*p*-1 is identified by dark gray boxes. The 2-, 4- and 6-sulfations are indicated with light gray stripped, solid and dotted ellipses, respectively. Brown algae (Phaeophyta) exhibit polymers of α-L-fucose bound by (1→3) and (1→4) glycosidic linkages, and with different patterns of sulfation (Pereira et al. 1999; Berteau and Mulloy 2003). Red algae (Rhodophyta) exhibit sulfated galactans composed mainly of the sequence [3-β-D-Gal*p*-1→4-α-D-Gal*p*-1]$_n$ (Farias et al. 2000; Pereira et al. 2005). Most of them are composed of 4-α-D-3,6-AnGal*p*-1 (3,6-anidrogalactose residues) and 3-β-D-Gal*p*-4(SO_4)-1, as found in carrageenans, the most common sulfated polysaccharides from red algae (Murano et al. 1997). The preponderant residue of the sulfated galactans from green algae (Clorophyta) is 3-β-D-Gal*p*-4(SO_4)-1 (Bilan et al. 2007; Farias et al. 2008). The marine angiosperms (Angiospermae, Spermatophyta) exhibit the repeating sequence: [3-β-D-Gal*p*-4(SO_4)-1→3-β-D-Gal*p*-4(SO_4)-1→4-α-D-Gal*p*-1→4-α-D-Gal*p*-1]$_n$, comprising structural features of algal and invertebrate sulfated polysaccharides (Aquino et al. 2005). In invertebrates, the sulfated polysaccharides from two species of sea urchins (Equinodermata, Echinoidea) *E. lucunter* (Alves et al. 1997) and *Glyptocidaris crenularis* (data not published) exhibit repeating sequences of [3-α-L-Gal*p*-2(SO_4)-1]$_n$ and [3-β-D-Gal*p*-2(SO_4)-1→3-β-D-Gal*p*-1→]$_n$, respectively. The clam *Meretrix petechialis* (Mollusca, Bivalvia) has a polysaccharide composed of the backbone 3-β-D-Gal*p*-1, mainly 2-sulfated and to some extent 6-sulfated (Amornrut et al. 1999). Some species of ascidians (Urochordata, Ascidiacea) *H.* monus, *S.* plicata and Ascidia *nigra*, *Clavelina oblonga* (Santos et al. 1992; Albano et al. 1990; Pavão et al. 1989, 1990; respectively) exhibit the unit [4-α-L-Gal*p*-3(OSO_4)-1]$_n$. The glycosaminoglycan keratan sulfate can be found in minor amounts as [3-β-D-Gal*p*-

$6(OSO_4)$-1$\rightarrow$4-β-D-GalNAc-$6(OSO_4)$-1]$_n$ (Scudder et al. 1986) such as fishes (Teleostei, Chordata).

Fig. 5. Structures of sulfated polysaccharides from three sea urchin egg jelly that co-habit the harbor at Rio de Janeiro, Brazil, and their respective activities as inducers of the acrosome reaction in homologous or heterologous sperm. The species *A. lixula* and *L. variegatus* express sulfated fucans while *E. lucunter* expresses sulfated galactan. Data modified from Alves et al. (1997).

Fig. 6. Phylogenetic relationship and divergence times of sea urchin species and a summary of the structure of the polysaccharides from their egg jelly. Data modified from Biermann *et al.* 2004. The sulfated polysaccharide-mediated mechanism of egg-sperm recognition may have played an important role in the separation of *S. droebachiensis* from *S. pallidus*. The bindin mechanism may have functioned as an isolation mechanism on the earlier separation of the joint lineage from *S. purpuratus* (that exhibit two different isotypes I and II, see also Figure 2E and F). Myr = million years of evolutionary divergence (Biermann et al. 2004; Mourão 2007). Experiments show that in *Echinometra*, the sperm bindin bound to the egg is more important than AR induction (Metz et al. 1994), indicating a preponderance of the bindin mechanism of species recognition.

Fig. 7. Schematic representation of the two hierarchical steps in sea urchin gamete recognition. (**A**) Sulfated polysaccharide-based species recognition: the sperm acrosome reaction is induced when a sperm with the correct receptor type contacts specific sulfated polysaccharide in the egg jelly coat (red triangles). This reaction exposes the protein bindin (shown in blue). (**B**) The bindin paradigm: the protein bindin, coating the outside of the acrosomal process reacts with a matching egg membrane receptor. Data from Biermann et al. (2004).

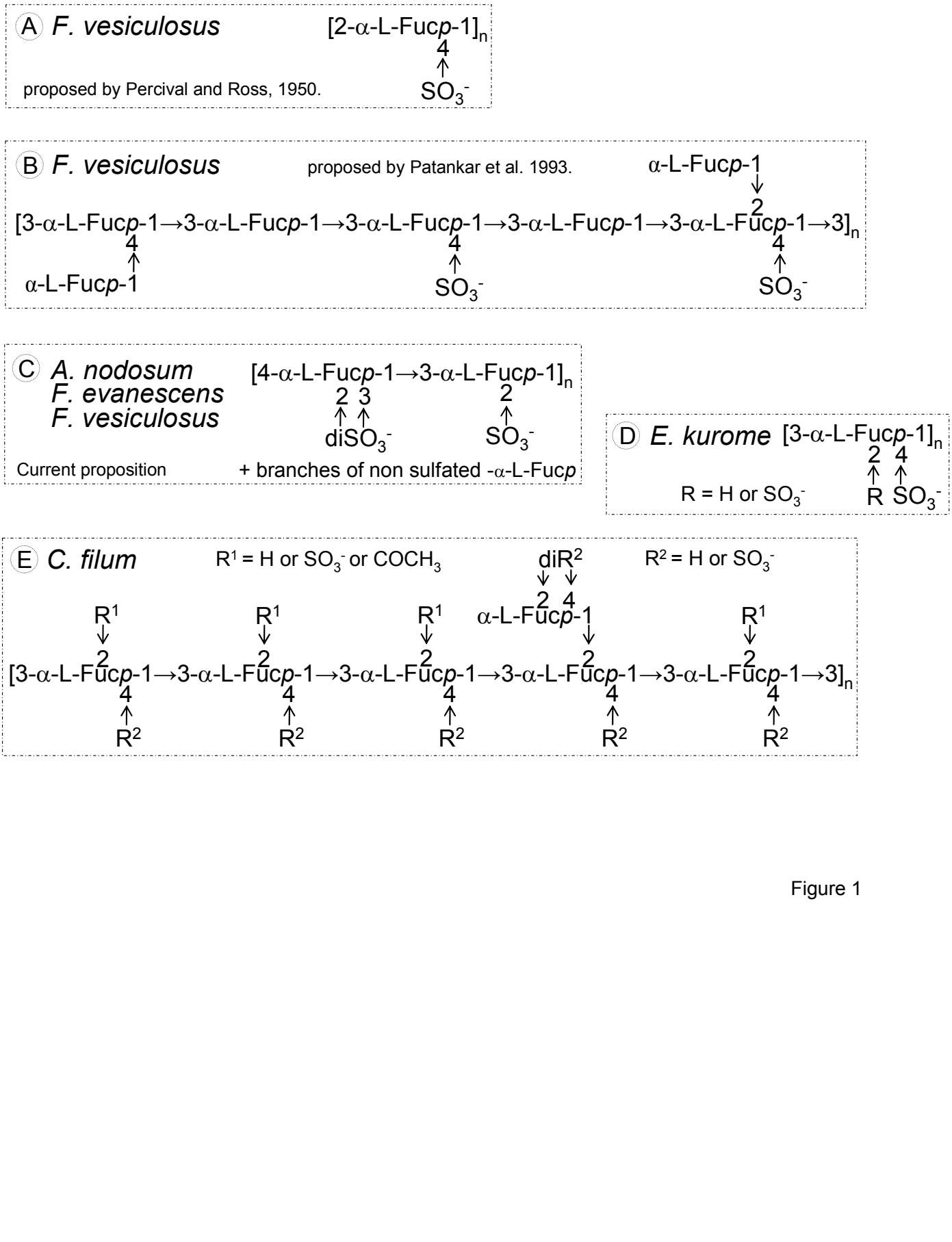
A F. vesiculosus
[2-α-L-Fucp-1]n
4
SO3-
proposed by Percival and Ross, 1950.
B F. vesiculosus
proposed by Patankar et al. 1993.
α-L-Fucp-1
2
[3-α-L-Fucp-1→3-α-L-Fucp-1→3-α-L-Fucp-1→3-α-L-Fucp-1→3-α-L-Fucp-1→3]n
4
α-L-Fucp-1
SO3-
SO3-
C A. nodosum
F. evanescens
F. vesiculosus
[4-α-L-Fucp-1→3-α-L-Fucp-1]n
2 3
2
diSO3-
SO3-
Current proposition
+ branches of non sulfated -α-L-Fucp
D E. kurome
[3-α-L-Fucp-1]n
2 4
R = H or SO3-
R SO3-
E C. filum
R1 = H or SO3- or COCH3
diR2
R2 = H or SO3-
2 4
R1
α-L-Fucp-1
[3-α-L-Fucp-1→3-α-L-Fucp-1→3-α-L-Fucp-1→3-α-L-Fucp-1→3-α-L-Fucp-1→3]n
4
R2

Figure 1

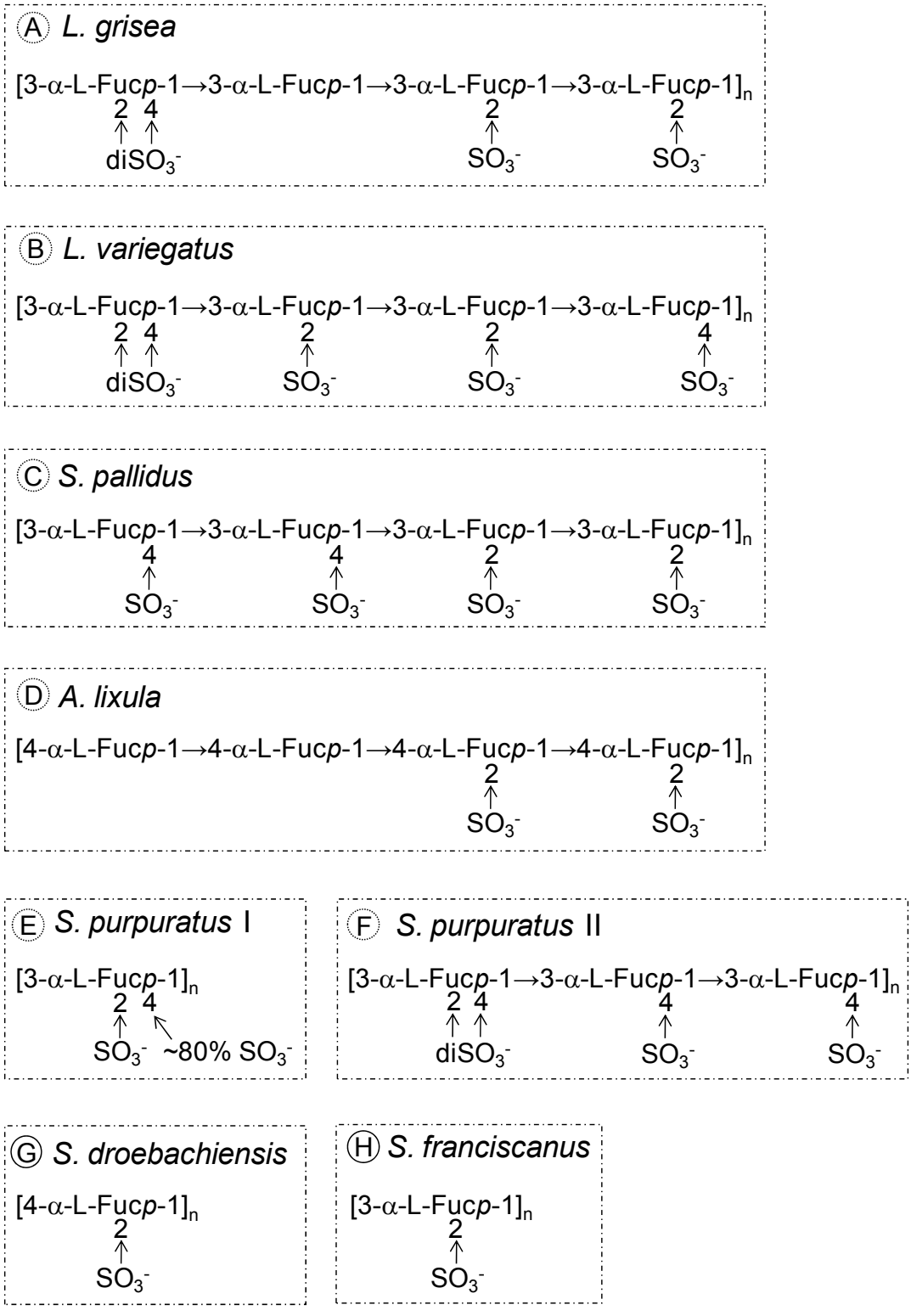
A L. grisea
[3-α-L-Fucp-1→3-α-L-Fucp-1→3-α-L-Fucp-1→3-α-L-Fucp-1]n
2 4
diSO3-
2
SO3-
2
SO3-
B L. variegatus
[3-α-L-Fucp-1→3-α-L-Fucp-1→3-α-L-Fucp-1→3-α-L-Fucp-1]n
2 4
diSO3-
2
SO3-
2
SO3-
4
SO3-
C S. pallidus
[3-α-L-Fucp-1→3-α-L-Fucp-1→3-α-L-Fucp-1→3-α-L-Fucp-1]n
4
SO3-
4
SO3-
2
SO3-
2
SO3-
D A. lixula
[4-α-L-Fucp-1→4-α-L-Fucp-1→4-α-L-Fucp-1→4-α-L-Fucp-1]n
2
SO3-
2
SO3-
E S. purpuratus I
[3-α-L-Fucp-1]n
2 4
SO3-
~80% SO3-
F S. purpuratus II
[3-α-L-Fucp-1→3-α-L-Fucp-1→3-α-L-Fucp-1]n
2 4
diSO3-
4
SO3-
4
SO3-
G S. droebachiensis
[4-α-L-Fucp-1]n
2
SO3-
H S. franciscanus
[3-α-L-Fucp-1]n
2
SO3-

Figure 2

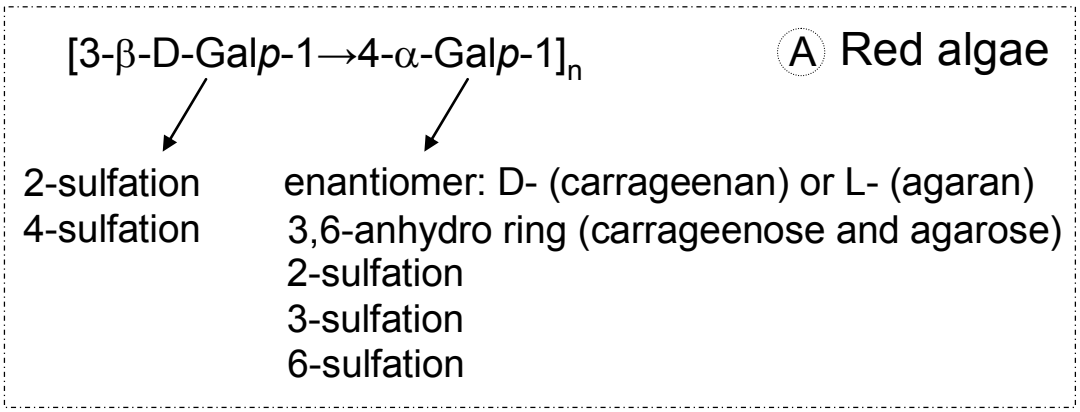
[3-β-D-Gal*p*-1→4-α-Gal*p*-1]n
A Red algae
2-sulfation
4-sulfation
enantiomer: D- (carrageenan) or L- (agaran)
3,6-anhydro ring (carrageenose and agarose)
2-sulfation
3-sulfation
6-sulfation

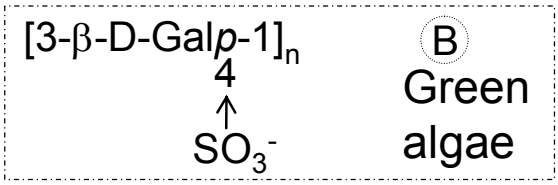
[3-β-D-Gal*p*-1]n
4
SO3-
B
Green
algae

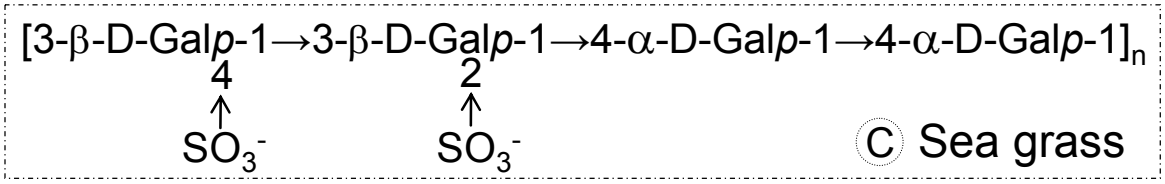
[3-β-D-Gal*p*-1→3-β-D-Gal*p*-1→4-α-D-Gal*p*-1→4-α-D-Gal*p*-1]n
4
SO3-
2
SO3-
C Sea grass

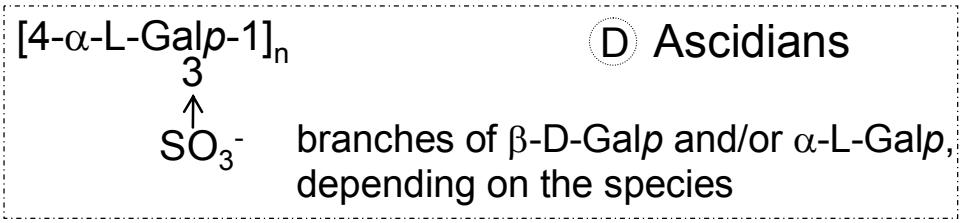
[4-α-L-Gal*p*-1]n
3
SO3-
D Ascidians
branches of β-D-Gal*p* and/or α-L-Gal*p*,
depending on the species

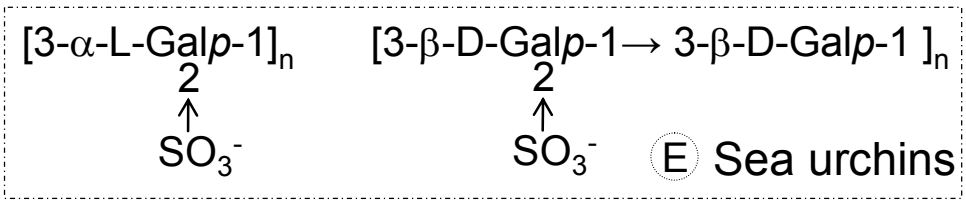
[3-α-L-Gal*p*-1]n
2
SO3-
[3-β-D-Gal*p*-1→ 3-β-D-Gal*p*-1]n
2
SO3-
E Sea urchins

Figure 3

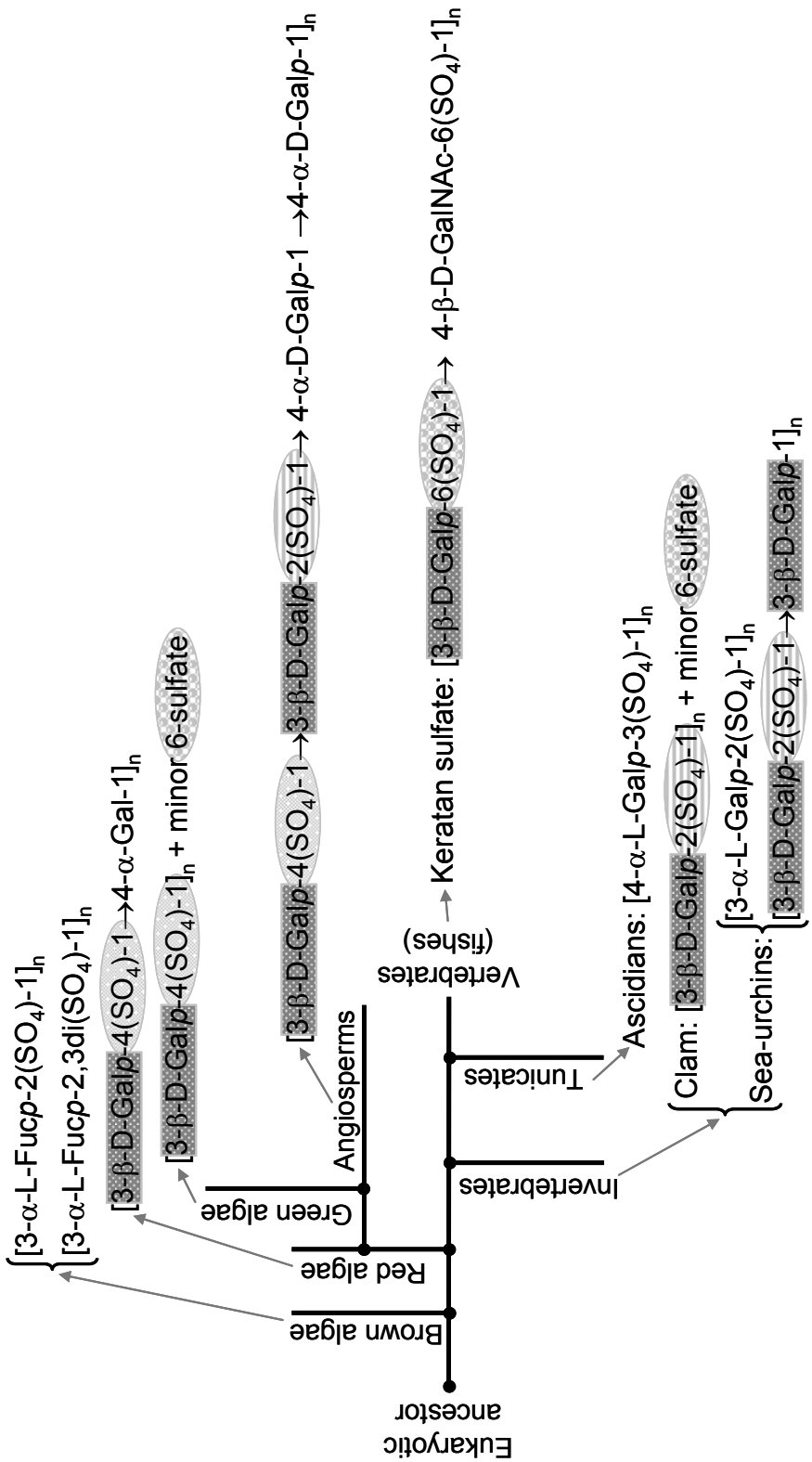
Eukaryotic ancestor
Brown algae
Red algae
Green algae
Angiosperms
Invertebrates
Tunicates
Vertebrates (fishes)
[3-α-L-Fucp-2(SO4)-1]n
[3-α-L-Fucp-2,3di(SO4)-1]n
[3-β-D-Galp-4(SO4)-1→4-α-Gal-1]n
[3-β-D-Galp-4(SO4)-1]n + minor 6-sulfate
[3-β-D-Galp-4(SO4)-1→3-β-D-Galp-2(SO4)-1→ 4-α-D-Galp-1 →4-α-D-Galp-1]n
Keratan sulfate: [3-β-D-Galp-6(SO4)-1→ 4-β-D-GalNAc-6(SO4)-1]n
Ascidians: [4-α-L-Galp-3(SO4)-1]n
Clam: [3-β-D-Galp-2(SO4)-1]n + minor 6-sulfate
Sea-urchins: [3-α-L-Galp-2(SO4)-1]n
[3-β-D-Galp-2(SO4)-1→3-β-D-Galp-1]n

Figure 4

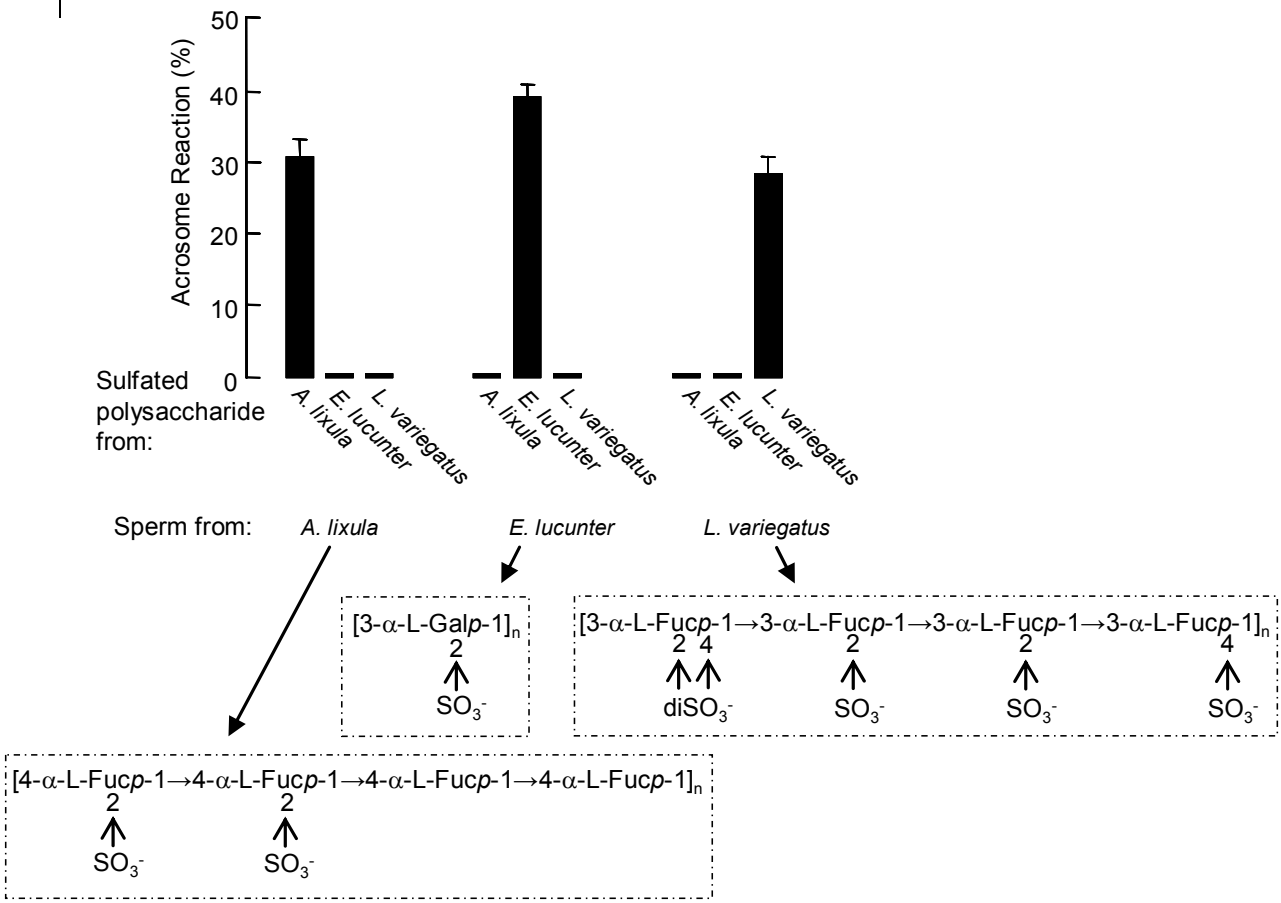
Acrosome Reaction (%)
50
40
30
20
10
0
Sulfated polysaccharide from:
A. lixula
E. lucunter
L. variegatus
A. lixula
E. lucunter
L. variegatus
A. lixula
E. lucunter
L. variegatus
Sperm from:
A. lixula
E. lucunter
L. variegatus
[3-α-L-Galp-1]n
2
SO3-
[3-α-L-Fucp-1→3-α-L-Fucp-1→3-α-L-Fucp-1→3-α-L-Fucp-1]n
2 4
diSO3-
2
SO3-
2
SO3-
4
SO3-
[4-α-L-Fucp-1→4-α-L-Fucp-1→4-α-L-Fucp-1→4-α-L-Fucp-1]n
2
SO3-
2
SO3-

Figure 5

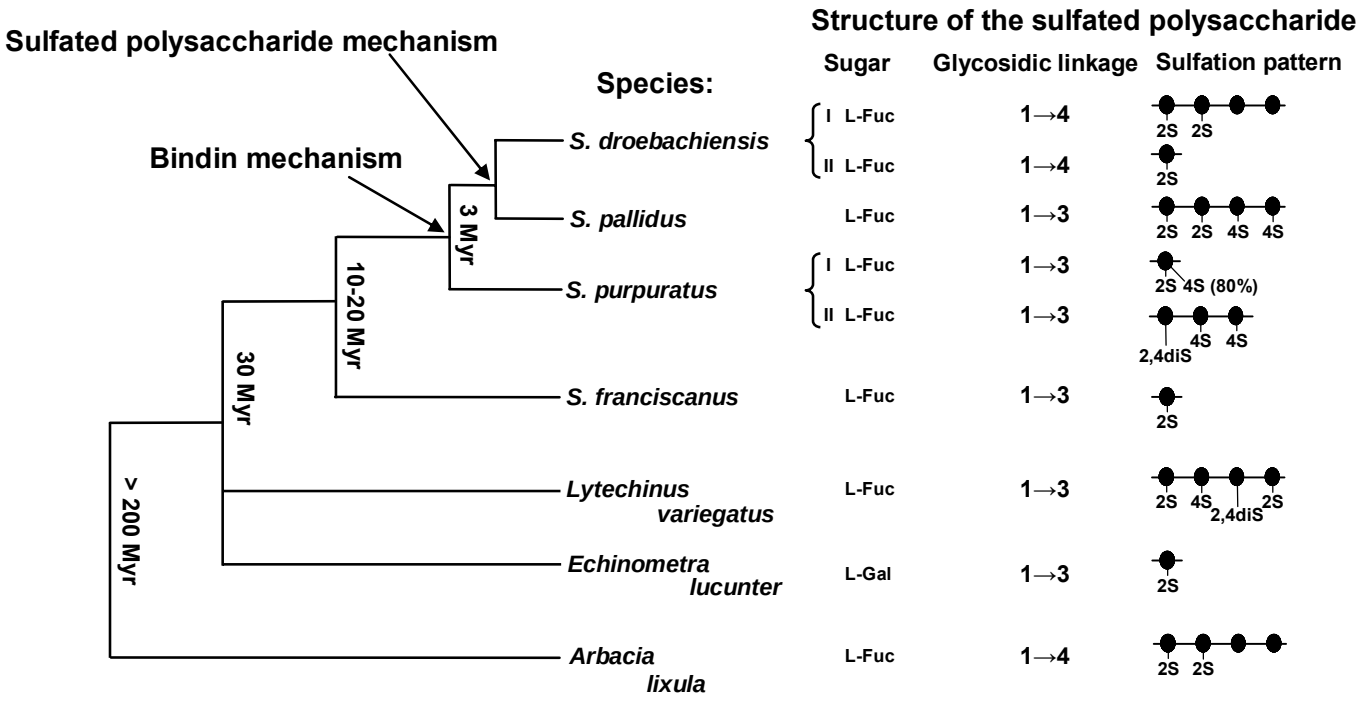

Myr = Million years of evolutionary divergence

Figure 6

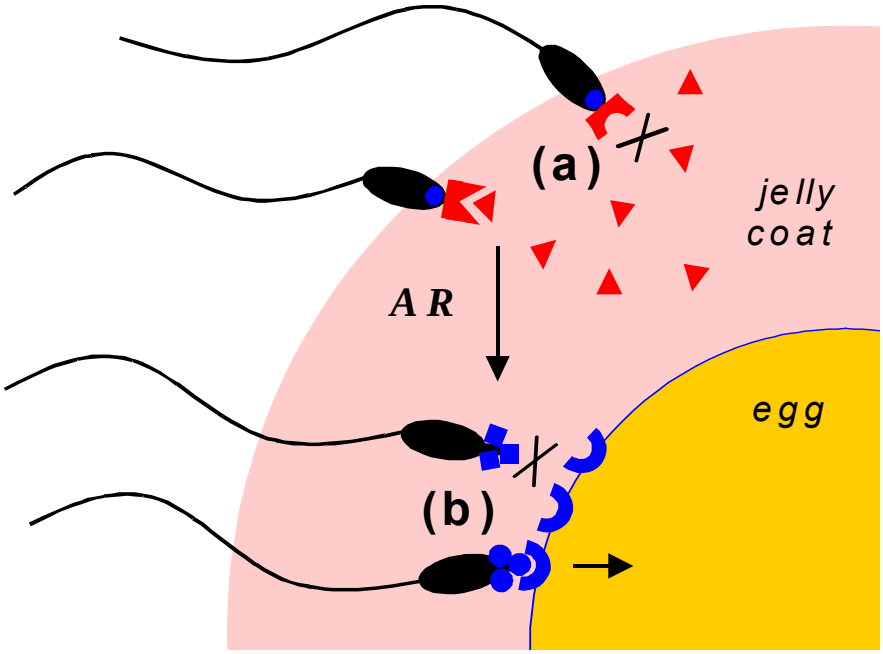

Figure 7

CAPÍTULO 2: FRAGMENTAÇÃO DE FUCANAS SULFATADAS

2.1 A importância da preparação de oligossacarídeos por hidrólise ácida branda

Além do tipo de ligação glicosídica, do padrão de sulfatação e do tipo de açúcar, o tamanho do polímero ou o peso molecular das fucanas sulfatadas também influenciam suas atividades biológicas. Por exemplo, Hirohashi e Vacquier (2002b) mostraram que um derivado de baixo peso molecular (60 ~kDa), obtido por hidrólise ácida branda da fucana sulfatadas de *S. purpuratus*, é incapaz de induzir a reação acrossômica, mas capaz de bloquear o efeito da fucana nativa ($\geq$ ~100 kDa). Os dados deste trabalho indicam que, esse derivado de baixo peso molecular abre apenas um dos dois canais de Ca^{+2} necessários para a reação acrossômica. Para a reação completa, os dois canais devem ser abertos (Hirohashi e Vacquier, 2002b).

Outro exemplo importante, mas envolvendo galactanas sulfatadas, é o trabalho de Melo *et al.* (2004). Nesse estudo, a atividade anticoagulante da galactana sulfatada de *B. occidentalis* (Figura 2A) mostrou dependência direta do tamanho molecular do polissacarídeo. Derivados de baixo peso molecular (de ~15 kDa à ~45 kDa), obtidos por hidrólise ácida branda, são capazes de se ligar a antitrombina, mas incapazes de aproximar o inibidor à protease para o conseqüente efeito anticoagulante. Para que este efeito ocorra, são necessárias moléculas acima de ~45 kDa.

Um avanço no estudo das atividades biológicas de polissacarídeos sulfatados envolve preparar derivados de baixo peso molecular. Este procedimento possibilita estudar não só a influência do tamanho do carboidrato na ação biológica, mas, também analisar regiões estruturais específicas necessárias para a interação com outras moléculas. A análise dessas interações é simplificada com o uso de derivados de tamanho molecular reduzido. Um exemplo clássico desta abordagem é o trabalho de Maimone e Tollefsen (1990). Esses autores mostraram que a seqüência específica do dermatam sulfato [4)-α-L-IdoA-(2SO_4)-

$(1\rightarrow3)$-β-D-GalNAc-$(4SO_4)$-$(1\rightarrow]_n$, onde $n \geq 3$ é necessária para a ligação do GAG ao HCII. Os oligossacarídeos utilizados para estas conclusões foram obtidos por N-deacetilação com hidrazina seguida da quebra deaminativa do GAG com ácido nitroso.

Porém, ainda não são conhecidas as enzimas ou métodos químicos adequados que clivem as fucanas sulfatadas em sítios específicos. Como alternativa, podemos usar métodos não-específicos, como a hidrólise ácida branda, para produzir oligossacarídeos (Hirohashi e Vacquier, 2002b). Uma abordagem similar também foi usada para as galactanas sulfatadas de algas marinhas (Melo *et al.*, 2004).

Um exemplo da utilização de hidrólise ácida branda para alterar o peso molecular e a sulfatação de polissacarídeos sulfatados foi o trabalho de Karlsson e Singh (1999). Estes autores incubaram cinco polissacarídeos sulfatados distintos [κ-, ι-, λ-carragenanas, heparina e dextram sulfato (DxS)] em tampão de hidrólise (0,008 M LiCl e 0,012 M HCl, pH 2), a 35 e 55 ^oC, durante duas horas e analisaram a perda de sulfatação e redução do peso molecular. O dextram sulfato sofreu a maior taxa de desulfatação, seguido da λ-, ι- e κ-carragenanas e por último, a heparina. Os autores correlacionaram a labilidade dos grupos sulfatos com a flexibilidade das cadeias desses polímeros. Quanto à redução do peso molecular, as carragenanas diminuíram em mais de 85 % a sua massa molecular, enquanto, o DxS e a heparina foram totalmente resistentes à clivagem nestas condições de hidrólise ácida. Nesse trabalho, também ficou comprovado que polissacarídeos com estruturas diferentes sofrem efeitos distintos no decorrer da hidrólise ácida branda, tanto na desulfatação quanto na redução do peso molecular.

Portanto, a hidrólise ácida de polissacarídeos sulfatados é um método alternativo para superar a ausência de enzimas ou métodos químicos mais específicos para a produção de oligossacarídeos, como por exemplo, no caso das fucanas sulfatadas.

2.2 Objetivos

Estudar a clivagem de fucanas sulfatadas durante a hidrólise ácida branda. Esse estudo visa preparar oligossacarídeos com estrutura repetitiva e regular, que possam ser utilizadas nos estudos de suas atividades biológicas a fim de determinar os mecanismos de ações biológicas das moléculas nativas.

2.3 Materiais e métodos

2.3.1 Extração e purificação de fucanas sulfatadas

Indivíduos adultos de ouriços-do-mar foram coletados e seus gametas foram retirados através de uma injeção intracelomática de 0,5 M de KCl (~5 mL por indivíduo), como descrito por Alves e colaboradores (1997, 1998), Mulloy e colaboradores (1994) e Vilela-Silva e colaboradores (1999, 2002). Os géis dos óvulos foram isolados por choque de pH, centrifugados e liofilizados após diálise contra água destilada, como descrito por SeGall e Lennarz (1979). Os polissacarídeos ácidos foram extraídos dos géis dos óvulos por digestão com papaína e parcialmente purificados pela precipitação com etanol (Albano e Mourão, 1986). As fucanas sulfatadas foram purificadas em cromatografia de troca-iônica e suas purezas conferidas por eletroforese em gel de agarose e espectroscopia de RMN (Vilela-Silva *et al*., 2002).

2.3.2 Hidrólise ácida branda de fucanas sulfatadas

As fucanas sulfatadas (5 mg) foram dissolvidas em 1 mL de HCl 0,01 M e mantidas a 60^{o}C por diferentes tempos. Após esse procedimento de depolimerização, o pH foi neutralizado com a adição de 1 mL de NaOH 0,01 M gelado. As amostras de oligosscarídeos foram analisadas por PAGE, como descritos no próximo item.

2.3.3 Eletroforese em gel de poliacrilamida (PAGE)

As fucanas sulfatadas nativas e seus respectivos derivados de baixo peso molecular obtidos pela hidrólise ácida branda (10 μg cada) foram aplicadas em um

gel de poliacrilamida 12%, em tampão barbital sódico 0,02 M (pH 8,6) e submetidos à migração eletroforética por ~45 min a 100 V. Após a eletroforese, os polissacarídeos foram corados com corante azul de toluidina 0.1% em 1% de ácido acético e lavados por 4 h em 1% de ácido acético. A massa molecular dos fragmentos de baixo peso das fucanas sulfatadas foi estimada por comparação da migração eletroforética com compostos padrões (Pavão *et al*. 1998; Pereira *et al*. 1999; Santos *et al*., 1992). Os padrões utilizados foram o DxS de alto peso (≥ ~100 kDa), o condroitim 4-sulfato de traquéia bovina (~40 kDa), o dermatam sulfato de pele de porco (~20 kDa) e o DxS de baixo peso (~10 kDa), todos obtidos da Sigma/Aldrich.

2.3.4 Espectros unidimensionais de ^{1}H-Ressonância Nuclear Magnética (RMN)

Os espectros de ^{1}H-RMN das fucanas nativas e seus respectivos derivados de baixo peso molecular foram realizados usando um magneto Bruker 400 MHz com um probe de tripla ressonância. Cerca de 3 mg de cada amostra foram dissolvidos em 0,5 mL de 99,9% D_2O (Cambridge Isotope Laboratory) (amostras nativas) ou 0,5 mL de HCl 0,01 M ou 0,02 M preparados com 99,9 % D_2O (derivados de baixo peso). Todos os espectros foram realizados a 60 ^{o}C com supressão de sinais HOD por pré-saturação. As soluções foram colocadas em um tubo 5 mm de RMN e espectros unidimensionais de ^{1}H-RMN foram gravados em diferentes tempos com 4 scans cada.

2.4 Resultados e discussão

2.4.1 Hidrólise ácida branda de fucanas sulfatadas: dependência da estrutura do polissacarídeo

No intuito de preparar derivados de baixo peso molecular, as fucanas sulfatadas de invertebrados marinhos (Figura 1), a galactana sulfatada de *E. lucunter* (Figura 2A) e a fucana sulfatada da alga parda *Laminaria brasiliensis* foram hidrolisadas com HCl 0.01M por 1 hora (Figura 4A) ou por 6 horas (Figu-

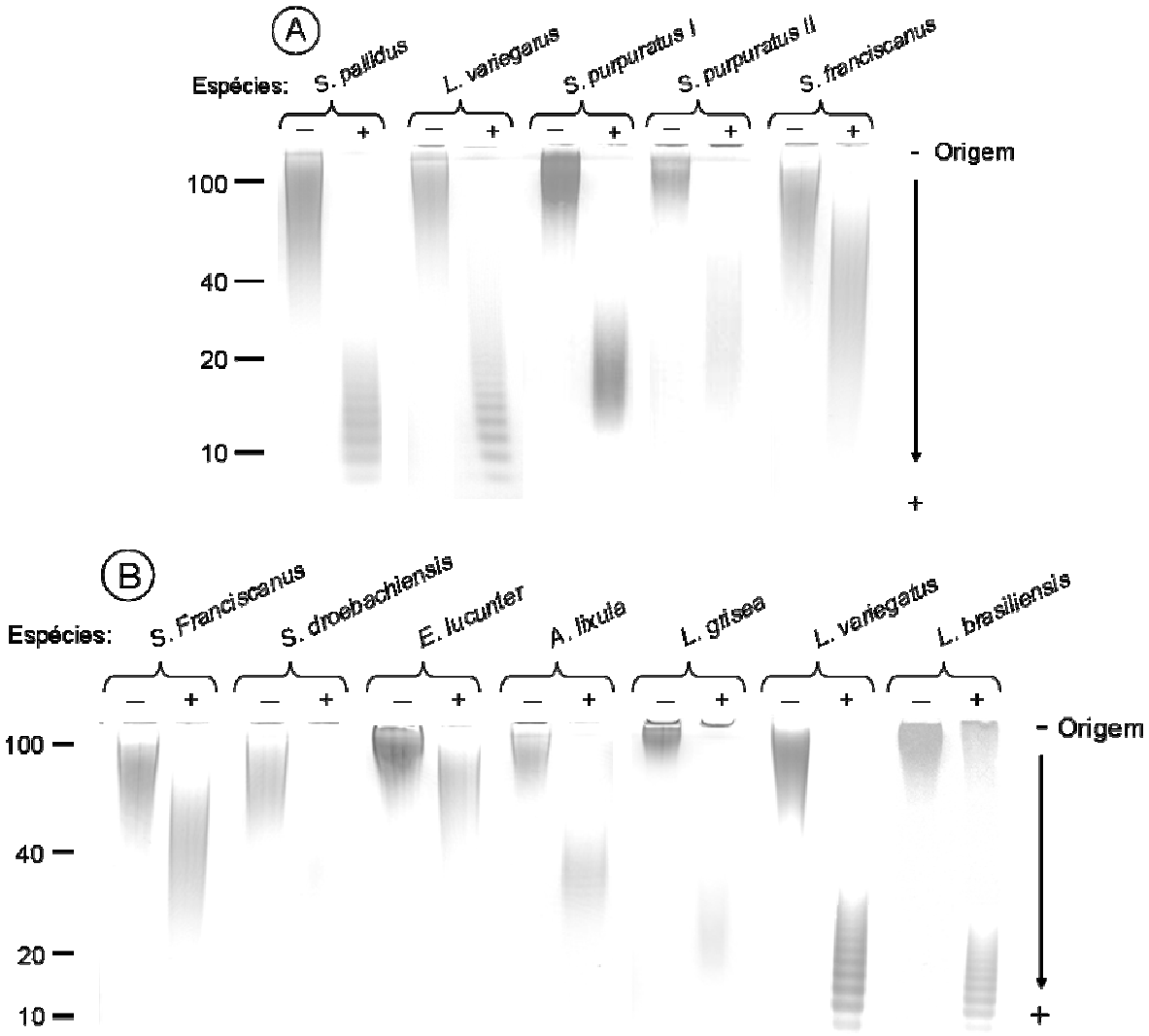

Figura 4. PAGE das fucanas sulfatadas intactas e submetidas à hidrólise ácida branda. As fucanas sulfatadas (100 μg cada) foram diluídas em 100 μL de água destilada (-) ou em uma solução de HCl 0,01 M (+) e aquecidas a 60 ^{o}C por 1 hora (A) ou 6 horas (B). Logo após, 100 μL de NaOH 0,01 M foi adicionado em cada solução. Os padrões de peso molecular são descritos no item 2.3.3 de Materiais e métodos.

ra 4B). Ao término desse período, a reação foi neutralizada e as amostras foram analisadas em uma PAGE (Figura 4). Os polissacarídeos sulfatados intactos têm peso molecular médio de ~100 kDa, com alta dispersão (Figura 4). Após a hidrólise ácida branda, os polissacarídeos sofreram uma redução significativa do peso molecular (amostras indicadas com sinal positivo na Figura 4), ou seja, todos os compostos foram sensíveis à clivagem com o ácido clorídrico. Mas, surpreendentemente, os pesos moleculares desses derivados variaram consideravelmente. Isto demonstra cinéticas de suscetibilidade à clivagem ácida, onde a eficácia da protonação responsável pela quebra da ligação glicosídica sofre influência direta das estruturas químicas desses polissacarídeos sulfatados (Figura 1 e 2A).

Contudo, o resultado mais intrigante foi a capacidade das fucanas sulfatadas das espécies de ouriço-do-mar *L. variegatus* (Figura 1B) e *S. pallidus* (Figura 1C) e da alga parda *L. brasiliensis* (estrutura não revelada devido a sua alta complexidade e heterogeneidade) produzirem oligossacarídeos com pesos moleculares regulares, como evidenciados pelas bandas bem definidas na PAGE (Figura 5A e B). Estes oligossacarídeos possuem pesos moleculares menores que 20 kDa.

Resolvemos prosseguir nossos estudos sobre a reação química de hidrólise ácida com as fucanas sulfatadas com as espécies de ouriços-do-mar, uma vez que suas estruturas já eram conhecidas facilitando a interpretação da reação de hidólise ácida branda (Mulloy *et al*. 1994; Alves *et al*. 1997).

2.4.2 Modificações estruturais das fucanas de *S. pallidus* e *L. variegatus* durante a reação de hidrólise ácida branda

Com o objetivo de identificar as modificações químicas causadas nas fucanas sulfatadas de *S. pallidus* e *L. variegatus* durante a hidrólise ácida branda, decidimos monitorar a reação através do emprego de espectroscopia de ^{1}H-RMN (Figuras 6A e B). As fucanas sulfatadas de *S. pallidus* e *L. variegatus* foram incubadas com HCl 0,01 M, dentro do tubo de RMN e vários espectros

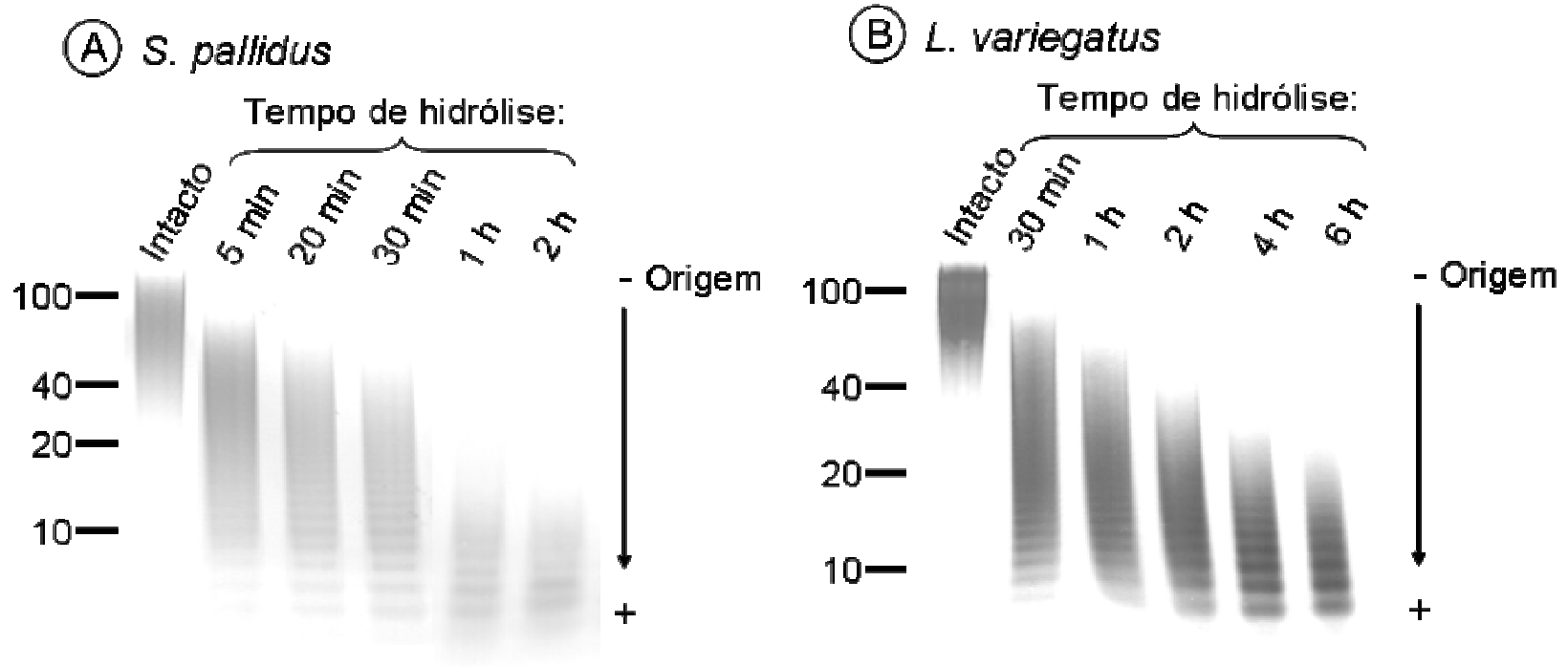

Figura 5. PAGE das cinéticas de hidrólise ácida branda das fucanas sulfatadas das espécies de ouriços-do-mar *S. pallidus* (A) e *L. variegatus* (B). As fucanas sulfatadas foram hidrolisadas com HCl 0,01 M a 60 ^{o}C em diferentes tempos. O peso foi estimado quando comparados com padrões de peso molecular conhecidos, como descrito no item 2.3.3 de Materiais e métodos.

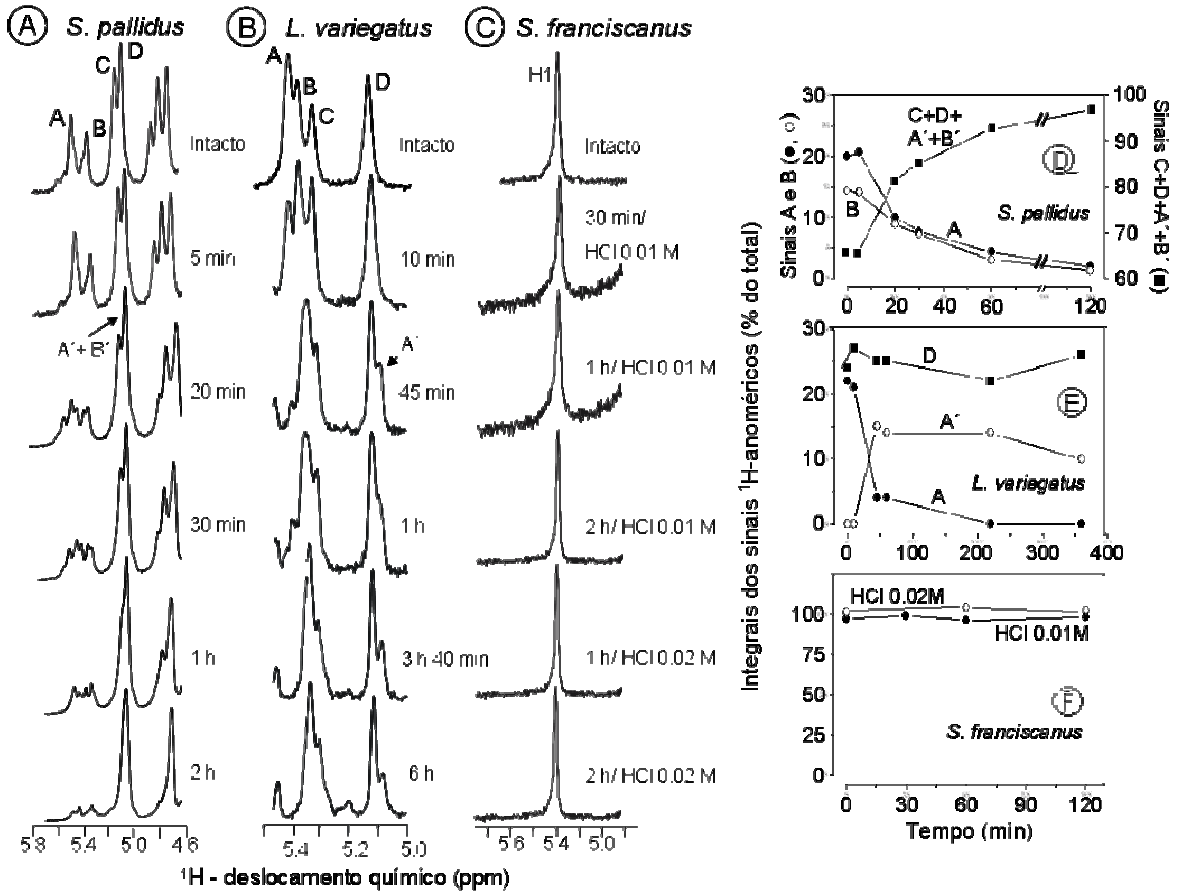

Fig. 6. Espectros ^{1}H-RMN das regiões anoméricas das fucanas sulfatadas de *S. pallidus* (**A**), *L. variegatus* (**B**) e *S. franciscanus* (**C**) em diferentes tempos de hidrólise ácida branda e suas respectivas integrais (**D**-**F**). As fucanas sulfatadas (3 mg) foram dissolvidas em 0,5 mL 99.9% de D_2O, contendo 0,01 M ou 0,02 M de HCl. A temperatura das soluções foi mantida a 60ºC durante o experimento. As integrais de todos os sinais de prótons anoméricos durante o tempo de hidrólise estão mostradas nos painéis **D-F**. Ver Pomin *et al.* (2005b) ***Glycobiology*** (Anexo II).

unidimensionais de ^{1}H-próton foram coletados durante diferentes períodos de tempo de reação.

A fucana de *S. pallidus* (Figura 6A) sofreu, nos primeiros 20 minutos de hidrólise, uma queda dos sinais ^{1}H-anoméricos (H1) dos resíduos assinalados como A e B (que representam os resíduos de fucose 2-sulfatados como representados na Figura 1C), localizados na região de ~5,5 ppm no espectro (espectro do intacto na Figura 6A). A queda desses sinais pode ser evidenciada pela diminuição de suas respectivas integrais (Figura 6D). Concomitantemente, houve um aumento dos sinais anoméricos A´+B´+C+D (que representam os dois resíduos de fucose 2-dessulfatados e os dois resíduos de fucose 4-sulfatados, respectivamente, como evidenciados pela integral na Figura 6D), em conseqüência do deslocamento dos sinais de ^{1}H1 de A e B para essa mesma região do espectro (~5,18 ppm).

Portanto, a hidrólise ácida branda da fucana sulfatada de *S. pallidus* tende a formar apenas um sinal anomérico em ~5,18 ppm, como observado no espectro de 2 h, onde a dessulfatação dos resíduos denominados A e B foi completa. De fato, esse sinal representa uma mistura de prótons anoméricos (A´+B´+C+D) coincidentes no espectro de 1D ^{1}H-próton da molécula hidrolisada. Esses sinais são claramente diferenciados nos espectros de 2D TOCSY e HMQC (discutidos no item 2, Anexo II). Os sinais A´ e B´ indicam claramente resíduos desulfatados na molécula. Portanto, a molécula sofreu uma 2-desulfatação estereoespecífica dos dois primeiros resíduos de fucose (A e B na Figura 1C). Os resíduos 4-sulfatados não sofreram dessulfatação como revelado nos espectros bidimensionais apresentados no item 2.6.2 Artigo III.

No caso da fucana sulfatada de *L. variegatus*, o sinal do próton anomérico A, do segundo resíduo 2-sulfatado da unidade oligossacarídica repetitiva (Figura 1B), diminui com o aparecimento paralelo de um novo sinal anomérico (representado por A´ na Figura 6B). Esta queda de sinal com o tempo de reação pode ser acompanhada pela integral do sinal anomérico deste resíduo 2-sulfatado (denominado A) e o respectivo aumento proporcional da integral do sinal A´, que

representa este mesmo resíduo de fucose, mas agora não-sulfatado (Figura 6E). Esta troca indica, portanto, uma desulfatação progressiva do resíduo 2-sulfatado, denominado como A na Figura 1B. Os sinais B, C e D dos demais resíduos (ver Figura 1B) permanecem inalterados, mostrando uma desulfatação seletiva apenas no segundo resíduo 2-sulfatado.

Comparando a cinética de hidrólise da fucana sulfatada de *S. pallidus* e *L. variegatus*, podemos concluir que houve exclusivamente uma 2-desulfatação nesses polissacarídeos. Para avaliar a susceptibilidade da remoção dos grupamentos 2-sulfato de fucanas pela hidrólise ácida branda, utilizamos o mesmo experimento de análise das modificações estruturais baseada na espectroscopia de ^{1}H-próton para a homofucana sulfatada de *S. franciscanus*, visto que essa molécula é totalmente constituída de resíduos 2-sulfatados (Figura 1G).

Surpreendentemente, a homofucana de *S. franciscanus* resistiu a desulfatação, mesmo usando o dobro da concentração de HCl (Figura 6C e F). A fucana sulfatada de *S. franciscanus* sofre apenas redução do peso molecular durante a hidrólise ácida branda (Figura 6C e F *vs* Figura 4). Esse experimento nos permite concluir que a 2-desulfatação de um resíduo de α-L-fucose durante a hidrólise ácida branda é influenciada pelo tipo de sulfatação da unidade vizinha, visto que todas as fucanas analisadas nos experimentos da Figura 6 possuem o mesmo tipo de ligação glicosídica $\alpha(1\rightarrow3)$ (comparar estruturas na figura 1B, C e G e na Tabela 1), concluindo que a susceptibilidade a 2-desulfatação é influenciada pelo padrão de sulfatação específico da molécula.

Coincidentemente, os resíduos 2-sulfatados que são suscetíveis a desulfatação pela hidrólise ácida nas fucanas de *S. pallidus* e *L. variegatus* são vizinhos de unidades de fucose 4-sulfatadas. Analisando a cinética de hidrólise dessas fucanas e a resistência da fucana de *S. franciscanus* (Figura 6), podemos concluir que a 2-desulfatação causada pela hidrólise ácida branda é uma reação regioseletiva influenciada diretamente pela presença de um resíduo vizinho 4-sulfatado.

Comparando a cinética de desulfatação (Figura 6) com a redução do peso molecular do polissacarídeo durante a hidrólise ácida branda (Figura 5), podemos concluir que a 2-desulfatação é um evento preliminar à redução do peso molecular da fucanas sulfatadas de *S. pallidus* e *L.variegatus*. Para a fucana sulfatada de *S. pallidus*, somente a partir de 1 h de hidrólise ácida branda a concentração dos oligossacarídeos de baixo peso aumenta significativamente (Figura 5A). Neste mesmo tempo de hidrólise, ocorreu praticamente toda a 2-desulfatação dos resíduos A e B (Figura 6A e D). Do mesmo modo que o observado para a fucana sulfatada de *L. variegatus*, mas, em diferentes intervalos de tempo, os oligossacarídeos de baixo peso são obtidos após 2 h de hidrólise ácida branda (Figura 5B), enquanto que a 2-desulfatação completa dos resíduos A ocorre até ~45 minutos (Figura 6E). Portanto, concluímos que a 2-desufatação antecede a clivagem específica das ligações glicosídicas.

2.5 Conclusões gerais sobre a hidrólise ácida branda de fucanas sulfatadas

A hidrólise ácida branda de fucanas sulfatadas é capaz de reduzir o peso molecular desses compostos com velocidades e mecanismos de degradação diferentes e influenciados diretamente por suas estruturas químicas. Para certas fucanas sulfatadas (*S. pallidus* e *L. variegatus*), a hidrólise ácida branda não é uma reação que modifica esses compostos aleatoriamente, mas age de forma bem ordenada, seja dessulfatando ou clivando o polissacarídeo em sítios específicos.

Na fucana sulfatada de *S. pallidus*, por exemplo, a hidrólise ácida promove, num primeiro estágio, a remoção seletiva dos dois grupamentos 2-sulfato e, posteriormente, a ligação glicosídica desses resíduos, agora não-sulfatados, sofre uma clivagem preferencial (Figura 7A). Provavelmente, a ligação glicosídica entre o segundo resíduo 2-sulfatado e a unidade 4-sulfatada é que sofre a clivagem, por analogia com a clivagem específica da fucana de *L. variegatus*.

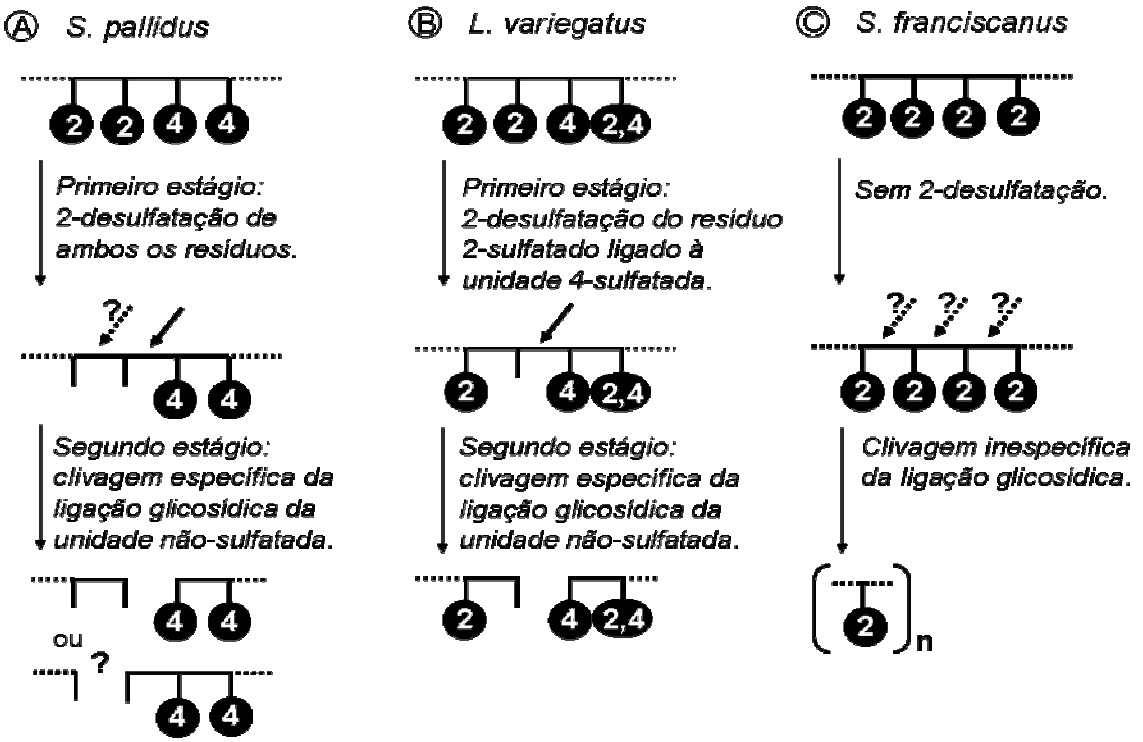

Figura 7. Esquema sumarizando os passos da hidrólise ácida branda de fucanas sulfatadas das espécies de ouriços-do-mar *S. pallidus* (A), *L. variegatus* (B) e *S. franciscanus* (C). Os números indicam a posição de sulfatação, as setas tracejadas indicam possíveis clivagens da ligação glicosídica, enquanto as setas contínuas indicam clivagens asseguradas pelos nossos dados experimentais. Ver também o item 2.6.2 Artigo III.

Na fucana sulfatada da espécie *L. variegatus*, a hidrólise ácida branda, numa primeira etapa, remove regioseletivamente o grupamento 2-sulfato do segundo resíduo (vizinho da unidade de fucose 4-sulfatada). Num segundo momento, a ligação glicosídica entre a unidade desulfatada e o resíduo 4-sulfatado sofre clivagem preferencial (Figura 7B).

A hidrólise ácida branda é, certamente, uma reação eficiente para redução do peso molecular das fucanas sulfatadas (Figura 4). Na maioria dos casos, a produção de derivados de baixo peso é resultado da quebra inespecífica de diferentes tipos de ligações glicosídicas. Como resultado, obtém-se uma mistura heterogênea de produtos com peso molecular reduzido, que não apresentam frações regulares (oligossacarídeos de peso e estrutura regular). De forma bem diferente, as fucanas sulfatadas das espécies *S. pallidus* e *L.* variegatus formam oligossacarídeos com peso molecular bem definido após a hidrólise ácida branda como evidenciados pela análise em PAGE (Figura 4). O motivo que leva à produção destes oligossacarídeos é a 2-desulfatação em sítios específicos na molécula, desencadeando a clivagem preferencial da ligação glicosídica do resíduo desulfatado (Figura 7A e B). A clivagem preferencial em resíduos que sofreram dessulfatação foi evidenciada pela comparação dos deslocamentos químicos dos sinais anoméricos (α e β) com resíduos não-sulfatados e sulfatados em diferentes posições. A presença de sinais β-anoméricos é devido a mutarotação da hidroxila na posição 1. Este sinal é mais evidenciado nos espectros de HSQC (anexos deste capítulo) devido a clivagem, visto que os polissacarídeo nativos possuem apenas ligações do tipo α.

No caso, por exemplo, da hidrólise ácida branda da fucana sulfatada de *S. franciscanus*, não acontece a 2-dessulfatação e, logo, não há clivagem preferencial para a produção de oligossacarídeos com peso molecular bem definido (Figura 7C). A ligação glicosídica de um resíduo não-sulfatado (e, por conseguinte, dessulfatado) é mais lábil à clivagem ácida (protonação) do que as ligações de unidades sulfatadas.

A 2-dessulfatação seletiva ocorre quando a unidade de fucose 2-sulfatada está obrigatoriamente ligada à, ou precedida por uma unidade 4-sulfatada. Portanto, a ocorrência de resíduo 4-sulfatado adjacente a uma unidade 2-sulfatada é um fator fundamental para a especificidade da remoção do sulfato. Com base nas estruturas químicas da Figura 1 e no tipo de produção de oligossacarídeos de baixo peso molecular (Figura 4), podemos perceber que, indubitavelmente, apenas as fucanas sulfatadas de *S. pallidus* e *L. variegatus* atendem às exigências estruturais para a 2-dessulfatação seletiva.

Durante a hidrólise ácida branda, a fucana sulfatada da alga parda *L. brasiliensis* produz oligossacarídeos com peso molecular bem definido (Figura 4B), semelhante às fucanas sulfatadas de ouriços-do-mar *S. pallidus* e *L. variegatus*. Este fato sugere que esse polissacarídeo também possui, na sua estrutura, regiões com unidades 2-sulfatadas ligadas a unidades 4-sulfatadas. Entretanto, uma parte significativa da fucana de *L. brasiliensis* resiste à hidrólise ácida branda, mantendo seu peso molecular elevado, como evidenciado por sua localização próxima da origem no gel de PAGE (Figura 4). Os espectros de 1D ^{1}H-próton e 2D NOESY da fucana sulfatada dessa alga são extremamente complexos (Pereira *et al*. 1999), não permitindo identificar claramente suas principais característica estruturais. Com base na produção de oligossacarídeos específicos pela hidrólise ácida branda (Figura 4), acreditamos que a fucana sulfatada de *L. brasiliensis*, mesmo heterogênea e ramificada, deve apresentar uma seqüência repetitiva. Uma possível interpretação para os nossos resultados seria que o polissacarídeo sulfatado desta alga apresente duas regiões com estruturas diferentes. Uma, com unidades repetitivas, suscetível à hidrólise ácida e capaz de produzir oligossacarídeos específicos e outra, resistente à hidrólise ácida branda (região com ~100 kDa da PAGE na Figura 4).

Podemos concluir que a hidrólise ácida ocorre de forma ordenada e dependente da estrutura da fucana sulfatada, principalmente do seu padrão de sulfatação. Essa reação, aparentemente não específica, é uma metodologia alternativa e eficaz para a produção de oligossacarídeos a partir de fucanas

sulfatadas, permitindo, inclusive, elucidar aspectos estruturais destas moléculas. Certamente, os oligossacarídeos de peso e estrutura definidos, obtidos por esta metodologia podem ser empregados em testes de atividades biológicas, onde o uso de derivados de baixo peso é necessário, visto que as moléculas nativas (≥ 100 kDa) não são capazes de revelar particularidades estruturais responsáveis pelos mecanismos desencadeados nas ações biológicas.

2.6.1 Artigo II

Glycobiology
Vol. 15 No 4, pp 369-381, 2005a

"Selective cleavage and anticoagulant activity of a sulfated fucan: stereospecific removal of a 2-sulfated ester from the polysaccharides, and heparin cofactor II-dependent anticoagulant activity."

Vitor H. Pomin, Mariana S. Pereira, Ana-Paula Valente, Douglas M. Tollefsen, Mauro S.G. Pavão e Paulo A.S. Mourão

Glycobiology vol. 15 no. 4 pp. 369–381, 2005
doi:10.1093/glycob/cwi021
Advance Access publication on December 8, 2004

Selective cleavage and anticoagulant activity of a sulfated fucan: stereospecific removal of a 2-sulfate ester from the polysaccharide by mild acid hydrolysis, preparation of oligosaccharides, and heparin cofactor II–dependent anticoagulant activity

Vitor H. Pomin[2,3], Mariana S. Pereira[2,4], Ana-Paula Valente[3,5], Douglas M. Tollefsen[6], Mauro S. G. Pavão[2,3], and Paulo A. S. Mourão[1,2,3]

[2]Laboratório de Tecido Conjuntivo, Hospital Universitário Clementino Fraga Filho, Universidade Federal do Rio de Janeiro, Caixa Postal 68041, Rio de Janeiro, RJ, 21941-590, Brazil; [3]Instituto de Bioquímica Médica, Universidade Federal do Rio de Janeiro, Caixa Postal 68041, Rio de Janeiro, RJ, 21941-590, Brazil; [4]Instituto de Ciências Biomédicas, Universidade Federal do Rio de Janeiro, Caixa Postal 68041, Rio de Janeiro, RJ, 21941-590, Brazil; [5]Centro Nacional de Ressonância Nuclear Magnética de Macromoléculas, Universidade Federal do Rio de Janeiro, Caixa Postal 68041, Rio de Janeiro, RJ, 21941-590, Brazil; and [6]Division of Hematology, Department of Internal Medicine, Washington University School of Medicine, St. Louis, MO 63110

Received September 16, 2004; revised on November 30, 2004; accepted on December 2, 2004

A linear sulfated fucan with a regular repeating sequence of [3)-α-L-Fuc*p*-(2SO_4)-(1→3)-α-L-Fuc*p*-(4SO_4)-(1→3)-α-L-Fuc*p*-(2,4SO_4)-(1→3)-α-L-Fuc*p*-(2SO_4)-(1→]$_n$ is an anticoagulant polysaccharide mainly due to thrombin inhibition mediated by heparin cofactor II. No specific enzymatic or chemical method is available for the preparation of tailored oligosaccharides from sulfated fucans. We employ an apparently nonspecific approach to cleave this polysaccharide based on mild hydrolysis with acid. Surprisingly, the linear sulfated fucan was cleaved by mild acid hydrolysis on an ordered sequence. Initially a 2-sulfate ester of the first fucose unit is selectively removed. Thereafter the glycosidic linkage between the nonsulfated fucose residue and the subsequent 4-sulfated residue is preferentially cleaved by acid hydrolysis, forming oligosaccharides with well-defined size. The low-molecular-weight derivatives obtained from the sulfated fucan were employed to determine the requirement for interaction of this polysaccharide with heparin cofactor II and to achieve complete thrombin inhibition. The linear sulfated fucan requires significantly longer chains than mammalian glycosaminoglycans to achieve anticoagulant activity. A slight decrease in the molecular size of the sulfated fucan dramatically reduces its effect on thrombin inactivation mediated by heparin cofactor II. Sulfated fucan with ~ 45 tetrasaccharide repeating units binds to heparin cofactor II but is unable to link efficiently the plasma inhibitor and thrombin. This last effect requires chains with ~ 100 or more tetrasaccharide repeating units. We speculate that the template mechanism may predominate over the allosteric effect in the case of the linear sulfated fucan inactivation of thrombin in the presence of heparin cofactor II.

[1]To whom correspondence should be addressed; e-mail: pmourao@hucff.ufrj.br

Key words: anticoagulant activity/heparin cofactor II/selective cleavage of sulfated polysaccharide/stereospecific desulfation/sulfated fucans

Introduction

Sulfated fucans are among the most abundant nonmammalian sulfated polysaccharides found in nature. They occur in brown algae and in marine invertebrates. Algal sulfated fucans have complex and heterogeneous structures, but recent studies revealed the occurrence of some ordered repeat units in the sulfated fucans from several species (Berteau and Mulloy, 2003; Mourão, 2004). In contrast, invertebrate polysaccharides have simple, ordered structures, which differ in the specific patterns of sulfation and/or position of the glycosidic linkage within their repeating units (Alves *et al*., 1997, 1998; Vilela-Silva *et al*., 1999, 2002).

Sulfated fucans have a wide variety of biological activities, but their potent anticoagulant action is by far the most widely studied. These polysaccharides are potent thrombin inhibitors whose action is mediated by antithrombin or heparin cofactor II. Attempts to identify in the algal polysaccharides specific structural features necessary for their anticoagulant activity have failed due to their complex and heterogeneous structures (Mourão, 2004). As we extend these studies to the invertebrate fucans, we were able to determine that their anticoagulant activity is not merely a consequence of the charge density but depends on specific structural motifs necessary for interaction with coagulation cofactors and their target proteases (Pereira *et al*., 2002). The major structural requirement for the interaction of linear sulfated fucans with heparin cofactor II is the presence of 4-sulfated fucose units. If we replace heparin cofactor II with antithrombin, 2,4-disulfated units are required for interaction with the cofactor. Apparently the presence of exclusively 2-sulfated fucose residues has a deleterious effect on the anticoagulant activity.

A further step for characterizing the anticoagulant activity of the sulfated fucans is to prepare low-molecular-weight derivatives and test their activities in specific assays. In the case of mammalian glycosaminoglycans, specific enzymatic and chemical methods can be used to provide tailored oligosaccharides for biological activity. This approach revealed that a specific sequence of [4)-α-L-IdUA-(2SO_4)-(1→3)-β-D-GalNAc-(4SO_4)-(1→]$_n$, where n = 3 is required for the binding of dermatan sulfate to heparin cofactor II (Maimone and Tollefsen, 1990) and n = 12 is the minimum size required to stimulate the thrombin–heparin cofactor II reaction (Tollefsen *et al*., 1986). Similar studies

Glycobiology vol. 15 no. 4 © Oxford University Press 2004; all rights reserved.

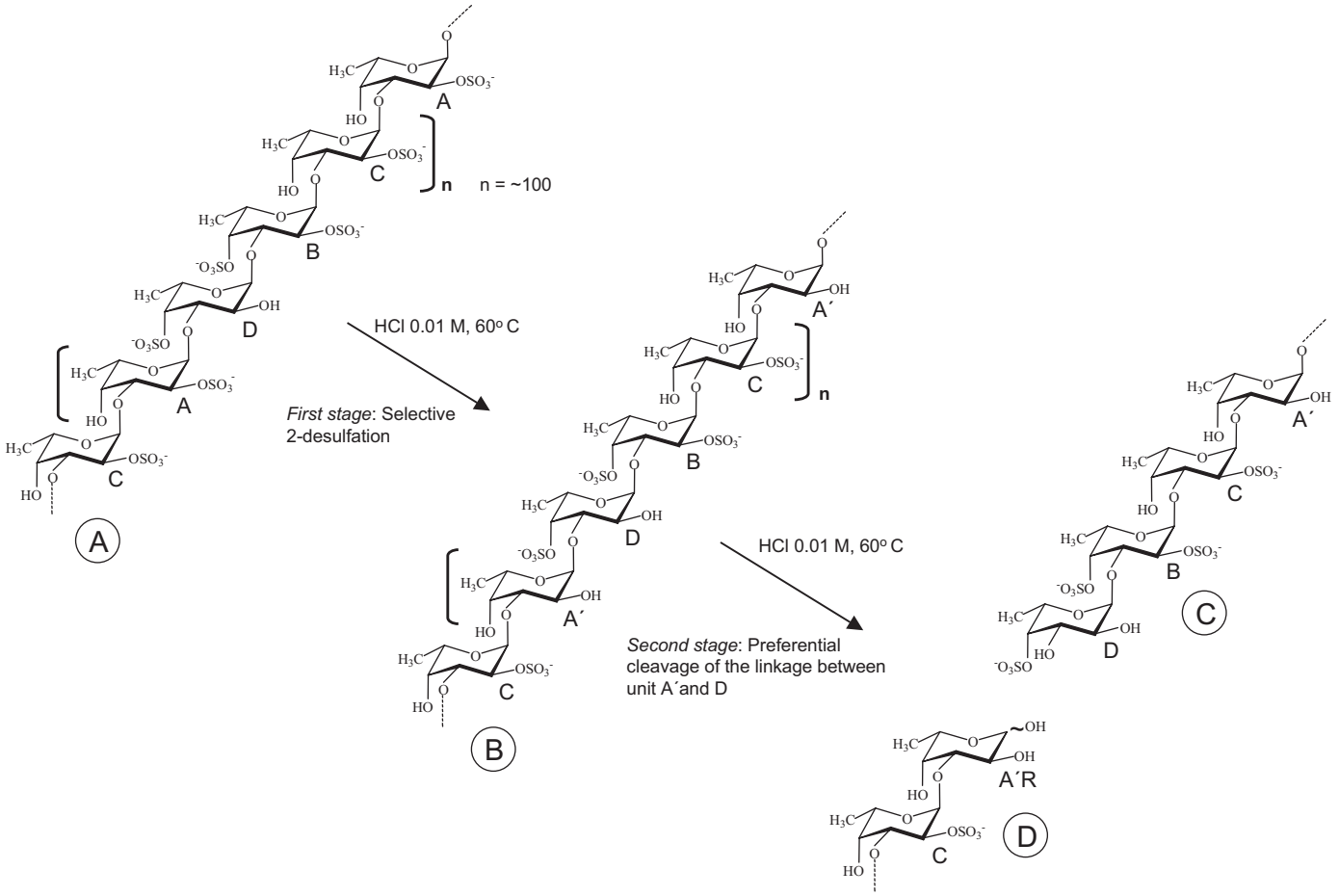

Fig. 1. Summary of the sulfated fucan structure before (**A**) and in the course of mild acid hydrolysis (**B**–**D**). A,sulfated fucan from *L. variegatus* is a linear polysaccharide, composed of a tetrasaccharide repeating sequence as follows: [3)-α-L-Fuc*p*-(2SO_4)-(1→3)-α-L-Fuc*p*-(4SO_4)-(1→3)-α-L-Fuc*p*-(2,4SO_4)-(1→3)-α-L-Fuc*p*-(2SO_4)-(1→]$_n$. Four types of fucose units are designated by the letters A–D. The average molecular weight of this fucan is = ~ 100 kDa, and its repeating tetrasaccharide unit has 980 Da. Therefore we estimated that the polysaccharide has an average of 100 tetrasaccharide units. (**B**) In the first stage of the acid hydrolysis, a sulfate ester is selectively removed from residue A, thereafter designated A′. (**C** and **D**) A preferential cleavage of the linkage formed by the nonsulfated fucose residue (A′ unit) occurs in the second stage of the acid hydrolysis. Oligosaccharides with well-defined molecular size are formed, containing nonsulfated fucose units at the reducing ends (A′R).

have been widely used for heparin (Conrad, 1998). However, it is not possible to apply this approach to sulfated fucans due to the absence of enzymes and chemical methods to cleave the polysaccharide and to produce oligosaccharides with well-defined structures. Enzymes that cleave the core of the sulfated fucans, leading to a rapid reduction of the molecular size, have been reported in marine invertebrates and bacteria (Daniel *et al.*, 1999; Furukawa *et al.*, 1992a; Kitamura *et al.*, 1992). However, the limitation for purification of these enzymes and the difficulties to identify different structures varying in their sensitivity to hydrolysis has limited their use for structural elucidation and the preparation of oligosaccharides. Preliminary reports have appeared in the literature concerning sulfatases able to act on sulfated fucans (Furukawa *et al.*, 1992b; Lloyd *et al.*, 1962) and nothing is known about their properties, particularly whether they can act alone or need glycosidases to achieve significant desulfation of sulfated fucans. Only one study has shown a sulfatase able to act specifically on some sulfate groups of sulfated fucan (Daniel *et al.*, 2001). But this enzyme does not act on a long polysaccharide chain and is able to release sulfate groups exclusively from mono- or disaccharides.

To overcome the limitation for preparation of low-molecular-weight derivatives from the sulfated fucan, we employ an apparently nonspecific methodology to cleave the polysaccharide, based on mild hydrolysis with acid. We concentrated our work on a sulfated fucan from the sea urchin *Lytechinus variegatus*, with a regular repeating sequence as follows: [3)-α-L-Fuc*p*-(2SO_4)-(1→3)-α-L-Fuc*p*-(4SO_4)-(1→3)-α-L-Fuc*p*-(2,4SO_4)-(1→3)-α-L-Fuc*p*-(2SO_4)-(1→]$_n$ (Figure 1A). Surprisingly, we observed that the sulfated fucan was cleaved by acid in an ordered sequence. Initially a 2-sulfate ester was selectively removed from the first fucose unit (residue A, Figure 1A). Then the glycosidic linkage between the nonsulfated fucose unit (residue A′) and the second, 4-sulfated unit (residue D) was preferentially cleaved by acid (Figure 1C), forming oligosaccharides with well-defined molecular size. Sulfated fucans with a reduced molecular weight were employed to determine

the requirement for interaction of this polysaccharide with heparin cofactor II. The molecular size required for binding to the serpin and to stimulate thrombin inhibition varies markedly between the mammalian glycosaminoglycans and the invertebrate sulfated fucan.

Results and discussion

Mild acid hydrolysis of the sulfated fucan yields oligosaccharides with well-defined molecular size

Mild acid hydrolysis gradually reduces the molecular size of the sulfated fucan, as indicated by metachromasia of fractions eluted from a Superose-6 column (Figure 2A). A similar profile was observed when the fractions were assayed by the phenol–sulfuric acid reaction for fucose (not shown in Figure 2A). Thus the decrease in molecular size by mild hydrolysis is not followed by a substantial disruption of the sulfation pattern of the molecule. Polyacrylamide gel electrophoresis (PAGE) reveals that mild acid hydrolysis produces a wide variety of metachromatic bands with well-defined sizes (Figure 2B). As the time of hydrolysis proceeds from 1 to 6 h, the proportions of bands with higher electrophoretic mobility increase but maintain the same well-defined pattern of narrow electrophoretic bands.

The oligosaccharides produced after 6 h of mild acid hydrolysis of the sulfated fucan were purified by gel chromatography on Bio-Gel P-10 (open circles in Figure 3A). A mixture of oligosaccharides were separated on this column and designated as I–VI. PAGE of the purified fractions (Figure 3B) shows that the oligosaccharides correspond to the well-defined size bands already observed in Figure 2B. As we increased the period of hydrolysis from 6 to 9 h (closed circles in Figure 3A), the proportions of low-molecular-mass oligosaccharides increase, but always with similar size as those obtained after 6 h of hydrolysis.

It is not possible to estimate the molecular masses of oligosaccharides I–VI due to the absence of appropriate standards. However, it is likely that the various metachromatic bands observed on PAGE (Figures 2B and 3B) differ from each other by one tetrasaccharide repeating unit, estimated as 901 Da (Figure 1C). This possibility is also supported by comparison between the electrophoretic mobility of these oligosaccharides with those obtained by chondroitin ABC lyase digestion of mammalian dermatan sulfate (data not shown).

Overall, our results show that mild acid hydrolysis of the sulfated fucan yields oligosaccharides with well-defined molecular size, indicative of preferential cleavage of a specific glycosidic linkage without substantial desulfation. Otherwise, we would expect a mixture of products with a wide dispersion in molecular size, as observed for the majority of sulfated polysaccharides.

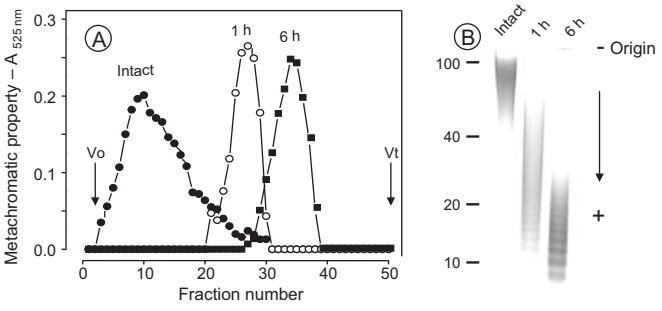

Fig. 2. Mild acid hydrolysis of the sulfated fucan. (**A**) Sulfated fucan from *L. variegatus* (2 mg) before (closed circles) and after partial acid hydrolysis with 1.25 ml of 0.01 M HCl at 60°C for 1 h (open circles) or 6 h (closed squares) was applied to a Superose-6 and eluted as described under *Materials and methods*. The fractions were assayed by metachromasia. A similar profile was obtained when the fractions were assayed by the phenol-sulfuric acid reaction (not shown in the panel). (**B**) Sulfated fucan, before and after mild acid hydrolysis (10 μg of each), were analyzed by PAGE, as described under *Materials and methods*. The molecular weights (kDa) of standard compounds are indicated at the left. These standards are: high-molecular-weight dextran sulfate (≥100 kDa), chondroitin 4-sulfate from bovine trachea (~40 kDa), dermatan sulfate from pig skin (~20 kDa), and low-molecular-weight dextran sulfate (~10 kDa).

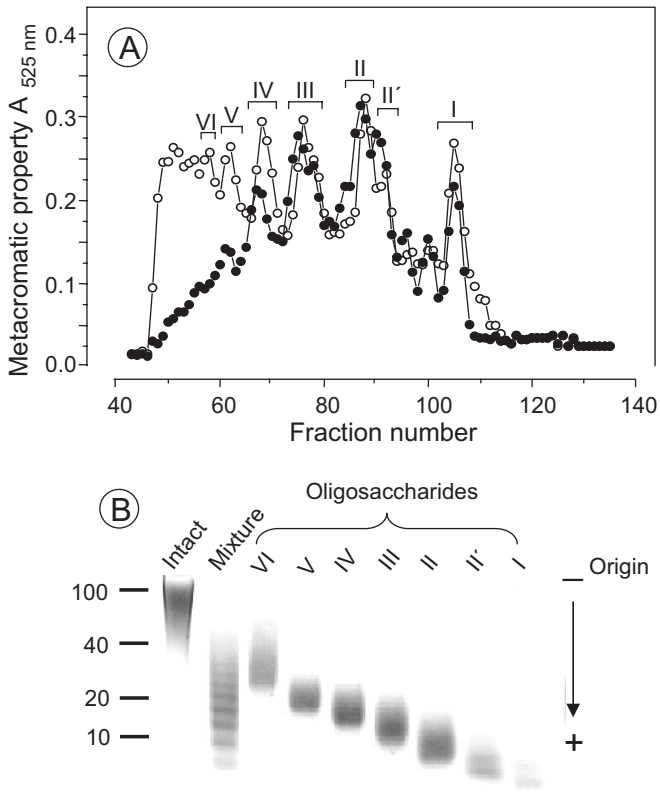

Fig. 3. Size fractionation of the sulfated fucan oligosaccharides. (**A**) Sulfated fucan (5 mg) partially hydrolyzed with 1 ml 0.01 M HCl at 60°C for 6 h (open circles) or 9 h (closed circles) were applied to a Bio-Gel P-10 column (200 × 0.9 cm), equilibrated with aqueous 10% ethanol, containing 1.0 M NaCl. The column was eluted as described under *Materials and methods*, and the fractions were assayed by metachromasia. The fractions containing the oligosaccharides (as indicated by the horizontal bars) were pooled, freeze-dried, desalted, and dissolved in distilled water. (**B**) Intact sulfated fucan, a mixture of unfractionated oligosaccharides, the seven major fractions obtained on Bio-Gel P-10 (10 μg each) were applied to a 10% polyacrylamide gel and analyzed as described in the legend of Figure 2. The molecular weights (kDa) of standard compounds are indicated at the left. See also the legend of Figure 2.

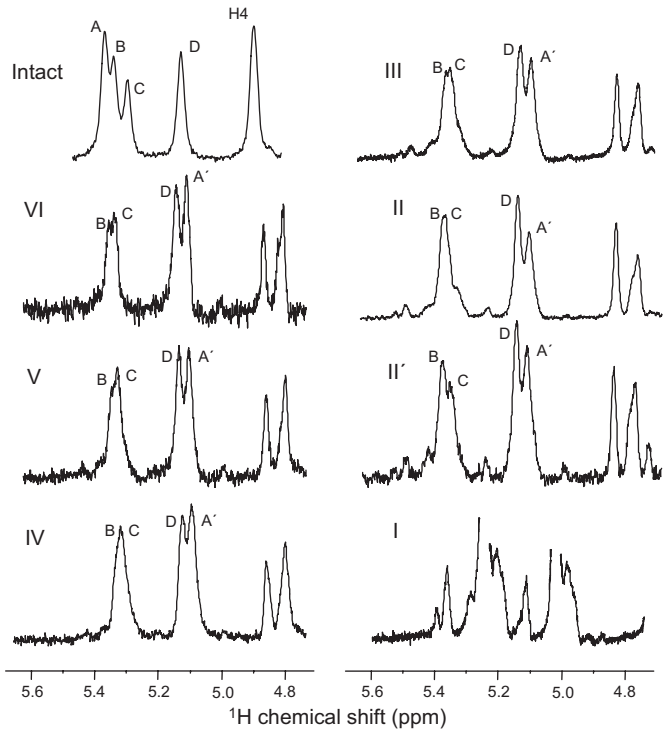

Fig. 4. Expansions of the 5.6–4.8 ppm regions of the ^{1}H-NMR spectra at 600 MHz of the intact sulfated fucan and of the purified oligosaccharides obtained by mild acid hydrolysis. The spectra were recorded at 60°C for samples in 99.9% D_2O solution. Chemical shifts are relative to external trimethylsilylpropionic acid at 0 ppm. The residual water signal has been suppressed by presaturation. Resonances marked A–D in the native sulfated fucan and as A′–D in the oligosaccharides are anomeric signals of the residues shown in Figure 1A and B, respectively.

A selective 2-desulfation occurs in the course of mild acid hydrolysis of the sulfated fucan

The ^{1}H-nuclear magnetic resonance (NMR) spectrum of the native sulfated fucan shows four well-defined anomeric signals, labeled with the letters A–D (Intact in Figure 4), which correspond to the four types of fucose residues in the sea urchin fucan (see structure in Figure 1A) (Alves *et al.*, 1998). Oligosaccharides II′–VI, obtained from gel filtration chromatography after mild acid hydrolysis of the sulfated fucan, show ^{1}H spectra very similar with each other but clearly different from the spectrum of the native polysaccharide. The peak corresponding to unit A is not present in any of the oligosaccharides, and a new peak could be assigned as A′. Concomitantly, the chemical shift of signal C is slightly to lowfield and overlaps with signal B. Oligosaccharide I, the smallest one, has a more heterogeneous ^{1}H-NMR spectrum, indicating that it does not contain a regular repeating structure as do oligosaccharides II′–VI.

Total correlation spectroscopy (TOCSY) and ^{1}H/^{13}C heteronuclear multiple quantum correlation spectroscopy (HMQC) spectra of oligosaccharides II′–VI confirmed that the four anomeric signals correspond to the four units labeled in Figure 4, as exemplified by the native fucan (Figures 5A and 6A) and by oligosaccharide III (Figures 5B and 6B).

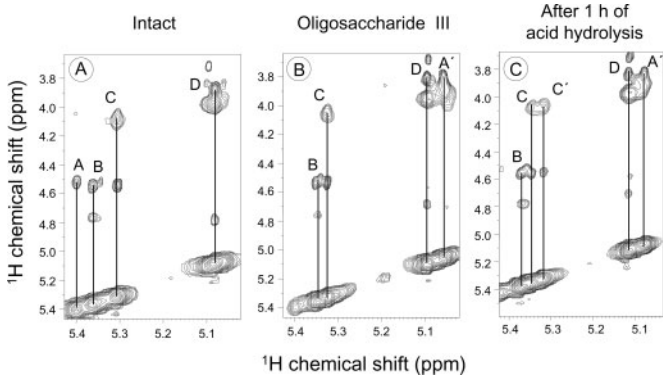

Fig. 5. Expansions of the TOCSY spectra of the native sulfated fucan and of the products obtained after 1 h mild acid hydrolysis. The TOCSY spectra of the intact sulfated fucan (**A**), the oligosaccharide III purified on a Bio-Gel P-10 column (**B**, see Figure 3) and the mixture of oligosac charides formed after 1 h mild acid hydrolysis (**C**, see Figure 2) show some cross-peaks used in the assignment of the fucose residues. The four fucose residues in the repeating units are marked A–D and A′–D for the intact and partially hydrolyzed fucan (see Figure 1A and B, respectively).

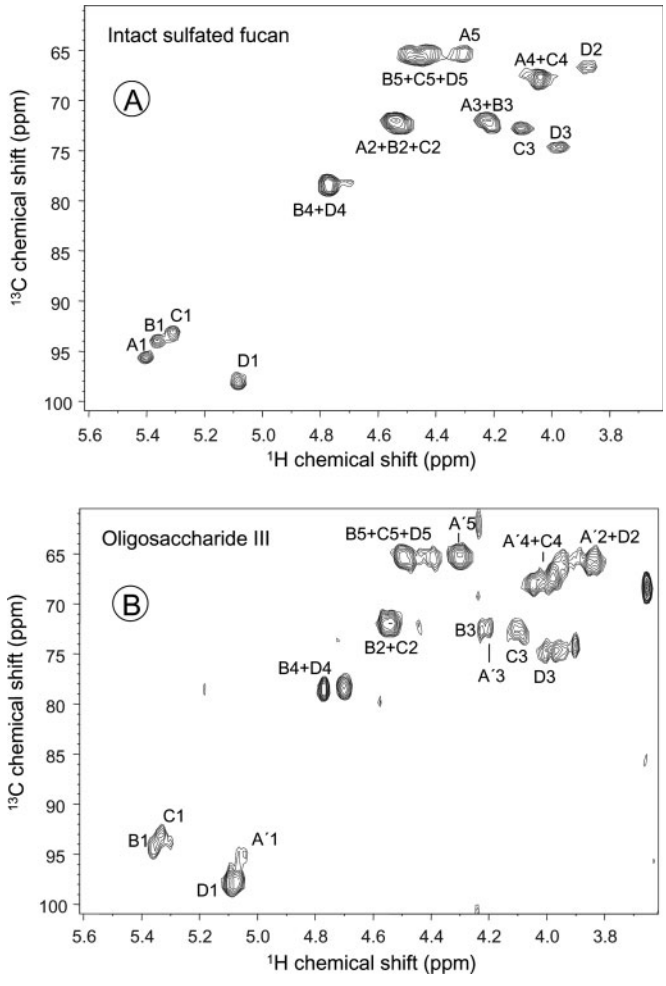

Fig. 6. ^{1}H/^{13}C HMQC spectra of intact sulfated fucan (**A**) and oligosaccharide III (**B**). The assignment was based on TOCSY and correlation spectroscopy spectra. The values of chemical shifts in Table II are relative to external trimethylsilylpropionic acid at 0 ppm for ^{1}H and to methanol for ^{13}C. The anomeric signals were identified by the characteristic carbon chemical shifts and are marked A–D for intact fucan and as A′–D for oligosaccharide III.

Table I. Proton and carbon chemical shifts (ppm) for residues of α-fucose in native fucan and in oligosaccharide III obtained by mild acid hydrolysis

	Native sulfated fucan (see Figure 1A)				Oligosaccharide III (see Figure 1C)			
	A	B	C	D	A′	B	C	D
Proton								
H-1	5.40	5.36	5.31	5.08	5.07	5.35	5.33	5.09
H-2	**4.55**	**4.55**	**4.55**	3.89	3.85	**4.56**	**4.56**	3.85
H-3	4.23	3.96	4.23	3.96	4.23	4.10	4.23	4.00
H-4	4.05	**4.78**	4.08	**4.78**	3.93	**4.77**	3.93	**4.77**
H-5	4.38	4.46	4.46	4.46	4.30	4.50	4.50	4.50
H-6	1.24–1.32	1.24–1.32	1.24–1.32	1.24–1.32	1.32–1.43	1.32–1.43	1.32–1.43	1.32–1.43
Carbon								
C-1	95.1	93.3	92.5	97.7	94.7	94.1	92.6	97.1
C-2	**71.8**	**71.8**	**71.8**	66.7	66.0	**71.8**	**71.8**	66.0
C-3	72.2	72.6	72.2	74.5	72.6	72.7	72.6	74.5
C-4	67.8	**78.0**	67.8	**78.0**	65.7	**78.2**	65.7	**78.2**
C-5	65.3	68.8	68.8	68.8	65.0	66.0	66.0	66.0
C-6	14–19	14–19	14–19	14–19	13–19	13–19	13–19	13–19

The spectra were recorded at 600 mHz in 99.9% D_2O. Chemical shifts are relative to external trimethylsilylpropionic acid at 0 ppm for ^1H and to methanol for ^{13}C. Values in boldface indicate positions bearing a sulfate ester.

Chemical shifts for the four types of fucose residues in oligosaccharide III as well as for the native sulfated fucan are listed in Table I. Residue A′ has H2 at ~ 0.7 ppm to highfield compared with H2 of residue A in the native fucan (Figure 5A and B), which typically indicates a desulfation at this site. No major differences can be observed among the chemical shifts of residues B, C, and D found in the native fucan and in oligosaccharide III. This observation was further confirmed by the $^1H/^{13}C$ HMQC spectra (Figure 6A and B) and the ^{13}C chemical shifts reported in Table I. Residue A′ has C2 at ~ 5.8 ppm to highfield compared with C2 of residue A of the native fucan, again as expected for a desulfated site.

The time course of mild acid hydrolysis of the sea urchin fucan was followed by 1D ^1H-NMR spectroscopy (Figure 7). The native sulfated fucan was incubated with acid inside the NMR tube and several ^1H spectra were obtained from 10 min to 6 h. Using this procedure, we could follow the chemical modifications that occur in the polysaccharide during mild acid hydrolysis. In the first 60 min of hydrolysis, most of the ^1H anomeric signal of residue A disappears with a concomitant increase of signal A′, whereas the integral of ^1H anomeric signal D does not change (Figure 7B). In the longer periods of hydrolysis, the ^1H-NMR spectra remain unchanged. The mixture of oligosaccharides obtained after 1 h of acid hydrolysis was analyzed by TOCSY (Figure 5C). Clearly, we can notice the similarity with the TOCSY spectrum of oligosaccharide III (Figure 5B), except that two spin systems of signal C coexist (designated C and C'), indicative that some 2-sulfation remains on residue A.

In conclusion, mild acid hydrolysis of the sulfated fucan from *L. variegatus* selectively removes 2-sulfate ester from the first fucose unit, which constitutes the regular repetitive tetrasaccharide units of the sea urchin fucan.

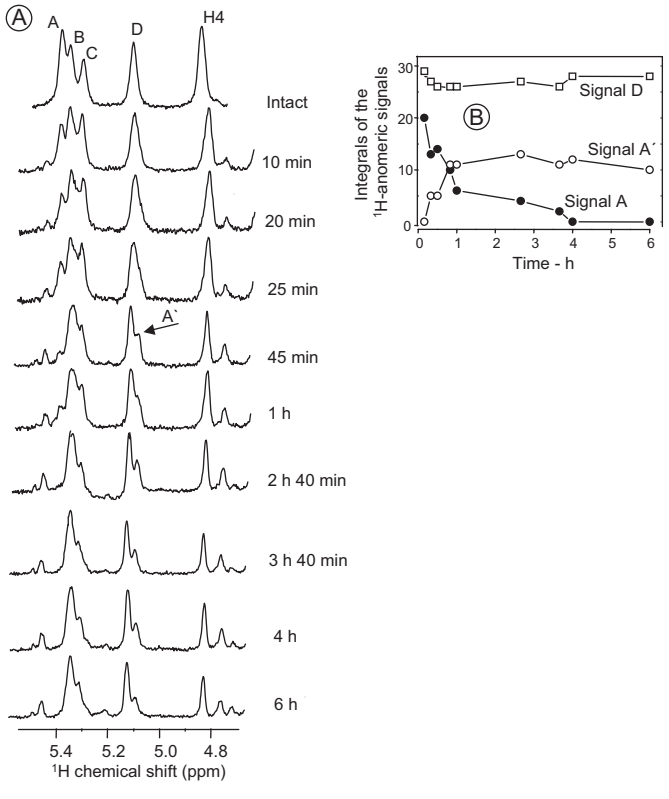

Fig. 7. Expansions of the 5.6–4.7 ppm regions of the ^1H-NMR spectra at 600 MHz of the sulfated fucan at different periods of mild acid hydrolysis at 60°C. (**A**) Sulfated fucan (3 mg) was dissolved in 1.0 ml 99.9% D_2O containing 0.01 M HCl in a 5-mm inner diameter NMR tube. This solution was heated at 60°C, and ^1H-NMR spectra were recorded from 10 min to 6 h, as indicated in the figure. Signals of the anomeric protons of residues A, A′, and D were integrated, and the integrals are shown in **B**.

A specific glycosidic linkage is preferentially cleaved by mild acid hydrolysis

The molecular size of the oligosaccharides formed from the sulfated fucan decreases as the period of acid hydrolysis proceeds from 1 to 6 h, but each oligosaccharide shows a very narrow band on PAGE (Figures 2 and 3). The preponderant chemical structure of these oligosaccharides remains unchanged, as revealed by ^{1}H-NMR spectra in the time course experiment of Figure 7. These observations suggest that a specific glycosidic linkage of the sulfated fucan is preferentially cleaved by acid hydrolysis; otherwise, we would expect oligosaccharides with a wide variety of molecular size as well as with a heterogeneous sulfation pattern. Identification of the specific linkage cleaved by acid hydrolysis is difficult, because the sulfated fucan contains a single type of glycosidic linkage, that is, α(1→3) linked units (Figure 1). We attempted to determine the cleavage site on the sulfated fucan using NMR spectroscopy. Anomeric protons from reducing terminals of fucose give very faint bands, and it was not possible to identify these signals and to trace spin systems on the 2D ^{1}H-NMR spectra. The presence of only faint bands of terminal reducing fucose units on the ^{1}H-NMR spectra indicates that the oligosaccharides obtained by mild acid hydrolysis of the sulfated fucan have a significant high number of repeating units, certainly = ~ 10 tetrasaccharide sequences. This is also supported by the observation that these oligosaccharides migrate on PAGE almost as a dextran sulfate with an average molecular weight of 10 kDa (Figures 2B and 3B). However, ^{1}H/^{13}C HMQC spectra show characteristic anomeric signals of reducing fucose—an equilibrium between α- and β-forms—as exemplified by oligosaccharide II in Figure 8. Comparison between the ^{1}H and ^{13}C chemical shifts of α- and β-anomeric signals of oligosaccharide II with standard compounds (Table II) clearly indicates that they originated from a nonsulfated fucose terminal. This observation indicates that the preferential cleavage site in the course of mild acid hydrolysis is the glycosidic linkage formed between residue A′ (the desulfated fucosyl unit) and residue D (a 4-sulfated fucose unit).

Conclusion concerning the ordered degradation of the sulfated fucan by mild acid hydrolysis

Taken together, the data of Figures 2–8 and Tables I and II indicate that sulfated fucan from the sea urchin *L. variegatus* is degraded in a specific order during mild hydrolysis with acid. In the initial stage of degradation, a 2-sulfate ester is selectively removed from the first fucose unit of a tetasaccharide (unit A). Thereafter, the molecular size of the polysaccharide is slowly reduced due to a preferential cleavage of the glycosidic linkage formed between the nonsulfated residue (A′ in Figure 1B) and the second, 4-sulfated unit (unit D). It has already been observed for a fucosylated chondroitin sulfate that the susceptibility of fucosyl residues to acid hydrolysis varies depending on the sulfation pattern. But in this case, branches of nonsulfated fucose are more resistant to acid hydrolysis than the sulfated units (Kariya *et al*., 1990; Mourão *et al*., 1996). No difference has been observed in the susceptibility of different *O*-sulfate esters to acid hydrolysis. However, 2-sulfate groups can be removed from heparin with considerable selectively under certain alkaline conditions. These treatments result in loss of 2-sulfate groups without any loss of 6-sulfates (Jaseja *et al*., 1989; Rej *et al*., 1989).

Evidence that the ordered degradation of the sulfated fucan from *L. variegatus* by mild acid hydrolysis is determined by its particular pattern of sulfation (and perhaps also by the position of the glycosidic linkage) comes from similar experiments using sulfated fucans from different species of invertebrate and from brown algae (Figure 9). The particular pattern of oligosaccharides with very narrow

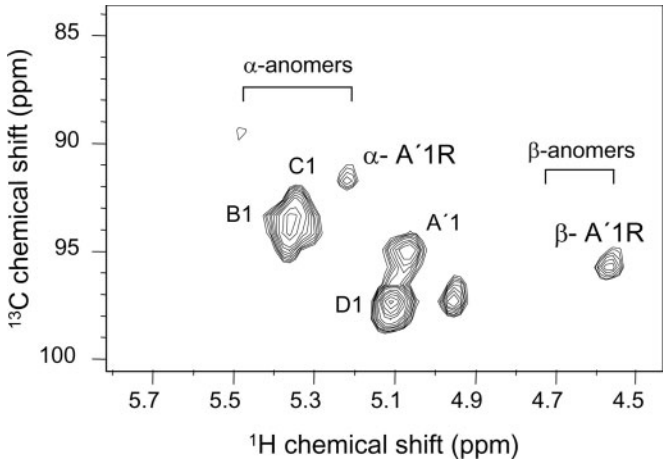

Fig. 8. Anomeric region of the ^{1}H/^{13}C HMQC spectrum of oligosaccharide II. The horizontal bars indicate the expected range of resonances for reducing α- and β-anomeric signals of nonsulfated and sulfated fucose units (see Table II). α-A´R and β-A'R are anomeric signals of nonsulfated fucose units at the reducing ends (see Figure 1D).

Table II. Chemical shifts (ppm) for anomeric ^{1}H protons and ^{13}C carbons from reducing terminals of fucosyl units of oligosaccharide II (see Figure 1D) and of standard compounds

	^{1}H chemical shifts[a]		^{13}C chemical shifts[a]	
	α-Anomer	β-Anomer	α-Anomer	β-Anomer
Oligosaccharide II	**5.20**	**4.55**	**92.0**	**96.0**
Unsulfated fucose[b]	**5.22**	**4.55**		
Unsulfated fucose[c]	**5.20**	**4.55**	**93.1**	**97.1**
Fucose 2-sulfate[c]	5.49	4.69	93.2	97.6
Fucose 3-sulfate[b]	5.26	4.65		
Fucose 3-sulfate[c]	5.26	4.66	95.1	98.9
Fucose 4-sulfate[b]	5.22	4.60		
Fucose 4-sulfate[c]	5.22	4.59	95.1	99.1
Fucose 2,4-sulfate[b]	5.49	4.73		
Fucose 3,4-sulfate[b]	5.28	4.68		

[a]The 600 MHz ^{1}H/^{13}C HMQC spectrum was recorded at 60°C. Chemical shifts are referenced to internal trimethylsilylpropionic acid at 0 ppm. Values in boldface indicate chemical shifts from nonsulfated fucosyl terminal units.
[b]Data from Mourão *et al*. (1996).
[c]Data from Daniel *et al*. (2001).

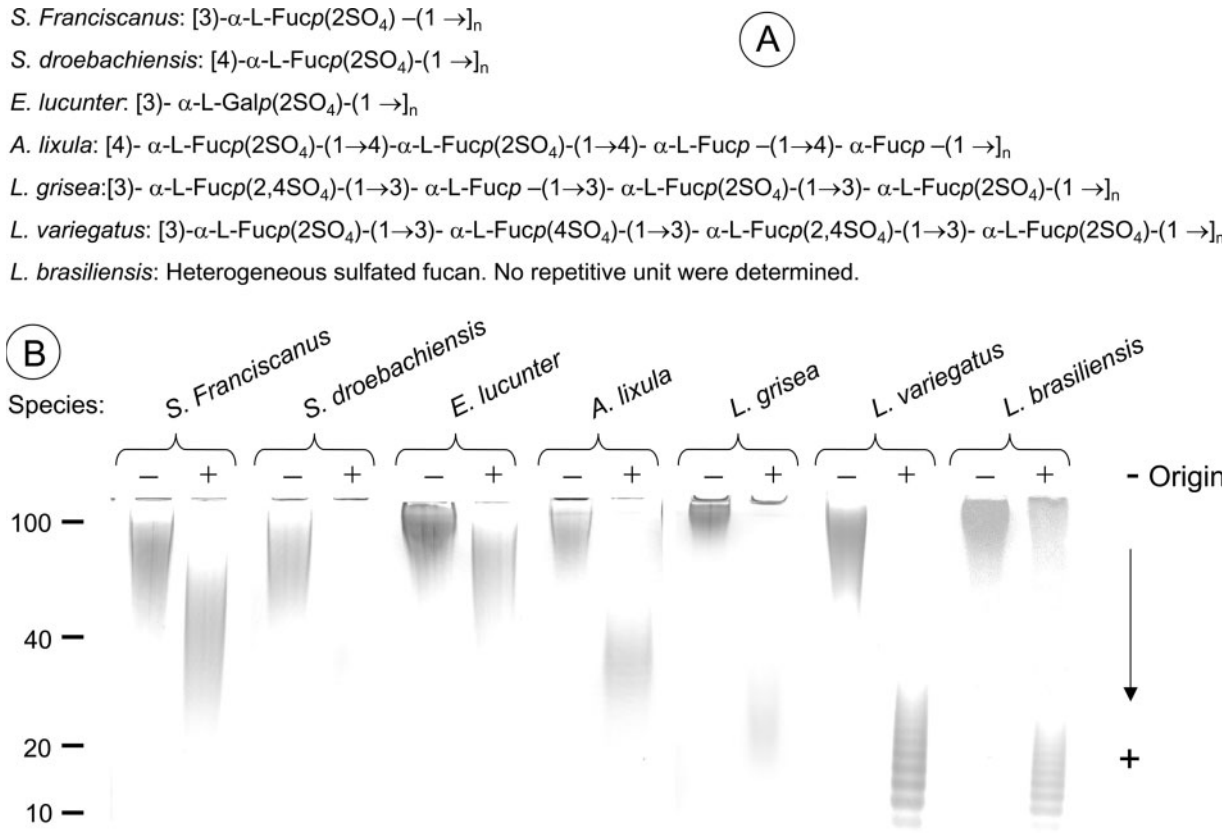

Fig. 9. Mild acid hydrolysis of sulfated fucans with different structures. (**A**) Structures of sulfated fucans and sulfated galactan used in the experiment. Sulfated polysaccharides isolated from invertebrates consist of 3- or 4-linked α-L-fucose or α-L-galactose units with 2-sulfate/4-sulfate substitution. The minimum repeating unit of each polysaccharide is shown. The sulfated fucan from the brown alga *L. brasiliensis* has not a clear repetitive unit. (**B**) the sulfated fucan (100 μg of each) was dissolved in 100 μl of distilled water (–) or aqueous 0.01 M HCl solution (+) and heated at 60°C for 6 h. The pH of the solution was then adjusted to 7.0 with the addition of 100 μl ice-cold 0.01 M NaOH. The samples (10 μg of each) were then analyzed by PAGE as described in the legend of Figure 2.

electrophoretic bands on PAGE is observed exclusively with the sulfated fucans from the sea urchin *L. variegatus* and from the brown alga *Laminaria brasiliensis*. The other sulfated fucans were either extensively digested or yielded widely dispersed electrophoretic bands, denoting a heterogeneous mixture of oligosaccharides. Therefore the ordered degradation of the sulfated fucan from *L. variegatus* is in fact determined by its particular structure.

Sulfated fucan stimulates thrombin inhibition by heparin cofactor II

The linear sulfated fucan from *L. variegatus* has an anticoagulant activity of 10 IU/mg, as evaluated by the activated partial thromboplastin time (APTT) assay standardized with the International Heparin Standard (220 IU/mg). Inhibition of thrombin by antithrombin is only marginally stimulated by the sulfated fucan (open squares in Figure 10A). As we replaced antithrombin by heparin cofactor II, the polysaccharide enhances thrombin inhibition with a sigmoid curve similar to that observed for mammalian dermatan sulfate (closed squares and closed circles in Figure 10A, respectively). However, the concentration of heparin cofactor II required to ensure the formation of an effective inhibitory complex varies significantly between assays performed with invertebrate sulfated fucan (Figure 10B) and mammalian dermatan sulfate (Figure 10C). Total thrombin inhibition occurs with 0.2 mM heparin cofactor II in the presence of mammalian dermatan sulfate, whereas ~ a fivefold higher concentration of this cofactor is required for total thrombin inhibition in the presence of the invertebrate sulfated fucan. One possibility that could explain the requirement for the higher concentration of heparin cofactor II for thrombin inhibition in the presence of sulfated fucan is that the serpin is preferentially cleaved by the protease rather than forming a covalent complex. This aspect requires future investigation.

Size dependence of the sulfated fucan required for thrombin inhibition mediated by heparin cofactor II

None of the oligosaccharides I–VI obtained by mild acid hydrolysis and purified by gel chromatography on Bio-Gel P-10 (Figure 3) show any anticoagulant activity in the APTT and the thrombin inhibition assays. Furthermore, the mixture of oligosaccharides obtained after 1 h of mild

hydrolysis, ranging from ~ 10 kDa to ~ 50 kDa (Figure 2), has only a modest anticoagulant activity (<1.0 IU/mg, based on APTT assay). These observations indicate that sulfated fucan requires fragments with longer size than mammalian dermatan sulfate to enhance thrombin inhibition by heparin cofactor II. The minimum sizes for complete thrombin inhibition in assays using mammalian dermatan sulfate (Tollefsen *et al.*, 1986) and heparin (Bray *et al.*, 1989; Sié *et al.*, 1988) are 12–14 and 26 monosaccharide units, respectively (Table III).

We further investigated this aspect using heparin cofactor II affinity chromatography. A sample of intact sulfated fucan was applied to a heparin cofactor II affinity column in buffer containing 0.05 M NaCl and eluted with 0.5 M NaCl. The elution profile of intact sulfated fucan shows a single population that is retained in the column (Figure 11A). In contrast, the fragments obtained after 1 h of mild hydrolysis

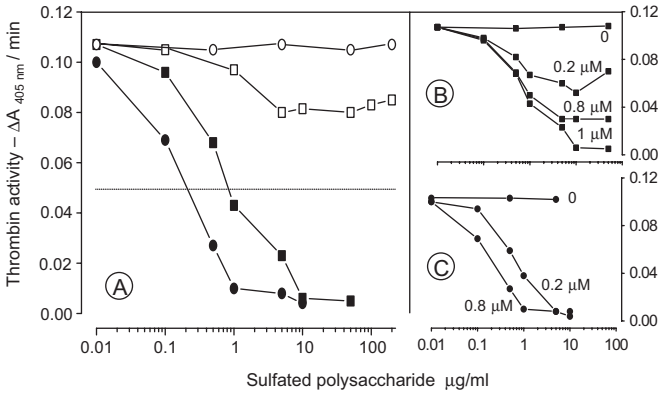

Fig. 10. Dependence on the concentration of invertebrate sulfated fucan (**A** and **B**) or mammalian dermatan sulfate (**A** and **C**) for inactivation of thrombin by heparin cofactor II (**A**–**C**) or antithrombin (**A**). (**A**) heparin cofactor II (1 µM) (closed squares, closed circles) or antithrombin (50 nM) (open squares) was incubated with thrombin in the presence of various concentrations of invertebrate sulfated fucan (closed and open squares) or mammalian dermatan sulfate (closed circles). After 60 s, the remaining thrombin activity was determined with a chromogenic substrate (A_{405nm}/min). Open circles indicate incubation with various concentrations of sulfated fucan in the absence of coagulation inhibitor. (**B** and **C**) Incubation with increasing concentrations of sulfated fucan (**B**) or dermatan sulfate (**C**) in the presence of the indicated concentrations of heparin cofactor II.

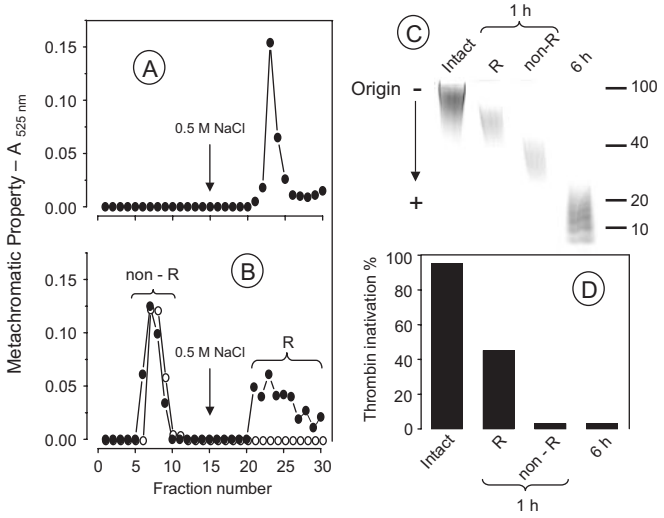

Fig. 11. Heparin cofactor II affinity chromatography of intact and low-molecular-weight sulfated fucans. (**A** and **B**) Intact sulfated fucan (**A**) and the low-molecular-weight fragments obtained after mild acid hydrolysis for 1 (closed circles in B) or 6 h (open circles) (70 µg of each) were applied to a heparin cofactor II column (HiTrap NHS-activated 1 ml, coupled with 7.3 mg heparin cofactor II). The column was washed with 15 ml 20 mM Tri-HCl (pH 7.4), 0.05 M NaCl at a flow rate of 1 ml/min. The fractions were checked for their metachromatic properties. (**C**) Fractions obtained on the affinity column of the fragments from 1 h acid hydrolysis of the sulfated fucan were pooled as indicated in **B**, desalted, and the retained (R) and nonretained (non-R) fractions, as well as the native sulfated fucan (intact) and the low-molecular-weight fragments obtained after 6 h mild hydrolysis (6 h) (10 µg of each) were run on 10% PAGE, as described in the legend of Figure 2. (**D**) Effect of the native fucan and of the retained and nonretained fractions obtained from the affinity column (**B**) on the inactivation of thrombin by heparin cofactor II. This experiment was as described in the legend of Figure 10, except that fixed concentrations of sulfated fucan (50 µg/ml) and of heparin cofactor II (1 µM) were used in the assays.

Table III. Comparison between the structural requirements for the heparin cofactor II (HCII)–mediated thrombin inhibition of sulfated fucan and mammalian glycosaminoglycans

	Sulfated fucan	Dermatan sulfate	Heparin
Structural motif for anticoagulant activity	[Fuc*p*-(4SO_4)][a]	[IdUA-(2SO_4)-GalNAc-(4SO_4)][b]	No specific structure but high charge regions of the molecule[e]
Minimum molecular size for interaction with HCII	~ 178 monosaccharide units (~ 40 kDa)[c]	6 monosaccharide units[b]	4 monosaccharide units[f]
Minimum size for complete thrombin inhibition	~ 408 monosaccharide units (~ 100 kDa)[c]	12–14 monosaccharide units[d]	26 monosaccharide units[g]

[a]See Pereira *et al.* (2002).
[b]See Maimone and Tollefsen (1990).
[c]We calculated the number of monosaccharide units for sulfated fucan activity assuming 901 and 980 Da as the molecular weight of tetrasaccharide repeating units of the degraded and native sulfated fucan, respectively (see Figure 1B).
[d]See Tollefsen *et al.* (1986).
[e]See Hurst *et al.* (1983) and Maimone and Tollefsen (1988).
[f]See Maimone (1990).
[g]See Sié *et al.* (1988) and Bray *et al.* (1989).

were heterogeneous, because only part of the oligosaccharides were retained on the column (closed circles in Figure 11B). On the other hand, the fragments obtained after 6 h of mild acid hydrolysis of the sulfated fucan do not bind at all to the heparin cofactor II affinity column (open circles in Figure 11B).

The molecular size of the oligosaccharides obtained from the heparin cofactor II column was determined by PAGE (Figure 11C). Clearly, binding of the sulfated fucan to heparin cofactor II depends on the molecular size. A comparison of the ability of the retained and nonretained fragments of sulfated fucan to stimulate thrombin inhibition by heparin cofactor II is shown in Figure 11D. We tested a single concentration of oligosaccharide due to the small amount of available material. Under the conditions of this assay, total inhibition of thrombin activity occurs in the presence of 50 μg/ml of intact sulfated fucan. But the retained oligosaccharides cause inhibition of only ~ 45% of the thrombin activity even at high concentration of heparin cofactor II (1.0 mM), whereas no inhibition of thrombin occurs in the presence of the nonretained oligosaccharides. In control experiments, neither the retained nor the nonretained oligosaccharides inhibit thrombin in the absence of heparin cofactor II. These results indicate that the oligosaccharides retained on the heparin cofactor II affinity column (average molecular weight of ~ 40 kDa) are less effective than the native fucan (average molecular weight of ~ 100 kDa) on thrombin inhibition.

The experiments based on the interaction of sulfated fucan oligosaccharides with heparin cofactor II-Sepharose were limited by the saturation of the heparin cofactor II affinity column with a very low amount of the carbohydrate (~ 70 μg). Therefore, we explored an alternative approach to obtain larger amounts of oligosaccharides with different activities toward heparin cofactor II. We initially prepared sulfated fucan oligosaccharides with different molecular size by gel chromatography (Figure 12A and B) and then tested the effect of the various fractions on thrombin inhibition assays (Figure 12C). In fact, we obtained fractions of oligosaccharides with molecular size similar to those from the heparin cofactor II affinity column (Figure 12B). Again, in contrast with the native sulfated fucan, which achieves total thrombin inhibition at a concentration of ~ 10 μg/ml (closed circles in Figure 12C), the sulfated fucan oligosaccharides with average size of ~ 40 kDa causes only 30% thrombin inhibition in the presence of heparin cofactor II even at a concentration of 100 μg/ml (closed squares in Figure 12C). No inhibition of thrombin occurs in the presence of oligosaccharides with molecular size lower than ~ 40 kDa (open circles in Figure 12C).

Overall, a linear sulfated fucan requires significantly longer chains than mammalian glycosaminoglycans to achieve complete thrombin inhibition with heparin cofactor II. Thus dermatan sulfate and heparin require 6 and 4 monosaccharide units to bind heparin cofactor II, respectively, whereas sulfated fucan needs ~ 178 monosaccharide units for this interaction (Table III). Furthermore, a slight decrease in the molecular size of the sulfated fucan dramatically reduces its effect on thrombin inhibition in the presence

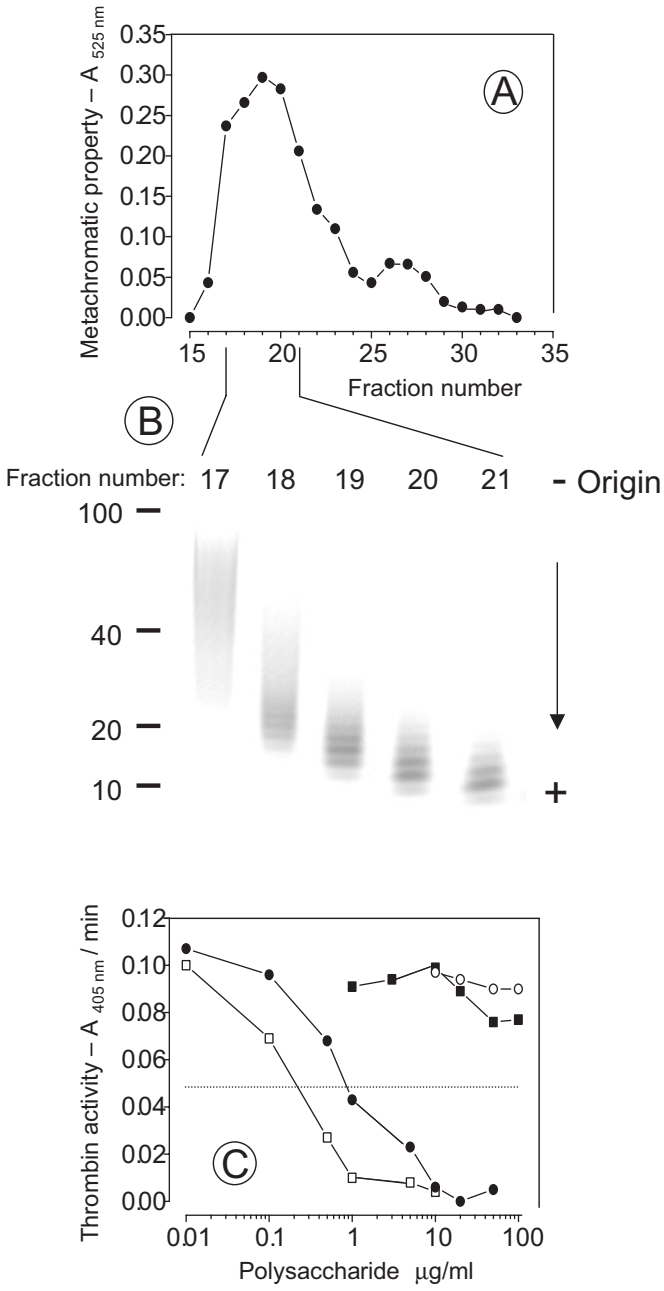

Fig. 12. Gel chromatography of the low-molecular-weight fragments from sulfated fucan (**A**), estimation of the molecular weight of the fractions (**B**), and determination of their effect on thrombin inhibition mediated by heparin cofactor II (**C**). (**A**) The low-molecular-weight derivatives obtained after 1 h of mild acid hydrolysis of the sulfated fucan (3 mg) were separated on an Superdex Peptide-HPLC. (**B**) The fractions from the column (10 μg of each) were analyzed on a 10% PAGE, as described in the legend of Figure 2. (**C**) Inactivation of thrombin in the presence of heparin cofactor II by fraction 17 (average molecular weight ~ 50 kDa) (closed squares), fraction 18 (average molecular weight ~ 30 kDa) (open circles), intact invertebrate sulfated fucan (closed circles), and mammalian dermatan sulfate (open squares). The assays were as described in the legend of Figure 10, using 1 μM heparin cofactor II.

of heparin cofactor II. Sulfated fucan of ~ 40 kDa binds to heparin cofactor II but is unable to efficiently stimulate the thrombin–heparin cofactor II reaction. This last effect

requires a molecular size = ~ 100 kDa (~ 408 monosaccharide units).

Possibility that the heparin cofactor II–dependent anticoagulant activity of the sulfated fucan is related to a rare and specific local structure in the polysaccharide chain

An aspect we need to consider is related to the possibility that the anticoagulant activity of the sulfated fucan is related to a rare and specific structure in the polysaccharide chain, rather than to the bulk pattern of sulfation. This point has been well clarified in the case of mammalian glycosaminoglycans (Conrad, 1998). Thus heparin preparations with similar bulk structure may vary in their antithrombin-dependent anticoagulant activity due to different proportions of a specific pentasaccharide sequence, which is almost undetectable on analysis of the native molecule (Conrad, 1998; Lindahl *et al.*, 1983; Thumberg *et al.*, 1982). If this is the case for the binding of sulfated fucan to heparin cofactor II, we would expect at least one binding site in the ~ 100-kDa native polymer, because the polysaccharide is totally retained on the heparin cofactor II affinity column (Figure 11A). If the average molecular size decreases to ~ 40 kDa and ~ 10 kDa after 1 and 6 h mild acid hydrolysis by random cleavage, ~ 50% and ~ 10% of the sulfated fucan should be retained on the affinity column, respectively. Certainly this is not the case for the sulfated fucan (Figure 11B). Furthermore, we would not expect a molecular size dependence for the retention of sulfated fucan on the heparin cofactor II affinity column, as in Figure 11C, if the binding is related to a specific local structure rather than to the bulk sulfation pattern.

Another possibility is that a specific sequence of oligosaccharide is selectively removed from the sulfated fucan during mild acid hydrolysis. Unless the oligosaccharide is located at the reducing or nonreducing ends, mild acid hydrolysis must be selective for the two linkages at the extreme ends of the oligosaccharide. Furthermore, the released oligosaccharide must be inactive; otherwise, we would detect significant anticoagulant activity on the mixtures obtained after 1 or 6 h hydrolysis. Finally, PAGE should reveal minor components formed in the course of mild hydrolysis besides those related to the tetrasaccharide repeating unit of the sulfated fucan (Figures 2 and 3).

Finally, we may consider that the rare and specific sequence is constituted by a fucose unit with a particular sulfation pattern, which is extremely labile to acid hydrolysis. However, we already demonstrated that 4-sulfated fucans, but not 2-sulfated ones, are heparin cofactor II–dependent anticoagulant polysaccharides (Pereira *et al.*, 2002). It is unlikely that a rare and active sulfation sequence is always present in 4-sulfated fucans and absent in the 2-sulfated ones.

Therefore our observations suggest that the heparin cofactor II–dependent anticoagulant activity of the linear sulfated fucan is in fact related to the bulk structure, rather than to a rare and specific oligosaccharide sequence. Of course, to provide unequivocal evidence for this, we would have to make a synthetic polymer and show that it had the same properties as the natural polysaccharide. This is not a feasible experiment due to the highly complex nature of the sulfated fucans.

Speculation concerning the mechanism of anticoagulant action of the sulfated fucan

It is well established that dermatan sulfate and heparin accelerate thrombin inactivation by heparin cofactor II through an allosteric mechanism in which the acidic N-terminal domain of the coagulation inhibitor interacts with exosite I of thrombin (Hortin *et al.*, 1989; Mitchell and Church, 2002; Ragg *et al.*, 1990; Rogers *et al.*, 1992; Van Deerlin and Tollefsen, 1991). In a more recent study (Verhamme *et al.*, 2004), it was proposed that the inactivation mechanism combines this allosteric effect with a template mechanism in which the glycosaminoglycan forms a temporary noncovalent ternary complex with the protease and the inhibitor. The template effect involves the preferential formation of a thrombin–glycosaminoglycan complex, which then interacts with heparin cofactor II rather than a cofactor–glycosaminoglycan interaction with thrombin (Verhamme *et al.*, 2004). A template mechanism was also proposed for the antithrombin-dependent anticoagulant activity of low-affinity heparin, that is, heparin fragments devoid of the specific pentasaccharide sequence with high affinity for antithrombin (Streusand *et al.*, 1995). It is still unclear what is the contribution of the allosteric and of the template effect to the overall mechanism of glycosaminoglycan-catalyzed thrombin inactivation by heparin cofactor II.

We hypothesize that linear sulfated fucan requires significantly longer chains than mammalian glycosaminoglycans to efficiently inactivate thrombin through heparin cofactor II because the template mechanism predominates over the allosteric effect in the case of the invertebrate polysaccharide. We already proposed a similar effect for sulfated galactan inactivation of thrombin mediated by antithrombin. In this case, the activation conformational change in antithrombin is less important for the anticoagulant activity of sulfated galactan than for heparin (Melo *et al.*, 2004).

We also speculate that different mechanisms may be involved in the action of sulfated fucan on heparin cofactor II–mediated thrombin inactivation. The polysaccharide may hold together more than one molecule of the protease and/or of the plasma cofactor in a noncovalent complex. In this case, the efficacy can be attributed to the longer chains that occur in the sulfated fucan. In fact, the observation that higher concentrations of heparin cofactor II are required for effective thrombin inactivation by sulfated fucan than by mammalian dermatan sulfate (Figure 10) suggests different stoichiometries for the reactions catalyzed by these two polysaccharides.

Our results concerning the heparin cofactor II–mediated anticoagulant activity of sulfated fucan may help design new drugs with specific actions on coagulation and thrombosis. Furthermore, this sulfated polysaccharide may be used as a research reagent to clarify different mechanisms for thrombin inactivation, which remain obscure in the case of mammalian glycosaminoglycans.

Materials and methods

Sulfated fucan

Eggs from mature females of the sea urchins were spawned into filtered sea water after intracelomic injection of 0.5 M KCl (~ 5 ml per specimen). The egg jelly was separated by pH shock, as described previously (SeGall and Lennarz, 1979). Sulfated polysaccharides were extracted from the egg jelly by protease digestion (Albano and Mourão, 1986). Sulfated fucans were purified by anion exchange chromatography, and their purity was checked by agarose gel electrophoresis and NMR spectroscopy (Alves *et al*., 1997, 1998; Vilela-Silva *et al*., 1999, 2002). A sulfated fucan from the brown alga *L. brasiliensis* was prepared as described (Pereira *et al*., 1999).

Depolymerization of sulfated fucan by mild acid hydrolysis

Sulfated fucan (10 mg) was dissolved in 1.25 ml 0.01 M HCl and maintained at 60°C for different periods of time. The pH of the solution was then adjusted to 7.0 with the addition of ~ 1.25 ml ice-cold 0.01 M NaOH. The products formed in the course of the mild acid hydrolysis were separated by gel chromatography and analyzed by PAGE, as described shortly.

Gel filtration chromatography

The products formed in the course of the mild acid hydrolysis of the sulfated fucan (2 mg) were applied to a Superose-6 (HR 10/30) column (Amersham Biosciences, Little Chalfont, U.K.), linked to a high-pressure liquid chromatography (HPLC) system from Shimadzu (Tokyo), equilibrated with 0.2 M NH_4HCO_3 (pH 8.0). The column was eluted with the same solution at a flow rate of 0.5 ml/min, and fractions of 0.5 ml were collected and assayed by metachromasia using 1,9-dimethylmethylene blue (Farndale *et al*., 1986) and by phenol–sulfuric acid reaction (Dubois *et al*., 1956). The fractions containing the low-molecular-weight sulfated fucans were pooled and freeze-dried.

The oligosaccharides formed after 6 or 9 h of mild acid hydrolysis of the sulfated fucan (5 mg) were fractionated on a Bio-Gel P-10 (Bio-Rad Laboratories, Hercules, CA) column (200 × 0.9 cm), equilibrated with aqueous 10% ethanol, containing 1.0 M NaCl. The column was eluted with the same solution at a flow rate of ~ 3 ml/h and fractions of 1.0 ml were collected and assayed by metachromasia using 1,9-dimethylmethylene blue (Farndale *et al*., 1986) and by the phenol–sulfuric acid reaction (Dubois *et al*., 1956). The elution volume of blue dextran and cresol red indicates the V_o and V_t of the column, respectively. The fractions containing the various oligosaccharides (as indicated by the positive metachromatic assay) were pooled, freeze-dried, and dissolved in 2.0 ml distilled water. These solutions were desalted on Superdex peptide column (Amersham Biosciences, Piscataway, NJ), linked to a HPLC system. Fractions of 0.5 ml were collected and their conductivities determined. The oligosaccharides were detected by metachromasia (Farndale *et al*., 1986). Fractions containing the desalted oligosaccharides were pooled and freeze-dried.

PAGE

The native and low-molecular-weight derivatives of the sulfated fucan (10 μg of each) were applied to a 10% 1-mm-thick polyacrylamide gel slab in 0.02 M sodium barbital (pH 8.6) and run for 30 min at 100 V. After electrophoresis the sulfated fucans were stained with 0.1% toluidine blue in 1% acetic acid and washed for about 4 h in 1% acetic acid. The molecular masses of the low-molecular-weight fragments of the sulfated fucan were estimated by comparison with the electrophoretic mobility of standard compounds (Pavao *et al*., 1998; Pereira *et al*., 1999; Sautos *et al*., 1992). The standards used were high-molecular-weight dextran sulfate (≥ ~100 kDa), chondroitin 4-sulfate from bovine trachea (~ 40 kDa), dermatan sulfate from pig skin (~ 20 kDa), and low-molecular-weight dextran sulfate (~ 10 kDa).

NMR experiments

^1H and ^{13}C spectra of the native sulfated fucan and its low-molecular-weight derivatives were recorded using a Bruker DRX 600 apparatus with a triple resonance probe. About 3 mg of each sample was dissolved in 0.5 ml 99.9% D_2O (Cambridge Isotope Laboratory, Cambridge, MA). All spectra were recorded at 60°C with HOD suppression by presaturation. In some experiments sulfated fucan (3 mg) was dissolved in 0.5 ml 0.01 M HCl, prepared in 99.9% D_2O. The solution was put into an NMR tube and maintained at 60°C; 1D ^1H-NMR spectra were recorded from 10 min to 6 h. Correlation spectroscopy, TOCSY, and $^1H/^{13}C$ HMQC spectra were recorded using states-time proportion phase incrementation for quadrature detection in the indirect dimension. TOCSY spectra were run with 4046 × 400 points with a spin-lock field of ~ 10 kHz and a mixed time of 80 ms. HMQC spectra were run with 1024 × 256 points and globally optimized alternating phase rectangular pulses for decoupling. Chemical shifts are relative to external trimethylsilylpropionic acid at 0 ppm for ^1H and to methanol for ^{13}C.

Anticoagulant activity measured by APTT

APTT clotting assays were carried out by the method of Anderson *et al*. (1976) using normal human plasma. In these assays, plasma samples (90 μl) were mixed with different amounts of sulfated polysaccharide in 0.9% NaCl (10 μl), warmed for 60 s at 37°C and then 100 μl prewarmed APTT reagent (Biomerieux, Rio de Janiero, Brazil) was added and allowed to incubate for 2 min at 37°C. Prewarmed 0.25 M $CaCl_2$ (100 μl) was then added, and the APTT recorded as the time for clot formation in a coagulometer (Amelung KC4A, Lemgo, Gemany). The activity was expressed as IU/mg using a parallel standard curve based on the fourth International Heparin Standard (220 U/mg) from the National Institute for Biological Standards and Control (Potters Bar, U.K.).

Inhibition of thrombin by heparin cofactor II or antithrombin in the presence of sulfated fucan

Incubations were performed in disposable UV semi-microcuvettes. The final concentrations of the reactants included 0.2–1.0 μM plasma-derived heparin cofactor II or 50 nM antithrombin, 15 nM bovine thrombin, and 0–1000 μg/ml sulfated fucan in 50 or 100 ml TS/PEG buffer

(0.02 M Tris–HCl, 0.15 M NaCl, and 1 μg/ml polyethyleneglycol, pH 7.4). Thrombin was added last to initiate the reaction. After a 60-s incubation at room temperature, 250 or 500 μl TS/PEG buffer containing 100 μM chromogenic substrate S-2238 (Chromogenix AB, Mondal, Sweden) was added, and the absorbance at 405 nm was recorded for 120 s. The change of absorbance was proportional to the thrombin activity remaining in the incubation. No inhibition occurred in control experiments in which thrombin was incubated with heparin cofactor II or antithrombin in the absence of sulfated fucan. In addition, no inhibition was observed when thrombin was incubated with sulfated fucan alone over the range of concentration tested.

Heparin cofactor II affinity chromatography

HiTrap NHS activated HP (5 ml) from Amersham Bioscience was mixed with 7.3 mg heparin cofactor II dissolved in 5 ml 200 mM $NaHCO_3$, containing 50 mM NaCl (pH 8.3), and coupling was carried out as described by the manufacturer. The immobilized heparin cofactor II maintained its expected binding specificities, because a dermatan sulfate sample with a high heparin cofactor II activity, obtained from the ascidia *Styela plicata* (Pavão *et al.*, 1998), bound to the heparin cofactor II affinity column, whereas both a dermatan sulfate with no heparin cofactor II activity, obtained from the ascidian *Ascidia nigra* (Pavão *et al.*, 1998), and vertebrate chondroitin 4-sulfate did not bind to the heparin cofactor II column. Intact sulfated fucan and its low-molecular-weight fragments (70 μg of each) were applied to the heparin cofactor II affinity column, preequilibrated with 20 mM Tris–HCl (pH 7.4), 0.05 M NaCl. The column was washed with 15 ml of the equilibrating buffer and the bound material eluted with 15 ml 20 mM Tris–HCl (pH 7.4), 0.5 M NaCl at a flow rate of 1.0 ml/min. Fractions of 1.0 ml were collected and analyzed for metachromasia using 1,9-dimethylmethylene blue (Farndale *et al.*, 1986). Under these conditions, all the bound polysaccharide still bound when reapplied to the column. The retained and nonretained fractions were desalted on a 5-ml HiTrap Desalting column (Amersham Biosciences), freeze dried and dissolved in ~ 0.1 ml of distilled water.

Acknowledgments

This investigation was supported by grants from Conselho Nacional de Desenvolvimento Científico e Tecnológico (CNPq), Fundação de Amparo à Pesquisa do Estado do Rio de Janeiro (FAPERJ), and the NIH Fogarty International Center (R03 TW05775). We are grateful to Adriana A. Piquet and Francisco Gomes Neto for technical assistance.

Abbreviations

APTT, activated partial thromboplastin time; HMQC, heteronuclear multiple quantum correlation spectroscopy; HPLC, high-pressure liquid chromatography; NMR, nuclear magnetic resonance; PAGE, polyacrylamide gel electrophoresis; TOCSY, total correlation spectroscopy.

References

Albano, R.M. and Mourão, P.A.S. (1986) Isolation, fractionation, and preliminary characterization of a novel class of sulfated glycans from the tunic of *Styela plicata* (Chordata, Tunicata). *J. Biol. Chem.*, **261**, 758–765.

Alves, A.P., Mulloy, B., Diniz, J.A., and Mourão, P.A.S. (1997) Sulfated polysaccharides from the egg jelly layer are species-specific inducers of acrosomal reaction in sperms of sea urchins. *J. Biol. Chem.*, **272**, 6965–6971.

Alves, A.P., Mulloy, B, Moy, G.W., Vacquier, V.D., and Mourão, P.A.S. (1998) Females of the sea urchin *Strongylocentrotus purpuratus* differ in the structures of their egg jelly sulfated fucans. *Glycobiology*, **8**, 939–946.

Anderson, L.O., Barrowcliffe, T.W., Holmer, E., Johnson, E.A., and Sims, G.E.C. (1976) Anticoagulant properties of heparin fractionated by affinity chromatography on matrix-bound antithrombin III and by gel filtration. *Thromb. Res.*, **9**, 575–580.

Berteau, O. and Mulloy, B. (2003) Sulfated fucans, fresh perspectives: structures, functions, and biological properties of sulfated fucans and an overview of enzymes active toward this class of polysaccharide. *Glycobiology*, **13**, 29R–40R.

Bray, B., Lane, D.A., Freyssinet, J-M., Pejler, G., and Lindahl, U. (1989) Antithrombin activities of heparin. Effect of saccharide chain length on thrombin inhibition by heparin cofactor II and by antithrombin. *Biochem. J.*, **262**, 225–232.

Conrad, H.E. (1998) *Heparin-binding proteins*. Academic Press, New York, pp. 203–238.

Daniel, R., Berteau, O., Jozefonvicz, J., and Goasdoue, N. (1999) Degradation of algal (*Ascophyllum nodosum*) fucoidan by an enzymatic activity contained in digestive glands of the marine mollusc *Pecten maximus*. *Carbohydr. Res.*, **322**, 291–297.

Daniel, R., Berteau, O., Chevolot, L., Varenne, A., Gareil, P., and Goasdoue, N. (2001) Regioselective desulfation of sulfated fucopyranoside by a new sulfoesterase from the marine mollusk *Pecten maximus.* Application to the structural study of algal fucoidan (*Ascophyllum nodosum*). *Eur. J. Biochem.*, **268**, 5617–5626.

Dubois, M., Gilles, K.A., Hamilton, J.K., Rebers, P.A., and Smith, F. (1956) Colorimetric method for determination of sugars and related substances. *Anal. Chem.*, **28**, 350–354.

Farndale, R.W., Buttle, D.J., and Barret, A.J. (1986) Improved quantification and discrimination of sulphated glycosaminoglycans by use of dimethylmethylene blue. *Biochim. Biophys. Acta*, **883**, 173–177.

Furukawa, S.I., Fujikawa, T., Koga, D., and Ide, A. (1992a) Growth and fucoidan sulfatase production in fucoidan-utilizing bacteria from sea sand. *Biosci. Biotech. Biochem.*, **56**, 1829–1834.

Furukawa, S.I., Fujikawa, T., Koga, D., and Ide, A. (1992b) Production of fucoidan-degrading enzymes, fucoidanas and fucoidan sulfatase by *Vibrio sp*. N-5. *Nippon Suisan Gakk.*, **58**, 1499–1503.

Hortin, G.L., Tollefsen, D.M., and Benutto, B.M. (1989) Antithrombin activity of a peptide corresponding to residues 54–75 of heparin cofactor II. *J. Biol. Chem.*, **264**, 13979–13982.

Hurst, R.E., Poon, M-C., and Griffith M.J. (1983) Structure-activity relationships of heparin. Independence of heparin charge density and antithrombin-binding domains in thrombin inhibition by antithrombin and heparin cofactor II. *J. Clin. Invest.*, **72**, 1042–1045.

Jaseja, M., Rej, R., Sauriol, F., and Perlin, A.S. (1989) Novel region- and stereoselective modifications of heparin in alkaline solution: nuclear magnetic resonance spectroscopic Evidence *Can. J. Chem.*, **67**,1449–1456.

Kariya, Y., Watabe, S., Hashimoto, K., and Yoshida, K. (1990) Occurrence of chondroitin sulfate E in glycosaminoglycan isolated from the body wall of sea cucumber *Stichopus japonicus*. *J. Biol. Chem.*, **265**, 5081–5085.

Kitamura, K., Matsuo, M., and Yasui, T. (1992) Enzimic degradation of Fucoidan by Fucoidanase from the hepatopancreas of *Patinopecten yessoensis*. *Biosci. Biotech. Biochem.*, **56**, 490–494.

Lindahl, U., Backström, G., and Thumberg, L. (1983) The antithrombin-binding sequence in heparin. Identification of an essential 6-O-sulfate group. *J. Biol. Chem.*, **258**, 9826–9830.

Lloyd, P.F., Lloyd, K.O., and Owen, O. (1962) Carbohydrate sulphatases of marine molluscs. Assay of glycosulphatases. *Biochem. J.,* **85**, 193–198.

Maimone, M.M. (1990) Characterization of heparin and dermatan sulfate molecules that bind and activate Heparin cofactor II. Ph.D. diss., Washington University, St. Louis.

Maimone, M.M. and Tollefsen, D.M. (1988) Activation of heparin cofactor II by heparin oligosaccharides. *Biochem. Biophys. Res. Commun.*, **152**, 1056–1061.

Maimone, M.M. and Tollefsen, D.M. (1990) Structure of a dermatan sulfate hexasaccharide that binds to heparin cofactor II with high affinity. *J. Biol. Chem.*, **265**, 18263–18271.

Melo, F.R., Pereira, M.S., Foguel, D., and Mourão, P.A.S. (2004) Antithrombin-mediated anticoagulant activity of sulfated polysaccharides: different mechanisms for heparin and sulfated galactans. *J. Biol. Chem.*, **279**, 20824–20835.

Mitchell, J.W. and Church, F.C. (2002) Aspartic acid residues 72 and 75 and tyrosine-sulfate 73 of heparin cofactor II promote intramolecular interactions during glycosaminoglycan binding and thrombin inhibition. *J. Biol. Chem.*, **277**, 19823–19830.

Mourão, P.A.S. (2004) Use of sulfated fucans as anticoagulant and antithrombotic agents: future perspectives. *Curr. Pharm. Des.*, **10**, 967–981.

Mourão, P.A.S., Pereira, M.S., Pavão, M.S.G., Mulloy, B., Tollefsen, D.M., Mowinckel, M.C., and Abildgaard (1996) Structure and anticoagulant activity of a fucosylated chondroitin sulfate from echinoderm. Sulfated fucose branches on the polysaccharide account for its high anticoagulant action. *J. Biol. Chem.*, **271**, 23973–23984.

Pavão, M.S.G., Aiello, K.R.M., Werneck, C.C., Silva, L.C.F., Valente, A.P., Mulloy, B., Colwell, N.S., Tollefsen, D.M., and Mourão, P.A.S. (1998) Highly sulfated dermatan sulfate from Ascidians: structure versus anticoagulant activity of these glycosaminoglycans. *J. Biol. Chem.*, **273**, 27848–27857.

Pereira, M.S., Mulloy, B., and Mourão, P.A.S. (1999) Structure and anticoagulant activity of sulfated fucans. Comparison between the regular, repetitive and linear fucans from echinoderms with the more heterogeneous and branched polymers from brown algae. *J. Biol. Chem.*, **274**, 7656–7667.

Pereira, M.S., Melo, F.R., and Mourão, P.A.S. (2002) Is there a correlation between structure and anticoagulant action of sulfated galactans and sulfated fucans? *Glycobiology*, **12**, 573–580.

Ragg, H., Ulshöfer, T., and Gerewitz, J. (1990) Glycosaminoglycan-mediated leuserpin-2/thrombin interaction. Structure-function relationships. *J. Biol. Chem.*, **265**,22386–22391.

Rej, R., Jaseja, M., and Perlin, A.S. (1989) Importance for blood anticoagulant activity of a 2-sulfate group on L-iduronic acid residues in heparin. *Thromb. Haemostas.*, **61**, 540–541.

Rogers, S.J., Pratt, C.W., Whinna, H.C., and Church, F.C. (1992) Role of thrombin exosites in inhibition by heparin cofactor II. *J. Biol. Chem.*, **267**, 3613–3617.

Santos, J.A., Mulloy, B., and Mourão, P.A.S. (1992) Strutural diversity among sulfated a-L-galactans from ascidians (tunicates): studies on the species *Ciona intestinalis* and *Herdmania monus*. *Eur. J. Biochem.*, **204**, 669–677.

SeGall, G.K. and Lennarz, W.L. (1979) Jelly coat and induction of the acrosome reaction in echinoid sperm. *Dev. Biol.*, **71**, 33–48.

Sié, P., Petitou, M., Lormeau, J-C., Dupouy, D., Boneu, B., and Choay, J. (1988) Studies on the structural requirements of heparin for the catalysis of thrombin inhibition by heparin cofactor II. *Biochim. Biophys. Acta*, **966**, 188–195.

Streusand, V.J., Björk, I., Gettins, P.G.W., Petitou, M., and Olson, S.T. (1995) Mechanism of acceleration of antithrombin-proteinase reactions by low affinity heparin. *J. Biol. Chem.*, **270**, 9043–9051.

Thumberg, L., Backström, G., and Lindahl, U. (1982) Further characterization of the antithrombin-binding sequence in heparin. *Carbohydr. Res.*, **100**, 393–410.

Tollefsen, D.M., Peacock, M.E., and Monafo, W.J. (1986) Molecular size of dermatan sulfate oligosaccharides required to bind and activate heparin cofactor II. *J. Biol. Chem.*, **262**, 8854–8858.

Van Deerlin, V.M.D. and Tollefsen, D.M. (1991) The N-terminal acidic domain of heparin cofactor II mediates the inhibition of a-thrombin in the presence of glycosaminoglycans. *J. Biol. Chem.*, **266**, 20223–20231.

Verhamme, I.M., Bock, P.E., and Jackson, C.M. (2004) The preferred pathway of glycosaminoglycan-accelerated inactivation of thrombin by heparin cofactor II. *J. Biol. Chem.*, **279**, 9785–9795.

Vilela-Silva, A.C.E.S., Alves, A.P., Valente, A.P., Vacquier, V.D., and Mourão, P.A.S. (1999) Structure of the sulfated α-L-fucan from the egg jelly coat of the sea urchin *Strongylocentrotus franciscanus:* patterns of preferential 2-*O*- and 4-*O*-sulfation determine sperm cell recognition. *Gycobiology*, **9**, 927–933.

Vilela-Silva, A.C.E.S., Castro, M.O., Valente, A.P., Biermann, C.H., and Mourão, P.A.S. (2002) Sulfated fucans from the egg jellies of the closely related sea urchins *Strongylocentrotus droebachiensis* and *Strongylocentrotus pallidus* ensure species-specific fertilization. *J. Biol. Chem.*, **277**, 379–387.

2.6.2 Artigo III

Glycobiology
Vol. 15 No 12, pp 1376-1385, 2005b

"Mild acid hydrolysis of sulfated fucans: a selective 2-desulfation reaction and an alternative approach for preparing tailored sulfated oligosaccharides."

Vitor H. Pomin, Ana-Paula Valente, Mariana S. Pereira e Paulo A.S. Mourão

Glycobiology vol. 15 no. 12 pp. 1376–1385, 2005
doi:10.1093/glycob/cwj030
Advance Access publication on August 23, 2005

Mild acid hydrolysis of sulfated fucans: a selective 2-desulfation reaction and an alternative approach for preparing tailored sulfated oligosaccharides

Vitor H. Pomin[2,3], Ana Paula Valente[3,4], Mariana S. Pereira[2,5], and Paulo A.S. Mourão[1,2,3]

[2]Laboratório de Tecido Conjuntivo, Hospital Universitário Clementino Fraga Filho; [3]Instituto de Bioquímica Médica; [4]Centro Nacional de Ressonância Magnética Nuclear Jiri Jonas; and [5]Instituto de Ciências Biomédicas, Universidade Federal do Rio de Janeiro, Caixa Postal 68041, Rio de Janeiro, RJ 21941-590, Brazil

Received on June 14, 2005; revised on August 1, 2005; accepted on August 17, 2005

Sulfated fucans from marine invertebrates have simple, linear structures, composed of repeating units of oligosaccharides. Most of these polysaccharides contain 3-linked fucosyl units, but each species of invertebrate has a specific pattern of sulfation. No specific enzyme able to cleave or to desulfate these polysaccharides has been described yet. Therefore, we employed an alternative approach, based on mild acid hydrolysis, in an attempt to obtain low molecular-weight derivatives from sulfated fucans. Surprisingly, we observed that sulfated fucans from *Lytechinus variegatus* and *Strongylocentrotus pallidus* (but not the sulfated fucans from other species) yield by mild acid hydrolysis oligosaccharides with well-defined molecular size as shown by narrow bands in polyacrylamide gel electrophoresis (PAGE). The sulfated oligosaccharides obtained by mild acid hydrolysis were purified by gel-filtration chromatography, and their structures were identified by ^{1}H-nuclear magnetic resonance (NMR) spectroscopy, revealing an identical chemical composition for all oligosaccharides. When we followed the acid hydrolysis by ^{1}H-NMR spectroscopy, we found that a selective 2-desulfation occurs in the fucans from *S. pallidus* and from *L. variegatus*. The reaction has two stages. Initially, 2-sulfate esters at specific sites are removed. Then the desulfated units are cleaved, yielding oligosaccharides with well-defined molecular size. The apparent requirement for the selective 2-desulfation is the occurrence of an exclusively 2-sulfated fucosyl unit linked to or preceded by a 4-sulfated residue. Thus, a homofucan from *Strongylocentrotus franciscanus* resists desulfation by mild acid hydrolysis, because it lacks the neighboring 4-sulfated unit. Overall, our results show a new approach for desulfating sulfated fucans at specific sites and obtaining tailored sulfated oligosaccharides.

[1]To whom correspondence should be addressed; e-mail: pmourao@hucff.ufrj.br

Key words: depolymerization/low molecular-weight fucans/sea urchin/specific desulfation/sulfated polysaccharides

Introduction

Sulfated fucans are among the most widespread nonmammalian-sulfated polysaccharides distributed in nature. They occur in algae (Percival and McDowell, 1967; Nishino *et al*., 1991) and marine invertebrates, particularly in echinoderms, such as sea cucumbers (Mourão and Bastos, 1987; Vieira and Mourão, 1988) and sea urchins (SeGall and Lennarz, 1979, 1981; Glabe *et al*., 1982). In the case of the sea urchins, such compounds are extracted from the egg jelly layer of female gametes. These sulfated polysaccharides are composed of simple, linear structures, and repeated units that differ principally in the pattern of sulfation. Several of these sulfated fucans have the $\alpha(1\rightarrow3)$-glycosidic linkage between 2-, 4-, and 2,4-sulfated fucopyranose residues (Mulloy *et al*., 1994; Alves *et al*., 1998; Pereira *et al*., 1999; Vilela-Silva *et al*., 1999, 2002). These singular structural characteristics confer an opportunity on the sulfated α-L-fucans of marine invertebrates to reveal the mechanism of their biological actions (Mourão and Pereira, 1999; Pereira *et al*., 1999; Hirohashi *et al*., 2002). On the other hand, algal-sulfated fucans are difficult tools for studying the biological activities because of their complex and heterogeneous structures (Pereira *et al*., 1999; Berteau and Mulloy, 2003; Mourão, 2004).

In addition to the simplicity of structures, the possibility of preparing low molecular-weight derivatives from the sulfated fucans of echinoderms makes it simple to study the relation between molecular size and biological activity (Pomin *et al*., 2005; Matsubara *et al*., 2005). However, a limited number of techniques for molecular reduction have been described. The enzymes that cleave the sulfated polysaccharide core lead to a rapid decrease in the molecular masses of these polymers (Kitamura *et al*., 1992), and the enzymatic kinetics or the biochemical properties of these fucanases are still unclear. Besides the influence of the molecular size, another important study of sulfated fucans is to reveal the significant role of the sulfated positions in the biological actions in mammalian systems (Pereira *et al*., 2002). One way to analyze the influence of these sulfated groups is to remove them with specific sulfatases. However, only one report has described a sulfatase able to cleave specifically certain sulfate groups of marine-sulfated fucans, and this enzyme acts only on disaccharide units (Daniel *et al*., 2001).

To overcome these limitations, in a previous work, we employed an alternative method based on mild acid hydrolysis

© The Author 2005. Published by Oxford University Press. All rights reserved. For permissions, please e-mail: journals.permissions@oupjournals.org

to specifically desulfate and depolymerize the sulfated fucans at determinated sites. We observed that 0.01 M HCl is able to produce specific-sulfated oligosaccharides from the sulfated fucan of *Lytechinus variegates* after a selective 2-sulfate removal. Using the oligosaccharides of well-defined molecular size obtained by this procedure, we were able to identify the minimum size that allowed this sulfated fucan to interact with heparin cofactor II, a plasmatic inhibitor of thrombin, the most important protease of hemostasis (Pomin *et al.*, 2005).

However, in the above study, we were unable to clarify the structural requirements for the selective desulfation and the specific cleavage. Some questions still remain as What specific structural characteristics are responsible for the 2-desulfation? Which glycosidic linkage is preferentially cleaved by mild acid hydrolysis to prepare oligosaccharides of well-defined molecular size? Here, we extend our studies of hydrolysis with acid to sulfated fucans from other species with regular and repetitive structures, differing only in the 2- and 4-sulfation pattern (Figure 1). Surprisingly, the sulfated fucan from the *Strongylocentrotus pallidus* was able to produce tailored oligosaccharides, in the same way described for *Lytechinus variegatus*. Two other species, *Strongylocentrotus purpuratus* and *Strongylocentrotus franciscanus*, were cleaved unspecifically, yielding heterogeneous-sulfated oligosaccharides. Correlating the chemical structures of these sulfated fucans with their susceptibilities to desulfation and the capacity for producing well-defined oligosaccharides, we were able to elucidate better the reaction mechanism of the mild acid hydrolysis of the sulfated fucans.

Results and discussion

Production of well-defined oligosaccharides from sulfated fucans by mild acid hydrolysis is influenced by the particular structure of the polysaccharides

Mild acid hydrolysis is an apparently nonspecific method for depolymerizing the sulfated polysaccharides. Even so, all of the sulfated fucans (Figure 1) maintained with 0.01 M HCl at 60°C for 1 h showed a reduction in molecular size (Figure 2), as previously reported for another sulfated fucan (Pomin *et al.*, 2005). Only the fucans of the species *S. pallidus* and *L. variegatus* produced specifically tailored oligosaccharides, as shown by their multiple metachromatic bands in polyacrylamide gel electrophoresis (PAGE). For the other species, although the molecular masses of the polysaccharides were reduced, no narrow bands appeared in the PAGE, indicating a heterogeneous mixture of oligosaccharides. Thus, the formation of well-defined molecular size oligosaccharides is notably dependent on the particular structure of the sulfated polysaccharides. As shown in Figure 1, all of the sulfated α-L-fucans used have the α(1→3)-glycosidic linkage, differing only in the pattern of sulfation (2-sulfate, 4-sulfate/substitutions). Thus, the specific cleavage of the polysaccharides by mild acid hydrolysis was influenced specifically by their pattern of sulfation.

Yielding of specific-sulfated oligosaccharides by the mild acid hydrolysis of the sulfated fucans, and increase of their proportion with the course of time

The PAGE shown in Figure 3A and B reveals the same higher electrophoretic mobility for the narrow bands after

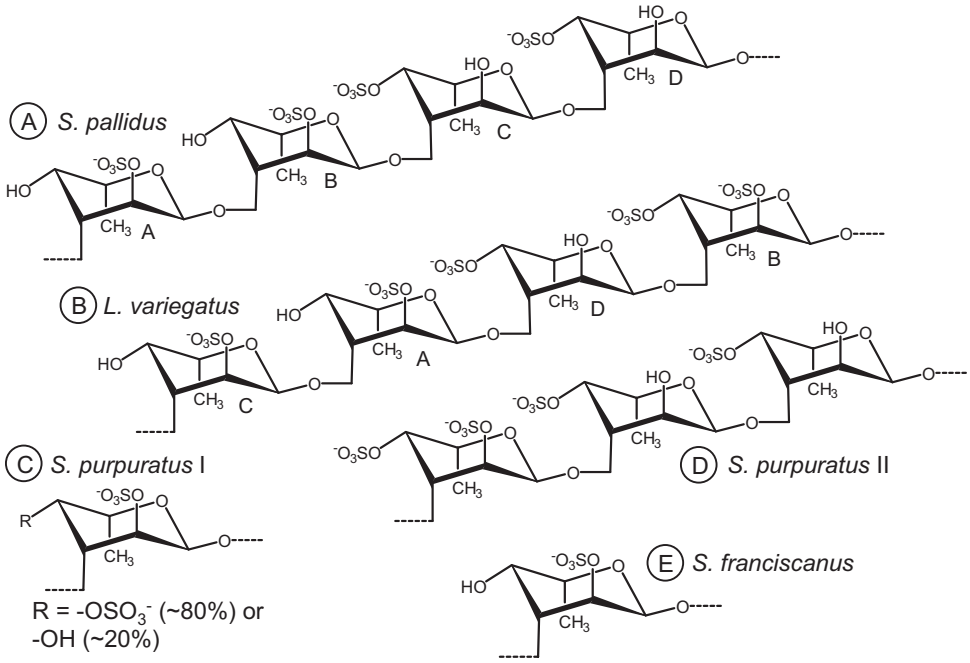

Fig. 1. Structures of sulfated α-L-fucans from sea urchin egg jelly coat. These polysaccharides consist of 3-linked, α-L-fucose units with 2-sulfate/4-sulfate substitutions. All these fucans are composed of repetitive oligosaccharides. Four types of fucose units are designated by letters A–D in the fucans from *Strongylocentrotus pallidus* and from *Lytechinus variegatus*. The species *Strongylocentrotus purpuratus* has two types of repetitive sulfated fucan (indicated as I and II).

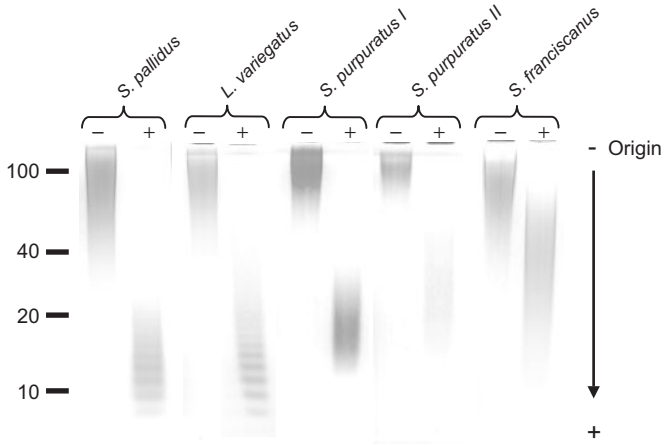

Fig. 2. Mild acid hydrolysis of different sulfated fucans. The sulfated fucans (100 μg of each) were dissolved in 100 μL of distilled water (–) or aqueous 0.01 M HCl solution (+) and heated at 60°C for 1 h. The pH of the solution was then adjusted to 7.0 with the addition of 100 μL of ice-cold 0.01 M NaOH. The samples (10 μg of each) were analyzed by PAGE, as described under *Materials and methods*. The molecular weights (kDa) of standard compounds are indicated at the left. These standards are high molecular-weight dextran sulfate (≥100 kDa), chondroitin 4-sulfate from bovine trachea (~40 kDa), dermatan sulfate from pig skin (~20 kDa), and low molecular-weight dextran sulfate (~10 kDa).

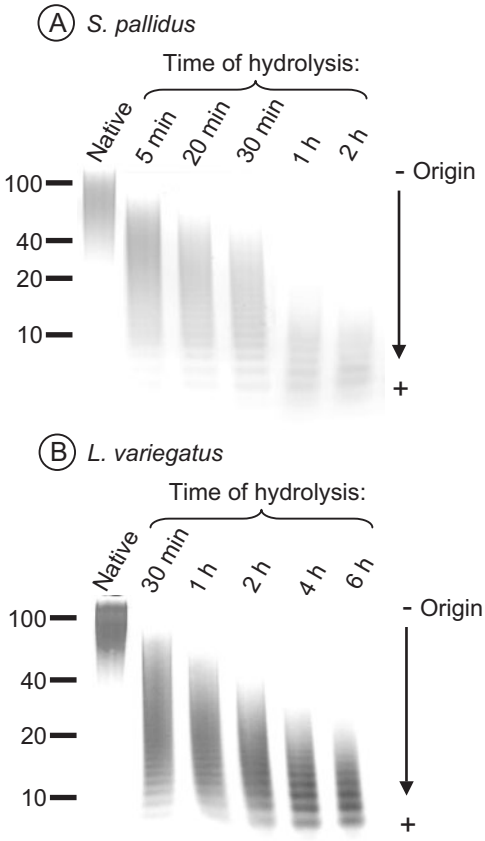

Fig. 3. Mild acid hydrolysis of sulfated fucans from *Strongylocentrotus pallidus* (**A**) and from *Lytechinus variegatus* (**B**) after different periods of time. Each sample (500 μg dry weight) was dissolved in 500 μL of aqueous 0.01 M HCl and heated at 60°C. After different periods of time (5 min, 20 min, 30 min, 1 h, and 2 h for the fucan from *S. pallidus* [**A**] and 30 min, 1 h, 2 h, 4 h, and 6 h for the fucan from *L. variegatus* [**B**]), aliquots of 100 μL of each sample were removed, and the pH was adjusted to 7.0 with the addition of 100 μL of ice-cold 0.01 M NaOH. The samples (10 μg of each) were analyzed by PAGE, as described under *Materials and methods*. The molecular weights (kDa) of standard compounds are indicated at the left, as described in legend of Figure 2.

different periods of time of hydrolysis. In fact, these defined metachromatic bands indicate that, as the time of hydrolysis proceeds, the same sulfated oligosaccharides are produced for each species. Although the cleavage of sulfated fucan from *S. pallidus* was faster than that from *L. variegates* (Figure 3A and B), both species showed the capacity to increase the proportion of low molecular-weight oligosaccharides in longer periods of hydrolysis, in detriment of the proportion of the high molecular-weight polysaccharides. The critical time to yield oligosaccharides from *S. pallidus* was after 30 min of hydrolysis (Figure 3A), while for *L. variegatus* it was 4 h (Figure 3B). For both species, these sulfated oligosaccharides ranged from <10 kDa to ~20 kDa.

The well-defined molecular size oligosaccharides obtained by mild acid hydrolysis have different molecular weights but the same chemical structure

The first step to characterize the structures of the sulfated oligosaccharides from the fucan of *S. pallidus* was to purify them. Thus, the oligosaccharides produced after 1 h of mild acid hydrolysis were fractionated by gel-filtration chromatography on Bio-Gel P10 (Bio-Rad Laboratories, Hercules, CA) (closed circles in Figure 4A). The oligosaccharides were separated, identified by their metachromatic property, and pooled as I→V. As we increased the time course of hydrolysis to 2 h (open circles in Figure 4A), the same elution profile was noticed, and the proportion of low molecular-weight masses rose as the high molecular-weight masses decreased. No oligosaccharides were identified by the phenol–sulfuric acid reaction after the elution of the smaller oligosaccharide (designated 'I' in Figure 4A), excluding the existence of possible desulfated oligosaccharides not assayed because of the absence of metachromatic property. PAGE of the purified fractions from the gel-filtration chromatography (Figure 4B) showed bands of a well-defined size, as already noted in Figure 3A. The absence of appropriate standards to compare with the electrophoretic mobility of the oligosaccharides I→V did not allow us to estimate precisely their respective molecular masses. However, the ^{1}H-nuclear magnetic resonance (NMR) spectrum of the sulfated oligosaccharides I→V (data not shown) revealed the same chemical structure for all of them, as exemplified for oligosaccharide IV (Figure 4C). Their structure will be described in full detail next.

Promotion of an exclusive desulfation of the 2-sulfated fucosyl unit necessarily linked to or preceded by a 4-sulfated residue in the sulfated fucans by the mild acid hydrolysis

In an attempt to identify the chemical modifications that occur in the polysaccharides during the mild acid hydrolysis, we followed the reaction by one dimensional ^{1}H-NMR

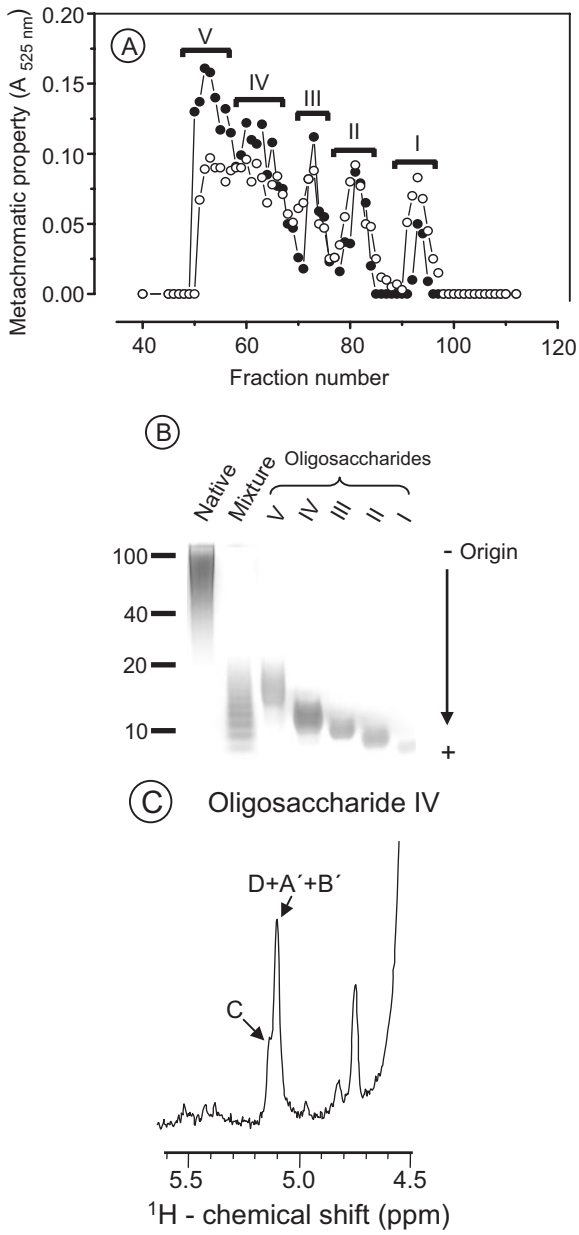

Fig. 4. Size fractionation and ^{1}H-NMR spectroscopy of the sulfated oligosaccharides from *Strongylocentrotus pallidus*. (**A**) Sulfated fucan (5 mg) partially hydrolyzed with 1 mL of 0.01 M HCl at 60°C during 1 h (closed circles) or 2 h (open circles) was applied to a Bio-Gel P10 column (200 × 0.9 cm), equilibrated with aqueous 10% ethanol, containing 1.0 M NaCl. The fractions (1 mL) were eluted as described under *Materials and methods*, and their metachromatic properties were assayed. The fractions containing the oligosaccharides (as indicated by the horizontal bars) were pooled, freeze-dried, desalted, and dissolved in distilled water. (**B**) Intact sulfated fucan, a mixture of unfractionated oligosaccharides, and five major fractions obtained by Bio-Gel P10 (10 µg of each) were applied to a 12% polyacrylamide gel and analyzed as described in the legend of Figure 2. The molecular weights (kDa) of standard compounds are indicated at the left. (**C**) Expansions of the 5.6–4.5 ppm regions of the ^{1}H-NMR spectrum at 600 MHz of the purified oligosaccharide IV obtained by Bio-Gel P10 column. The spectrum was recorded at 60°C for samples in 99.9% D_2O. Chemical shifts are relative to external trimethylsilylpropionic acid at 0 ppm. The residual water signal has been suppressed by presaturation. The respective anomeric signals are indicated by arrows (Figure 1). All the oligosaccharides (I→V) showed the same ^{1}H-NMR spectra (data not shown) as exemplified for oligosaccharide IV.

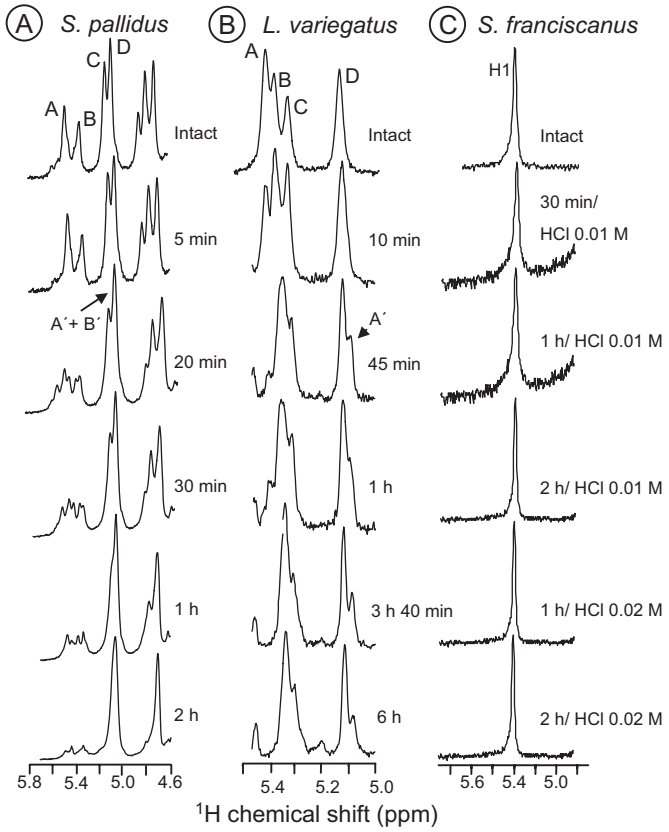

Fig. 5. Expansions of the anomeric regions of the ^{1}H-NMR spectra at 600 MHz of the sulfated fucans from *Strongylocentrotus pallidus* (**A**), *Lytechinus variegatus* (**B**), and *Strongylocentrotus franciscanus* (**C**) at different periods of mild acid hydrolysis. The sulfated fucans (3 mg of each) were dissolved in 1.0 mL of 99.9% D_2O containing 0.01 M HCl (for all sulfated fucans) or 0.02 M HCl (exclusively for *S. franciscanus*) in a 5-mm inner diameter NMR tube. These solutions were heated at 60°C, and ^{1}H-NMR spectra were recorded at different periods of time, as indicated. The A′ and B′ indicate desulfated residues.

spectroscopy (Figure 5A–C). The fucans from *S. pallidus*, *L. variegatus*, and *S. franciscanus* were incubated with 0.01 M HCl inside the NMR tube, and several ^{1}H spectra were recorded at different periods of time.

In the case of the sulfated fucan from *S. pallidus* (Figure 5A), the first 20 min of hydrolysis showed a regression of the ^{1}H-anomeric signals of the residues A and B (Figure 1A) with a parallel increase in the signal A′ + B′ + C + D, as indicated by their respective integrals (Figure 6A). The mild acid hydrolysis tends to form only one peak resonating at ~5.18 ppm, as observed in the ^{1}H-NMR spectrum of 2 h of hydrolysis. This wide peak represents all the ^{1}H-anomeric signals of the molecule (A′ + B′ + C + D), identified in total correlation spectroscopy (TOCSY) spectrum (Figure 7B) and in ^{1}H/^{13}C heteronuclear multiple quantum coherence (HMQC) spectrum (Figure 7D) of the unfractionated oligosaccharides obtained by 1 h of hydrolysis. The ^{1}H-anomeric signals of A′ and B′ both indicate desulfated residues, confirmed by the displacement of their H1 signals to high field shifts (~0.34 ppm to A′ and ~0.25 ppm to B′) (Figure 7A versus B and C versus D), and the disappearance of their

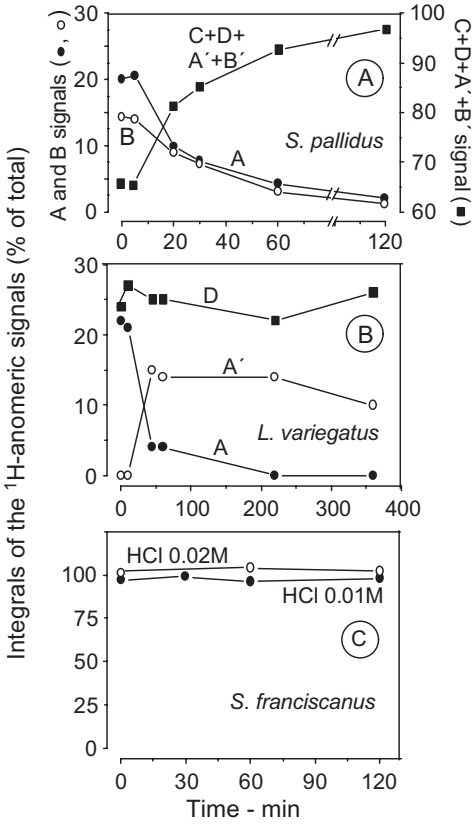

Fig. 6. ^{1}H-anomeric signals modifications in sulfated fucans during different periods of the mild acid hydrolysis determined by their respective integrals (% of total area of the anomeric peaks). The anomeric protons of residues (A, B, and C + D + A′ + B′) of the fucan from *Strongylocentrotus pallidus* (**A**) and of the residues (A, A′, and D) of the fucan from *Lytechinus variegatus* (**B**), indicated in Figure 5, were quantified by their integrals when incubated with 0.01 M HCl at 60°C. The A′ and B′ correspond to desulfated residues. The only ^{1}H-anomeric signal of the fucan from *Strongylocentrotus franciscanus* (**C**) was also integrated in incubations with 0.01 M and 0.02 M HCl at 60°C.

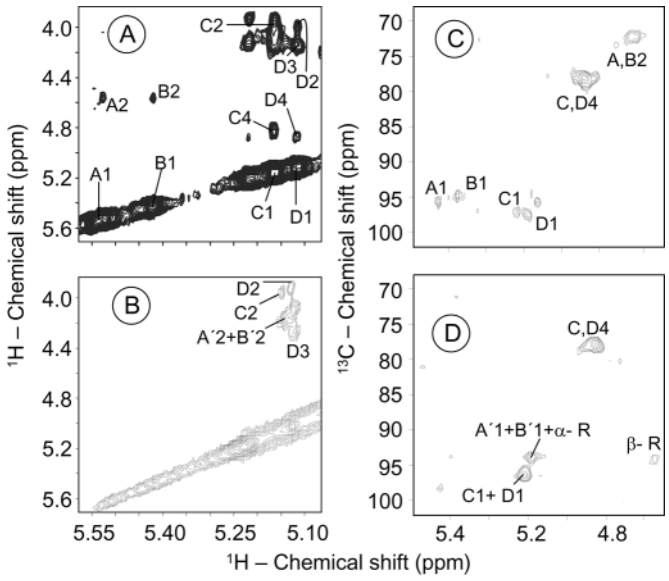

Fig. 7. Part of the TOCSY spectra (**A** and **B**) and the ^{1}H/^{13}C HMQC spectra (**C** and **D**) of native sulfated fucan from *Strongylocentrotus pallidus* (**A** and **C**) and of the mixture of oligosaccharides obtained by mild acid hydrolysis during 1 h (**B** and **D**). The reducing α- and β-anomeric signals of the nonsulfated and sulfated fucose units (Table II) range from 5.50 to 5.20 and from 4.73 to 4.55 ppm, respectively. α-R and β-R are anomeric signals of the reducing ends from nonsulfated fucose units. Oligosaccharide IV shows the same spectra as in **B** and **D**.

H2 signals from the ^{1}H/^{13}C HMQC spectra of the native fucan (Figure 7C versus D). These data agree with those previously reported for a desulfated fucan: high field shifts of ~0.3 and ~0.2 ppm to H1 of desulfated A and B residues, respectively (Table I). In contrast, no alterations were observed in HMQC spectrum of the anomeric signals of C and D residues (Figure 7D versus C; Table I). Both these signals represent 4-sulfated residues (Figure 1A), indicating clearly that 4-O-sulfated fucose units resist desulfation when incubated with acid.

In conclusion, the mild acid hydrolysis promotes in the sulfated fucan from *S. pallidus* a selective 2-desulfation. We can deduce that the predominant-repeating structure found in the products after 20 min of acidification is composed of two consecutive 2-desulfated fucosyl units linked to two following 4-sulfated fucose residues. Thus, the spectra obtained from the oligosaccharides purified by Bio-Gel P10 column (Figure 4C) are similar to those observed in the unfractionated sample after 1 h of hydrolysis (Figure 5A). These data indicate that all oligosaccharides produced by mild acid hydrolysis have the same structure.

Oligosaccharide IV showed the same HMQC spectrum as the mixture of oligosaccharides (not shown but similar to Figure 7D). In this case, the signal of β-anomeric proton at 4.55 ppm is ~3% of the total anomeric protons. Assuming an equilibrium of 4:6 between the α- and β-forms of reducing fucoses, we can estimate that signals of non-reducing α-protons that resonate between 5.18 and 5.22 ppm are ~97% of the total anomeric protons. This indicates that oligosaccharide IV contains ~20 fucose units per reducing terminal, that is, approximately five repeating tetrasaccharide units. Of course this is a rough calculation, but it emphasizes that the oligosaccharides obtained by mild acid hydrolysis are still high molecular-size compounds. These values are not too far from the molecular sizes estimated by PAGE (Figures 3A and 4B).

The same procedure was used to analyze the hydrolysis of the sulfated fucan from *L. variegatus* (Figure 5B). The ^{1}H-anomeric signal of the first 2-sulfated residue (designated as A in Figure 1B) decreases after 45 min with a concomitant appearance of the new anomeric signal of a desulfated residue (indicated A′). The integrals of anomeric signals of A and A′ residues interchange proportionally (Figure 6B). These data indicate not only the 2-desulfation, but, in this case, that a specific 2-sulfate ester is removed. The second residue, indicated as C signal (Figure 5B), resisted hydrolysis, probably because of the influence of its adjacent 2,4-disulfated fucose residue (Figure 1B).

To study the susceptibility of the 2-sulfate esters to desulfation caused by the mild acid hydrolysis, we followed possible structure modifications by several ^{1}H-NMR spectra in a homofucan constituted of 2-sulfated fucose units (Figure 5C). The only anomeric signal stayed unchanged, even at higher concentration of acid (0.02 M HCl). These results are supported by the unaffected integrals of the signals of the only constituent unit (Figure 6C). Thus, the sulfated fucan

Table I. Proton chemical shifts (ppm) for residues of α-fucose in native, chemically desulfated fucan, and mixture of oligosaccharides obtained by 1 h of mild acid hydrolysis of the fucan from *Strongylocentrotus pallidus*

	Native sulfated fucan[a]					Mixture of oligosaccharides obtained by 1 h of mild acid hydrolysis			
Próton	A	B	C	D	Desulfated[a]	A′	B′	C	D
H-1	5.52	5.43	5.20	5.12	5.23	5.18	5.18	5.22	5.14
H-2	**4.59**	**4.60**	4.01	4.06	4.09	4.10	4.10	4.06	4.06
H-3	4.18	3.18	4.19	4.19	4.09	4.09	3.15	4.11	4.11
H-4	4.12	4.12	**4.85**	**4.89**	4.13	4.13	4.13	**4.87**	**4.90**
H-5	4.69–4.56	4.47–4.56	4.46–4.56	4.46–4.56	4.43	4.40	4.41	ND	ND
H-6	1.32–1.43	1.32–1.43	1.32–1.43	1.32–1.43	1.38	1.30–1.40	1.30–1.40	1.30–1.40	1.3–1.4

ND, not determined.
The spectra were recorded at 600 MHz in 99.9% D_2O. Chemical shifts are relative to external trimethylsilylpropionic acid at 0 ppm for ^1H. Values in boldface type indicate positions bearing a sulfate ester. Similar chemical shifts were observed for the spectra of the purified oligosaccharide IV.
[a]Data from Vilela-Silva *et al.* (2002).

from *S. franciscanus* was observed totally resistant to desulfation, probably because of the absence of neighboring 4-sulfated fucose residue. It was not possible to follow chemical modifications by ^1H-NMR spectra of the fucans from *S. purpuratus* I and *S. purpuratus* II because of the limited amount of material.

Comparing the kinetics of acid hydrolysis of the sulfated fucans from *S. pallidus*, *L. variegatus*, and *S. franciscanus* (Figure 5A–C), we can conclude that the desulfation occurs exclusively on the 2-sulfated fucosyl unit obligatorily linked to or preceded by a 4-sulfated fucose unit. If the neighboring residue contains sulfation in the 2-position or in both 2- and 4-positions, as for *S. franciscanus* (only 2-sulfated neighboring units) and for *L. variegatus* (2,4-disulfated neighboring unit), respectively, the desulfation stops.

The glycosidic linkage of the desulfated fucose residue is more susceptible to acid cleavage than the sulfated units

It was already concluded that the oligosaccharides from *S. pallidus* produced in the course of the mild acid hydrolysis have a well-defined molecular size due to the narrow bands indicated by PAGE (Figures 2 and 3) and the elution profile in Bio-Gel P10 column (Figure 4A). Their preponderant chemical structure also remains unchanged as seen by ^1H-NMR spectra in Figure 4C. These observations suggest that this α-L-fucan is preferentially cleaved by HCl in a specific site. In an attempt to determine which glycosidic linkage is more susceptible to cleavage, we analyzed the unfractionated products of 1 h of mild acid hydrolysis (because all oligosaccharides have the same structure) using $^1H/^{13}C$ HMQC spectrum (Figure 7D). Therefore, the $^1H/^{13}C$ HMQC spectrum of the hydrolyzed products showed small, but detectable anomeric signals of reducing fucose units. These signals represent the equilibrium in aqueous solution between the α- and β-forms of the reducing ends (indicated as α-R and β-R in Figure 7D). Comparison between the ^1H and ^{13}C chemical shifts of the α- and β-reducing ends anomeric signals with standard compounds (Table II) clearly indicates that the glycosidic linkage was cleaved in a nonsulfated fucose unit. All these data are

Table II. Chemical shifts (ppm) for anomeric ^1H protons and ^{13}C carbons from reducing terminals of fucosyl units of the mixture of oligosaccharides obtained by 1 h of mild acid hydrolysis of the sulfated fucan from *Strongylocentrotus pallidus* and of standard compounds

	^1H chemical shifts[a]		^{13}C chemical shifts[a]	
	α-anomer	β-anomer	α-anomer	β-anomer
Mixture of oligosaccharides from 1 h of acid hydrolysis	**5.22**	**4.55**	**93.1**	**96.1**
Unsulfated fucose[b]	**5.22**	**4.55**		
Unsulfated fucose[c]	**5.20**	**4.55**	**93.1**	**97.1**
Fucose 2-sulfate[c]	5.49	4.69	93.2	97.6
Fucose 4-sulfate[b]	5.22	4.60		
Fucose 4-sulfate[c]	5.22	4.59	95.1	99.1
Fucose 2,4-sulfate[b]	5.49	4.73		

[a]The 600 MHz $^1H/^{13}C$ HMQC spectrum was recorded at 60°C. Chemical shifts are referenced to internal trimethylsilylpropionic acid at 0 ppm for ^1H and to methanol for ^{13}C. Values in boldface type indicate chemical shifts of nonsulfated fucosyl terminal units. Similar chemical shifts were observed for the spectrum of the purified oligosaccharide IV.
[b]Data from Mourão *et al.* (1996).
[c]Data from Daniel *et al.* (2001).

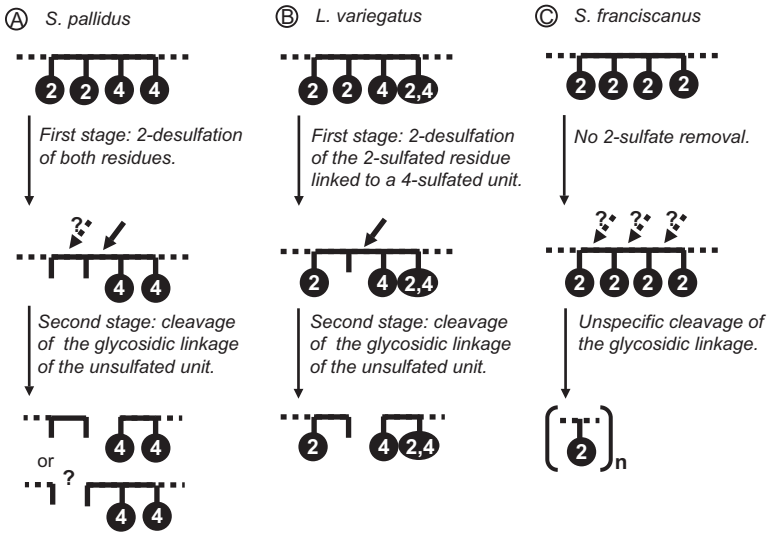

Fig. 8. Scheme summarizing the stages of mild acid hydrolysis of the sulfated fucans from *Strongylocentrotus pallidus* (**A**), *Lytechinus variegatus* (**B**), and *Strongylocentrotus franciscanus* (**C**). The numbers correspond to the sulfate positions in the fucose chain. Stippled arrows indicate the possible cleavage sites, and solid arrow indicates certainty cleavage site. In analogy with the ordered degradation already described for *L. variegatus*, the sulfated fucan from *S. pallidus* is probably cleaved after the second desulfated residue, yielding well-defined oligosaccharides. The oligosaccharides produced from *S. franciscanus* are totally homogeneous, constituted of only 2-sulfated fucose units and different exclusively by their molecular sizes.

coincident to the ordered degradation already described for the sulfated fucan of *L. variegatus* (Pomin *et al.*, 2005) (Figure 8B). In the case of the acid hydrolysis of *S. pallidus*, we were not able to determine which desulfated unit was cleaved (residues designated A′ or B′). But, certainly the cleavage did not occur after the 4-sulfated units (Table II).

Considering the particular characteristics of the acid hydrolysis method, like the selective 2-desulfation of a unit obligatorily linked to or preceded by a 4-sulfated fucose residue and the specific cleavage of the glycosidic linkage of the desulfated residue, we can trace a hypothetical analogy between the ordered degradation of the fucan from *S. pallidus* with that of the fucan from *L. variegatus*. Respecting these similarities, we deduce that probably the acid cleaves the glycosidic linkage of the second desulfated residue of the sulfated fucan from *S. pallidus* (Figure 8A and B). But, it was not possible to accomplish an appropriate experiment to ascertain which 2-sulfated residue has its glycosidic linkage cleaved, because of the absence of a sulfated fucan composed of a non-sulfated fucopyranose residue linked to a 4-sulfated fucose unit.

In the case of the fucan from *S. franciscanus*, we already observed an unspecific cleavage of the glycosidic linkage by the mild acid hydrolysis because of the widely dispersed electrophoretic bands (Figure 2). No 2-desulfation occurred in this fucan either (Figure 5C). These data suggest that probably the resistance to desulfation confers on this fucan a random cleavage of the linkage between the 2-sulfated fucose residues (Figure 8C). Overall, we can deduce that the glycosidic linkage of a desulfated unit is more labile to acid cleavage than one resistant to desulfation.

Conclusion

In synthesis, we presented evidence that mild acid hydrolysis, an apparently nonspecific approach, could be used as an alternative methodology to specifically desulfate and to produce sulfated oligosaccharides of a well-defined molecular size. In some specific cases, this approach showed the capacity to remove only the 2-sulfate esters, in an interesting way not described previously. After this first stage of the hydrolysis, a glycosidic linkage is preferentially cleaved (Figures 8A and B). This methodology depends on the particular sulfated pattern of the polysaccharides. Finally, the 2-sulfated fucose unit content in the sulfated polysaccharides influenced significantly the kinetics of the acid hydrolysis.

Some authors have reported that a desulfation method that differs from the mild acid hydrolysis, solvolysis in dimethyl sulfoxide (DMSO), promotes a first and complete 2-desulfation. Curiously, they show that 4-sulfate esters persist partially resistant to desulfation (Vilela-Silva *et al.*, 1999; Aquino *et al.*, 2005). These data corroborate ours, in that the 2-sulfate ester is more labile than a 4-sulfate group when they are exposed to harsh conditions.

Another relevant observation for the acid hydrolysis approach is that the desulfation in the fucan from *S. pallidus* was faster than in the fucan from *L. variegatus*, as seen by the earlier structural modifications analyzed by ^{1}H-NMR spectrum (Figure 5A versus B). Maybe this occurs because of the presence of two sites of desulfation in the first sulfated fucan (two 2-sulfated residues [A and B]). Like the desulfation, the formation of oligosaccharides with time shown in PAGE (Figure 3A versus B) was also faster. Another comparison is noticed between the yielding of sulfated oligosaccharides in PAGE of Figure 2. During 1 h of mild acid hydrolysis, all of the molecular sizes of the products from *S. pallidus* are smaller than 20 kDa. However, in the case of *L. variegatus*, there are some populations of not well-defined oligosaccharides with the weights above 20 kDa, and the products of the fucan from *S. franciscanus* ranged almost from ~60 to ~15 kDa. In addition, a clear difference can be noted in the molecular sizes of the products of the

acid hydrolysis from *S. purpuratus* I and *S. purpuratus* II. The different molecular weights of these oligosaccharides appear in the same time of hydrolysis (lanes 6 and 8 in Figure 2), indicates that the velocity of the hydrolytic cleavage is directly influenced by the particular structures of these sulfated fucans, mostly by the sulfated pattern.

An important point to be explained is how the presence of 4-sulfate groups increases the susceptibility of 2-sulfate esters of a preceding residue to hydrolysis. Such phenomenon can be related to intramolecular interactions. In fact, because of the acidic pH of the medium, many sulfate groups would be in a protonated form, so making possible the occurrence of intramolecular hydrogen bonds between two adjacent sulfate groups. These interactions would facilitate the removal of a sulfate group in a nucleophilic substitution reaction. Based on preliminary molecular modeling results on sulfated fucan disaccharides, and depending on the carbohydrate ring conformation, the molecular orientation necessary to supply such hydrogen bonds can be 100 kJ/mol less stable when only 2-sulfate groups are present than in molecules presenting a 4-sulfate group near a 2-sulfate group. In addition, this energy can be considerably bigger in great polysaccharide chains, because the entire molecule is less flexible than a simple oligosaccharide.[1] Regarding the increase in susceptibility to acid cleavage in a desulfated fucose unit compared with one of a nondesulfated unit, the sulfate groups can promote a steric and/or electrostatic protection of the glycosidic linkage of the polysaccharide. After its removal, the linkage becomes more susceptible to hydrolysis. These data are evidenced by the different degradation of the sulfated fucans from *S. pallidus*/*L. variegatus* and *S. franciscanus* (Figure 8).

Certainly the methodology based on mild acid hydrolysis can be used as an efficient tool to study the relationship between molecular weight of the sulfated polysaccharides and their biological activities. However, the choice of this approach as a depolymerization procedure needs to be carefully analyzed. As described, the loss of the sulfated residues by solvolysis can promote a great decrease in the biological activity of the sulfated polysaccharide (Koyota *et al.*, 1997; Farias *et al.*, 2000). However, another report has used the mild acid hydrolysis to show that the reduction of the molecular mass can cause a decrease in the biological action of the sulfated fucan (Hirohashi and Vacquier, 2002). Probably, this loss of activity occurs not only because of the reduction of the molecular size, but may also be influenced by the desulfation at specific sites. Therefore, this report that used mild acid hydrolysis to establish the effect of the molecular weight on the biological activity needs to be reexamined.

Materials and methods

Extraction and purification of sulfated fucans

Adults of *S. pallidus*, *S. purpuratus*, *S. franciscanus* and *L. variegatus* were spawned into filtered sea water after intracelomic injection of 0.5 M KCl (~5 mL per specimen). The egg jellies were isolated from the female gametes by the pH 5.0 method, centrifuged, and lyophilized after dialysis against distilled water, as described previously (SeGall and Lennarz, 1979). The acidic polysaccharides were extracted from the jelly coats by papain digestion and partially purified by EtOH precipitation (Albano and Mourão, 1986). Sulfated fucans were purified by anion-exchange chromatography, and the purity was checked by agarose gel electrophoresis and NMR spectroscopy (Mulloy *et al.*, 1994; Alves *et al.*, 1998; Pereira *et al.*, 1999).

Mild acid hydrolysis of sulfated fucans

Sulfated fucans (5 mg) were dissolved in 1 mL of 0.01 M HCl and maintained at 60°C for different periods of time. After this depolymerization procedure, the pH was neutralized by the addition of 1 mL of ice-cold 0.01 M NaOH, as described previously (Pomin *et al.*, 2005). The amount of oligosaccharides formed was analyzed by PAGE, as described below. The oligosaccharides of *S. pallidus* were separated by gel-filtration chromatography and analyzed by PAGE.

PAGE

The native and low molecular-weight derivatives of the sulfated fucans (10 μg of each) were applied to a 12% 1-mm thick polyacrylamide gel slab in 0.02 M sodium barbital (pH 8.6) and run for ~45 min at 100 V. After the electrophoresis, the sulfated polysaccharides were stained with 0.1% toluidine blue in 1% acetic acid and washed for about 4 h in 1% acetic acid. The molecular masses of the low molecular-weight fragments of sulfated fucans were estimated by comparison with the electrophoretic mobility of standard compounds (Santos *et al.*, 1992; Pavão *et al.*, 1998; Pereira *et al.*, 1999; Pomin *et al.*, 2005). The standards used were high molecular-weight dextran sulfate (≥~100 kDa), chondroitin 4-sulfate from bovine trachea (~40 kDa), dermatan sulfate from pig skin (~20 kDa), and low molecular-weight dextran sulfate (~10 kDa).

Gel-filtration chromatography

The oligosaccharides formed after 1 and 2 h of mild acid hydrolysis of sulfated fucan from *S. pallidus* (5 mg) were fractionated on a Bio-Gel P10 column (200 × 0.9 cm), equilibrated with aqueous 10% ethanol, containing 1.0 M NaCl, as described previously (Pomin *et al.*, 2005). The fractions (1 mL) were eluted with the same solution at a flow rate of ~3 mL/h and assayed by their metachromatic property using 1,9-dimethylmethylene blue (Fardale *et al.*, 1986) and by phenol–sulfuric acid reaction (Dubois *et al.*, 1956). The fractions containing the various sulfated oligosaccharides were pooled, freeze-dried, and dissolved in 2.0 mL of distilled water. These solutions were desalted on a Superdex Peptide column (Amersham Biosciences, Piscataway, NJ), coupled to a fast protein liquid chromatography (FPLC) system. Fractions of 0.5 mL of these solutions were collected, and the oligosaccharides were detected by their metachromatic property. The fractions corresponding to the desalted oligosaccharides were pooled and freeze-dried.

[1]A more extensive study of the molecular modeling of sulfated fucan is now being undertaken by Dr. Hugo Verli. This study may help to understand in further detail the molecular mechanism of mild acid hydrolysis of these polysaccharides.

NMR experiments

^{1}H and ^{13}C spectra of the native sulfated fucan and its low molecular-weight derivatives were recorded using a Bruker DRX 600 apparatus (Bruker BioSpin GmbH, Rheinstetten, Germany) with a triple resonance probe. About 3 mg of each sample was dissolved in 0.5 mL of 99.9% D_2O (Cambridge Isotope Laboratory, Andover, MA). All spectra were recorded at 60°C with water suppression by presaturation. In some experiments, sulfated fucans (3 mg) were dissolved in 0.5 mL of 0.01 or 0.02 M HCl, prepared in 99.9% D_2O. The solution was put into an NMR tube, maintained at 60°C, and one dimensional ^{1}H-NMR spectra were recorded after different periods of time. TOCSY and $^{1}H/^{13}C$ HMQC spectra were recorded using states–time proportion phase incrementation for quadrature detection in the indirect dimension. TOCSY spectra were run with 4046×400 points with a spin-lock field of ~10 kHz and a mixed time of 80 ms. HMQC spectra were run with 1024×256 points and globally optimized alternating phase rectangular pulses for decoupling. Chemical shifts are relative to external trimethylsilylpropionic acid at 0 ppm for ^{1}H and to methanol for ^{13}C.

Supplementary Data

Supplementary data are available at *Glycobiology* online (http://glycob.oxfordjournals.org).

Acknowledgments

We are grateful to Adriana A. Piquet for technical assistance, Ana-Cristina E.S. Vilela-Silva for supply of *S. franciscanus* egg jelly, and Martha M. Sorenson for revision of the manuscript. This work was supported by grants from Conselho Nacional de Desenvolvimento Científico e Tecnológico (CNPq) and Fundação de Amparo à Pesquisa do Estado do Rio de Janeiro (FAPERJ).

Abbreviations

FPLC, fast protein liquid chromatography; HMQC, heteronuclear multiple quantum coherence; NMR, nuclear magnetic resonance; PAGE, polyacrylamide gel electrophoresis; TOCSY, total correlation spectroscopy.

References

Albano, R.M. and Mourão, P.A.S. (1986) Isolation, fractionation, and preliminary characterization of a novel class of sulfated glycans from the tunic of *Styela plicata* (Chordata, Tunicata). *J. Biol. Chem.*, **261**, 758–765.

Alves, A.P., Mulloy, B., Moy, G.W., Vacquier, V.D., and Mourão, P.A.S. (1998) Females of the sea urchin *Strongylocentrotus purpuratus* differ in the structures of their egg jelly sulfated fucans. *Glycobiology*, **8**, 939–946.

Aquino, R.S., Landeira-Fernandez, A.M., Valente, A.P., Andrade, L.R., and Mourão, P.A.S. (2005) Occurrence of sulfated galactans in marine angiosperms: evolutionary implications. *Glycobiology*, **15**, 11–20.

Berteau, O. and Mulloy, B. (2003) Sulfated fucans, fresh perspectives: structures, functions, and biological properties of sulfated fucans and an overview of enzymes active toward this class of polysaccharide. *Glycobiology*, **13**, 29R–40R.

Daniel, R., Bertau, O., Chevolot, L., Varenne, A., Gareil, P., and Goasdoue, N. (2001) Regioselective desulfation of sulfated fucopyranoside by a new sulfoesterase from the marine mollusk *Pecten maximus*. Application to the structural study of algal fucoidan (*Ascophyllum nodosum*). *Eur. J. Biochem.*, **268**, 5617–5626.

Dubois, M., Gilles, K.A., Hamilton, J.K., Rebers, P.A., and Smith, F. (1956) Colorimetric method for determination of sugars and related substances. *Anal. Chem.*, **28**, 350–354.

Fardale, R.W., Buttle, D.J., and Barret, A.J. (1986) Improved quantification and discrimination of sulphated glycosaminoglycans by use of dimethylmethylene blue. *Biochim. Biophys. Acta*, **883**, 173–177.

Farias, W.R.L., Valente, A.P., Pereira, M.S., and Mourão, P.A.S. (2000) Structure and anticoagulant activity of sulfated galactans. Isolation of a unique sulfated galactan from the red algae Botryocladia occidentalis and comparison of its anticoagulant action with that of sulfated galactans from invertebrates. *J. Biol. Chem.*, **275**, 29299–29307.

Glabe, C.G., Grabel, L.B., Vacquier, V.D., and Rosen, S.O. (1982) Carbohydrate specificity of sea urchin sperm bindin: a cell surface lectin mediating sperm-egg adhesion. *J. Cell Biol.*, **94**, 123–128.

Hirohashi, N. and Vacquier, V.D. (2002) High molecular mass egg fucose sulfate polymer is required for opening both Ca2+ channels involved in triggering the sea urchin sperm acrosome reaction. *J. Biol. Chem.*, **277**, 1182–1189.

Hirohashi, N., Vilela-Silva, A.C.E.S., Mourão, P.A.S., and Vacquier, V.D. (2002) Structural requirements for species-specific induction of the sperm acrosome reaction by sea urchin egg sulfated fucan. *Biochem. Biophys. Res. Commun.*, **298**, 403–407.

Kitamura, K., Matsuo, M., and Yasui, T. (1992) Enzimic degradation of fucoidan by fucoidanase from the hepatopancreas of *Patinopecten yessoensis*. *Biosci. Biotechnol. Biochem.*, **56**, 490–494.

Koyota, S., Wimalasiri, K.M., and Hoshi, M. (1997) Structure of the main saccharide chain in the acrosome reaction-inducing substance of the starfish, Asterias amurensis. *J. Biol. Chem.*, **272**, 10372–10376.

Matsubara, K., Xue, C., Zhao, X., Mori, M., Sugawara, T., and Hirata, T. (2005) Effects of middle molecular weight fucoidans on in vitro and ex vivo angiogenesis of endothelial cells. *Int. J. Mol. Med.*, **15**, 695–699.

Mourão, P.A.S. (2004) Use of sulfated fucans as anticoagulant and antithrombotic agents: future perspectives. *Curr. Pharm. Des.*, **10**, 967–981.

Mourão, P.A.S. and Bastos, I.G. (1987) Highly acidic glycans from sea cucumbers. Isolation and fractionation of fucose-rich sulfated polysaccharides from the body wall of Ludwigothurea grisea. *Eur. J. Biochem.*, **166**, 639–645.

Mourão, P.A.S. and Pereira, M.S. (1999) Searching for alternatives to heparin: sulfated fucans from marine invertebrates. *Trends Cardiovasc. Med.*, **9**, 225–232.

Mourão, P.A.S., Pereira, M.S., Pavão, M.S.G., Mulloy, B., Tollefsen, D.M., Mowinckel, M.C., and Abildgaard, U. (1996) Structure and anticoagulant activity of a fucosylated chondroitin sulfate from echinoderm. Sulfated fucose branches on the polysaccharide account for its high anticoagulant action. *J. Biol. Chem.*, **271**, 23973–23984.

Mulloy, B., Ribeiro, A.C., Alves, A.P., Vieira, R.P., and Mourão, P.A.S. (1994) Sulfated fucans from echinoderms have a regular tetrasaccharide repeating unit defined by specific patterns of sulfation at the 0-2 and 0-4 positions. *J. Biol. Chem.*, **269**, 22113–22123.

Nishino, T., Kiyohara, H., Yamada, H., and Nagumo, T. (1991) An anticoagulant fucoidan from the brown seaweed *Ecklonia kurome*. *Phytochemistry*, **30**, 535–539.

Pavão, M.S.G., Aiello, K.R.M., Werneck, C.C., Silva, L.C.F., Valente, A.P., Mulloy, B., Colwell, N.S., Tollefsen, D.M., and Mourão, P.A.S. (1998) Highly sulfated dermatan sulfate from ascidians: structure versus anticoagulant activity of these glycosaminoglycans. *J. Biol. Chem.*, **273**, 27848–27857.

Percival, E. and McDowell, R.H. (1967) *Chemistry and Enzymology of Marine Algal Polysaccharides*. Academic Press, New York, pp. 157–175.

Pereira, M.S., Mulloy, B., and Mourão, P.A.S. (1999) Structure and anticoagulant activity of sulfated fucans. Comparison between the regular, repetitive, and linear fucans from echinoderms with the more heterogeneous and branched polymers from brown algae. *J. Biol. Chem.*, **274**, 7656–7667.

Pereira, M.S., Melo, F.R., and Mourão, P.A.S. (2002) Is there a correlation between structure and anticoagulant action of sulfated galactans and sulfated fucans? *Glycobiology*, **12**, 573–580.

Pomin, V.H., Pereira, M.S., Valente, A.P., Tollefsen, D.M., Pavão, M.S.G., and Mourão, P.A.S. (2005) Selective cleavage and anticoagulant activity of a sulfated fucan: stereospecific removal of a 2-sulfate ester from the polysaccharide by mild acid hydrolysis, preparation of oligosaccharides, and heparin cofactor II-dependent anticoagulant activity. *Glycobiology*, **15**, 369–338.

Santos, J.A., Mulloy, B., and Mourão, P.A.S. (1992) Structural diversity among sulfated a-L-galactans from ascidians (tunicates): studies on the species *Ciona intestinalis* and *Herdmania monus*. *Eur. J. Biochem.*, **204**, 669–677.

SeGall, G.K. and Lennarz, W.J. (1979) Jelly coat and induction of the acrossome reaction in echnoid sperm. *Dev. Biol.*, **71**, 33–48.

SeGall, G.K. and Lennarz, W.J. (1981) Jelly coat and induction of the acrosome reaction in echinoid sperm. *Dev. Biol.*, **86**, 87–93.

Vieira, R.P. and Mourão, P.A.S. (1988) Occurrence of a unique fucose-branched chondroitin sulfate in the body wall of a sea cucumber. *J. Biol. Chem.*, **263**, 18176–18183.

Vilela-Silva, A.C.E.S., Alves, A.P., Valente, A.P., Vacquier, V.D., and Mourão, P.A.S. (1999) Structure of the sulfated alpha-L-fucan from the egg jelly coat of the sea urchin Strongylocentrotus franciscanus: patterns of preferential 2-O- and 4-O-sulfation determine sperm cell recognition. *Glycobiology*, **9**, 927–933.

Vilela-Silva, A.C.E.S., Castro, M.O., Valente, A.P., Biermann, C.H., and Mourão, P.A.S. (2002) Sulfated fucans from the egg jellies of the closely related sea urchins *Strongylocentrotus droebachiensis* and *Strongylocentrotus pallidus* ensure species-specific fertilization. *J. Biol. Chem.*, **277**, 379–387.

CAPÍTULO 3: β-GALACTANA SULFATADA DE ALGA VERDE

3.1 Objetivos

Esta parte da tese tem como objetivo descrever a estrutura da galactana sulfatada extraída da espécie de alga verde *Codium isthmocladum*.

3.2 Materiais e métodos

3.2.1 Extração da galactana sulfatada da alga verde *C. isthmocladum*

A alga verde *C. istmocladum* foi coletada na costa-sublitoral de Natal, Rio Grande do Norte, Brazil. Imediantamente após a sua obtenção, a alga foi seca com ar quente (50^{o}C), triturada em um liquidificador, e colocada em etanol e acetona, a temperatura ambiente durante 24 h, para a remoção de pigmentos e lipídios. Cem gramas de alga triturada, delipidada e seca foram suspensas em 500 mL de uma solução aquosa de NaCl 250 mM e o pH foi ajustado para 8,0 com a adição de NaOH. Cerca de 20 mg de maxatase de *Esporobacillus* (Biobrás, Montes Claros, Minas Gerais, Brazil) foi adicionada à solução contendo pedaços da alga para digestão proteolítica. Após incubação por 18 horas a 60^{o}C sobre agitação constante, a mistura foi filtrada através de um filtro de algodão. O filtrado foi fracionado através de precipitação seriada com volumes crescentes de acetona (1:0,3; 1:0,5; 1:0,7; 1:0,9 e 1:1,2; v/v). Para cada precipitação, o volume de acetona gelada foi adicionado sob baixa agitação e mantido a 4^{o}C por 24 horas. Os precipitados formados foram coletados separadamente por centrifugação (10.000 x *g* por 20 min), secos no vácuo, resuspendidos em água destilada e analisados quanto a sua composição química (conteúdo de açúcar e razão molar de sulfato, como descritos abaixo).

3.2.2 Análise química dos precipitados obtidos com diferentes volumes de acetona

O conteúdo de açúcar total de cada precipitado foi analisado pela reação de fenol-H_2SO_4, descrita por Dubois e colaboradores (1956), usando D-galactose

como padrão. Após a hidrólise ácida dos polissacarídeos (HCl 6 M a 100^{o}C por 4 horas), o conteúdo de sulfato foi estimado pela método de toluidina como descrito por Nader e Dietrich (1977). Os polissacarídeos de cada precipitação foram novamente hidrolizados (HCl 6 M 100^{o}C por 2 horas) e os tipos de derivados alditol-acetato foram determinados por cromatografia gás-líquida (Kircher, 1960), como descrito no próximo item. Os padrões utilizados foram: fucose, glicose, ramnose, arabinose, manose, galactose e xilose, todos convertidos em seus respectivos alditóis-acetatos.

3.2.3 Purificação da galactana sulfatada da alga verde *C. isthmocladum*

Para obtenção da galactana sulfatada pura da alga verde *C. isthmocladum*, os polissacarídeos precipitados com 1:0,9 volumes de acetona foram fracionados por cromatografia de troca-iônica. Resumidamente, 12 mg da mistura foram dissolvidos em 5 mL de água destilada e aplicados a uma coluna (19,0 x 4,5 cm) com resina MP500 Lewatit (Bayer Chemicals, São Paulo, Brazil). Primeiramente, a coluna foi lavada com 300 mL de água destilada. Em seguida, foi utilizado um procedimento de “stepwise” para eluição, usando 300 mL de solução aquosa com diferentes concentrações de NaCl (300 mM; 500 mM; 700 mM; 1 M; 1,5 M; 2 M; 3 M e 4 M), e um fluxo de eluição ajustado para 1 mL/min. Posteriormente, 300 mL de cada concentração salina foi coletado em um recipiente único. Depois, um segundo recipiente foi utilizado para coletar os 300 mL adicionais com a mesma molaridade para certificação da eluição completa dos polissacarídeos. Para precipitar os polissacarídeos, o dobro do volume (600 mL) de metanol foi adicionado aos recipientes de cada concentração salina. Entretanto, apenas os primeiros recipientes (primeiros 300 mL) das concentrações salinas de 300 mM, 2 M e 3 M tiveram polissacarídeos precipitados com a adição de metanol. Estas suspensões foram centrifugadas separadamente (10.000 x *g* por 20 min), secas a vácuo, dissolvidas em água destilada até a concentração final de 10 mg/mL e

analisadas quanto ao teor de hexose (Dubois *et al*., 1956) e razão molar de sulfatação (Nader e Dietrich, 1977).

3.2.4 Eletroforeses em géis de agarose e poliacrilamida

O polissacarídeo total obtido antes da precipitação seriada, o precipitado com 1:0,9 volume de acetona e as frações obtidas da coluna de cromatografia com as concentrações salinas de 2 M e 3 M (galactanas sulfatadas: GS 1 e GS 2) foram analisadas por eletroforese em gel de agarose, como descrito previamente por Dietrich e Dietrich (1977). As amostras (~ 20 µg) foram aplicadas em um gel de 5 mm de espessura de 0,5 % agarose e submetidos à eletroforese por 1 h a 110 V, em tampão 50 mM de 1,3 diaminopropano-acetato (pH 9.0). Em seguida, os polissacarídeos sulfatados foram fixados no gel com a adição de uma solução de 0,1 % *N*-cetil-*N*,*N*,*N*-trimetil-amônia. Após 12 h de fixação e secagem do gel, os polissacarídeos foram corados com 0,1 % de azul de toluidina em ácido acético:etanol:água (0,1:5:5, v/v).

As massas moleculares das galactanas sulfatadas (GS 1 e GS 2) foram estimadas por PAGE, comparando-se a migração eletroforética com à de padrões de peso molecular conhecidos, como já descrito em Pomin *et al*. 2005a. Os polissacarídeos sulfatados (~ 10 µg de cada) foram aplicados a um gel de 10% de poliacrilamida, com espessura de 1 milímetro em tampão barbital sódico 20 mM (pH 8,6). Após a eletroforese (100 V por 30 min), os polissacarídeos sulfatados foram corados com 0,1 % de azul de toluidina em 1 % de ácido acético e o gel foi lavado por 1 h em ácido acético para remoção do corante residual. Os marcadores de massa molecular utilizados foram: o dextram sulfato de alto-peso-molecular (~500 kda), o condroitim 6-sulfato de cartilagem de tubarão (~60 kda), o condroitim 4-sulfato de cartilage de baleia (~40 kda), heparina não-fracionada de mucosa intestinal de porco (~15 kda), heparina de baixo-peso-molecular (~7,5 kDa) e dextram sulfato de baixo-peso-molecular (~8 kDa).

3.2.5 Reações químicas de dessulfatação e metilação

A dessulfatação da galactana sulfatada foi realizada como descrito por Vieira e colaboradores (1991). Cerca de 20 mg de cada galactana sulfatada (GS 1 e GS 2) foram dissolvidos em 5 mL de água destilada e misturados com 1 g (peso seco) de resina Dowex 50-W (H^+, malha de 200-400). As soluções foram liofilizadas após neutralização com piridina. O sal piridina resultante foi dissolvidos em 2,5 mL de dimetil-sulfóxido:metanol (9:1, v/v). A mistura foi aquecida a 80^{o}C por 4 h e os produtos dessulfatados foram exaustivamente dializados em água destilada e liofilizados. A dessulfatação foi mensurada pela razão molar de sulfato/açúcar total. Este método permitiu uma detecção de sulfatação a uma razão molar ≤ 0,1 sulfato/açúcar total. Cerca de 5 mg de cada galactana dessulfatada foi obtida com este procedimento.

As galactanas nativas e dessulfatadas foram submetidas a três etapas de metilação como descrito po Ciucanu e Kerek (1984). As amostras metiladas foram hidrolizadas com ácido tri-flúor-acético por 5 h a 100^{o}C, reduzidas com boroidreto de sódio e os derivados alditóis foram acetilados com 1:1 anidro acético/piridina (Kircher, 1960). Os derivados alditóis-acetatos dos açúcares metilados foram dissolvidos em clorofórmio e analisados em espectroscopia de massa e cromatografia a gás Hewlett-Packard modelo 5987-A. Injeções foram feitas em uma coluna capilar DB-1 (25 m x 0.3 mm). A corrida cromatográfica foi programada para 120^{o}C por 2 min, com aquecimento posterior até 230^{o}C por 2^{o}C/min, e mantido por 5 min.

3.2.6 Experimentos de RMN

Espectros de RMN unidimensionais ou bidimensionais das galactanas nativas e dessulfatadas, obtidas das espécies de alga verde *C. isthmocladum*, foram realizados usando um espectomêtro de RMN Bruker DRX 400 MHz com probe de tripla ressonância, como já descrito em Pomin *et al*. (2005b). Cerca de 5 mg de cada amostra de polissacarídeo foi dissolvido em 500 µL de 99,9 % óxido deutério (Cambridge Isotope Laboratory, Cambridge, MA). Todos os espectros

foram realizados a 50 ^{o}C com supressão de HOD por presaturação. Os espectros unidimensionais de ^{1}H foram realizados com 16 scans. Os spectros 2D ^{1}H/^{1}H COSY, TOCSY, NOESY e ^{1}H/^{13}C HSQC foram realizados usando estado de incrementação de fase proporcional ao tempo ("states-TPPI") para detecção por quadratura na dimensão indireta. Os espectros TOCSY foram realizados com 4046 x 400 pontos com campo de "spin-lock" ajustado para 10 kHz e tempo de mistura de 80 ms. Os espectros NOESY foram realizados com tempo de mistura de 100 ms. Os espectros heteronucleares ^{1}H/^{13}C DEPT-HSQC e ^{1}H/^{13}C HSQC foram realizados com 1024 x 256 pontos e GARP ("globally optimized alternating phase rectangular pulses") para desacoplamento. O espectro ^{1}H/^{13}C HMBC foi realizado com 1024 x 256 pontos, com um "delay" de 60 ms para evolução de acoplamentos de longa distância e ausência de desacoplamento durante o tempo de aquisição. Os deslocamentos químicos foram ajustados para 0 ppm relacionados com os padrões externos ácido trimetilsilil-propiônico para a escala de ^{1}H e metanol para a escala de ^{13}C.

3.3 Resultados e discussão

3.3.1 Purificação da galactana sulfatada da alga verde

Os polissacarídeos extraídos da alga pela digestão com maxatase (veja item 3.2.1 de Materiais e métodos) foram fracionados por precipitação seriada com volumes crescentes de acetona (1:0,3; 1:0,5; 1:0,7; 1:0,9; 1:1,2; v/v de amostra e acetona). Todas as frações precipitadas, exceto a que foi obtida com 1:1,2 volume de acetona, revelaram um conteúdo heterogêneo de açúcares (Tabela II). Manose foi o constituinte predominante das frações precipitadas com 1:0,3 e 1:0,5 volume de acetona. Galactose e arabinose foram igualmente predominantes nas frações precipitadas com 1:0,7 e 1:0,9 acetona. O precipitado com 1:1,2 volumes de acetona revelou, curiosamente, um único tipo de açúcar, a arabinose.

Tabela II. Dosagem de açúcar nas frações precipitadas em diferentes volumes de acetona, conteúdo de sulfato e massa molecular das galactanas sulfatadas da alga verde *C. isthmocladum*.

Frações (v/v)[a]	Composição (razão molar)[b]				Massa molecular média[c] (kDa)
	Gal	Ara	Man	(SO_4) / açúcares totais	
1:0,3	0,29	0,14	0,57	-	-
1:0,5	0,07	0,34	0,59	-	-
1:0,7	0,43	0,52	0,05	-	-
1:0,9	0,42	0,50	0,08	-	-
1:1,2	0,14	0,78	0,08	-	-
Galactana Sulfatada 1 (GS 1)	1,00	< 0,01	< 0,01	1,4	~ 14
Galactana Sulfatada 2 (GS 2)	1,00	< 0,01	< 0,01	1,9	~ 20

[a] As frações foram obtidas por adição de diferentes volumes de acetona (1:0.,3; 1:0,5; 1:0,7; 1:0,9 and 1:1,2, v:v da amostra e acetona) na solução dos polissacarídeos totais. As galactanas sulfatadas (GS 1 e GS 2) foram obtidas através da precipitação com 1:0,9 de acetona em cromatografia de troca-iônica com resina Bayer Lewatit (veja Figura 8).

[b] O conteúdo de açúcar nas diferentes precipitações foi determinado por GLC-MS dos derivados alditóis-acetatos como descrito em Materiais e Métodos. Os padrões de açúcar foram: fucose, glicose, ramnose, arabinose, manose, galactose e xilose, convertidos em seus respectivos derivados alditóis-acetatos.

[c] A massa molecular média (kDa) das SG foram estimadas por PAGE (veja Figura 10).

A mistura de polissacarídeos obtidas pela precipitação com 1:0,9 volume de acetona foi adicionalmente purificada por cromatografia de troca-iônica (resina Lewatit Bayer) (Figura 8). A fração eluída com 300 mM de NaCl representou quase 60% de todo o conteúdo do polissacarídeo aplicado na coluna. Entretanto, a baixa concentração de sulfato desta fração indicou que esses polissacarídeos são constituídos predominantemente por resíduos neutros. As frações eluídas com 2 M e 3 M de NaCl representam ~ 16% e ~13% da quantidade de polissacarídeo total aplicado na coluna de Lewatit, respectivamente. Essas frações revelaram um alto conteúdo de sulfato com razões molares de 1,4 e 1,9 sulfato/resíduo de açúcar, respectivamente (Tabela II). A análise de açúcar dessas duas frações (denominadas como GS 1 e GS 2) revelou a presença majoritária de resíduos de galactose (Tabela II).

A pureza das frações de polissacarídeos foi verificada por eletroforese em gel de agarose (Figura 9). Para ambas as frações de GS, há apenas uma banda no gel, indicando amostras puras quando comparadas com os polissacarídeos das amostras precipitadas com 1:0,9 volume de acetona e com o polissacarídeo total, antes da precipitação seriada com acetona. Como conclusão, essas duas frações (GS 1 e GS 2) contêm exclusivamente cadeias puras de galactose sulfatada e foram escolhidas para estudos estruturais subseqüentes.

As massas moleculares de GS 1 e de GS 2 foram determinadas por PAGE (Figura 10). Suas mobilidades eletroforéticas foram comparadas com as de diferentes marcadores moleculares (como indicado na esquerda da Figura 10). Ambas as frações de galactanas sulfatadas mostraram uma migração polidispersa devido à heterogeneidade de peso molecular, característica muito comum dos polissacarídeos sulfatados. Entretanto, bandas predominantes em ~14 kDa e ~20 kDa puderam ser notadas para GS 1 e GS 2, respectivamente. Obviamente, a massa molecular maior da GS 2, juntamente com seu alto conteúdo de sulfato, (Tabela II) explica sua eluição da coluna de Lewatit com a concentração de sal mais elevada (3 M NaCl) quando comparado com a GS 1, eluída com 2 M de NaCl (Figura 8).

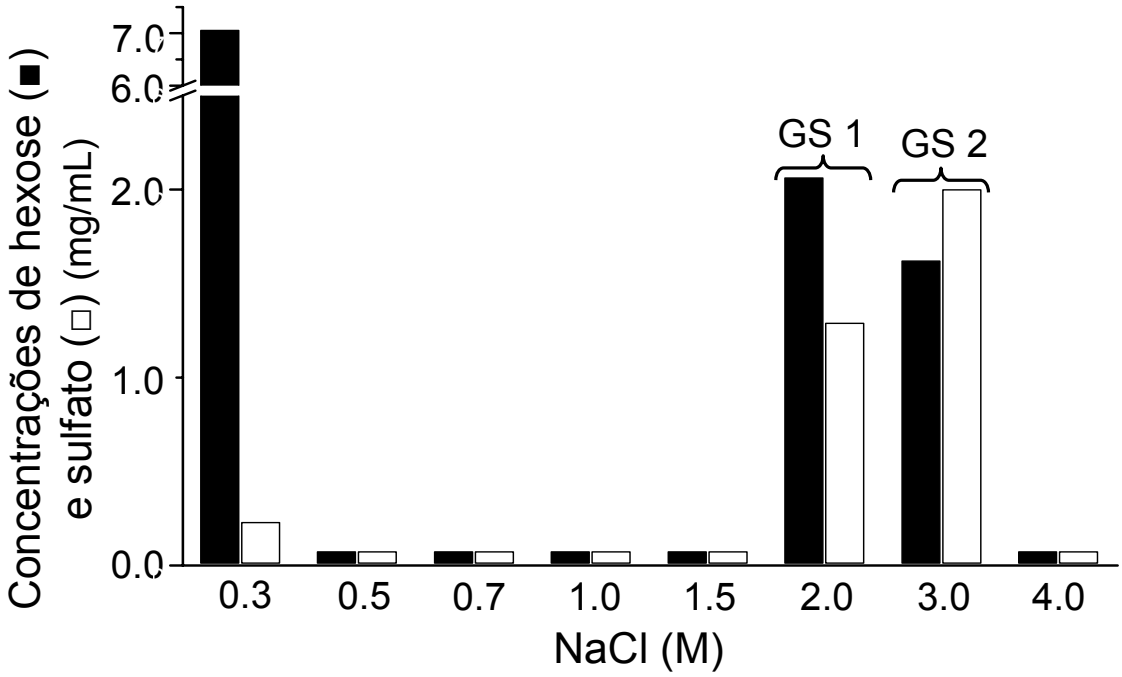

Figura 8. Purificação das frações de galactanas sulfatadas (GS 1 e GS 2) da alga verde *C. isthmocladum* por cromatografia de troca-iônica. A fração precipitada com 1:0,9 volumes de acetona (~12 mg) foi aplicada a uma coluna de Lewatit e a eluição do material foi realizada com concentrações crescentes de NaCl, iniciando com 0,3 M, seguido de 0,5 M; 0,7 M; 1,0 M; 1,5 M; 2,0 M; 3,0 M e 4,0 M. As frações eluídas foram analisadas quanto ao seu conteúdo de hexose (barras pretas) e conteúdo de sulfato (barras brancas).

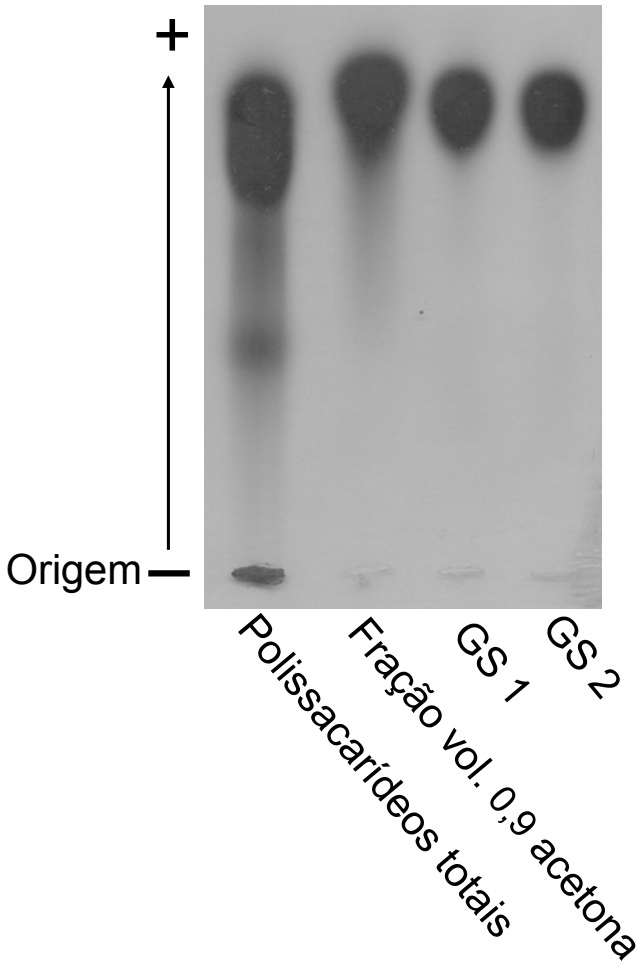

Figura 9. Análise dos polissacarídeos da alga *C. isthmocladum* por gel de agarose. Os polissacarídeos totais (antes da precipitação seriada com diferentes concentrações de acetona), a fração precipitada com 1:0,9 volume de acetona e as frações eluídas com 2,0 M e 3,0 M de NaCl da coluna de Lewatit (GS 1 e GS 2, respectivamente) foram aplicadas em um gel de 0,5% agarose em 1,3-diaminopropano:acetato (pH 9,0) e submetidas a migração eletroforética (como indicado pela seta) foi realizada por 1h a 110V. Os polissacarídeos foram fixadaos no gel, o gel foi secado, e corado com descrito no item 3.2.4..

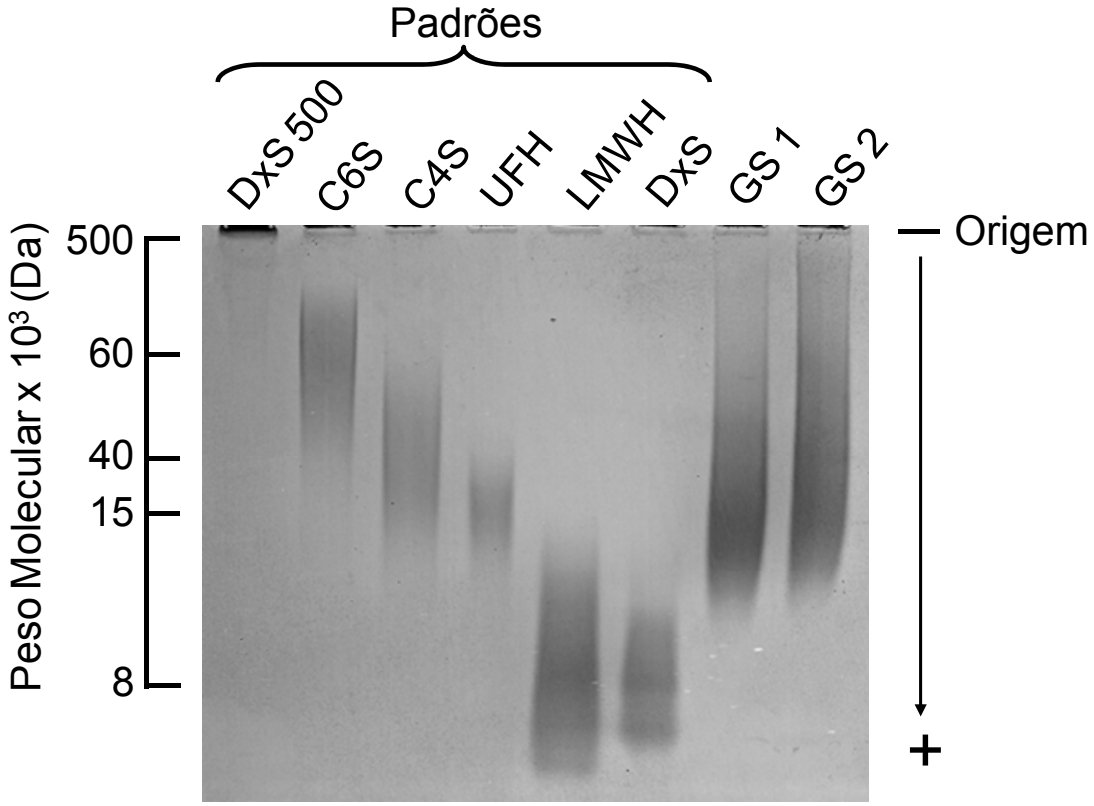

Figura 10. Análise dos polissacarídeos da alga *C. isthmocladum* por gel de poliacrilamida. As frações de galactanas sulfatadas (GS 1 e GS 2), cerca de 10 µg cada, foram aplicadas em um gel de poliacrilamida para estimativa de seus pesos moleculares. Os padrões utilizados como referência (como indicados na figura) foram: o dextran sulfato de alto-peso-molecular (~500 kDa), o condroitim 6-sulfato de cartilagem de tubarão (~60 kDa), o condroitim 4-sulfato de cartilagem de baleia (~40 kDa), a heparina não-fracionada de mucosa intestinal de porco (~15 kDa), a heparina de baixo-peso-molecular (~7,5 kDa) e o dextran sulfato de baixo-peso-molecular (~8 kDa). O sentido de migração eletroforética está indicado pela seta na figura.

3.3.2 Presença de 4- e 6-sulfatação nas galactanas sulfatadas da alga verde

Na tentativa inicial de determinar a estrutura das galactanas sulfatadas obtidas da alga verde, empregamos análises de metilação do polissacarídeo nativo e de seu derivado quimicamente dessulfatado. Mesmo com as limitações dessa metodologia, decorrente de dessulfatação e metilação parciais ou sítios preferênciais de metilação no anel do açúcar, os resultados obtidos forneceram informações valiosas sobre a estrutura das GS (Tabela III).

De fato, comparando os derivados metil-galactitóis produzidos a partir da galactana sulfatada nativa com aqueles produzidos pelo derivado dessulfatado, podemos observar o desaparecimento do derivado 2-*O*-metil galactitol e o aumento significativo dos derivados 2,4-di-*O*-metil galactitol (indicativo de 4-sulfatação) e 2,4,6-tri-*O*-metil galactitol (indicativo de 4- e 6-sulfatação). A produção de quantidades significativas de 2,4,6-tri-metil galactitol na metilação das galactanas dessulfatadas sugere que há predominância de unidades de galactose 3-ligadas. Além disso, a produção de quantidades significativas de 2,4 e 2,6-di-*O*-metil galactitóis pode indicar dessulfatação parcial na molécula ou a presença de resíduos ramificados ou presença de outros tipos de grupamentos substituintes, como será explicado mais adiante.

3.3.3 Preponderância de resíduos β-D-galactopiranose 4-sulfatado e 3-ligado nas galactanas sulfatadas da alga verde

Para maior detalhamento da análise estrutural das galactanas sulfatadas da alga verde, empregamos experimentos de espectroscopia de RMN unidimensional e bidimensional. As frações das galactanas nativas (GS 1 e GS 2) e seus respectivos derivados dessulfatados mostraram sinais similares nos espectros de ^{1}H-RMN (Figura 11), indicando estruturas similares para GS 1 e GS 2. Portanto, escolhemos a fração SG 2, por ser mais sulfatada, e seu respectivo derivado dessulfatado para realizar os espectros 2D RMN para uma determinação estrutural mais completa.

Tabela III. Análise dos produtos metilados das GS nativas e de seus respectivos derivados dessulfatados obtidos da alga verde *C. isthmocladum.*

Açúcares metilados[a] (como alditol-acetatos)		% da soma das áreas dos picos[b]			
		GS 1		GS 2	
	t_R[c] (min)	Nativo	Dessulfatado	Nativo	Dessulfatado
2,4,6-Met_3-Gal	34.4	10	34	7	36
2,6-Met_2-Gal	36.9	40	41	32	38
2,4-Met_2-Gal	40.8	<1	25	<1	22
2-Met-Gal	42.3	50	<1	61	4
	4-substituído	49%	-	51%	-
	6-substituído	24%	-	29%	-

[a] Após a reação de metilação, os polissacarídeos metilados foram hidrolisados e seus derivados alditol-acetatos foram analisados por GLC-MS usando uma coluna capilar DB-1 (25 m x 0.3 mm).

[b] As proporções dos metilados acetatos estão baseadas na porcentagem da integral de cada pico em relação à soma das integrais.

[c] Tempo de retenção dos derivados alditol-acetato na coluna capilar DB-1 (25 m x 0.3 mm) no GLC-MS.

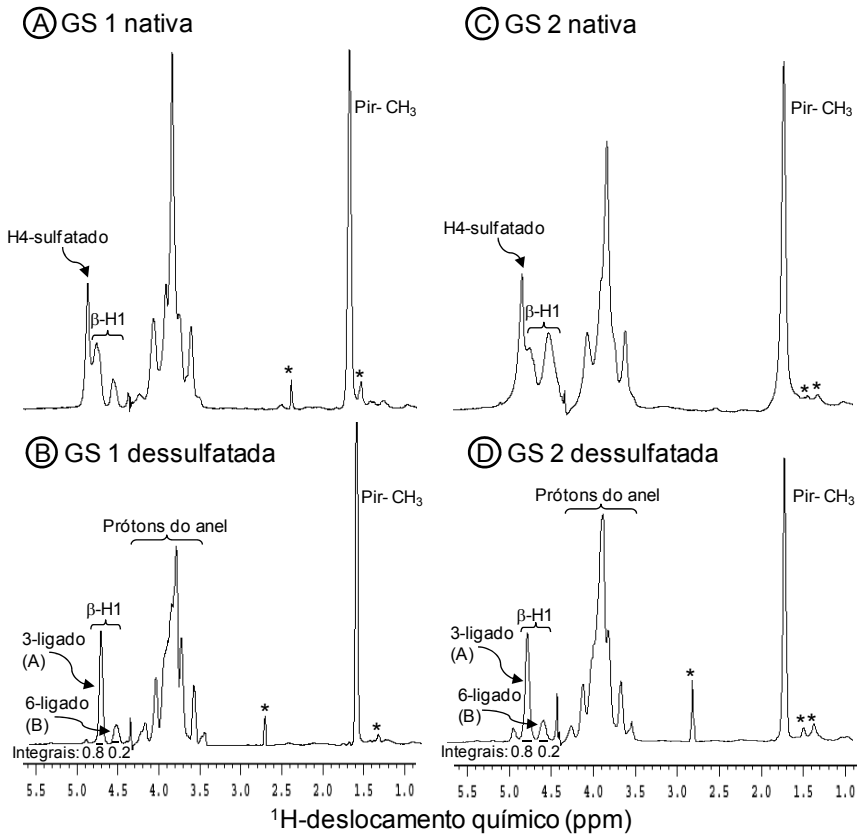

Figura 11. Espectros 1D de ^{1}H-RMN em 400 MHz da GS 1 nativa (**A**), da GS 2 nativa (**B**) da alga verde *C. isthmocladum* e os respectivos derivados dessulfatados de GS 1 (**C**) e GS 2 (**D**). Cerca de 5 mg de cada amostra foram dissolvidos em 0.5 mL de D_2O e os espectros 1D-RMN foram realizados a temperatura de 50 ^{o}C. O sinal residual da água foi suprimido por presaturação. Os deslocamentos químicos estão referenciados ao padrão externo ácido trimetilsilil-propiônico para 0 ppm. Os sinais H4 correspondem aos hidrogênios de unidades de galactose 4-sulfatada. Os sinais β-H1 correspondem aos prótons β-anoméricos. Os sinais assinalados com A e B correspondem às unidades de galactose 3- e 6-ligadas, respectivamente. As integrais de cada pico anomérico das galactanas dessulfatadas estão indicadas abaixo de cada pico. Os sinais indicados com Pir-CH_3 correspondem aos hidrogênios do grupamento metila dos ácidos pirúvicos. Os sinais marcados com asteriscos representam contaminantes.

Os sinais de próton (^{1}H) entre 4,4 e 4,9 ppm nos espectros unidimensionais das SG representam uma mistura de sinais H-1 dos β-anômeros de resíduos de galactopiranose e também sinais de H-4 do anel de hexose que demonstra um deslocamento para campo baixo de ~0,6 ppm, típico de sulfatação (Pomin *et al*., 2005a; 2005b; Bilan *et al*., 2007). Esses resultados também são comprovados pelos espectros de $^{1}H/^{13}C$ DEPT-HSQC do polissacarídeo nativo (Figura 12A) e do desaparecimento do sinal $\delta_H/\ \delta_C$ 4,94/77,8 ppm, após a reação de dessulfatação (Figura 12B).

Os espectros 1D de ^{1}H (Figura 11B e D) e especialmente o espectro $^{1}H/^{13}C$ DEPT-HSQC (Figura 12) revelaram dois sinais anoméricos predominantes para a galactana nativa GS 2, denominados A e B (Figura 12A), assim como para seu derivado dessulfatado (Figura 12B). Através dos espectros 2D COSY (Figura13A e C) e dos espectros TOCSY (Figura 13B e D) foi possível traçar o sistema de spins desses dois sinais anoméricos (A e B), especialmente para a GS 2 dessulfatada (Figura 13A e B). Portanto, conseguimos determinar os deslocamentos químicos de próton para esses sinais, como mostrados na Tabela IV. Apenas o deslocamento químico dos H-6 não pôde ser facilmente determinado. Entretanto, esses valores de deslocamentos químicos foram deduzidos devido aos sinais de fase-negativa relativos aos gruamentos CH_2 (sinais com contornos azuis na Figura 12B) do espectro $^{1}H/^{13}C$ DEPT-HSQC. Assinalamos dois sinais de H-6/C-6, associados com os sistemas de spins das unidades A e B - sinais predominates e minoritários, respectivamente na Figura 12B. A análise dos valores de deslocamentos químicos de ^{13}C indicaram inequivocamente que as unidades designadas A e B (estruturas 1 e 2 na Tabela IV, respectivamente) estavam associados a resíduos de β-D-galactopiranose 3- e 6-ligados, respectivamente, como indicados pelo típico deslocamento de carbonos para campo baixo (~10 ppm) em sítios de glicosilação (Tabela IV). Este deslocamento de ^{13}C foi também observado nos compostos de referência, formados por unidades de β-D-galactopi-

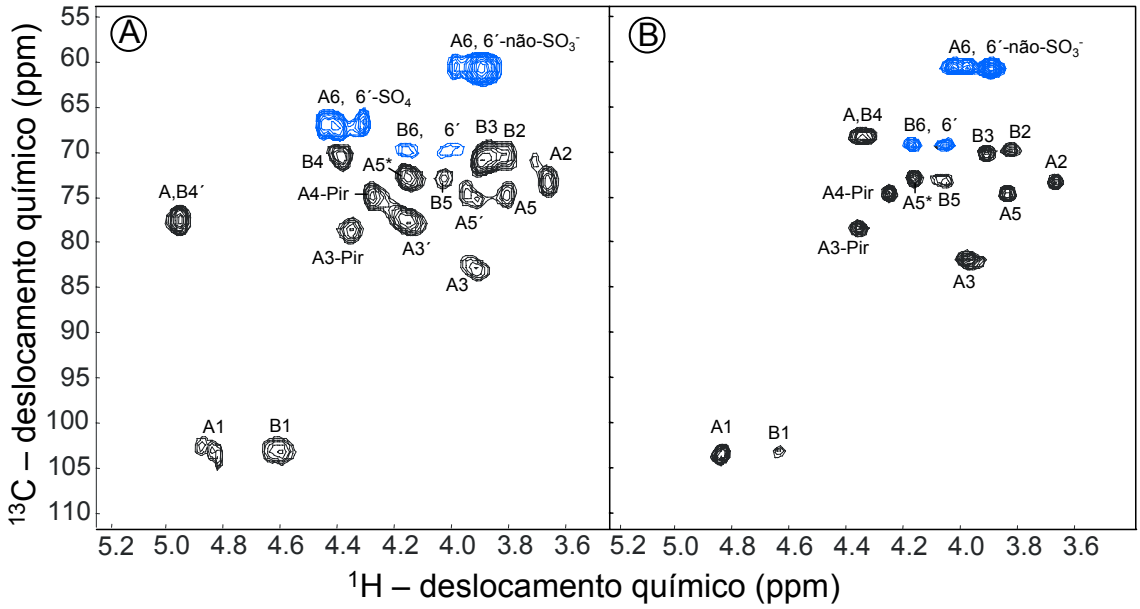

Figura 12. Espectros $^{1}H/^{13}C$ DEPT-HSQC da GS 2 nativa (**A**) e seu derivado dessulfatado (**B**). Os assinalamentos se baseiam nos experimentos 2D homonucleares (COSY e TOCSY) e do espectro HSQC do derivado dessulfatado e depiruvatado (dados não mostrados). Os picos em contornos azuis representam fase negativa dos grupamentos CH_2 e os picos de contornos pretos representam a fase positiva dos grupamentos CH e CH_3**.** Os deslocamentos químicos de ^{1}H e ^{13}C estão referenciados para 0 ppm com os padrões externos ácido trimetilsilil-propiônico e metanol, respectivamente. Os sinais denotados com A e B representam resíduos de galactose 3- e 6-ligados, respectivamente. Os picos denotados A3-Pir, A4-Pir e A5* correspondem as posições 3, 4 e 5 dos resíduos de galactose 3,4-(1´carboxi)-etilideno nos terminais não-redutores. Os picos denotados A3´, A, B4´ e A5´ representam respectivamente as posições 3 e 4 das unidades de galactose 4-sulfatada e 3-ligada, a posição 4 das galactoses 4-sulfatadas e 6-ligadas e a posição 5 das unidades de galactose 4-sulfatada e 3-ligada.

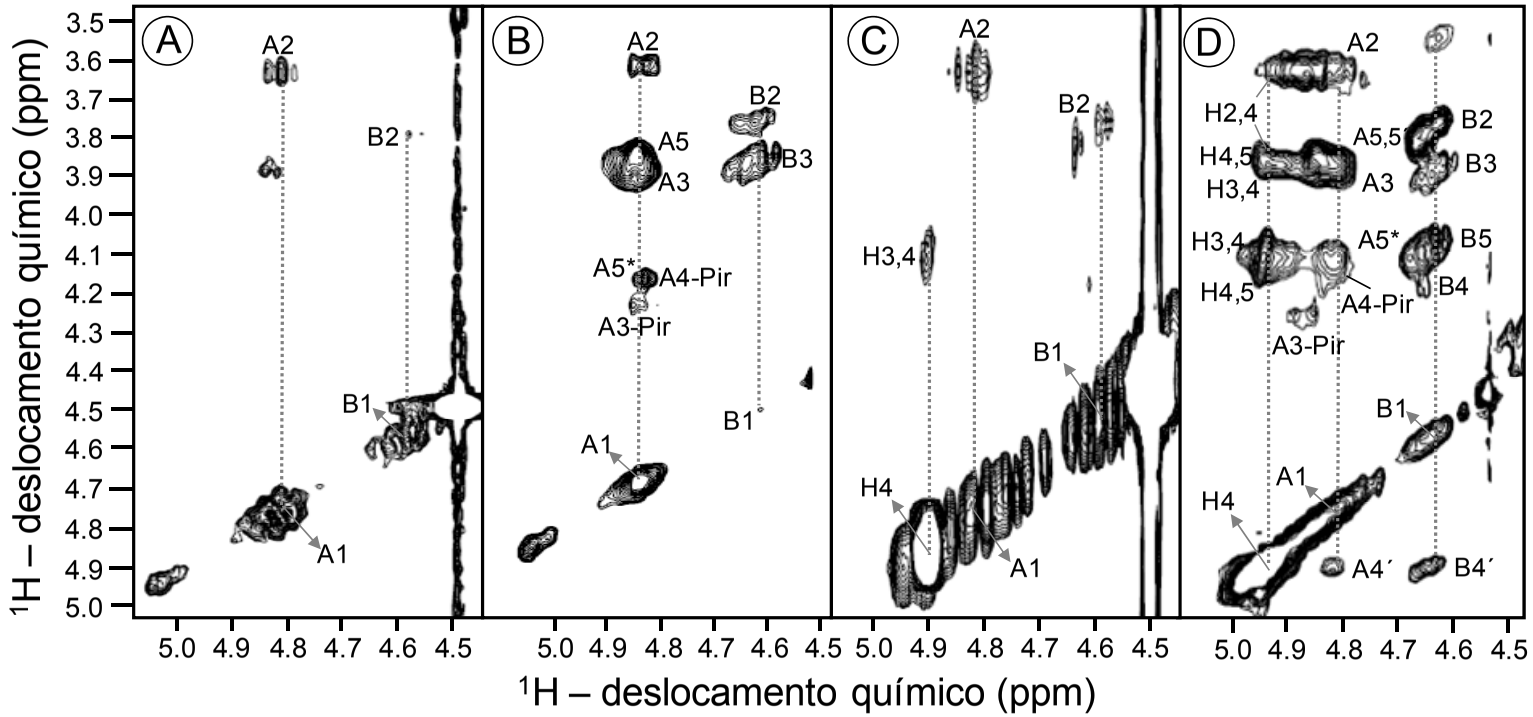

Figura 13. Regiões anoméricas (de 5,1 a 4,5 ppm) dos espectros 2D COSY (**A** e **C**) e TOCSY (**B** e **D**) da galactana 2 dessulfatada (**A** e **B**) e da GS 2 nativa (**C** e **D**) de *C. isthmocladum*. Cerca de 5 mg de cada amostra foram dissolvidas em 0,5 mL de D_2O e os espectros 2D foram realizados a 50ºC em 400 MHz. Os sistemas de spins foram denominados A e B para unidades de galactose 3- e 6-ligadas. Os sinais denominados A3-Pir, A4-Pir e A5* indicam, respectivamente, H3, H4 e H5 de resíduos de galactose com 3,4-(1´carboxi)-etilideno. Os sinais denotados A4´ e B4´ correspondem, respectivamente, aos H4 dos resíduos de galactose 3- e 6-ligadas.

Tabela IV. Deslocamento químico (ppm) dos ^{1}H-prótons e ^{13}C-carbonos para as estruturas propostas da GS 2 da alga verde *C. isthmocladum*, seu respectivo derivado dessulfatado e, para comparação, da galactana sulfatada nativa da alga verde *C. yezoense* e seu respectivo derivado dessulfatado.

Polissacarídeos	Estrutura	Deslocamento químico dos ^{1}H e ^{13}C[a] (ppm)					
		H-1 C-1	H-2 C-2	H-3 C-3	H-4 C-4	H-5 C-5	H-6,6´ C-6
Galactana dessulfatada de *C. isthmocladum*	1) Unit A[c]: 3-β--D-Gal*p*-1	4,81 102,6	3,64 73,8	*3,92* *82,9*	4,39 67,1	3,86 75,2	3,94;3,85 60,3
	2) Unit B[d]:6-β-D-Gal*p*-1	4,62 103,1	3,82 70,1	3,89 70,2	4,38 67,0	4,09 73,9	*4,36;4,01* *69,9*
Galactana nativa de *C. Isthmocladum*	3.1) Unit A: 3-β-D-Gal*p*-4(SO_4)-1 (preponderante)	4,84 103,1	3,71 71,9	*4,16* *77,6*	**4,94** **77,8**	3,95 74,8	3,96;3,86 60,4
	3.2) Unit A: 3-β-D-Gal*p*-4,6-di(SO_4)-1 (minoritário)	4,84 103,1	3,71 71,9	*4,16* *77,6*	**4,94** **77,8**	3,95 74,8	**4,42;4,32** **66,8**
	4) Unit B: 6-β-D-Gal*p*-4(SO_4)-1 (minoritário)	4,63 103,2	3,83 70,2	3,89 70,2	**4,94** **77,8**	4,13 73,7	*4,36;4,01* *69,9*
Galactana dessulfatada de *C. yezoense*[b]	5) 3-β-D-Gal*p*-1	4,69 105,4	3,79 71,5	*3,86* *83,2*	4,21 69,7	3,73 76,0	3,79 62,3
	6) 6-β-D-Gal*p*-1	4,47 104,8	3,57 72,2	3,69 73,9	3,97 69,9	3,92 74,8	*4,04;3,91* *70,5*
	7) β-D-Gal*p*-1	4,62 105,7	3,54 72,2	3,65 73,9	3,92 69,9	3,70 76,4	3,78 62,2
Galactana nativa de *C. yezoense*[b]	8) 3-β-D-Gal*p*-4(SO_4)-1	4,70 105,4	3,82 72,2	*4,08* *79,0*	**4,82** **78,8**	3,81 76,0	*3,74* *62,3*

[a] Os espectros foram registrados em 400 MHz com 99.9% D_2O. Os deslocamentos químicos são relativos ao ácido trimetilsililpropiônico em 0 ppm para ^{1}H e etanol para ^{13}C. Valores em negrito indicam posições de sulfato e em itálico indicam posições glicosiladas.
[b] Valores de referência de Bilan *et al*. (2007).
[c] β-D-Galactopiranose 3-ligada.
[d] β-D-Galactopiranose 6-ligada.

ranose 3- e 6-ligados (estruturas 5 e 6 na Tabela IV) e nos resíduos de galactose localizados em terminais não-redutores (estrutura 7 na Tabela IV).

Os sistemas de spins traçados para a GS 2 nativa foi mais complexo devido a grande hetergeneidade desse polímero. Entretanto, identificamos claramente, dois tipos de sistemas, denominados como A e B (Figura 13C e D) (Tabela IV). Novamente, foi difícil identificar os sinais que correspondem ao H-6, mas o espectro DEPT-HSQC (Figura 12A) foi extremamente útil para este assinalamento (sinais de contornos azuis). Sinais de glicosilação na posição-6 ($\delta_{H,H'}/\delta_C$ 4,16; 4,01/69,9 ppm das unidades denominadas B) e não substituídos na posição 6 (unidades A) foram identificados pela comparação com o espectro da GS 2 dessulfatada (Figura 12B). Mais ainda, identificamos outro sinal ($\delta_{H,H'}/\delta_C$ 4,42; 4,32/66,8 ppm) com um típico deslocamento de próton para campo baixo (~ 0,6 ppm), indicativo de 6-sulfatação (Figura 12A).

A 6-sulfatação está necessariamente relacionada ao sistema A, enquanto o sistema B é glicosilado nessa posição. O sistema A é principalmente sulfatado no C-4, como indicado pelo típico deslocamento químico para campo baixo (~0,65 ppm) do sinal H-4 (estrutura 3 da Tabela IV). Mas, há também quantidades menores de unidades não-sulfatadas, como indicada pela análise de metilação. O sistema B é principalmente 4-sulfatado, como indicado pelo deslocamento químico para campo baixo do H-4 (estrutura 4 na Tabela IV). Unidades não sulfatadas também co-existem com essas unidades sulfatadas.

Em síntese, esses dados indicam que a galactana sulfatada da alga verde tem uma constituição preponderante de unidades 3-β-D-Gal*p*-1 [cerca de 80% dos resíduos totais, como indicado pelas integrais dos sinais de RMN (Figura 11B e D)]. Muitos desses resíduos são 4-sulfatados, mas também há resíduos não sulfatados e 6-sulfatados, porém em quantidades menores. A galactana sulfatada da alga também possui unidades 6-ligadas de β-D-Gal*p*-4(SO_4) e, em quantidades menores, há também resíduos de β-D-galactopiranose 6-ligados e não sulfatados.

3.3.4. Ocorrência de resíduos 3,4-*O*-(1´carboxi)-etilideno nas galactanas sulfatadas

Curiosamente, além dos sinais de ^{1}H e de ^{13}C do anel de galactose e dos prótons e carbonos anoméricos, as GS 1 e GS 2 nativas e seus derivados dessulfatados mostraram um sinal ^{1}H bem intenso a campo alto em ~1,77 ppm (Figura 11), o que sugere, fortemente, grupamentos metila na molécula. Também, a análise dos derivados metilados das galactanas dessulfatadas mostrou que os compostos adlitóis-acetatos são altamente substituídos nos C-3 e C-4, como observado pela produção do derivado 2,6-di-*O*-metil galactitol (Tabela III). Globalmente, esses dados sugerem a presença de substituição adicional na hexose, com grupamentos metila ligados ao C-3 e/ou C-4 de alguns resíduos de galactose.

Os experimentos de RMN heteronucleares $^{1}H/^{13}C$ nos permitiram provar que o grupamento metila no polissacarídeo de alga advém de grupamentos piruvatos. O espectro HSQC (Figura 14A) revelou apenas um singleto em $\delta_H/\ \delta_C$ 1,77/23,4 ppm, que corresponde ao sinal metila do ácido pirúvico. Mas, no HMBC (Figura 14B) esse sinal apresenta-se como um dubleto em $\delta_H/\ \delta_C$ 1,87/23,4 ppm e $\delta_H/\ \delta_C$ 1,67/23,4 ppm, devido ao não-desacoplamento durante a aquisição na seqüência de pulso desse experimento. Mais ainda, devido a sinais de núcleos de prótons ligados a núcleos de carbono, que estão separados por mais de uma ligação química, pudemos, indubitavelmente, assinalar dois outros sinais acoplados à freqüência de δ_H 1,77 ppm. Esses picos ressonam em freqüências δ_C 109,1 e δ_C 186,6 ppm, que correspondem, respectivamente aos grupamentos C-O-C e COOH do anel piruvato no resíduo de galactose (Figura 14B e Tabela V). O deslocamento químico de próton em campo baixo nesse sistema (~1,77 ppm) claramente revela um ácido pirúvico envolvido em um quetal cíclico de cinco elementos, que incluem as posições *O*-3 e *O*-4 de um resíduo de β-D-galactose em terminal não-redutor, ao invés de um ácido pirúvico envolvido em um quetal cíclico de seis elementos, que incluem as posições *O*-4 e *O*-6 (Shashkov *et al*., 2000; Bilan *et al*., 2007). Estes dados indicam que a galactana sulfatada da alga verde *C. isthmocladum* possui resíduos de quetal cíclico 3,4-*O*-(1´carboxi)-etilideno.

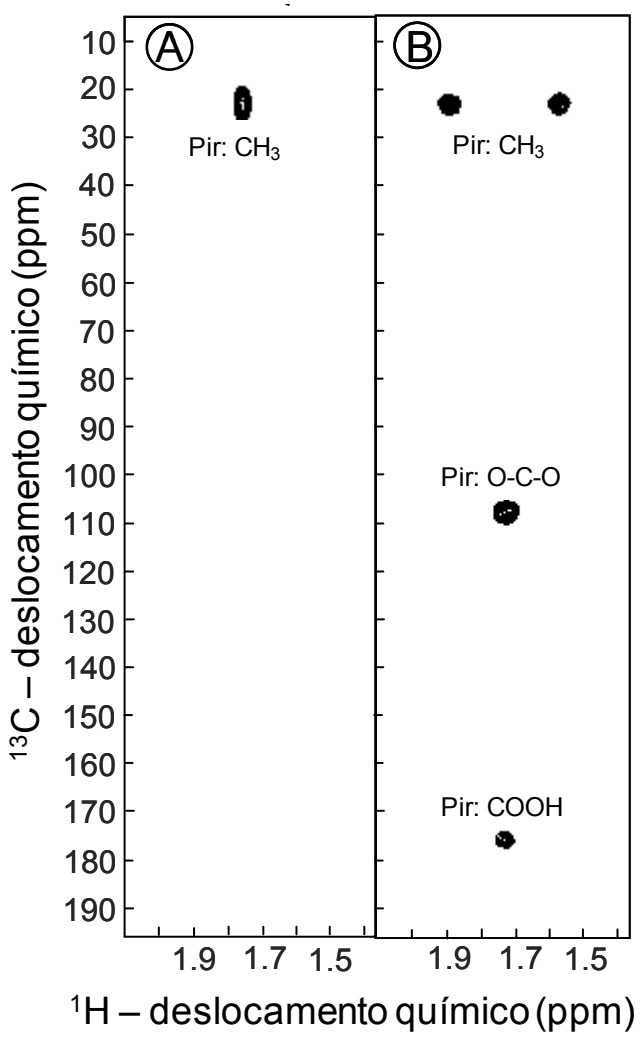

Figura 14. Espectros heteronucleares $^{1}H/^{13}C$ HSQC (**A**) e HMBC (**B**) da região correspondente ao sinal metil do grupamento piruvato da molécula da GS 2 nativa. Pir: CH_3, Pir: O-C-O e Pir: COOH indicam respectivamente os sinais dos grupos CH_3, O-C-O e COOH das unidades de β-galactose com 3,4-*O*-(1´carboxi)-ethilideno. Os sinais singleto e dubleto do Pir: CH_3 nos espectros de HSQC (**A**) e HMBC (**B**), respectivamente, ocorrem devido ao desacoplamento e ausência de desacoplamento durante a aquisição das seqüências de pulso.

Tabela V. Deslocamento químico (ppm) dos picos de correlação - δ_H/δ_C – (ppm) obtidos nos espectros de $^1H/^{13}C$ HMBC do piruvato em quetal ciclíco da galactopiranose do terminal não-redutor da SG 2 e da galactana sulfatada nas algas verdes *C. isthmocladum* e *C. yezoense*[b] respectivamente.

		Valores de referência[b]	
Grupo químico	Galactose piruvatada encontrada em *C. isthmocladum*	Anel de 5-elementos (substituídos em *O*-3 e *O*-4)	Anel de 6-elementos (substituídos em *O*-4 and *O*-6)
CH_3	1,77/23,4	1,62/26,4	1,48/26,4
O-C-O	1,77/109,1	1,62/108,3	1,48/102,0
COOH	1,77/186,6	1,62/178,5	1,48/177,2

[a]Os espectros foram registrados em 400 MHz com 99.9% D_2O. Os deslocamentos químicos são relativos ao ácido trimetilsililpropiônico em 0 ppm para ^1H e etanol para ^{13}C.

[b] Dados obtidos de Bilan *et al*. (2007).

A ocorrência de resíduos de β-D-galactose 3,4-*O*-(1´carboxi)-etilideno nos levou a re-interpretar os dados de metilação dessa galactana sulfatada da alga. A observação de quantidades significativas do derivado 2,6-di-*O*-metil obtido da galactana dessulfatada (Tabela III) pode ser explicada pela presença de unidades de galactose piruvatadas, substituídas nas posições C-3 e C-4 de resíduos obrigatoriamente localizados nos terminais não-redutores da cadeia glicídica desse polissacarídeo. Além disso, a re-análise do sistema de spins correspondente aos resíduos nomeados de A nos espectros de RMN TOCSY e DEPT-HSQC revela uma heterogeneidade adicional, compatível com unidades de β-D-galactopiranose 3,4-*O*-(1´carboxi)-etilideno e, especialmente, sinais coincidentes de H-3 e H-4 de unidades piruvatadas (3-Pir e 4-Pir), mais o deslocamento químico a campo baixo do H-5 adjacente (denominado como A5*) (Figuras 12, 13B e D).

3.4 Principais conclusões sobre os componentes estruturais da galactana sulfatada e piruvatada da alga verde *C. isthmocladum*

A galactana sulfatada e também piruvatada da alga verde *C. isthmocladum* é um polissacarídeo complexo, que apresenta diferentes componentes estruturais. As maiores variações advêm de diferentes sítios de glicosilação (unidades de galactose 3- e 6-ligadas), diferentes sítios de sulfatação (posições 4 e/ou 6) e da presença de ácidos pirúvicos, que formam um quetal cíclico, envolvendo as posições *O*-3 e *O*-4 de β-D-galactoses localizadas em terminais não-redutores. As análises de derivados metilados e dos espectros de RMN asseguram que a unidade 3-β-Gal*p*-4(SO_4) é a unidade preponderante neste polissacarídeo (Figura 15A). Entretanto, unidades de galactopiranose di-sulfatadas nas posições 4 e 6 e com ligações gicosídicas β(1→3) também ocorrem (Figura 15B), assim como resíduos 4-sulfatados e 6-ligados (Figura 15C). Finalmente, unidades contendo 3,4-*O*-(1´carboxi)-etilideno (Figura 15D) constituem os terminais não-redutores desse polissacarídeo. Outra fonte de heterogeneidade nessa molécula é a presença de unidades não-sulfatadas. A tentativa de determinar algum padrão repetitivo na distribuição desses componentes ao longo do polímero, usando espectros de RMN (principalmente NOESY), provou ser infrutífera.

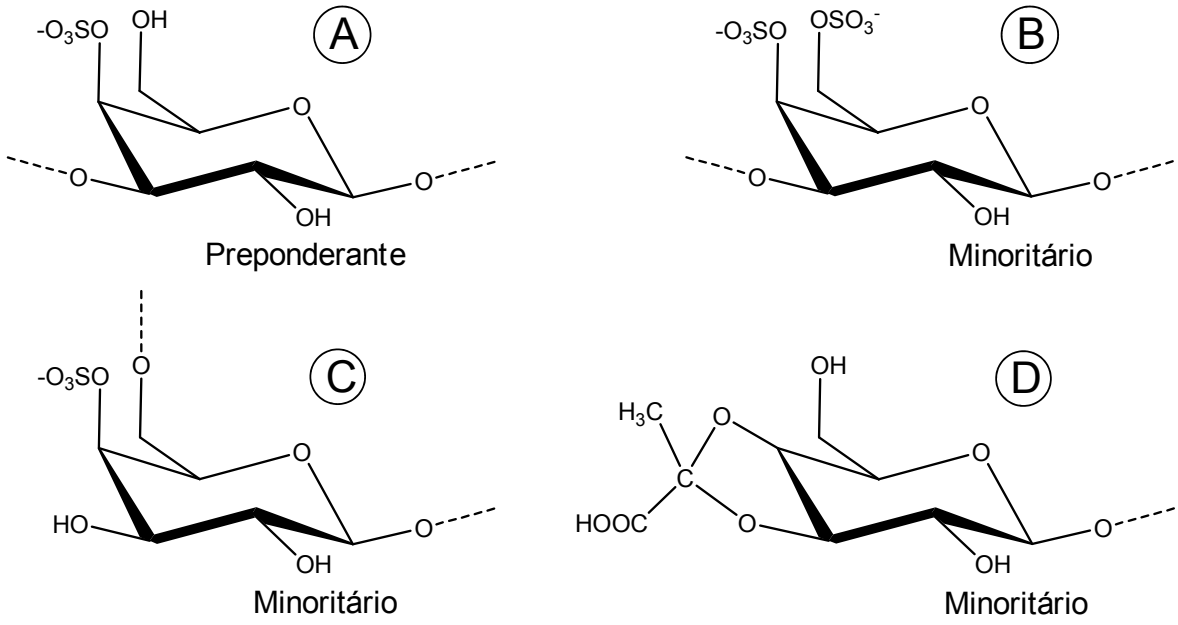

Figura 15. Principais componentes estruturais encontrados na galactana sulfatada da alga verde *C. isthmocladum*. A unidade predominante (**A**) é 3-β-D-Gal*p*-4(SO_4)-1. Outros componentes também encontrados, mas em quantidades menores são: (**B**) 3-β-D-Gal*p*-4,6di(SO_4)-1, (**C**) 6-β-D-Gal*p*-4(SO_4)-1 e (**D**) β-D-Gal*p*-1 3,4-*O*-(1´carboxi)-etilideno em terminais não-redutores. Unidades de galactose não-sulfatada 3- e 6-ligadas também são encontradas nesta galactana sulfatada.

Aparentemente, a galactana sulfatada das algas verdes *C. isthmocladum* e *C. yezoense* (Bilan *et* al., 2007) são polissacarídeos bem similares. Porém, uma análise mais detalhada dos componentes estruturais desses dois polissacarídeos revela algumas diferenças importantes. A galactana sulfatada da alga *C. isthmocladum* possui uma estrutura mais simples do que o polissacarídeo da alga *C. yezoense*, como revelado nos espectros de DEPT-HSQC (Figura 12) e no espectro de HSQC (ver Bilan *et al*., 2007). As análises de metilação também apoiam a maior simplicidade do polissacarídeo de *C. isthmocladum*. Claramente, e em contraste com o polímero de *C.* yezoense, o polissacarídeo descrito neste trabalho não possui unidades 3,6-ligadas (unidades de ramificação) e também resíduos formando quetal cíclico de seis elementos, que envolvem as posições *O*-4 e *O*-6. Além disso, a galactana de *C. yezoense* é altamente ramificada.

3.5 Artigo IV

Glycobiology

Vol. 18 No 3, pp 250-259, 2008

"A preponderantly 4-sulfated, 3-linked galactan from the green alga *Codium isthmocladum*."

Eduardo H.C. Farias, Vitor H. Pomin, Ana-Paula Valente, Helena B. Nader, Hugo A.O. Rocha e Paulo A.S. Mourão

Glycobiology vol. 18 no. 3 pp. 250–259, 2008
doi:10.1093/glycob/cwm139
Advanced Access publication January 3, 2008

A preponderantly 4-sulfated, 3-linked galactan from the green alga *Codium isthmocladum*

Eduardo H C Farias[2,3], Vitor H Pomin[2,4,5], Ana-Paula Valente[5,6], Helena B Nader[7], Hugo A O Rocha[1,3], and Paulo A S Mourão[1,4,5]

[3]Laboratório de Biotecnologia de Polímeros Naturais - BIOPOL, Departamento de Bioquímica, Universidade Federal do Rio Grande do Norte, Natal, RN, 59072-970; [4]Laboratório de Tecido Conjuntivo, Hospital Universitário Clementino Fraga Filho; [5]Instituto de Bioquímica Médica, Centro de Ciências da Saúde, Universidade Federal do Rio de Janeiro, Caixa Postal 68041, Rio de Janeiro, RJ, 21941-590; [6]Centro Nacional de Ressonância Magnética Nuclear Jiri Jonas, Universidade Federal do Rio de Janeiro, Rio de Janeiro, RJ, 21941-590; and [7]Departamento de Bioquímica, Universidade Federal de São Paulo, SP, 04044-020, Brazil

Received on October 9, 2007; revised on November 28, 2007; accepted on December 28, 2007

The green algae of the genus *Codium* have recently been demonstrated to be an important source of sulfated galactans from the marine environment. Here, a sulfated galactan was isolated from the species *Codium isthmocladum* and its structure was studied by a combination of chemical analyses and NMR spectroscopy. Two fractions (SG 1, ∼14 kDa, and SG 2, ∼20 kDa) were derived from this highly polydisperse and heterogeneous polysaccharide. Both exhibited similar structures in ^{1}H 1D NMR spectra. The structural features of SG 2 and its desulfated derivative were analyzed by COSY, TOCSY, DEPT-HSQC, HSQC, and HMBC. This sulfated galactan is composed preponderantly of 4-sulfated, 3-linked β-D-galactopyranosyl units. In minor amounts, it is sulfated and glycosylated at C-6. Pyruvate groups are also found, forming five-membered cyclic ketals as 3,4-*O*-(1'carboxy)-ethylidene-β-D-galactose residues. A comparison of sulfated galactans from different marine taxonomic groups revealed similar backbones of 3-β-D-Gal*p*-1.

Keywords: Codium isthmocladum/green alga/green seaweed/phylogeny/pyruvylated-sulfated galactan

Introduction

The sulfated polysaccharides comprise a complex group of macromolecules with a large range of important biological activities (Verli 2007). These anionic polymers can occur as glycosaminoglycans, widely distributed in vertebrate tissues (Mathews 1975). In marine organisms (invertebrates and algae), the sulfated polysaccharides are found predominantly as sulfated fucans or sulfated galactans. The sulfated fucans are constituted mainly of α-L-fucose residues in which the species-specific molecular structures vary in the glycosidic position and in the pattern of sulfation (Berteau and Mulloy 2003; Mourão 2004, 2007). The most common source of sulfated fucans is the cell wall of brown algae (Phaeophyta) (Pereira et al. 1999; Rocha et al. 2005), but they can also be found in the egg jelly layer of sea urchins (Mulloy et al. 1994; Alves et al. 1997) and in the body wall of the sea cucumber (Echinodermata, Holothuroidea)(Ribeiro et al. 1994).

The most common source of sulfated galactans is the cell wall of red algae (Rhodophyta) (Lahaye 2001; van de Velde et al. 2004). Like the sulfated fucans, the sulfated galactans can also be isolated from the outer layer of the sea-urchin egg (Echinodermata, Echinoidea) (Alves et al. 1997), or extracted from other classes of invertebrates, such as tunicates (Urochordata, Ascidiacea) (Pavão et al. 1989; Albano et al. 1990; Santos et al. 1992) and clams (Mollusca, Bivalvia) (Amornrut et al. 1999). Recently, a novel sulfated galactan was isolated from sea grass (Aquino et al. 2005), leading for the first time to a description of sulfated polysaccharides in the marine angiosperms, a group of vascular plants. Thus, sulfated galactans with different structures are widely distributed among marine organisms from distant phyla.

Recently, the green algae, particularly the genus *Codium* (Bryopsidales, Chlorophyta) (Love and Percival 1964; Matsubara et al. 2001; Bilan et al. 2007), have proved to be another important source of sulfated galactans in the marine environment. Fewer structures of sulfated polysaccharides from green seaweed are known than are those from red or brown algae. In the genus *Codium*, different species demonstrate structural heterogeneity and complexity in their sulfated galactans. Bilan et al. (2007) described a complex and highly pyruvylated and sulfated galactan from *C. yezoense*, composed essentially of linear backbone segments of 3-linked β-D-galactopyranosyl units, ramified by short oligosaccharides attached by linkages at C-6. Sulfate groups were localized mainly at C-4 and in lower amounts at C-6. A few pyruvate groups (about 25% of total residues) were present, forming 3,4-*O*-(1′-carboxy)-ethylidene-β-D-galactopyranose residues located at nonreducing terminals of the chains of galactose. The sulfated galactans from *C. fragile* and *C. cylindricum* were heterogeneous polymers. In addition to its galactose content, *C. fragile* also contained arabinose residues (sulfated arabinogalactan) (Love and Percival 1964) and *C. cylindricum* contained glucose residues, probably forming a sulfated glucogalactan (Matsubara et al. 2001).

Here, we describe the isolation and structural characterization of the sulfated galactan from *Codium isthmocladum*, a green alga that occurs abundantly along the coast of Natal, Rio Grande do Norte, Brazil. We analyzed this sulfated galactan by a combination of chemical methods (desulfation and methylation reactions and measurements of sulfate content) and nuclear magnetic resonance (NMR) spectroscopy (^{1}H 1D and 2D correlation spectroscopy (COSY), total correlation spectroscopy (TOCSY),

[1]To whom correspondence should be addressed: e-mail: pmourao@hucff.ufrj.br
[2]These two authors contributed equally to the work.

© The Author 2008. Published by Oxford University Press. All rights reserved. For permissions, please e-mail: journals.permissions@oxfordjournals.org

distortionless enhancement by polarization transfer-heteronuclear single quantum coherence (DEPT-HSQC), HSQC, and heteronuclear multiple bound correlation (HMBC)). The sulfated galactan from *C. isthmocladum* is composed preponderantly of 3-linked β-D-galactopyranose residues that are extensively 4-sulfated and occasionally 6-sulfated. In minor amounts, the β-D-galactopyranosyl units are 6-linked. Also, based on HMBC experiments, the sulfated galactans from *C. isthmocladum* contain pyruvate groups that form five-membered cyclic ketals located in 3,4-*O*-(1′carboxy)-ethylidene-β-D-galactose units.

A comparison among different sulfated polysaccharides indicates that sulfated galactans with glycosidic linkage (β1→3) occur in some taxonomic groups of marine eukaryotic organisms (rhodophytes, chlorophytes, angiosperms, echinoderms, and molluscs). The sulfated galactans found among these phyla differ in sulfation sites, with a marked tendency toward 4-sulfation in algae and 2-sulfation in invertebrate animals. In minor amounts, 6-sulfation is dispersed throughout the phylogenetic tree.

Results and discussion

Purification of the sulfated galactans from the green alga C. isthmocladum

The polysaccharides extracted from the alga with maxatase digestion (see the Materials and methods section) were fractionated by precipitation with increasing volumes of acetone (1:0.3, 1:0.5, 1:0.7, 1:0.9, and 1:1.2, v/v of sample and acetone). All the precipitated fractions, except the one that was obtained with 1:1.2 acetone, revealed a heterogeneous content of sugars (Table I). Mannose was the major constituent in fractions precipitated with 1:0.3 and 1:0.5 acetone. Galactose and arabinose were equally predominant in fractions precipitated with 1:0.7 and 1:0.9 acetone. The precipitate obtained with 1:1.2 acetone contained primarily one type of sugar, arabinose.

The mixture of polysaccharides obtained by precipitation with 1:0.9 acetone was purified additionally by ion-exchange chromatography (Bayer Lewatit) (Figure 1A). The fraction eluted with 0.3 M NaCl contained almost 60% of the total polysaccharides applied to the column. However, the low sulfate content indicated that these polysaccharides were composed predominantly of neutral residues. The fractions eluted with 2.0 M and 3.0 M NaCl contained ∼16% and ∼13% of the total polysaccharides applied to the Lewatit column. These fractions were highly sulfated with a molar ratio of 1.4 and 1.9 sulfate/residue, respectively (Table I). The sugar analysis of these two fractions revealed mainly galactopyranose residues (Table I) and they were denominated as SG 1 and SG 2.

The purity of these fractions was demonstrated by agarose gel electrophoresis (Figure 1B). For both fractions, there was only a single band in the gel, indicating purified polysaccharides when compared with the polysaccharides precipitated with 1:0.9 acetone and with the crude polysaccharide before the serial precipitation with acetone. In conclusion, these two fractions contained exclusively sulfated galactan and were chosen for subsequent structural studies.

The molecular masses of SG1 and SG2 were determined by PAGE (Figure 1C). Their electrophoretic mobilities were compared with different molecular markers as indicated in the figure. Both fractions of sulfated galactan showed a dispersive migration due to a heterogeneous molecular weight as is the characteristic for the sulfated polysaccharides. However, the predominance of bands at ∼14 kDa and ∼20 kDa can be noted for SG1 and SG2, respectively. Obviously, the greater molecular weight of SG 2 together with its higher sulfate content (Table I) explains its elution from the Lewatit column with a higher saline concentration (3.0 M NaCl) than that observed for SG 1 (2.0 M NaCl) (Figure 1A).

Presence of 4- and 6-sulfation in the galactans

In an initial attempt to determine the structure of the sulfated galactan obtained from the green alga, we methylated the native polysaccharides and their chemically desulfated derivatives. In spite of limitations to this type of methodology, such as partial desulfation and methylation or preferential sites of methylation in the sugar ring, this analysis provides valuable information about the structure (Table II).

In fact, comparing the methyl galactitols produced from the native sulfated galactan and desulfated derivative, we can observe the disappearance of the 2-*O*-methyl galactitol and a significant increase in 2,4-di-*O*-methyl galactitol (indicative of 4-sulfation) and of the 2,4,6-tri-*O*-methyl galactitol (indicative

Table I. Sugar and sulfate contents of the fractions precipitated with different volumes of acetone and average molecular mass of the fractions of sulfated galactans from the green alga *C. isthmocladum*

Fractions (v/v)[a]	Composition (molar ratios)[b]				Average molecular mass[c] (kDa)
	Gal	Ara	Man	(SO_4)/total sugars	
1:0.3	0.29	0.14	0.57	–	–
1:0.5	0.07	0.34	0.59	–	–
1:0.7	0.43	0.52	0.05	–	–
1:0.9	0.42	0.50	0.08	–	–
1:1.2	0.14	0.78	0.08	–	
Sulfated galactan 1 (SG 1)	1.00	<0.01	<0.01	1.4	∼14
Sulfated galactan 2 (SG 2)	1.00	<0.01	<0.01	1.9	∼20

[a]The fractions were obtained by adding different volumes of acetone (1:0.3, 1:0.5, 1:0.7, 1:0.9, and 1:1.2, v/v of sample and acetone) to the solution of the crude polysaccharide. The sulfated galactans (SG 1 and SG 2) were obtained from the fraction precipitated by 1:9 acetone using ion-exchange chromatography on Bayer Lewatit resin (see Figure 1A).
[b]The sugar contents were determined by GLC-MS of alditol acetates as described under the Materials and methods section. Standard sugars were fucose, glucose, rhamnose, arabinose, mannose, galactose, and xylose converted to their respective alditol acetate derivatives.
[c]The average molecular masses (kDa) were estimated by PAGE (see Figure 1C).

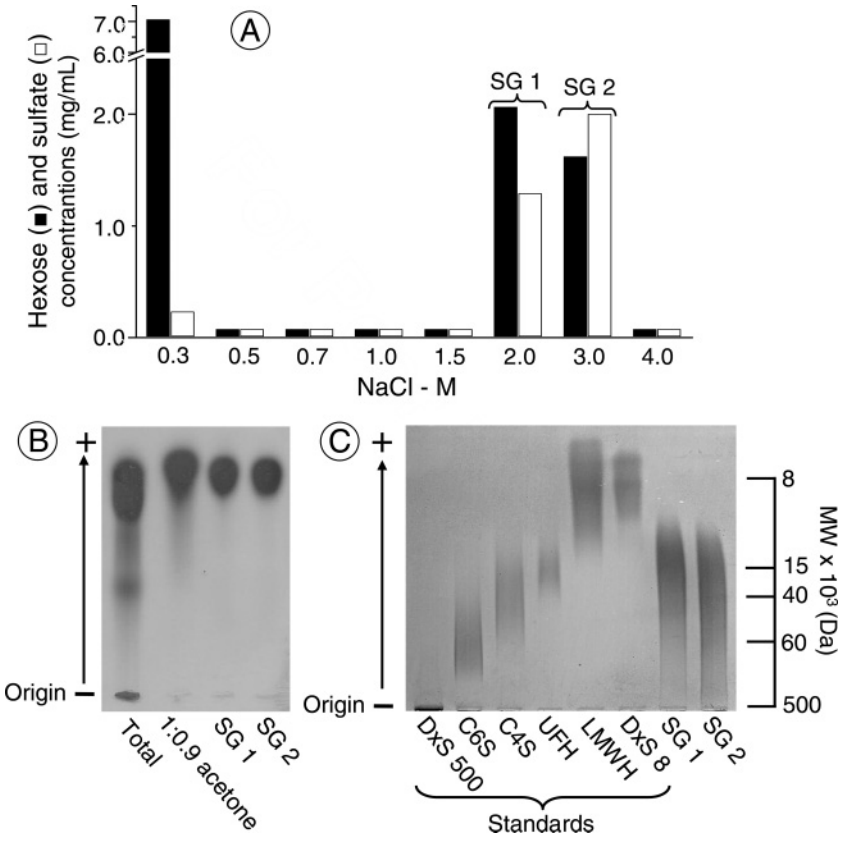

Fig. 1. Purification of the fractions of sulfated galactan (SG 1 and SG 2) from *C. isthmocladum* by ion-exchange chromatography (**A**) and electrophoretic analysis by agarose gel (**B**) and polyacrylamide gel (**C**). (**A**) The fraction precipitated with 1:0.9 acetone (∼12 mg) was applied to a Lewatit column and the elution was carried out in a stepwise system, initializing with 0.3 M NaCl, followed by 0.5 M, 0.7 M, 1.0 M, 1.5 M, 2.0 M, 3.0 M, and 4.0 M NaCl. The eluted fractions were analyzed for their hexose content (black bars) and for sulfate content (white bars). (**B**) The crude polysaccharides before acetone precipitation (Total), the fraction precipitated with 1:0.9 acetone, and SG 1 and SG 2 were applied to a 0.5% agarose gel in 1,3-diaminopropane:acetate (pH 9.0) and run for 1 h at 110 V as indicated by the arrow. The sulfated polysaccharides in the gel were fixed, dried, and stained as described under the Materials and methods section. (**C**) SG 1 and SG 2 (∼10 μg of each) were analyzed by PAGE as described under the Materials and methods section. The molecular weights (MW-Da) of standard compounds are indicated at the right. These standards were: high-molecular-weight dextran sulfate (∼500 kDa), chondroitin 6-sulfate from shark cartilage (∼60 kDa), chondroitin 4-sulfate from whale cartilage (∼40 kDa), unfractionated heparin from porcine intestinal mucosa (∼15 kDa), low-molecular-weight heparin (∼7.5 kDa), and low-molecular-weight dextran sulfate (∼8 kDa).

of 4- and 6-sulfation). The production of significant amounts of 2,4,6-tri-*O*-methyl galactitol from the methylation of the desulfated galactans suggests the predominance of 3-linked galactose units. In addition, the production of significant amounts of 2,4- and 2,6-di-*O*-methyl galactitols may indicate partial desulfation of the molecules, the presence of branching residues or the presence of other types of substituents, as discussed below.

Table II. Methylated galactose derivatives obtained from native and desulfated SG 1 and SG 2 from the green alga *C. isthmocladum*

Methylated sugars[a] (as alditol acetates)	t_R^c (min)	Total peak area[b] (%)			
		SG 1		SG 2	
		Native	Desulfated	Native	Desulfated
2,4,6-Met_3-Gal	34.4	10	34	7	36
2,6-Met_2-Gal	36.9	40	41	32	38
2,4-Met_2-Gal	40.8	<1	25	<1	22
2-Met-Gal	42.3	50	<1	61	4
	4-substituted	49%	–	51%	–
	6-substituted	24%	–	29%	–

[a]After the methylation reaction, the methylated galactans were hydrolyzed and the products analyzed as their alditol acetate derivatives by GLC-MS using a DB-1 capillary column (25 m × 0.3 mm).
[b]The proportions of the methylated acetates are based on the integral of each peak compared with the sum of integrals.
[c]Retention time of the alditol acetate derivatives in the GLC-MS on the DB-1 capillary column (25 m × 0.3 mm).

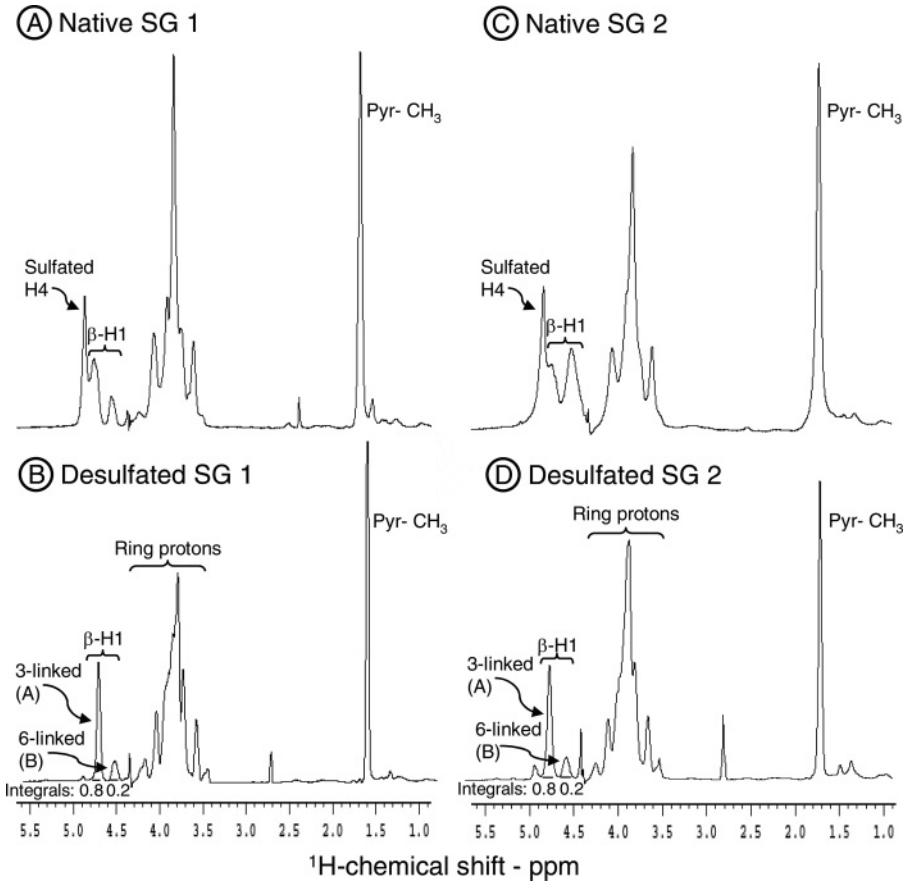

Fig. 2. ^{1}H NMR spectra at 400 MHz of the native SG 1 (**A**), native SG 2 (**C**) from *C. isthmocladum*, and the desulfated derivatives of SG 1 (**B**) and SG 2 (**D**). About 5 mg of each were dissolved in 0.5 mL D_2O and the 1D NMR spectra were recorded at 50°C. The residual water signal was suppressed by presaturation. Chemical shifts are relative to external trimethylsilylpropionic acid at 0 ppm. The H4 signals correspond to 4-sulfated galactose units. The β-H1 signals correspond to the β-anomeric protons. The signals denoted by A and B correspond to 3-linked and 6-linked galactose units, respectively. The integrals of each anomeric peak of the desulfated galactan are indicated under the peak. Pyr-CH_3 indicates methyl signals from pyruvate groups.

Preponderance of 4-sulfated, 3-linked β-D-*galactopyranose residues*

For a more detailed structural analysis of the sulfated galactans from the green alga, we employed one-dimensional and two-dimensional NMR spectroscopy. The fractions of native sulfated galactans and their desulfated derivatives produced similar signals in the ^{1}H 1D NMR spectra (Figure 2), which indicates similar structures for SG 1 and SG 2. Therefore, the 2D NMR spectra were recorded exclusively with fraction SG 2 and its desulfated derivative.

The ^{1}H-signals between 4.4 and 5.0 ppm in the spectra of the sulfated galactan contained a mixture of signals of H-1 from the β-anomers of galactopyranoses and of H-4 from the sugar rings; these exhibited a down-field shift (~0.6 ppm) due to sulfation (Pomin, Pereira, et al. 2005; Pomin, Valente, et al. 2005; Bilan et al. 2007). This conclusion is reinforced by the analysis of the ^{1}H/^{13}C DEPT-HSQC of the native polysaccharide (Figure 3A) and the disappearance of the signal at δ_H/δ_C 4.94/77.8 ppm, after the desulfation reaction (Figure 3B).

The ^{1}H 1D spectra (Figure 2C and D) and especially the ^{1}H/^{13}C DEPT-HSQC (Figure 3) showed two preponderantly anomeric signals, denominated as A and B, for the native sulfated galactan SG 2, as well as for its desulfated derivative. Through the 2D COSY spectra (Figure 4A and C) and TOCSY spectra (Figure 4B and D), it was possible to trace the spin systems of these two signals, especially for the desulfated SG 2 (Figure 4A and B). Thus, we obtained the ^{1}H chemical shifts indicated in Table III. Only the chemical shifts of H-6 could not be determined. However, these values were easily deduced due to the negative-phase signals relative to CH_2 (blue-contour peaks in Figure 3B) in the ^{1}H/^{13}C DEPT-HSQC spectrum. We identified two signals of H-6/C-6 associated with spin systems A and B (preponderant and minority blue signals, respectively). The analysis of the ^{13}C chemical-shift values indicated unequivocally that the units designated A and B (structures 1 and 2 in Table III, respectively) were associated with 3- and 6-linked β-D-galactopyranose residues, respectively, as indicated by the typical low-field shift of carbons (~10 ppm) in sites of glycosylation (Table III). This ^{13}C shift was also seen in reference compounds of 3- and 6-linked β-D-galactosyl units (structures 5 and 6 in Table III) and in galactose residues located at nonreducing terminals (structure 7 in Table III).

The spin system traced for the native SG 2 was more complex due to the greater heterogeneity of the polymer. However, we identified two spin systems, denoted by A and B (Figure 4C and D) (Table III). Again, it was difficult to identify the signals that correspond to H-6, but the DEPT-HSQC spectrum (Figure 3A) was especially useful for this assignment (blue-contour peaks).

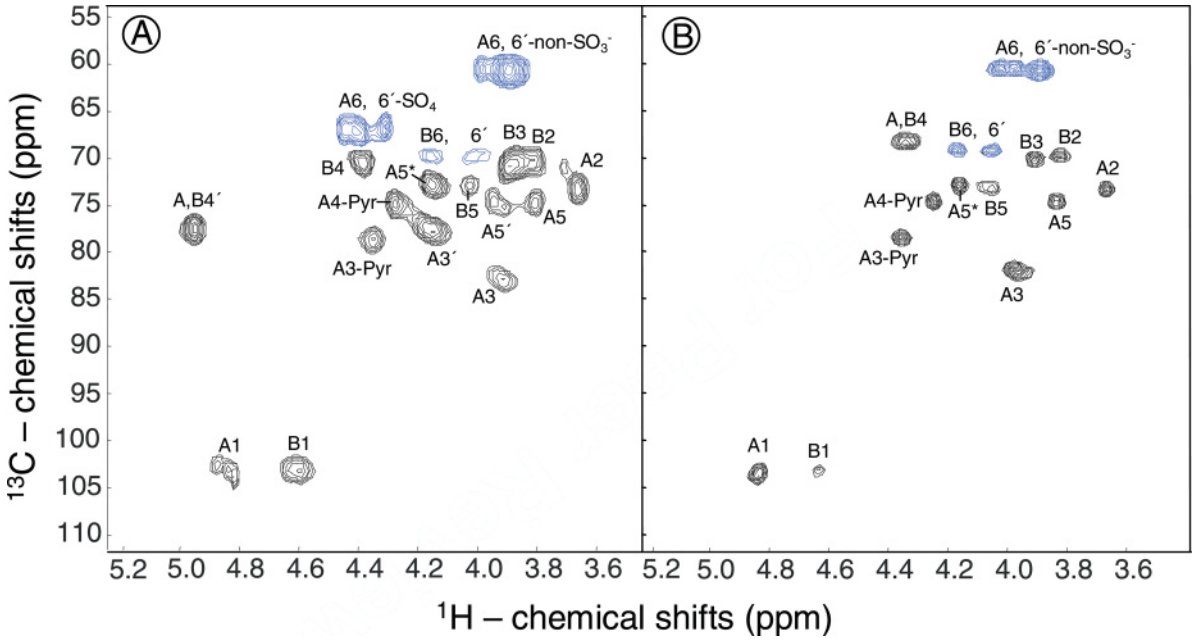

Fig. 3. $^{1}H/^{13}C$ DEPT-HSQC spectra of the native SG 2 (**A**) and its desulfated derivative (**B**). The assignments were based on 2D NMR experiments (COSY and TOCSY), and HSQC of the depyruvylated and desulfated derivative (see supplementary material). The blue-contour peaks are due to the negative phase from CH_2 groups, and the black-contour peaks are due to the positive phase from CH and CH_3 groups. The values of chemical shifts are relative to external trimethylsilylpropionic acid at 0 ppm for ^{1}H and methanol for ^{13}C. The signals are denoted by A for 3-linked and by B for 6-linked β-D-galactopyranosyl units. The peaks denoted by A3-Pyr, A4-Pyr and A5* indicate ^{1}H-chemical shifts of H3, H4, and H5 of the 3,4-(1′carboxy)-ethylidene-β-D-galactopyranose residues, respectively. The peaks denoted by A3′, A, B4′, and A5′ correspond respectively to signals from H3 and H4 of the 4-sulfated, 3-linked β-D-galactopyranosyl units; H4 of the 4-sulfated, 6-linked β-D-galactopyranosyl units; and H5 of the 4-sulfated, 3-linked β-D-galactopyranosyl units.

Signals fromglycosylated 6-position ($\delta_{H,H'}/\delta_C$ 4.36, 4.01/69.9 ppm of units denominated as B) and unsubstituted 6-position (units A) were identified by comparison with the spectra of the desulfated SG 2 (Figure 3B). Moreover, we identified another signal ($\delta_{H,H'}/\delta_C$ 4.42, 4.32/66.8 ppm) with a typical ^{1}H low-field shift (∼0.6 ppm) that indicates 6-sulfation (Figure 3A).

The 6-sulfation is necessarily associated with the system A, while the system B is glycosylated at this site. The system A is mainly sulfated at C-4, as indicated by the typical low-field shift (∼0.65 ppm) of the H-4 (structure 3 in Table III). But, there are also minor amounts of nonsulfated units, as indicated by the methylation analysis. The system B is mainly 4-sulfated

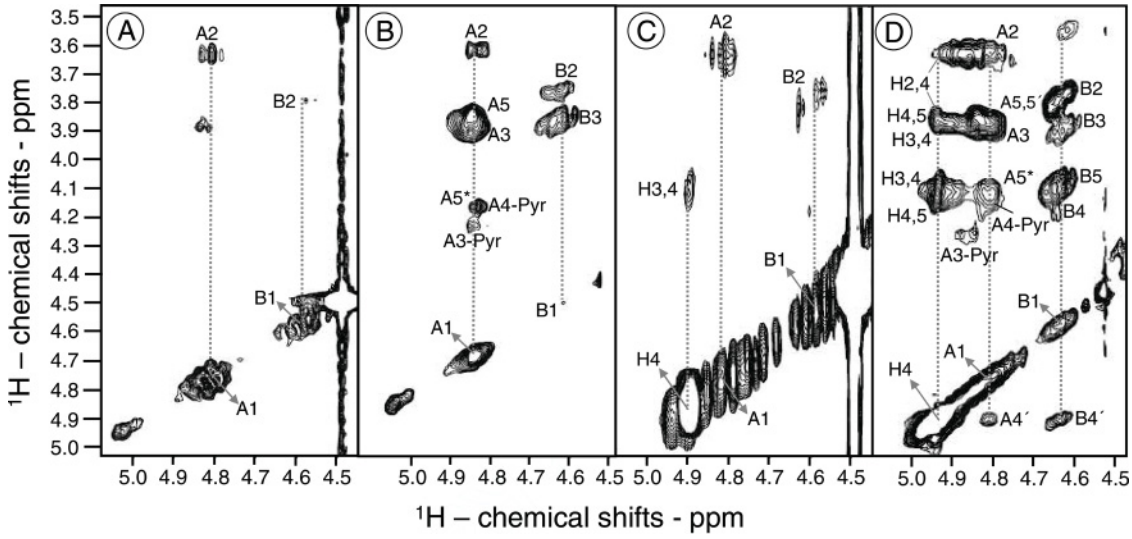

Fig. 4. Strips of the anomeric regions (expansions from 5.1 to 4.5 ppm) from the COSY (**A** and **C**) and TOCSY (**B** and **D**) spectra of the desulfated galactan 2 (**A** and **B**) and the native SG 2 (**C** and **D**) from *C. isthmocladum*. About 5 mg of each were dissolved in 0.5 mL D_2O and the 2D NMR spectra were recorded at 50°C at 400 MHz. The spin systems are denoted by A for 3-linked and by B for 6-linked β-galactose units. The peaks denoted by A3-Pyr, 4-Pyr and A5* indicate ^{1}H-chemical shifts of H3, H4, and H5 of the 3,4-(1′carboxy)-ethylidene-β-D-galactopyranose residues, respectively. The peaks denoted by A4′ and B4′ correspond to signals H4 of the 4-sulfated, 3-linked, and 6-linked galactosyl units, respectively.

Table III. ^{1}H and ^{13}C chemical shifts (ppm) for native SG 2 from the green alga *C. isthmocladum* and its desulfated derivative

Polysaccharide	Structure	^{1}H and ^{13}C chemical shift[a] (ppm)					
		H-1	H-2	H-3	H-4	H-5	H-6,6′
		C-1	C-2	C-3	C-4	C-5	C-6
Desulfated galactan from *C. isthmocladum*	(1) Unit A[c]: 3-β-D-Gal*p*-1	4.81	3.64	*3.92*	4.39	3.86	3.94,3.85
		102.6	73.8	*82.9*	67.1	75.2	60.3
	(2) Unit B[d]:6-β-D-Gal*p*-1	4.62	3.82	3.89	4.38	4.09	*4.36,4.01*
		103.1	70.1	70.2	67.0	73.9	*69.9*
Native galactan from *C. Isthmocladum*	(3.1) Unit A: 3-β-D-Gal*p*-4(SO_4)-1 (preponderant)	4.84	3.71	*4.16*	**4.94**	3.95	3.96,3.86
		103.1	71.9	*77.6*	**77.8**	74.8	60.4
	(3.2) Unit A: 3-β-D-Gal*p*-4,6-di(SO_4)-1 (minor)	4.84	3.71	ND	**4.94**	ND	**4.42,4.32**
		103.1	71.9	ND	**77.8**	ND	**66.8**
	(4) Unit B: 6-β-D-Gal*p*-4(SO_4)-1 (minor)	4.63	3.83	3.89	**4.94**	4.13	*4.36,4.01*
		103.2	70.2	70.2	**77.8**	73.7	*69.9*
Desulfated galactan from *C. yezoense*[b]	(5) 3-β-D-Gal*p*-1	4.70	3.79	*3.86*	4.21	3.73	3.79
		105.4	71.5	*83.4*	69.8	76.1	62.3
	(6) 6-β-D-Gal*p*-1	4.47	3.57	3.69	3.97	3.92	*4.04,3.91*
		104.8	72.2	73.9	69.9	74.8	*70.5*
	(7) β-D-Gal*p*-1	4.61	3.61	3.68	3.93	3.69	3.79
		105.7	72.5	73.9	70.0	76.5	62.3

[a]Chemical shifts are relative to external trimethylsilylpropionic acid at 0 ppm for ^{1}H and methanol for ^{13}C. Values in boldface indicate sulfate position and those in italic indicate glycosylated positions.
[b]Reference values from Bilan et al. (2007).
[c]3-linked -β-D-galactopyranose.
[d]6-linked -β-D-galactopyranose.
ND, not determined.

(as indicated by the down-field shift of H-4 and structure 4 in Table III), but nonsulfated units also co-exist with these units.

In synthesis, these results indicate, for the sulfated galactan from the green alga, a preponderant constitution of 3-β-D-Gal*p*-1, about 80% of the total residues, as indicated by the integrals of the NMR signals (Figure 2B and D). Most of these units are 4-sulfated, but, in minor amounts, there are also units sulfated at the 6-position, as well as nonsulfated units. The sulfated galactan also contains 6-linked units of β-D-Gal*p*-4(SO_4), and, in minor amounts, 6-linked nonsulfated galactopyranose residues. The nuclear overhauser enhancement spectroscopy (NOESY) spectra (data not shown) did not reveal a clear distribution pattern for these minority residues in the structure of the polymer.

Occurrence of 3,4-O-(1′carboxy)-ethylidene residues in the sulfated galactans

Curiously, in addition to the ^{1}H- and ^{13}C-signals from the galactose ring and its anomeric protons and carbons, the native SG 1 and SG 2 and their desulfated derivatives showed an intense high-field ^{1}H-signal at ~1.7 ppm (Figure 2), which strongly indicates methyl groups. Furthermore, in the methylation analysis the desulfated galactan was still highly substituted at C-3 and C-4, as observed from the production of 2,6-di-*O*-methyl galactitols (Table II). These data together suggest the presence of an extra-ring methyl group bound to C-3 and/or C-4 of the galactose ring.

We used $^{1}H/^{13}C$ heteronuclear NMR experiments to prove that this methyl group comes from pyruvate groups. The HSQC spectrum (Figure 5A) revealed only a singlet at δ_H/δ_C 1.77/23.4 ppm that may correspond to methyl signals from pyruvic acid. The HMBC spectrum (Figure 5B) showed a doublet signal at

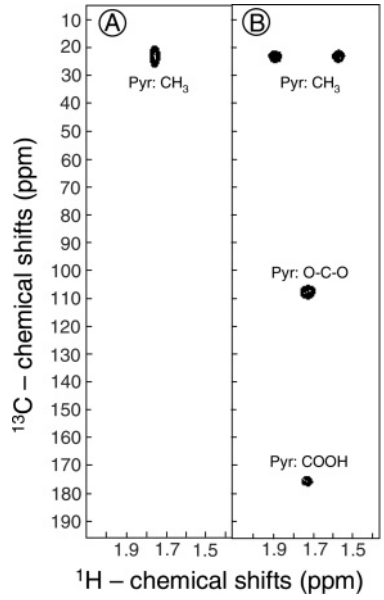

Fig. 5. $^{1}H/^{13}C$ HSQC (**A**) and HMBC (**B**) spectra of the methyl region of the pyruvate group from the native SG 2. Pyr:CH_3, Pyr:O–C–O, and Pyr:COOH indicate signals from the CH_3, O–C–O, and COOH groups of the 3,4-*O*-(1′carboxy)-ethylidene β-D-galactopyranosyl units, respectively. The singlet and doublet signals of the Pyr:CH_3 in HSQC and HMBC spectra, respectively, are due to the decoupling and no-decoupling during the acquisition of the pulse sequences.

δ_H/δ_C 1.87/109.3 ppm and δ_H/δ_C 1.67/109.3 ppm due to nondecoupling during the acquisition of the pulse sequence. Moreover, due to identified signals of proton nuclei bound to carbon nuclei that are separated by more than one bond, we assigned two

Table IV. ^{1}H and ^{13}C chemical shifts[a] of the correlation peaks, δ_H/δ_C (ppm), of pyruvate involved in cyclic ketals with nonreducing-terminal galactopyranoses derived from the $^{1}H/^{13}C$ HMBC spectra

		Reference values[b]	
Chemical group	Pyruvylated galactose found in *C. isthmocladum*	Five-membered ring (*O*-3 and *O*-4 substituted)	Six-membered ring (*O*-4 and *O*-6 substituted)
CH_3	1.77/23.4	1.62/26.4	1.48/26.4
O-C-O	1.77/109.1	1.62/108.3	1.48/102.0
COOH	1.77/176	1.62/178.5	1.48/177.2

[a]Chemical shifts are relative to external trimethylsilylpropionic acid at 0 ppm for ^{1}H and methanol for ^{13}C.
[b]Data from Bilan et al. (2007).

other signals coupled to the δ_H 1.77 ppm frequency. These peaks resonate at δ_C 109.1 ppm and δ_C 176.6 ppm and correspond respectively to the groups O–C–O and COOH of the pyruvate (Figure 5B and Table IV). The low-field proton chemical shift of this system (∼1.77 ppm) clearly reveals a typical pyruvate involved in a five-membered cyclic ketal including *O*-3 and *O*-4 of the nonreducing-terminal galactoses, instead of a six-membered cyclic ketal including *O*-4 and *O*-6 positions (Shashkov et al. 2000; Bilan et al. 2007). These data together indicate the presence of galactose residues with 3,4-*O*-(1′carboxy)-ethylidene cyclic ketals.

The occurrence of 3,4-*O*-(1′carboxy)-ethylidene-galactose residues in the sulfated galactans from the green alga allows us to reinterpret the methylation analysis of these polysaccharides. The observation that significant amounts of 2,6-di-*O*-methyl derivative obtained from the desulfated galactans (Table II) may be explained by the presence of pyruvylated groups substituted at 3- and 4-positions of the galactoses that are located at nonreducing ends of the polysaccharide. In addition, a re-analysis of the NMR spectra (TOCSY and DEPT-HSQC) of the spin system A reveals an additional heterogeneity compatible with 3,4-*O*-(1′carboxy)-ethylidene-β-D-galactopyranosyl units from nonreducing terminals, especially coincident signals of H-3 and H-4 of pyruvated units and the low-field shift of the adjacent H-5 (denoted by A5*) (Figures 3 and 4).

Major conclusions about the structure of the sulfated galactans from the green alga C. isthmocladum

The sulfated galactan from the green alga *C. isthmocladum* is a complex polysaccharide with different structural components. The main variations come from different positions of glycosidic linkages (3- and 6-linked units), from different sulfation sites (positions 4 and/or 6), and from the presence of pyruvate groups involved in cyclic ketals with the positions *O*-3 and *O*-4 of the β-D-galactoses located at nonreducing ends. The studies of methylation and the NMR spectra ensure that the 3-β-Gal*p*-4(SO_4)-1 is the preponderant unit of these polysaccharides (Figure 6A). However, galactopyranosyl units linked by β1→3 linkages and disulfated at 4- and 6-positions are also found (Figure 6B), as are 4-sulfated, 6-linked residues (Figure 6C). Finally, units at nonreducing terminals contain 3,4-*O*-(1′carboxy)-ethylidene (Figure 6D). The structural complexity of this polysaccharide prevented us from determining the sites of substitution of the nonreducing terminals of the main backbone. Another possible source of heterogeneity in these molecules is the presence of minor amounts of nonsulfated units. The attempt to determine a repetitive pattern of distribution in the polymer using NMR (especially the NOESY spectra) proved to be unsuccessful.

Apparently, the sulfated galactans from *C. isthmocladum* and *C. yezoense* are similar polysaccharides. But a more in-depth analysis of the structure of these two polysaccharides reveals some differences. In particular, the sulfated galactan from *C. isthmocladum* has a more simple structure than the polysaccharide from *C. yezoense*, as revealed by the HMQC spectra (compare Figure 3 and the results of Bilan et al. 2007) and the methylation analysis. Clearly, the sulfated galactan from *C. isthmocladum* has no 3,6-linked units and no six-membered cyclic ketals including *O*-4 and *O*-6 positions. In addition, the sulfated galactan from *C. isthmocladum* is less branched than the polymer from *C. yezoense*.

The preponderance of the 3-β-D-Gal*p*-4(SO_4)-1 unit in these sulfated galactans from the green alga stimulated us to review the distribution of this structure in the animal and vegetal kingdoms (Whittaker 1969). The sulfated 3-β-D-Gal*p*-1 units are preserved among species of phyla that cohabit the

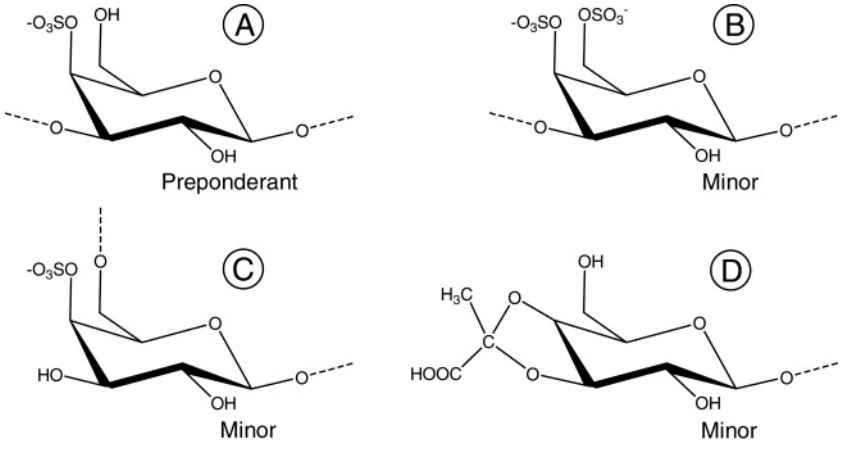

Fig. 6. Proposed structures of the components found in the sulfated galactan from the green alga *C. isthmocladum*. (**A**) The preponderant component is 3-β-D-Gal*p*-4(SO_4)-1. Other components also found but in minor amounts are (**B**) 3-β-D-Gal*p*-4,6di(SO_4)-1, (**C**) 6-β-D-Gal*p*-4(SO_4)-1, and (**D**) 3,4-*O*-(1′carboxy)-ethylidene-β-D-Gal*p*-1 of the nonreducing terminals.

marine environment. These species appear among brown algae (Phaephyta), green algae (Chlorophyta), red seaweeds (Rhodophyta), marine seagrass (Angiospermae, Spermatophyta), invertebrates [sea urchins (Echinodermata, Echinoidea), clams (Mollusca, Bivalvia), tunicates (Urochordata, Ascidiacea)], and vertebrates such as fishes (Teleostei, Chordata) that express keratan sulfate, although 6-sulfation is less evident in this glycosaminoglycan (Scudder et al. 1986). Although the 3-β-D-Gal*p*-1 units are preserved in these phyla, the preferential sulfation site varies: 4-sulfation in the algae and marine angiosperm and 2- or 6-sulfation in the galactans from invertebrates and in the keratan sulfate (and the marine angiosperm).

Materials and methods

Extraction of polysaccharides

The green alga *C. isthmocladum* was collected from the sublittoral coast of Natal, Rio Grande do Norte, Brazil. Immediately after collection, the alga was air-dried at 50°C (under ventilation) and ground in a blender. The seaweed was then treated with ethanol and acetone to remove pigments and lipids, respectively. One hundred grams of delipidated, dry powdered alga was suspended in 500 mL of an aqueous solution of 0.25 M NaCl and adjusted to pH 8.0 with NaOH. About 20 mg of maxatase, an alkaline protease from *Esporobacillus* (Biobrás, Montes Claros, Minas Gerais, Brazil) was added to the solution for proteolytic digestion. After incubation for 18 h at 60°C under agitation, the mixture was filtered through cheesecloth. The filtrate was fractionated through a serial precipitation with increasing volumes of acetone (1:0.3, 1:0.5, 1:0.7, 1:0.9, and 1:1.2, v/v). For each precipitation, the volume of ice-cold acetone was added under gentle agitation and maintained at 4°C for 24 h. The pellets formed in each suspension were collected by centrifugation separately (10,000 × *g* for 20 min), dried under vacuum, resuspended in distilled water, and analyzed for chemical composition (content of sugars and sulfate molar ratio were estimated as described below). The measurements are indicated in Table I.

Chemical analyses of the precipitates obtained with different volumes of acetone

Total sugar content of each pellet was measured by the phenol–H_2SO_4 reaction (Dubois et al. 1956), using D-galactose as standard. After acid hydrolysis of the polysaccharides (6 M HCl for 4 h at 100°C), the sulfate contents were measured by the toluidine method as previously described (Nader and Dietrich 1977). Again, the polysaccharides of each pellet were hydrolyzed (2 M HCl for 2 h at 100°C) and the type of hexose was determined by gas–liquid chromatography of alditol acetate derivatives (Kircher 1960), as described below. As standards, fucose, glucose, rhamnose, arabinose, mannose, galactose, and xylose were converted to their respective alditol acetates.

Purification of the sulfated galactan

To obtain the sulfated galactan, the precipitate formed with 1:0.9 acetone was fractionated by ion-exchange chromatography. After centrifugation and drying, 12 mg was dissolved in 5 mL of distilled water and applied to a column (19.0 × 4.5 cm) of MP500 Lewatit resin (Bayer Chemicals, São Paulo, Brazil). First, the column was washed with 300 mL of distilled water and developed by a stepwise gradient system using 300 mL of aqueous solutions with different concentrations of NaCl (0.3 M, 0.5 M, 0.7 M, 1.0 M, 1.5 M, 2.0 M, 3.0 M, and 4.0 M) at 1 mL/min. The first 300 mL at each step was collected in a single recipient; then, a second recipient was used to collect an additional 300 mL of the same saline molarity to check for the complete elution of the polysaccharides. To precipitate the polysaccharides, two volumes (600 mL) of methanol were added to both recipients for each step. However, only the first 300 mL of the steps at 0.3 M, 2.0 M, and 3.0 M precipitated polysaccharides when methanol was added. These suspensions were centrifuged separately (10,000 × *g* for 20 min), dried under vacuum, dissolved in distilled water to a final concentration of 10 mg/mL, and analyzed for hexose (Dubois et al. 1956) and sulfate molar ratio (Nader and Dietrich 1977).

Agarose and polyacrylamide gel electrophoresis

The precipitate with 1:0.9 acetone and the fractions of sulfated galactan (SG 1 and SG 2) were analyzed by agarose gel electrophoresis as described previously (Dietrich CP and Dietrich SMC 1977). The samples (~20 μg) were applied to a 5-mm-thick 0.5% agarose gel and run for 1 h at 110 V in 0.05 M 1,3-diaminopropane–acetate (pH 9.0). The sulfated polysaccharides in the gel were fixed with 0.1% *N*-cetyl-*N*,*N*,*N*-trimethylammonium bromide solution. After 12 h, the gel was dried and stained with 0.1% toluidine blue in acetic acid:ethanol:water (0.1:5:5, v/v).

The molecular masses of the sulfated galactan (SG 1 and SG 2) were estimated by PAGE in comparison with the electrophoretic mobility of standard compounds (Pomin, Pereira, et al. 2005). The sulfated polysaccharides (~10 μg of each) were applied to a 1-mm-thick 10% polyacrylamide slab gel in 0.02 M sodium barbital (pH 8.6). After electrophoresis (100 V for 30 min), the sulfated polysaccharides were stained with 0.1% toluidine blue in 1% acetic acid and washed for about 1 h in 1% acetic acid. The molecular-mass markers used were high-molecular-weight dextran sulfate (~500 kDa), chondroitin 6-sulfate from shark cartilage (~60 kDa), chondroitin 4-sulfate from whale cartilage (~40 kDa), unfractionated heparin from porcine intestinal mucosa (~15 kDa), low-molecular-weight-heparin (~7.5 kDa), and low-molecular-weight dextran sulfate (~8 kDa).

Desulfation and methylation reactions

Desulfation of the sulfated galactan was performed as detailed previously (Mourão and Perlin 1987; Vieira et al. 1991). About 20 mg of each sulfated galactan (SG 1 and SG 2) was dissolved in 5 mL of distilled water and mixed with 1 g (dry weight) of Dowex 50-W (H^+, 200–400 mesh). After neutralization with pyridine, solutions were lyophilized. The resulting pyridinium salts were dissolved in 2.5 mL of dimethyl sulfoxide:methanol (9:1, v/v). The mixtures were heated at 80°C for 4 h, and the desulfated products were exhaustively dialyzed against distilled water and lyophilized. The extent of desulfation was estimated by the molar ratio of sulfate/total sugars. This method allows us to detect desulfation down to a molar ratio of ≤0.1 sulfate/total sugar. About 5 mg of each desulfated fraction was obtained. The native and desulfated galactans were subjected to three rounds of methylation, as described (Ciucanu and Kerek 1984)

and with the modifications suggested by Patankar et al. (1993). The methylated galactans were hydrolyzed with 6.0 M trifluoroacetic acid for 5 h at 100°C, reduced with borohydride, and the alditols were acetylated with 1:1 acetic anhydride/pyridine (Kircher 1960). The alditol acetates from the methylated sugars were dissolved in chloroform and analyzed in a Hewlett-Packard gas chromatography/mass spectrometry unit, model 5987-A. Injection was made in the splitless mode in a DB-1 capillary column (25 m × 0.3 mm). The column was programmed to run at 120°C for 2 min, then raised to 230°C at 2°C/min, and held for 5 min.

NMR experiments

^{1}H and ^{13}C, one-dimensional and two-dimensional spectra of the native sulfated galactan and the desulfated galactan were recorded using a Bruker DRX 400 MHz apparatus with a triple resonance probe as detailed previously (Pomin, Valente, et al. 2005). About 5 mg of each sample was dissolved in 0.5 mL 99.9% deuterium oxide (Cambridge Isotope Laboratory, Cambridge, MA). All spectra were recorded at 50°C with HOD suppression by presaturation. The 1D ^{1}H NMR spectra were recorded with 16 scans. The 2D ^{1}H/^{1}H COSY, TOCSY, NOESY, and ^{1}H/^{13}C HSQC spectra were recorded using states-time proportion phase incrementation (states-TPPI) for quadrature detection in the indirect dimension. The TOCSY spectra were run with 4046 × 400 points with a spin-lock field of 10 kHz and a mixed time of 80 ms. The NOESY spectra were recorded with a mixing time of 100 ms. The ^{1}H/^{13}C DEPT-HSQC and ^{1}H/^{13}C HSQC spectra were run with 1024 × 256 points and globally optimized alternating phase rectangular pulses (GARP) for decoupling. The ^{1}H/^{13}C HMBC spectrum was recorded with 1024 × 256 points, with a 60-ms delay for evolution of long-range couplings and was set with no decoupling during acquisition time. Chemical shifts are displayed relative to external trimethylsilylpropionic acid at 0 ppm for ^{1}H and relative to methanol for ^{13}C.

Supplementary Data

Supplementary data for this article is available online at http://glycob.oxfordjournals.org.

Funding

Conselho Nacional de Desenvolvimento Científico e Tecnológico (CNPq), Fundação de Amparo à Pesquisa do Estado do Rio de Janeiro (FAPERJ) and Coordenação de Aperfeiçoamento de Pessoal de Nível Superior (CAPES).

Acknowledgements

We are grateful to Anderson Pinheiro and Fabiana Albernaz from the Centro Nacional de Ressonância Magnética Nuclear Jiri Jonas, CCS, Brazil for help with the NMR experiments and figures and especially to Martha Sorenson for editing the manuscript.

Conflict of interest statement

None declared.

Abbreviations

COSY, correlation spectroscopy; DEPT, distortionless enhancement by polarization transfer; HMBC, heteronuclear multiple bound coherence; HSQC, heteronuclear single quantum coherence; NMR, nuclear magnetic resonance; NOESY, nuclear overhauser enhancement spectroscopy; PAGE, polyacrylamide gel electrophoresis; SG, sulfated galactan; TOCSY, total correlation spectroscopy..

References

Albano RM, Pavão MSG, Mourão PAS, Mulloy B. 1990. Structural studies of a sulfated L-galactan from *Styela plicata* (Tunicate): Analysis of the Smith-degraded polysaccharide. Carbohydr Res. 208:163–174.

Alves AP, Mulloy B, Diniz JA, Mourão PAS. 1997. Sulfated polysaccharides from the egg jelly layer are species-specific inducers of acrosomal reaction in sperms of sea urchins. J Biol Chem. 272:6965–6971.

Amornrut C, Toida T, Imanari T, Woo E-R, Park H, Linhardt R, Wu SJ, Kim YS. 1999. A new sulfated beta-galactan from clams with anti-HIV activity. Carbohydr Res. 321:121–127.

Aquino RS, Landeira-Fernandez AM, Valente A-P, Andrade LR, Mourão PAS. 2005. Occurrence of sulfated galactans in marine angiosperms: Evolutionary implications. Glycobiology. 15:11–20.

Berteau O and Mulloy B. 2003. Sulfated fucans, fresh perspectives: Structures, functions, and biological properties of sulfated fucans and an overview of enzymes active toward this class of polysaccharide. Glycobiology. 13:29R–40R.

Bilan MI, Vinogradova EV, Shashkov AS, Usov AI. 2007. Structure of a highly pyruvylated galactan sulfate from the Pacific green alga *Codium yezoense* (Bryopsidales, Chlorophyta). Carbohydr Res. 342:586–596.

Ciucanu I and Kerek F. 1984. Rapid and simultaneous methylation of fatty and hydroxy fatty acids for gas chromatographic analysis. J Chromatogr. 286:179–185.

Dietrich CP and Dietrich SMC. 1977. Electrophoretic behaviour of acidic mucopolysaccharides by agarose gel electrophoresis. J Chromatogr. 130:299–304.

Dubois M, Gilles KA, Hamilton JK, Rebers PA, Smith F. 1956. Colorimetric method for determination of sugars and related substances. Anal Chem. 28: 350–354.

Estevez JM, Ciancia M, Cerezo AS. 2004. The system of low-molecular-weight carrageenans and agaroids from the room-temperature-extracted fraction of *Kappaphycus alvarezii*. Carbohydr Res. 339:2575–2592.

Kircher HW. 1960. Gas–liquid partition chromatography of methylated sugars. Anal Chem. 32:1103–1106.

Lahaye M. 2001. Development on gelling algal galactans, their structure and physico-chemistry. J Appl Phycol. 13:173–184.

Love J and Percival E. 1964. The polysaccharides of green seaweed *Codium fragile*: Part III. A β-1,4-linked mannan. J Chem Soc. 3345–3350.

Mathews MB. 1975. Connective Tissue, Macromolecular Structure and Evolution. Berlin: Springer.

Matsubara K, Matsuura Y, Bacic A, Liao M-L, Hori K, Miyazawa K. 2001. Anticoagulant properties of a sulfated galactan preparation from a marine green alga. Codium cylindricum Biol Macromol. 28:395–399.

Mourão PAS. 2004. Use of sulfated fucans as anticoagulant and antithrombotic agents: Future perspectives. Curr Pharm Des. 10:967–981.

Mourão PAS. 2007. A carbohydrate-based mechanism of species recognition in sea urchin fertilization. Braz J Med Biol Res. 40:5–17.

Mourão PA and Perlin AS. 1987. Structural features of sulfated glycans from the tunic of *Styela plicata* (Chordata-Tunicata). A unique occurrence of L-galactose in sulfated polysaccharides. Eur J Biochem. 166:431–436.

Mulloy B, Ribeiro A-C, Alves A-C, Vieira RP, Mourão PAS. 1994. Sulfated fucans from echinoderms have a regular tetrasaccharide repeating unit defined by specific patterns of sulfation at the *O*-2 and *O*-4 positions. J Biol Chem. 296:22113–22123.

Murano E, Toffanin R, Cecere E, Rizzo R, Knutsen SH. 1997. Investigation of the carrageenans extracted from *Solieria filiformis* and *Agardhiella subulata* from Mar Piccolo, Taranto. Mar Chem. 58:319–325.

Nader HB and Dietrich CP. 1977. Determination of sulfate after chromatography and toluidine blue complexation. Anal Biochem. 78:112–118.

Patankar MS, Oehninger S, Barnett T, Williams RL, Clark GF. 1993. A revised structure for fucoidan may explain some of its biological activities. J Biol Chem. 268:21770–21776.

Pavão MSG, Albano RM, Lawsom AM, Mourão PAS. 1989. Structural heterogeneity among unique sulfated L-galactans from different species of ascidians (tunicates). J Biol Chem. 264:9972–9979.

Pavão MSG, Mourão PA, Mulloy B. 1990. Structure of a unique sulfated alpha-L-galactofucan from the tunicate Clavelina. Carbohydr Res. 208:153–161.

Pereira MS, Mulloy B, Mourão PAS. 1999. Structure and anticoagulant activity of sulfated fucans. Comparison between the regular, repetitive and linear fucans from echinoderms with the more heterogeneous and branched polymers from brown algae. J Biol Chem. 274:7656–7667.

Pereira MG, Benevides NMB, Melo MRS, Valente A-P, Melo FR, Mourão PA. 2005. Structure and anticoagulant activity of a sulfated galactan from the red alga, *Gelidium crinale*. Is there a specific structural requirement for the anticoagulant action? Carbohydr Res. 340:2015–2023.

Pomin VH, Pereira MS, Valente A-P, Tollefsen DM, Pavão MSG, Mourão PA. 2005. Selective cleavage and anticoagulant activity of a sulfated fucan: Stereospecific removal of a 2-sulfated ester from the polysaccharide by mild acid hydrolysis, preparation of oligosaccharides, and heparin cofactor II-dependent anticoagulant activity. Glycobiology. 15:369–381.

Pomin VH, Valente A-P, Pereira MS, Mourão PA. 2005. Mild acid hydrolysis of sulfated fucans: A selective 2-desulfation reaction and an alternative approach for preparing tailored sulfated oligosaccharides. Glycobiology. 15:1376–1385.

Ribeiro A-C, Vieira RP, Mourão PAS, Mulloy B. 1994. A sulfated alpha-L-fucan from sea cucumber. Carbohydr Res. 255:225–240.

Rocha HA, Moraes FA, Trindade ES, Franco CR, Torquato RJ, Veiga SS, Valente A-P, Mourão PA, Leite EL, Nader HB et al. 2005. Structural and hemostatic activities of a sulfated galactofucan from the Brown alga *Spatoglossum schroederi*. An ideal antithrombotic agent? J Biol Chem. 280:41278–41288.

Santos JA, Mulloy B, Mourão PAS. 1992. Structural diversity among sulfated alpha-L-galactans from ascidians (tunicates). Studies on the species *Ciona intestinalis* and *Herdmania monus*. Eur J Biochem. 204:669–677.

Scudder P, Tanq PW, Hounsell EF, Lawson AM, Mehmet H, Feizi T. 1986. Isolation and characterization of sulphated oligosaccharides released from bovine corneal keratin sulphate by the action of endo-beta-galactosidase. Eur J Biochem. 157:365–373.

Shashkov AS, Senchenkova SN, Vinogradov EV, Zatonsky GV, Knirel YA, Literacka E, Kaca W. 2000. Full structure of the *O*-specific polysaccharide of *Proteus mirabilis* O24 containing 3,4-*O*-[(S)-1-carboxyethylidene]-D-galactose. Carbohydr Res. 329:453–457.

van de Velde F, Pereira L, Rollema HS. 2004. The revised NMR chemical shift data of carrageenans. Carbohydr Res. 339:2309–2313.

Verli H. 2007. Insights into Carbohydrate Structure and Biological Function. Kerala (India): Transworld Research Network.

Vieira RP, Mulloy B, Mourão PA. 1991. Structure of a fucose-branched chondroitin sulfate from sea cucumber. Evidence for the presence of 3-*O*-sulfo-beta-D-glucuronosyl residues. J Biol Chem. 266:13530–13536.

Whittaker RH. 1969. New concepts of kingdoms of organisms. Science. 163:150–160.

CAPÍTULO 4: β-GALACTANA SULFATADA EM OURIÇO-DO-MAR

4.1 Objetivos

Extrair, purificar e analisar a estrutura química e conformacional da β-galactana sulfatada da espécie de ouriço-do-mar *G. crenularis*. Verificar quais são as características estruturais dessa galactana sulfatada responsáveis pela indução na reação acrossômica em espermatozóides de ouriços-do-mar.

4.2 Materiais e métodos

4.2.1 Extração e purificação

Gametas femininos maduros da espécie de ouriço-do-mar G. *crenularis* foram coletados na Baía de Noheji, Japão. Os gametas foram liberados na água-do-mar por uma injeção intracelômica de KCl 0,5 M. Os envóltórios gelatinosos totais foram isolados dos óvulos por choque de pH, filtrados e centrifugados a 30,000 x g. O sobrenadante foi dializado contra água destilada e liofilizados, como descrito por Vacquier e Moy (1997). Os polissacarídeos totais foram extraídos da camada gelatinosa do óvulo por digestão com papaína e parcialmente purificados por precipitação com etanol, como descrito previamente (Albano and Mourão, 1986). Aproximadamente 10 mg de polissacarídeo total foram aplicadas a uma coluna de Mono-Q (HR5/5; Amershan Biosciences. Inc.), acoplada a sistema de FPLC e equilibrada com Tris-HCl 20 mM (pH 8,0). A coluna foi lavada com 10 mL do mesmo tampão e então eluída com um gradiente linear de sal de NaCl 0-3M no mesmo tampão. O fluxo da coluna foi de 0,45ml/min e frações de 0,5 ml foram coletadas. As frações foram analisadas quanto aos conteúdos de galactose e ácido siálico, respectivamente pelos métodos de Dubois e Erlich (Dubois et al. 1971; Kabat and Mayer, 1971), e também, quanto sua propriedade metacromática (Farndale *et al.* (1986). As concentrações de NaCl foram estimadas por leitura de condutividade. As frações contendo os polissacarídeos sulfatados, foram agrupadas, dialisadas contra água destilada e liofilizadas.

4.2.2 Eletroforeses e dessulfatação dos polissacarídeos

As amostras de polissacarídeos foram analisadas por eletroforeses em gel de agarose e de policarilamida como descrito no item 3.2.4. A reação de dessulfatação foi realizada como descrita em 3.2.5.

4.2.3 Experimentos de RMN

Os experimentos de RMN foram feitos exatamente como descritos em 3.1.2.6.

4.2.4 Dinâmica molecular (DM)

Todos os cálculos e simulações foram realizados pelo programa GROMACS (van der Spoel *et al.* 2005) e campo de força GROMOS96 (van Gunsteren *et al.* 1996). As estruturas das unidades dissacarídicas: α-L-Gal*p*-(1→3)-α-L-Gal*p*, α-L-Gal*p*-2(SO_4)-(1→3)-α-L-Gal*p*-2(SO_4), β-D-Gal*p*-(1→3)-β-D-Gal*p*, β-D-Gal*p*-2(SO_4)-(1→3)-β-D-Gal*p* and β-D-Gal*p*-(1→3)-β-D-Gal*p*-2(SO_4) foram fornecidos pelo servidor PRODRG (Schuettelkopf *et al.* 2004). As geometrias iniciais foram restringidas. Essas geometrias foram fornecidas com cargas atômicas Löwdin HF/6-31G** (Verli e Guimarães, 2004; Becker *et al.*, 2005) e submetidas à análise conformacioanl pela variação dos ângulos diedros Φ e Ψ de −180 a 180 graus, com passos de 30^o, num total de 144 confôrmeros para cada ligação. Cada conformação foi posteriormente refinada em DM por 20 ps a 10 K, com passos de integração de 0.5 fs (Pol-Fachin e Verli, 2008). As estabilidades relativas de cada conformação obtida foram usadas para construir os mapas de energia. As conformações de mínima energia observadas nesses mapas foram submetidas a simulações de MD por 0.1 μs em solução aquosa usando modelo de água-SPC (Berendsen *et al.*, 1987), seguido do protocolo previamente descrito em Verli e Guimarães (2004, 2005); Becker *et al.* (2005). Uma caixa de água sob condições de ligação periódicas foi empregada, usando uma distância mínima de 10 Å do soluto para as faces da caixa. Contra-íons (Na^+) foram adicionados para neutralizar o sistema. O método Lincs (Hess *et al.*, 1997) foi aplicado para contração de comprimentos de ligação, permitindo a integração por passos de 2 fs após uma minimização da energia inicial usando o algorítmo Steepest Descents. Todas as simulações aplicadas utilizaram o método de Particle-Mesh Ewald (Darden

et al. 1993). A temperatura e pressão foram mantidas constantes para carboidratos, ìons e solvente acoplados à temperature externa e banhos de pressão com constantes de acoplamento de τ = 0.1 e 0.5 ps, respectivamente (Berendsen *et al.*, 1984). A temperature referencial foi ajustada para 310 K. As recomendações e símbolos de nomenclatura propostos pela IUPAC (IUPAC-IUBMB, 1996) foram respeitados. A orientação relativa de cada par contínuo de carboidratos foi descrita pelos ângulos de torção da ligação glicosídica, denominados Φ e Ψ, como descrito: Φ = O-5–C-1–O-1–C-3´ e Ψ = C-1–O-1–C-3´–C-2´.

4.3 Resultados e discussão

4.3.1 O gel do óvulo do ouriço-do-mar *G. crenularis* contém uma D-galactana sulfatada

Os polissacarídeos extraídos da camada gelatinosa de *G. crenularis* foram purificados por cromatografia de troca-aniônica em coluna Mono-Q, acoplada a um sistema de FPLC, e suas frações foram monitoradas quanto a hexose (círculos fechados, Figura 16A) e metacromasia (círculos abertos, Figura 16A). Este perfil, mostrou apenas uma fração única de polissacarídeo sulfatado, que elui com uma molaridade de ~1,3 M NaCl. O sialo-glicoconjugado não foi observado nos géis dos óvulos desta espécie de ouriço-do-mar, como indicado pela reação de Erlich negativa (triângulos fechados, Figura 16A). Estes glicoconjugados de ácido siálico são comumente observados na camada gelatinosa dos óvulos de outras espécies de ouriços-do-mar, eluindo da coluna de Mono-Q com uma concentração salina de ~0,7 M (Alves *et al*., 1997, 1998; Vilela-Silva *et al*., 1999, 2002).

O polissacarídeo sulfatado de *G. crenularis* revelou apenas uma banda na eletroforese em gel de agarose (Figura 16B), e um peso molecular alto analisado por PAGE (Figura 16C). Esta massa molecular alta (≥ 100 kDa) é comumente observada para os fucanas e galactanas sulfatadas de géis do óvulo de ouriços-do-mar (Alves *et al*., 1997, 1998; Vilela-Silva *et al*., 1999, 2002). Análises químicas deste polissacarídeo sulfatado purificado de *G. crenularis* revelaram exclusivamente galactoses e sulfatos. O galactosídeo (-)-2-butil acetato obtido deste polissacarídeo mostrou o mesmo tempo de reten-

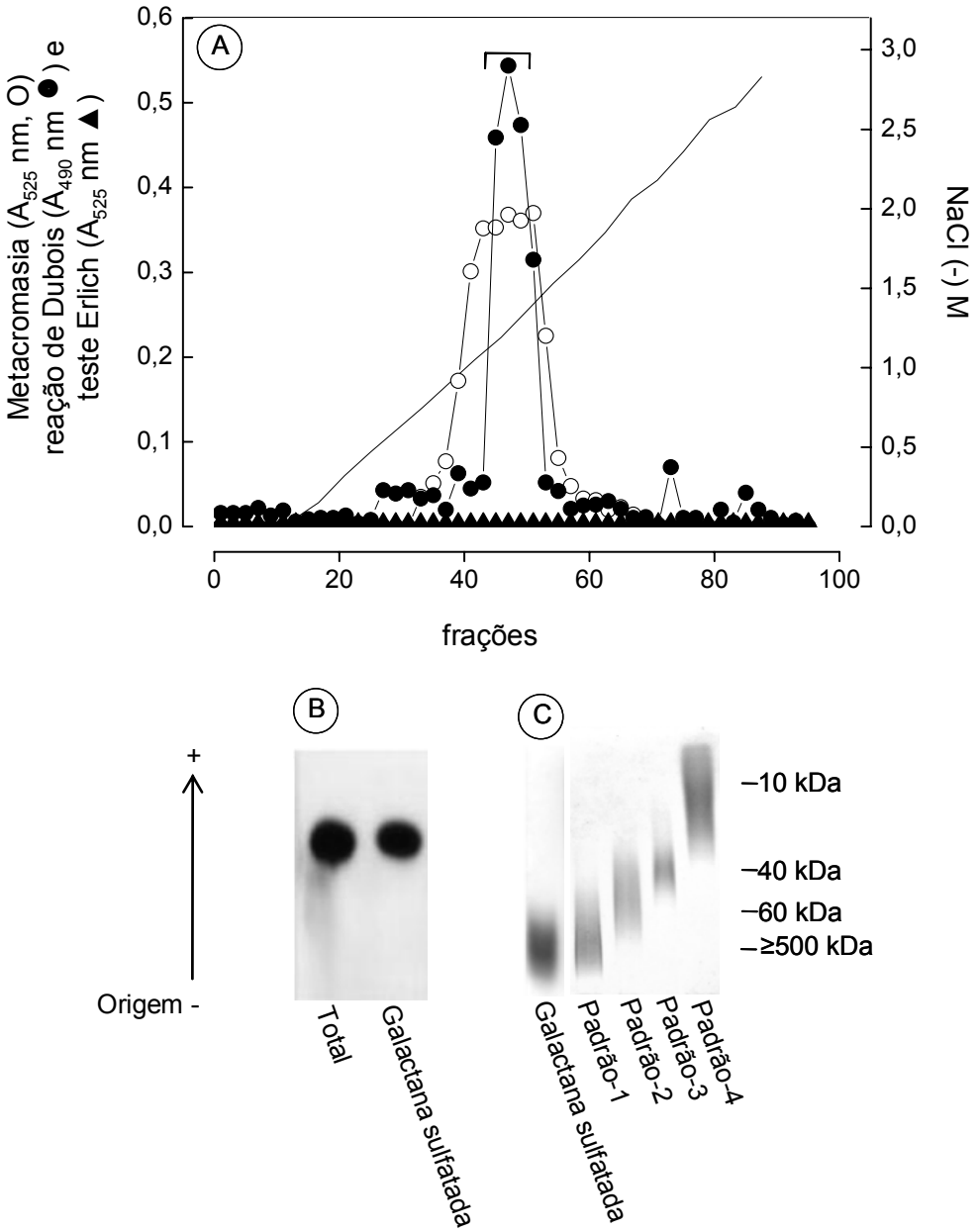

Figura 16. Purificação da galactana sulfatada do envoltório gelatinoso dos óvulos de *G. crenularis*. (**A**) Os polissacarídeos totais (Total) do gel do óvulo foram purificados por cromatografia em troca-iônica em coluna de Mono-Q acoplada a um sistema de FPLC, como descrito no item 4.2.1. A única fração obtida da coluna foi analisada por suas propriedades metacromáticas (círculos abertos), ácido siálico (triângulo fechado) e hexose (círculo fechado). As concentrações de NaCl foram estimadas pela leitura de condutância. A única fração de polissacarídeo sulfatado foi agrupada, dialisada contra água destilada e liofilizada. (**B**) Os polissacarídeos sulfatados (totais e galactana sulfatada) foram aplicados a um gel de 0,5% de agarose como descrito no item 4.2.2. (**C**) Os polissacarídeos purificados foram aplicados a um gel de poliacrilamida 10% como descrito no item 4.2.2. Os padrões foram: 1- dextran sulfato de alto peso (~500 kDa), 2- condroitim 6-sulfato (~60 kDa), 3- condroitim 4-sulfato (~40 kDa) e dextram sulfato de baixo peso (~8kDa).

ção do padrão de D-galactose. Portanto, resíduos de galactose ocorrem no polímero de *G. crenularis* como D-enantiômeros.

Em conclusão, o gel do óvulo do ourilo-do-mar *G. crenularis* contém uma única fração de D-galactana sulfatada. Esta ocorrência difere dos polissacarídeos sulfatados das outras espécies de ouriços-do-mar, formadas por fucoses e galactoses sempre na configuração-L (Alves *et al*., 1997, 1998; Vilela-Silva *et al*., 1999, 2002).

4.3.2. A galactana sulfatada de *G. crenularis* tem uma unidade dissacarídica regular composta por resíduos de β-galactopiranose 3-ligada, alternando 2-sulfatação e não-sulfatação

Para uma análise estrutural da galactana sulfatada de *G. crenularis*, empregamos experimentos de espectroscopia de RMN 1D e 2D do polissacarídeo nativo e seu derivado dessulfatado (Figuras 17-19).

O espectro de RMN-^{1}H 1D (Figura 17A) e especialmente o espectro heteronuclear ^{1}H/^{13}C HSQC (Figura 18A) da galactana sulfatada nativa mostrou proporções equimolares de dois sinais anoméricos, denominados como A1 e B1. A1 ressona com um deslocamento químico de campo-baixo (~0,2 ppm), possivelmente devido à sulfatação (Pomin et al 2005a). Esta conclusão foi obtida pela observação do sinal anomérico A1 no espectro ^{1}H/^{13}C HSQC do polissacarídeo sulfatado (Figura 18A) e seu conseqüente desaparecimento no espectro ^{1}H/^{13}C HSQC da amostra dessulfatada (Figura 18B). Estas observações sugerem que a galactana sulfatada de *G. crenularis* contem proporções equimolares de resíduos de galactose não-sulfatados e sulfatados.

Picos de correlação nos espectros COSY 2D (Figuras 19A e D) e nos espectros TOCSY (Figuras 19B e E) permitiram traçar o sistema de spins completo para os sistemas de sinais A e B da galactana nativa e para o sistema de sinais B da galactana dessulfatada. O espectro COSY da galactana nativa mostrou dois sinais de correlação (A1-2 e B1-2) devido ao acoplamento escalar entre os prótons anoméricos (^{1}H1) e os hidrogênios 2 (H2) de cada resíduo (Figura 19A). A presença única do sinal de correlação B1-2 é observada no espectro da galactana dessulfatada (Figura 19D). Seguindo à identificação dos picos de correlação nos espectros COSY, os experimentos de

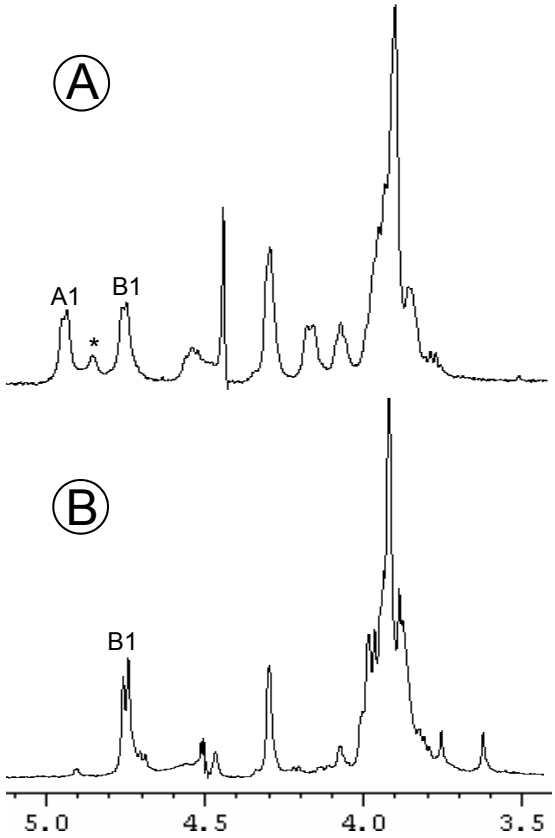

Figura 17. Espectros 1D de ^{1}H-RMN em 400 MHz (de ~ 5.5 a ~ 3.0 ppm) da galactana sulfatada nativa (**A**) do ouriço-do-mar *G. crenularis* e seu derivado dessulfatado (**B**). Cerca de 5 mg de cada amostra foram dissolvidos em 0.5 mL de D_2O e os espectros 1D foram realizados a 50^{o}C. O sinal de aágua residual foi surimido por pré-saturação. Os deslocamentos químicos de protons estão relacionados ao padrão externo ácido trimetilsilipropiônico em 0 ppm. Os sinais A1 e B1 correspondem respectivamente aos sinais H1-anoméricos das unidades de β-D-galactopiranose 2-sulfatada e não-sulfatada. O pico marcado com o asterístico corresponde a um contaminante.

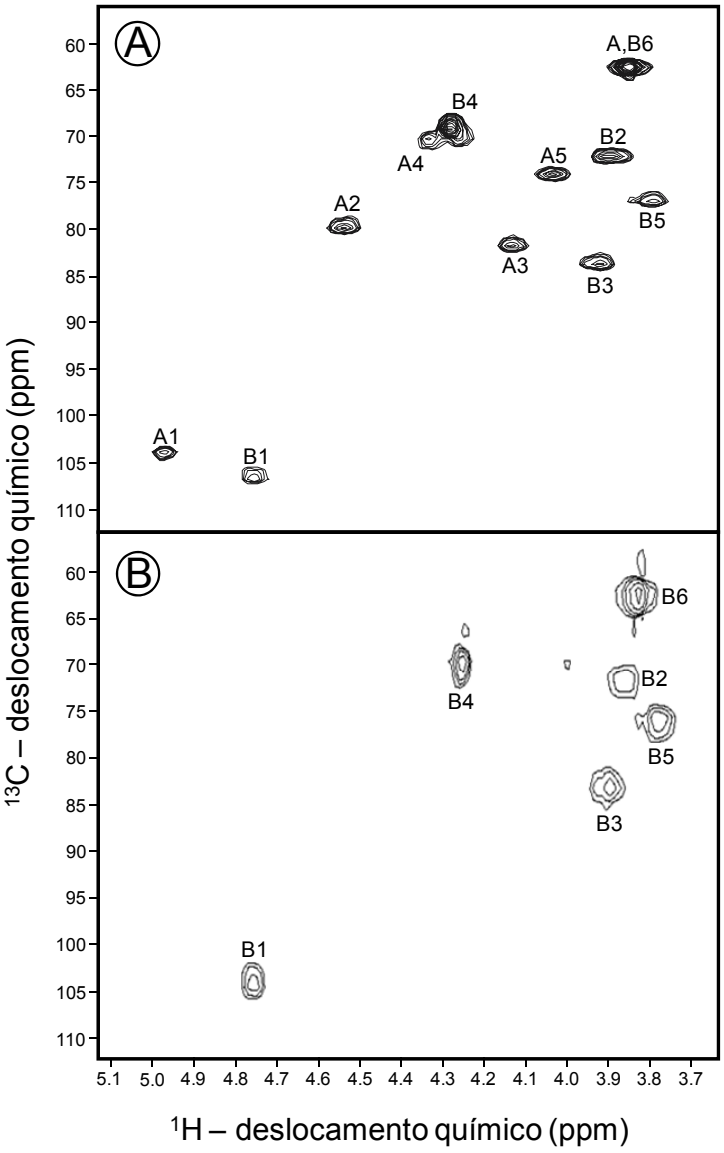

Figura 18. Espectros de $^{1}H/^{13}C$ HSQC da galactana sulfatada do ouriço-do-mar *G. crenularis* (**A**) e seu derivado dessulfatado (**B**). Os deslocamentos químicos estão relacionados aos padrões externos ácido trimetilsililpropiônico em 0 ppm para ^{1}H e metanol para ^{13}C. Os sistemas de spins foram denominados A e B para as unidades de β-D-galactopiranose 2-sulfatada e não-sulfatada, respectivamente.

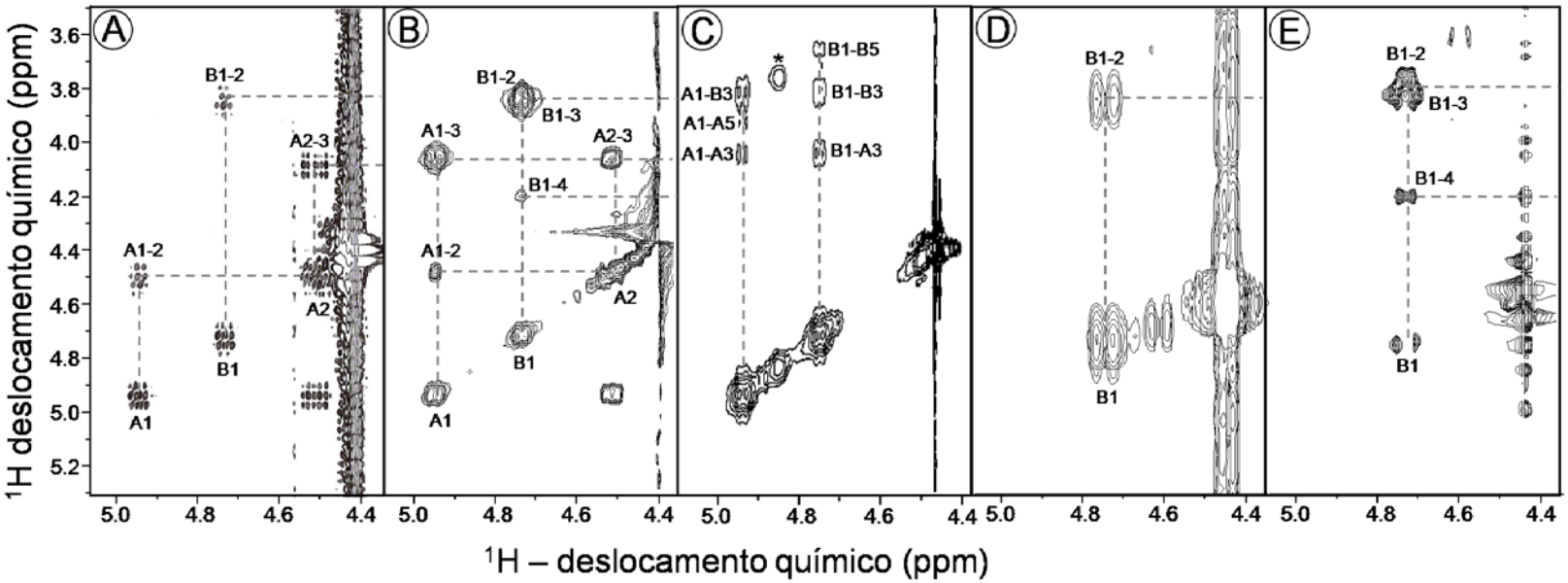

Figura 19. Faixas espectrais das regiões anoméricas (de ~ 4.5 a ~ 5.1 ppm) dos espectros COSY (**A** e **D**), TOCSY (**B** e **E**) e NOESY (**C**) da galactana sulfatada (**A-C**) do ouriço-do-mar *G. crenularis* e seu derivado dessulfatado (**D** e **E**). Cerca de 5 mg de cada amostra foram dissolvidos em 0.5 mL de D_2O e os espectros de 2D RMN foram realizados a 50ºC em 400 MHz. Os deslocamentos químicos estão relacionados ao padrão externo ácido trimetilsililpropiônico em 0 ppm para ^{1}H. Os sistemas de spins foram denominados como A e B para as unidades de β-D-galactopiranose 2-sulfatadas e não-sulfatadas, respectivamente. O pico no espectro NOESY (**C**) marcado com asterístico corresponde a um contaminante.

TOCSY (Figs 19B e E) permitiu assinalar inequivocamente os sistemas de spins A e B e obter os valores de deslocamentos químicos de prótons (ppm), como indicados na Tabela VI. Baseado nos deslocamentos químicos de ^{1}H, os picos de correlação heteronuclear nos espectros $^{1}H/^{13}C$ HSQC (Figura 18) foram assinalados e obtivemos os valores para os deslocamentos químicos de carbono ^{13}C (Tabela VI). Análises desses deslocamentos químicos de ^{13}C revelaram que a galactana contém resíduos de β-galactopiranose 3-ligados, como indicado pelo típico deslocamento a campo-baixo deste carbono (~10 ppm) em sítios de glicosilação (Tabela VI) (ver Anexo II e III do capítulo 2 desta tese).

Os sistemas de spins A e B traçados para a galactana sulfatada diferem principalmente para o típico deslocamento ^{1}H em campo-baixo (~0,6 ppm) do H2 que indica 2-sulfatação (Tabela VI). As regiões de ^{1}H do H1 e H3 mostraram um deslocamento típico de ~0,2 ppm a campo-baixo devido a 2-sulfatação.

Em síntese, esses resultados indicam que a galactana sulfatada de *G. crenularis* possui proporções equimolares de 2-sulfatação e não-sulfatação em resíduos de β-galactopiranose. Ainda fica a dúvida se esses resíduos se alternam ao longo do polímero ou ocorrem em distribuições aleatórias, ou ainda, em regiões sulfatadas e outras não sulfatadas. Esta dúvida foi esclarecida com o espectro 2D NOESY da galactana nativa (Figura 19C). O espectro revelou NOE´s intra-residuais entre o ^{1}H-anomérico com H3 e H5, comumente encontrados em resíduos de β-galactopiranose (Ravenscroft *et al* 1995). Prótons H1, H3 e H5 de galactose estão orientados no mesmo plano (equatorialmente ou axialmente) com contatos espaciais de até 5 Å de distancia, que permite a detecção de sinais NOE. Porém, mais significativamente, o espectro NOESY também revelou NOEs inter-resíduais entre H1 com o H3 do resíduo adjacente (A1-B3 e B1-A3) (Figura 19C). Estas observações indicam que os resíduos 2-sulfatados e não-sulfatados se intercalam ao longo da cadeia do polissacarídeo, em unidades dissacarídicas repetitivas. Portanto, a galactana sulfatada do gel do óvulo de *G. crenularis* é composta por uma unidade dissacarídica repetitiva de: [-3-β-D-Gal*p*-2(OSO_4)-1→3-β-D-Gal*p*-1-]$_n$ (Figura 20).

Tabela VI. Deslocamentos químicos de ^{1}H e ^{13}C (ppm), $^{3}J_{H-H}$ e $^{1}J_{C-H}$ dos espectros de RMN das α-L- e β-D-galactanas sulfatadas dos ouriços-do-mar *E. lucunter* e *G. crenularis*, respectivamente.

Polissacarídeos dos ouriços-do-mar	Deslocamentos químicos de ^{1}H and ^{13}C [a] (ppm)					
	H-1 C-1	H-2 C-2	H-3 C-3	H-4 C-4	H-5 C-5	H-6 C-6
α-L-galactana sulfatada[b] (Figura 3A)	5.47 97.2	**4.66** **76.2**	*4.23* *75.9*	4.33 72.5	4.35 69.5	3.82 63.8
β-D-galactana sulfatada (A) unidade 2-sulfatada	4.94 104.1	**4.52** **80.2**	*4.11* *81.8*	4.37 70.5	4.02 74.3	3.82 62.5
β-D-galactana sulfatada (B) unidade não-sulfatada	4.73 107.2	3.87 72.0	*3.90* *83.5*	4.24 69.1	3.75 77.0	3.82 62.5
	$^{3}J_{H-H}$ (Hz)					
	H-1,H-2	H-2,H-3	H-3,H-4	H-4,H-5	H-5,H-6	
α-L-galactana sulfatada (Figura 3A)	3.0	10.5	ND[c]	ND	4.5	
β-D-galactana sulfatada	7.4	7.9	2.7	ND	ND	
	$^{1}J_{C-H}$ (Hz)					
	C-1,H-1	C-2,H-2	C-3,H-3	C-4,H-4	C-5,H-5	C-6,H-6
α-L-galactana sulfatada (Figura 3A)	177.5	151.3	146.2	146.5	146.8	143.3
β-D-galactana sulfatada (A) unidade 2-sulfatada	164.7	156.8	143.4	151.4	143.0	143.9
β-D-galactana sulfatada (B) unidade não-sulfatada	163.5	141.2	143.1	150.5	139.9	143.9

[a]Os deslocamentos qu´micos estão calibrados em relação a padrão externo ácido trimetilsilpropiônico em 0 ppm para ^{1}H e metanol para ^{13}C. Os valores indicados em negrito correspondem as posições de sulfatação e em itálico, as posições glicosiladas.

[b]Referências de Pereira *et al*., 2002.

[c]ND, não determinado.

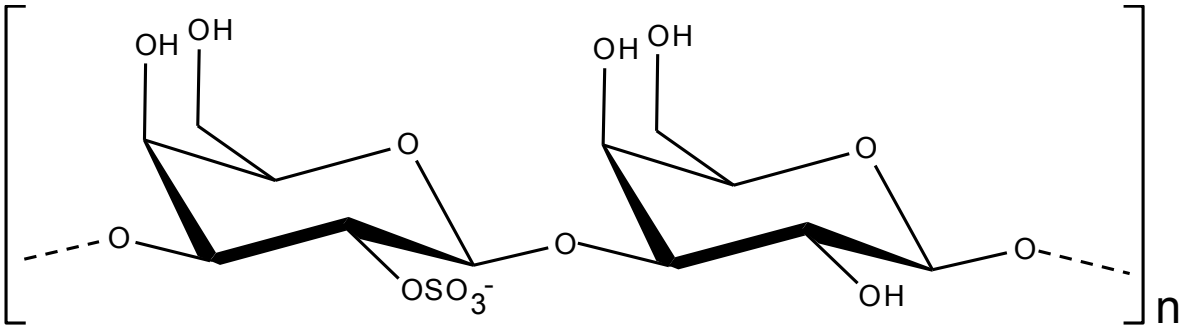

Figura 20. Unidade dissacarídica repetitiva da galactana sulfatada do gel do óvulo do ouriço-do-mar *G. crenularis*.

4.3.3 As constantes de acopamento $^{3}J_{H-H}$ e $^{1}J_{C-H}$ das α- e β-galactanas sulfatadas de ouriços-do-mar indicam conformações distintas

A β-galactana sulfatada do ouriço-do-mar *G. crenularis* revelou, interessantemente, dubletos bem nítidos de acoplamento ^{1}H-^{1}H nos sinais anoméricos dos espectros 1D (Figura 16A e B), cujos valores são 7,4 Hz para ambos os resíduos (Tabela VI). Estes sinais de acoplamento ^{1}H-^{1}H são bem evidentes pelos multipletos nos picos de correlação do espectro COSY (Figura 19A) e nos dubletos dos outros espectros 2D homonucleares (TOCSY e NOESY, Figura 19B e C). Este padrão de acoplamento particular e diferenciado já foi observado em outras β-galactanas sulfatadas de invertebrados, como na do mexilhão *Meretrix petenchialis* (Amornrut *et al*., 1999). Porém, este parâmetro é pouco evidente na maioria das α-galactanas sulfatadas (Alves *et al*., 1997; Pereira *et al*., 2002) (Tabela VI). Esta diferença nos valores de acoplamento escalar (*J*-, medido em Hz) é devido aos diferentes arranjos moleculares (e obviamente das diferentes conformações dos hidrogênios envolvidos nestes acoplamentos), sugerindo, assim, clara difereça nas conformações espaciais das α- e β-galactanas sulfatadas. Provavelmente, as β-galactanas sulfatadas são mais dinâmicas e flexíveis que as α-galactanas sulfatadas. Este dado fica claro quando comparamos os valores de $^{3}J_{H-H}$ e $^{1}J_{C-H}$ da β-D-galactana sulfatada do ouriço-do-mar *G. crenularis* com a α-L-galactana sulfatada de outra espécie de ouriço-do-mar *Echinometra lucunter* que é composta exclusivamente por unidades monossacarídicas [→3-α-L-Gal*p*-2(SO_4)-1→]$_n$ (Figura 3A) (Alves *et al*., 1997).

Notavelmente, as α- e β-galactanas exibem diferenças significativs em seus valores de constantes de acoplamento, principalmente $^{3}J_{H-H}$ (Tabela VI). Ambas as unidades constituintes da β-D-galactana de *G. crenularis* (2-sulfatada e não-sulfatada) revelaram o mesmo valor de $^{3}J_{H-H}$, embora com discreta diferença nos valores de $^{1}J_{C-H}$ (Tabela VI). Isto indica que a presença ou ausência de sulfatação não altera dramaticamente as constantes de acoplamento. Mas, quando se altera os estereoisomêros (α ou β) os valores podem mudar consideravelmente, indicando mudança conformacional para estes polímeros de galactose. Para provar tais resultados, empregamos

estudos de DM para uma análise mais elaborada das influências conformacionais dessas galactanas sulfatadas.

4.3.4 Diferentes estados conformacionais das α- e β-galactanas sulfatadas são observados pela dinâmica molecular

As simulações de DM consistem atualmente de uma potente metodologia para calcular e representar as preferências conformacionais dos carboidratos, como evidenciados em trabalhos descrevendo as geometrias e flexibilidades dos dissacarídeos de heparina (Pol-Fachin and Verli, 2008) e outros oligossacarídeos (Verli and Guimarães, 2004; Verli and Guimarães, 2005), e também para as α-L-fucana sulfatadas e α-L-galactana sulfatadas (Figuras 1 e 2) (Becker *et al.*, 2007). Neste mesmo contexto, e considerando os parâmetros de RMN (NOE e acoplamentos escalares – $^{3}J_{H,H}$) obtidos para as galactanas sulfatadas de diferentes padrões de sulfatação e diferentes formas enantioméricas (*E. lucunter* e *G. crenularis*), empregamos os estudos conformacionais das unidades dissacarídicas α-D-Gal*p*-(1→3)-α-D-Gal*p*, α-D-Gal*p*-2(SO_4)-(1→3)-α-D-Gal*p*-2(SO_4), β-D-Gal*p*-(1→3)-β-D-Gal*p*, β-D-Gal*p*-2(SO_4)-(1→3)-β-D-Gal*p* and β-D-Gal*p*-(1→3)-β-D-Gal*p*-2(SO_4) na tentativa de estimar os estados conformacionais e a flexibilidade de cada composto em solução aquosa (Becker *et al.*, 2007; Pol-Fachin and Verli, 2008).

Baseado em tais análises, pode ser observado que as unidades não-sulfatadas apresentam maiores padrões de flexibilidade e dinâmica quando comparadas com suas partes sulfatadas (Figura 21), indicando que a sulfatação promove uma rigidez na cadeia de polissacarídeo, como já descrito nas comparações de DM das α-L-fucanas e α-L-galactans (Becker *et al.*, 2007). De forma similar, a configuração do carbono anomérico também parece influenciar na flexibilidade das galactanas sulfatadas, como nos polissacarídeos compostos por unidades β-D-Gal*p* apresentam um aumento na flexibilidade da ligação glicosídica quando comparados com os polissacarídeos de cadeias de α-D-Gal*p* (Figura 21).

Na intenção de refinar as análises obtidas para cada mapa de contorno com a adição das moléculas de solvente, cada estado de corformação com mínimo de energia foi submetido por 0.1μs de simulação de em solução aquo-

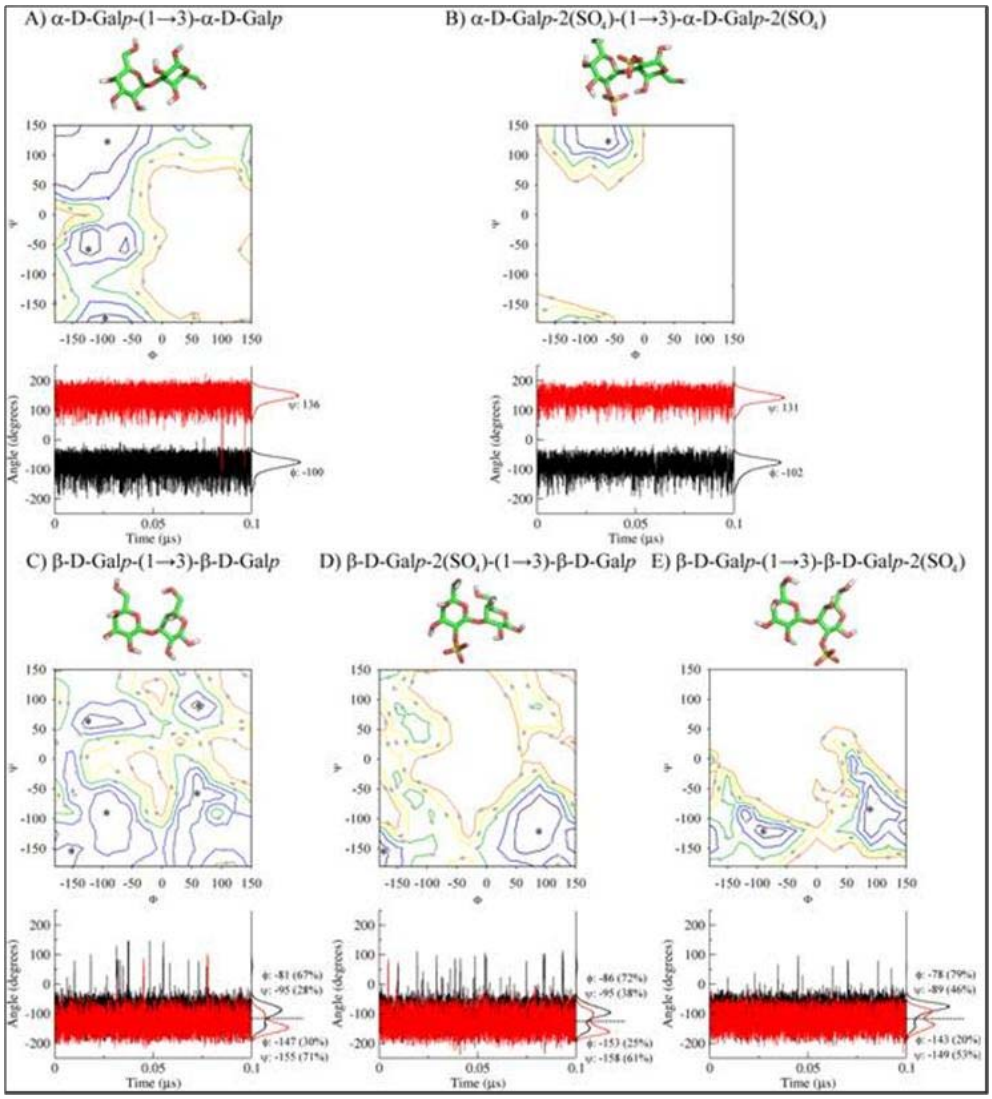

Figura 21. Descrição conformacional das galactanas compostas pelas unidades disscarídicas: (**A**) α-D-Gal*p*-(1→3)-α-D-Gal*p*, (**B**) α-D-Gal*p*-2(SO_4)-(1→3)-α-D-Gal*p*-2(SO_4), (**C**) β-D-Gal*p*-(1→3)-β-D-Gal*p*, (**D**) β-D-Gal*p*-2(SO_4)-(1→3)-β-D-Gal*p* and (**E**) β-D-Gal*p*-(1→3)-β-D-Gal*p*-2(SO_4). Os mapas de contornos são mostrados para cada 10 kJ.mol^{-1} de 10 a 50 kJ.mol^{-1}. Os asteríscos (*) indicam os estados conformacionais de menor energia pelo refinamento da DM. As geometrias mais prevalentes dos ângulos diedros avaliados durante 0.1 μs de simulações de DM para cada disscarídeo estudado estão ilustradas pelas representações de *e*struturas em bastão. A flutuação e a distribuição dos ângulos diedros: Φ (preto) e Ψ (vermelho) também estão representados, juntamente com a média e os valores de porcentagem de cada população de confôrmeros. Os confôrmeros predominantes (de maior porcentagem de ângulos diedros) para cada dissacarídeo simulado estão representados pelas estruturas em bastão no topo de cada painel. Os desvios-padrões para cada valor em média varia em ~20º.

sa. A análise da cada simulação confirma a observação de que a galactana composta por unidades de α-L-Galp apresenta maior rigidez que a galactana composta por unidades β-D-Galp. Enquanto os dissacarídeos da configuração α-enantiomérica, como da molécula extraída de E. lucunter (Figura 3A), apresenta uma única conformação predominante (com ângulos de ligação glicosídica de Φ/Ψ= -102°/131°, Figura 21B), as unidades dissacarídicas com o carbono anomérico na forma β, como observados na galactana sulfatada de G crenularis, apresenta no mínimo duas populações de conformações principais para cada ângulo diedro (Figura 21C, D e E), resultando em quatro confôrmeros totais co-existindo simultaneamente em solução. Isto decorre da combinação dos quatro ângulos diedros predominantes em cada simulação (Figura 21C, D e E). Como conseqüência, parece que as ligações glicosídicas nas β-galactanas sulfatadas não possuem estados muito estáveis em soluções, e uma série de estados conformacionais existem em equilíbrio, representando uma molécula de alta dinâmica conformacional. De fato, as populações de confôrmeros existentes na galactana sulfatada na β-configuração não superpõem com as mesmas populações de confôrmeros observadas para a molécula na forma-α.

Curiosamente, quando nós comparamos a DM dos derivados dessulfatado de ambas as formas enantioméricas (α ou β) das galactanas sulfatadas de ouriços-do-mar (Figura 21A *vs* C), ainda podemos observar um comportamento de dinâmica molecular menor para o polissacarídeo na forma-α. Isso nos leva a concluir que, embora saibamos que os grupamentos sulfatos causem impedimentos estéricos [como já observado na cinética de clivagem pela hidrólise ácida branda (item 2.4.2)], e que as ligações glicosídicas (e, conseqüentemente, suas torções) fiquem restritas e/ou até protegidas em ocasionais protonações ácidas (como descrito no item 2.5), fica evidente que a organização tridimensional das galactanas sulfatadas está sendo dominada ou modulada, predominantemente, pela conformação do anel de galactose decorrente de sua forma enantiomérica. Logo, a galactana sulfatada da espécie *G. crenularis* parece ser um polissacarídeo muito mais dinâmico devido à altamente influência da configuração-β, e não pela influência de seu menor

conteúdo de sulfatação (50% do nível de sulfatação da α-galactana sulfatada de *E. lucunter* - comparar Figura 20 com Figura 3A).

4.4 Conclusões gerais

A estrutura do polissacarídeo sulfatado isolado da camada gelatinosa dos óvulos do *G. crenularis* é bem distinta dos carboidratos já descritos para as outras espécies de ouriços-do-mar (Figura 1 B-G e 3A) (Mulloy *et al*., 1994; Alves *et al*., 1997; Alves *et al*., 1998; Vilela-Silva *et al*., 1999; Vilela-Silva *et al*., 2002). O polissacarídeo sulfatado de *G. crenularis* é formado por uma unidade dissacarídica repetitiva de resíduos de β-D-galactopiranose, sendo um, 2-sulfatado e outro, não-sulfatado, e ambos unidos pela ligação glicosídica (1→3). Além da primeira descrição de uma unidade dissacarídica repetitiva para os polissacarídeos sulfatados de equinodermas (Figura 1 e 3A), o polímero de *G. crenularis* também apresenta a inusitada forma-β enantiomérica para seus açúcares constituintes. Este tipo de configuração anomérica foi observado somente nas galactoses dos polissacarídeos sulfatados de algas verdes, como para a espécie *C. isthmocladum* e *C. yezoense* (Farias *et al*., 2008, Bilan *et al*. 2007), assim como, em menor ocorrência, nos polissacarídeos de alga vermelha e de grama-marinha (Figura 2), esta última apresentando metade de seus resíduos constituintes na forma-β (Figura 2B). Até agora, nós havíamos caracterizados polissacarídeos sulfatados de invertebrados compostos de unidades de configuração α-anoméricos (Figura 1 e 3).

Cadeias de galactopiranose na configuração-α são carboidratos menos dinâmicos que as cadeis compostas de β-galactopiranoses. A presença de ésteres de sulfato na molécula não interfere tanto na flexibilidade do polissacarídeo como a configuração anomérica do anel de açúcar. Isto nos leva a acreditar que efeitos biológicos distintos podem ser provocados por estes carboidratos, uma vez que esses polissacarídeos não apresentam os mesmos estados conformacionais predominantes.

De fato, em ensaios de fertilização, estes polissacarídeos apresentam efeitos indutores diferentes na reação acrossômica (estes dados estão descritos detalhadamente no artigo V deste capítulo). A ausência de

reconhecimento, e, consequentemente ausência da reação acrossômica nos espermatozóides de *E. lucunter* quando incubados com a β-galactana sulfatada de *G. crenularis* é explicada pelo fato de que a conformação adequada da galactana ao reconhecimento e interação com o receptor no espermatozóide de *E. lucunter*, não está presente nas populações conformacionais da β-galactana sulfatada de *G. crenularis*. Realmente, a α-galactana sulfatada de *E. lucunter*, que é responsável por induzir a reação acrossômica em espermatozóides da mesma espécie (ver anexo) apresenta apenas um estado conformacional com ângulos diedros de Φ/Ψ= -102°/131° (Figura 21B). Este estado conformacional é adequadamente identificado e reconhecido pelos receptores de polissacarídeos sulfatados nos espermatozóides de *E. lucunter*. Estes dados são comprovados uma vez que a fucana sulfatada da espécie de ouriço-do-mar *S. franciscanus* (Figura 1G) também pode induzir a reação acrossômica em espermatozóides de *E. lucunter*. Quando comparamos as estruturas dos polissacarídeos sulfatados de *E lucunter* (Figura 3A) e de *S. franciscanus* (Figura 1G), verificamos que ambos são constituídos de α-hexoses 2-sulfatadas, diferindo apenas na presença de galactose e fucose. Mais ainda, já observamos que a fucana sulfatada de *S. franciscanus* apresenta um mapa conformacional (âgulos diedros em função da energia) similar ao da galactana sulfatada de *E. lucunter*.

Os resultados dos estudos de conformação e de indução da reação acrossômica claramente exemplificam a ocorrência e o efeito importante dos estados conformacionais dos polissacarídeos sulfatados regulando suas ações biológicas. De maneira geral, estes efeitos biológicos estão diretamente relacionados às geometrias espaciais dos carboidratos, e não, decorrentes de seu comportamento natural em se ajustar com diferentes formas e afinidades a um ligante. Isto prova que as características estruturais dos carboidratos (tipo de resíduo, conformação do anel - bote ou cadeira, padrão de sulfatação e tipos de ligação glicosídica) podem ser consideradas responsáveis indiretos por suas ações biológicas, uma vez que essas características influenciam determinantemente a preferência, proporção e comportamento dinâmico dos estados conformacionais que realmente mostram-se ser requerimentos estruturais para a ação destes compostos.

4.5 Artigo V

Manuscrito em revisão para submissão.

"A unique 2-sulfated β-galactan from the egg jelly of the sea urchin *Glyptocidaris crenularis*: conformation flexibility *versus* induction of the sperm acrosome reaction"

Michelle O. Castro, Vitor H. Pomin, Livia L. Santos, Ana-Cristina E.S. Vilela-Silva, Noritaka Hirohashi, Laércio Pol-Fachin ,Hugo Verli e Paulo A.S. Mourão

A unique 2-sulfated β-galactan from the egg jelly of the sea urchin *Glyptocidaris crenularis*: conformation flexibility *versus* induction of the sperm acrosome reaction[2]

Michelle O. Castro[a,b], Vitor H. Pomin[a,b] Livia L. Santos[a,b], Ana-Cristina E.S. Vilela-Silva[a,c], Noritaka Hirohashi[d], Laércio Pol-Fachin[e] ,Hugo Verli[e,f], and Paulo A.S. Mourão[a,b,3]

From the [a]Laboratório de Tecido Conjuntivo, Hospital Universitário Clementino Fraga Filho, [b]Instituto de Bioquímica Médica, [c]Instituto de Ciências Biomédicas, Universidade Federal do Rio de Janeiro, Caixa Postal 68041, Rio de Janeiro, RJ, 21941–590, Brazil. [d]Genetic Counseling Course, Graduate School of Humanities and Sciences, Ochanamizu University, Japan. [e]*Programa de Pós-Graduação em Biologia Celular e Molecular, Centro de Biotecnologia, and* [f]*Faculdade de Farmácia, Universidade Federal do Rio Grande do Sul, Caixa Postal 15005, Porto Alegre 91500-970, RS, Brazil.*

Running title: Sulfated β-galactan from sea urchin

[2]This work was supported by Conselho Nacional de Desenvolvimento Científico e Tecnológico (CNPq), Fundação de Amparo à Pesquisa do Estado do Rio de Janeiro (FAPERJ) and Coordenação de Aperfeiçoamento de Pessoal de Nível Superior (CAPES).

[3]To whom correspondence should be addressed (e-mail): pmourao@hucff.ufrj.br

Abstract

Sulfated polysaccharides from the sea urchin egg jelly are involved in fertilization acting as species-specific inducers of the sperm acrosome reaction. It is important to investigate the molecular details of this phenomenon because it is a very rare case of pure carbohydrate-induced signal-transduction mechanism in animal cells. The sea urchin polysaccharides differ in their monosaccharide types (L-fucose or L-galactose), glycosilation and sulfation sites, but they always belong to the α-anomeric configuration. Herein, structural analysis of the polysaccharide from the sea urchin *Glyptocidaris crenularis* surprisingly revealed a unique sulfated β-D-galactan. Nuclear Magnetic Resonance experiments showed the following repeating unit: [-3-β-D-Gal*p*-2(OSO_4)-1→3-β-D-Gal*p*-1-]$_n$. Subsequently, we compared different 2-sulfated polysaccharides as inducers of the acrosome reaction using sperm from a distinct sea urchin species, aiming to trace relationships between activity and structural features of the echinoderm polysaccharides, including those based on conformational arrangements. Intriguingly, the anomeric configuration of the glycosidic linkage rather than monosaccharide composition (galactose or fucose) is the preferential structural requirement for the effect of these polysaccharides on sea urchin fertilization. NMR data and molecular dynamics indicate that sulfated α-galactan or α-fucan have less dynamic structural behavior, exhibiting lower conformational populations, with an almost exclusive conformational state with glycosidic dihedral angles Φ/Ψ= -102°/131°. The preponderant conformer experimented by the active sulfated α-galactan or α-fucan is not observed among populations in the β-form besides its more flexible structure in solution. Possibly a proper spatial conformation is required for interaction of the sea urchin sulfated polysaccharides with the specific sperm receptor.

Keywords: sulfated polysaccharides; sulfated fucan; fertilization; conformation of polysaccharide; species differentiation

Introduction

The evolution of barriers to inter-specific hybridization is a crucial step in the fertilization of free spawning marine invertebrates. In sea urchins, the molecular recognition between sperm and egg ensures species recognition. The jelly surrounding sea urchin eggs is not a simple accessory structure; it is considerably complex on a molecular level and intimately involved in gamete recognition. It contains sulfated polysaccharides, sialoglycans and peptides. The sulfated polysaccharides show species-specific structures, composed of repetitive units (mono-, tri- and tetrasaccharides), which differ in the monosaccharides of the backbone (L-fucose or L-galactose), positions of glycosilation (3 or 4-linked) and sulfation (2- and/or 4-sulfation), but they always belong to the α-enantiomeric configuration (Mourão 2007, Vilela-Silva *et al* 2008).

Sulfated polysaccharides from the sea urchin egg jellies show species-specificity in inducing the sperm acrosome reaction, which is regulated by the structure of the saccharide chain and its sulfation pattern (Vilela-Silva *et al*., 1999, 2002; Biermann et al., 2004). Other components of the egg jelly do not possess acrosome reaction inducing activity, but sialoglycans act in synergy with the sulfated polysaccharide, potentiating its activity (Hirohashi and Vacquier, 2002b). Structural changes in egg jelly sulfated polysaccharide modulate cell-cell recognition and species specificity leading to exocytosis of the acrosomal vesicle. This distinct sulfated polysaccharide-mediated mechanism for cell-cell recognition co-exists with the sperm bindin regulation by its egg receptor (Vacquier and Moy, 1977). Therefore, sulfated polysaccharides, in addition to their known functions as growth factors, coagulation factors and selectin binding partners, also function in fertilization (Berteau and Mulloy, 2003; Vilela-Silva *et al*., 2008). Of course it is important to investigate the molecular details of this event because it constitutes another of the rare cases of a pure carbohydrate-induced signal-transduction process in animal cells.

We now extended our studies to the sea urchin *Glyptocidaris crenularis*, which inhabits high depth and low temperature sea water (Hirai, 1963). Surprisingly, we observed this species contains a unique sulfated β-D-galactan, composed of repetitive disaccharide units alternating 2-sulfated and non-sulfated β-D-galactopyranosyl units. This polymer is markedly distinct from all other sea urchin sulfated polysaccharides described so far, which are composed of units on α-L-configuration. Furthermore, this sea urchin does not contain sialoglycans, which are commonly found in the echinoderm egg jelly.

We used this new sulfated β-galactan to investigate the acrosome reaction in a further molecular detail using sperm from the species *Echinometra lucunter*. We tested three 2-sulfated polysaccharides, which differ in their conformation (α or β) and monosaccharide composition (galactose or fucose), as inducers of the sperm acrosome reaction. We aimed to establish the structure *versus* biological activity of the echinoderm polysaccharides, including structural features at a conformational level. The anomeric configuration of the glycosidic linkage (α or β) rather than monosaccharide composition (galactose or fucose), was the dominant structural requirement responsible for inducing the acrosome reaction of these sea urchin polysaccharides during fertilization.

Molecular dynamics and NMR data of $^{3}J_{H\text{-}H}$ and $^{1}J_{C\text{-}H}$ strongly indicated that α- and β-isomers of sulfated galactan and fucan exhibit distinct conformational preferences. In particular, the preponderant conformer population experimented by the active sulfated α-galactan or α-fucan (Φ/Ψ= -102°/131°) is not observed among populations of the β-form, besides its much more flexible structure in solution. Therefore, our results extend the observation about the structural stringency of the sea urchin polysaccharides as inducer of the sperm acrosome reaction to a conformational level.

Experimental Procedures

Extraction of sulfated galactan from egg jelly of sea urchins

Mature females of *G. crenularis* were collected at Noheji Bay, Japan. Eggs were spawned into sea water by intracelomic injection of 0.5 M KCl. The crude egg jelly was isolated by pouring eggs repeatedly through nylon mesh, prepared as a 30,000 x *g* supernatant, and stored at -20°C, lyophilized and dialyzed against distilled water (Hirohashi and Vacquier, 2002a). The acidic polysaccharides were extracted from the jelly coat by papain digestion and partially purified by ethanol precipitation, as described previously (Albano and Mourão, 1986).

Purification of sulfated galactan

Approximately 20 mg of the crude polysaccharides from *G. crenularis* was applied to a Mono-Q FPLC-column (HR5/5; Amershan Biosciences. Inc.), equilibrated with 20 mM Tris-HCl (pH 8.0) and coupled to a FPLC-system. The column was washed with 10 mL of the same solution and then eluted by a linear gradient of 0-3 M NaCl. The flow rate of the column was 0.45 mL/min, and fractions of 0.5 mL were collected. These fractions

were checked for hexose (Dubois *et al.* 1956), sialic acid (Kabat and Mayer, 1971) and metachromatic property (Farndale *et al.,* 1986). The NaCl concentration was estimated by conductivity. Fractions were pooled, dialyzed against distilled water, and lyophilized.

Chemical analyses

After acid hydrolysis of the polysaccharide (5.0 M trifluoroacetic acid for 5 h at 100°C), sulfate was measured by the $BaCl_2$/gelatin method (Saito *et al*., 1968). The presence of hexoses and 6-deoxy-hexoses in the acid hydrolysates was estimated by paper-chromatography in 1-butanol/pyridine/water (3:2:1, v/v) for 48 h. In addition, alditol acetate derivatives of these sugars were analyzed by gas-liquid chromatography/mass spectrometry (Kircher, 1960).

Determination of D or L configuration of galactose

The enantiomeric form of the galactose was assigned based on analysis of the acetated (-)-2-butyl glycoside, as described (Gerwig *et al.*, 1979). Galactose obtained after acid hydrolysis of the polysaccharide from *G. crenularis* (1 mg, see above) was mixed with 0.5 mL of (-)-2-butanol (Aldrich), containing 1 M HCl. After butanolysis for 18 h at 80°C, the solution was neutralized with Ag_2CO_3, the supernatant concentrated, and dissolved in 50 μL. Thereafter, alditol acetate derivative was prepared (Kircher, 1960) and analyzed on a DB-5 GLC column. The temperature was programmed from 120 to 240°C at 2°/min. The injector and detector temperatures were 220 and 260°C, respectively. Appropriate controls of acetated (-)-2-butyl-D- and L-galactosides were analyzed under the same conditions.

Agarose and polyacrylamide gel electrophoresis

The sulfated galactan was analyzed by agarose gel electrophoresis, as described previously (Vieira *et al*., 1991; Alves *et al*., 1997). About 15 μg of the purified sulfated polysaccharide was applied to a 0.5% agarose gel and run for 1 h at 110 V in 0.05 M 1.3-diaminopropane acetate (pH 9.0). The sulfated polysaccharides in the gel were fixed with 0.1% *N*-cetyl-*N,N,N*-trymethylammonium bromide solution. After 12 h, the gel was dried and stained with 0.1% toluidine blue in acetic acid:ethanol:water (0.1:5:5, v/v).

The average molecular mass of the sulfated galactan was estimated by comparison with the electrophoretic mobility of standard compounds (Pomin *et al*., 2005a). The sulfated polysaccharides (~10 μg of each) were applied to a 1-mm-thick 10% polyacrylamide slab gel in 0.02 M sodium barbital (pH 8.6). After electrophoresis

(100 V for 30 min), the sulfated polysaccharides were stained with 0.1% toluidine blue in 1% acetic acid and washed for about 1 h in 1% acetic acid.

Desulfation procedure

Desulfation of the sulfated galactan was performed as described previously (Mourão and Perlin, 1987**;** Vieira, *et al.*, 1991). About 20 mg of the polysaccharide was dissolved in 5 mL of distilled water and mixed with 1 g (dry weight) of Dowex 50-W (H^+, 200–400 mesh). After neutralization with pyridine, the solution was lyophilized. The resulting pyridinium salt was dissolved in 2.5 mL of dimethyl sulfoxide/methanol (9:1, v/v). The mixture was heated at 80°C for 4 h, and the desulfated product was exhaustively dialyzed against distilled water and lyophilized. The extent of desulfation was estimated by the molar ratio of sulfate/total sugars. This method allows us to detect desulfation up to a molar ratio of ≤0.1 sulfate/total sugar. About 5 mg of desulfated polysaccharide was obtained at the end of the reaction.

NMR experiments

^1H and ^{13}C, 1D and 2D spectra of the native sulfated galactan and of its desulfated derivative were recorded using a Bruker DRX 400 MHz apparatus with a triple resonance probe, as detailed previously (Pomin, *et al*., 2005a). About 5 mg of each sample was dissolved in 0.5 ml 99.9% deuterium oxide (Cambridge Isotope Laboratory, Cambridge, MA). All spectra were recorded at 50^{o}C with HOD suppression by presaturation. 1D ^1H-NMR spectra were recorded with 16 scans. 2D $^1H/^1H$ COSY, TOCSY, NOESY and $^1H/^{13}C$ HSQC spectra were recorded using states-TPPI (states-time proportion phase incrementation) for quadrature detection in the indirect dimension. TOCSY spectra were run with 4046 x 400 points with a spin-lock field of 10 kHz and a mixed time of 80 ms. NOESY spectra were recorded with a mixing time of 100 ms. $^1H/^{13}C$ HSQC spectra were run with 1024 x 256 points and GARP (globally optimized alternating phase rectangular pulses) for decoupling. Chemical shifts are relative to external trimethylsilylpropionic acid at 0 ppm for ^1H and to methanol for ^{13}C.

Molecular dynamic (MD)

All calculations were performed using GROMACS simulation suite (van der Spoel *et al.*, 2005) and GROMOS96 force field (van Gunsteren *et al.*, 1996). Briefly, structures of disaccharide units containing α-L-Gal*p*-(1→3)-α-L-Gal*p*, α-L-Gal*p*-2(SO_4)-(1→3)-α-L-Gal*p*-2(SO_4), β-D-Gal*p*-(1→3)-β-D-Gal*p*, β-D-Gal*p*-2(SO_4)-(1→3)-β-D-Gal*p* and β-D-Gal*p*-(1→3)-β-D-Gal*p*-2(SO_4) were submitted to the PRODRG server (Schuettelkopf *et al.*, 2004) and the initial geometries and crude topologies were retrieved. These

topologies were supplied with Löwdin HF/6-31G** atomic charges (Verli and Guimarães, 2004; Becker *et al.*, 2005) and submitted to conformational analysis by varying the ϕ and ψ dihedral angles from -180 to 180°, with a 30° step, in a total of 144 conformers for each linkage. Each conformation was further refined in a 20 ps molecular dynamics at 10 K, with an integration step of 0.5 fs (Pol-Fachin and Verli, 2008). The relative stabilities of the conformations were used to construct relaxed energy contour plots. The minimum energy conformations described in these plots were submitted to 0.1 μs MD simulations in aqueous solutions, using the SPC water model (Berendsen *et al.*, 1987), following a protocol previously described (Verli and Guimarães, 2004; Verli and Guimarães, 2005; Becker *et al.*, 2005). A triclinic water box under periodic boundary conditions was employed, using a 10 Å minimum distance from solute to the box faces. Counter ions (Na^+) were added to neutralize the system. The Lincs method (Hess *et al.*, 1997) was applied to constrain covalent bond lengths, allowing an integration step of 2 fs after an initial energy minimization using the Steepest Descents algorithm. All simulations applied the Particle-Mesh Ewald method (Darden *et al.*, 1993). Temperature and pressure were kept constant by coupling carbohydrate, ions, and solvent to external temperature and pressure baths with coupling constants of 0.1 and 0.5 ps, respectively (Berendsen et al., 1984). The reference temperature was adjusted to 310 K. The relative orientation of a pair of contiguous carbohydrate residues is described by two torsional angles at the glycosidic linkage, denoted ϕ and ψ, as follows: ϕ = O-5–C-1–O-1–C-3´ (1) and ψ = C-1–O-1–C-3´–C-2´ (2).

Acrosome reaction assays

The method used was slightly modified from Su and Vacquier (2005). Briefly, sperm were spawned by intracelomic injection of 0.5 M KCl (0.5 mL/animal), collected undiluted and stored on ice before dilution. They were diluted 1:5 in 10 mM HEPES-buffered sea water, pH 7.9. Immediately after dilution, Twenty-five μL of the sperm suspension were mixed with 50 μL of the polysaccharide solution. The sugar content of these solutions was previously quantified by the phenol-sulfuric acid assay (Dubois *et al.*, 1956). After 5 min in ice, sperm were fixed by the addition of 350 μL of 3.7% formaldehyde in sea water. After 30 min, sperm were washed two times with 500 μL phosphate buffered solution and stained for at least two hours with 1 U of rhodamine phalloidin (Molecular Probes R415, Invitrogen Corporation, Carlsbad, CA) in 50 μL of 0.1 M glycine, 1 mg/mL bovine serum albumin, 0.02% sodium azide in phosphate-buffered saline, pH 7.4. The solution was then washed twice in 500 μL of phosphate-

buffered saline and incubated with 30 µL of DAPI (4'6'-diamino-2-phenylindole, Sigma) for 6 min. Then, the cells were washed again twice in 500 µL of phosphate-buffered saline and then re-suspended in 30 µL of 70% glyceraldehyde in the same solution, mounted in a thin layer, and the cover slip sealed. Sperm were scored blindly using a Zeiss Axioskop 2 plus fluorescent microscope. Photos were acquired from a Zeiss LSM 510 Meta confocal microscope (Jeha, Germany). We simultaneously collected red (phalloidin), blue (DAPI), and transmitted light channels.

Measurements of Increases in Intracellular Ca^{+2}

This methodology was slightly modified from Hirohashi and Vacquier (2002a). Briefly, sperm from *E. lucunter* were collected and immediately experimented, always on ice and in darkness. Undiluted semen was suspended in 4 volumes of dye loading buffer (artificial sea water containing 10 mM HEPES, 1 mM $CaCl_2$ and 0.1 mg/mL soybean trypsin inhibitor at pH 7.0). The sperm suspension was put in a tube with dimethyl sulfoxide (final concentration 0.6%) containing fura-2/AM, at a final concentration of 12 µM, and incubated for 4 h in darkness, at 4°C. Then cells were washed twice with PBS in a swinging bucket rotor at 430 x *g* for 5 min. The final pellet was re-suspended in fresh dye loading buffer without soybean trypsin inhibitor. Finally, 50 µL of fura-2 loaded sperm were placed in 11-mm diameter glass tube containing 1.5 mL of dye loading buffer without soybean trypsin inhibitor, and mounted in a FP-6300 spectrofluorimeter from Jasco, at 16°C and continual agitation. Fluoresce was measured continuously at Ex/Em 340/500 nm in order to follow the effect of sulfated polysaccharide addition to the sperm suspension. The sugar content of the polysaccharide solutions was quantified by the phenol-sulfuric acid assay (Dubois et al., 1956).

Results and discussion

The egg jelly of the sea urchin G. crenularis contains a sulfated D-galactan-The polysaccharides extracted from the egg jelly of *G. crenularis* were purified by anion-exchange chromatography on Mono-Q column, coupled to a FPLC-system, and fractions were monitored for hexose and metachromasia (Fig. 1*A*). We observed a single fraction of sulfated polysaccharide, eluted from the column with ~1.3 M NaCl, as indicated by the hexose assay (closed circles in Fig. 1*A*) and the metachromasia (open circles). The sialoglycan is absent in the egg jelly of this sea urchin, as indicated by the negative Erlich-reaction (closed triangles in Fig. 1*A*). Sialoglycans extracted from the

egg jelly of other species of sea urchins eluted from Mono-Q at ~0.7 M NaCl (Alves *et al*., 1997, 1998; Vilela-Silva *et al*., 1999, 2002).

The purified sulfated polysaccharide from *G. crenularis* showed a single component on agarose gel electrophoresis (Fig. 1*B*), with a high molecular mass (Fig. 1*C*), as already observed for the sulfated polysaccharides from the egg jelly of other species of sea urchins (Alves *et al*., 1997, 1998; Vilela-Silva *et al*., 1999, 2002). Chemical analyses of the purified sulfated polysaccharide from *G. crenularis* revealed exclusively galactose and sulfate. The acetated (-)-2-butyl galactosides obtained from this polysaccharide had the same retention times and peak areas as the standard D-galactose. Therefore, galactose occurs on the *G. crenularis* galactan exclusively as D-enantiomer.

Thus, the egg jelly of the sea urchin *G. crenularis* contains a single fraction of sulfated D-galactan. It differs from the sulfated polysaccharides found in other species of sea urchins, which contain fucose or galactose always belonging to the L-configuration (Alves *et al*., 1997, 1998; Vilela-Silva *et al*., 1999, 2002).

The sulfated galactan from G. crenularis has a regular disaccharide repeating unit composed of alternating 2-sulfated and non-sulfated 3-linked β-galactopyranosyl units- For a detailed structural analysis of the sulfated galactan from *G. crenularis*, we employed 1D and 2D NMR spectroscopy of the native polysaccharide and of its desulfated derivative (Figs 2-4).

The ^{1}H 1D spectrum (Fig. 2*A*) and especially the ^{1}H/^{13}C HSQC spectrum (Fig. 3*A*) of the native sulfated galactan showed equimolar proportions of two anomeric signals, denominated as A1 and B1. A1 exhibited a down-field shift (~0.2 ppm), possibly due to sulfation (Pomin et al 2005b). This conclusion was reinforced by analysis of the ^{1}H/^{13}C HSQC spectrum of the native polysaccharide (Fig. 3*A*) and the disappearance of signal A1 after the desulfation reaction (Figs 2*B* and 3*B*). These observations suggest that the sulfated galactan from *G. crenularis* contains equimolar proportions of non-sulfated and sulfated galactoses.

Correlation-peaks in 2D COSY spectra (Figs 4*A* and *D*) and TOCSY spectra (Figs 4*B* and *E*) allowed us to trace the entire spin systems of A and B signals in the native sulfated galactan and of B signal in the desulfated derivative. The COSY spectrum of the native sulfated galactan showed two correlation signals (A1-2 and B1-2) due to scalar-couplings between ^{1}H-anomeric proton and H2 for both residues (Fig. 4*A*). A single B1-2 correlation signal is observed in the spectrum of the desulfated derivative (Fig. 4*D*). Following identification of the cross peaks in the COSY spectra,

the TOCSY experiments (Figs 4*B* and *E*) allowed to assign unequivocally the whole spin systems A and B and to obtain the ^{1}H chemical shifts, as indicated in Table I. Based on the ^{1}H-chemical shifts, we assigned the peaks of correlation in the $^{1}H/^{13}C$ HSQC spectra (Fig. 3) and obtained the values of ^{13}C chemical shifts shown in Table I. Analysis of these ^{13}C chemical-shifts revealed that the galactan contains 3-linked β-galactopyranosyl residues, as indicated by the typical low-field shift of carbon (~10 ppm) in sites of glycosilation (Table I). This ^{13}C shift was also seen in reference compounds (structures 4 and 6-8 *vs* structure 5, Table I).

The spin systems A and B traced for the native sulfated galactan differ mainly due to typical ^{1}H low-field shift (~0.6 ppm) of H2 that indicates 2-sulfation (Table I). The neighbors H1 and H3 protons showed characteristic ~0.2 ppm low- field shifts. The spin systems B traced for native sulfated galactan and for its desulfated derivative show almost similar chemical shifts for ^{1}H and ^{13}C.

In synthesis, these results indicate that sulfated galactan from *G. crenularis* has equimolar proportions of 2-sulfated and non-sulfated β-galactopyranosyl units. It remains to clarify whether these units alternate along the polysaccharide chain or occur in a random distribution or even as clusters in the molecule. This aspect was investigated using 2D NOESY spectrum of the native sulfated galactan (Fig. 4*C*). The spectrum revealed intra-residue NOE´s between ^{1}H-anomeric and H3 and H5, as typically found in β-galactopyranose residues in their regular chair-conformation (Ravenscroft *et al* 1995). Protons H1, H3 and H5 are on the same plane (equatorially or axially) and commonly show <5 Å space contacts, which allow to detect their NOE´s. But, more significant, the NOESY spectrum also showed inter-residue NOE´s between H1 and H3 of the adjacent residue (A1-B3 and B1-A3). These observations indicated that the 2-sulfated and non-sulfated units are intercalating along the polysaccharide chain, as a repeating disaccharide unit.

Overall, NMR analysis indicated that the sulfated galactan from the egg jelly of *G. crenularis* has the following disaccharide repeating units: [-3-β-D-Gal*p*-2(OSO_4)-1→3-β-D-Gal*p*-1-]$_n$ (Fig. 5*A*).

The anomeric configuration of the glycosidic linkage is an important structural feature for recognition of sulfated polysaccharides by sea urchin sperm-We already tested a variety of sulfated polysaccharides with well-defined structures as inducers of acrosome reaction in sea urchin sperm. These studies indicated that sulfated polysaccharides show species-specificity in inducing the sperm acrosome reaction, which is regulated by the structure of the saccharide chain and its sulfation pattern

(Alves *et al*., 1997, 1998; Vilela-Silva *et al*., 1999, 2002; Biermann et al. 2004). However, the glycosidic linkages in all these previously tested polysaccharides were in the α-anomeric configuration. The sulfated β-D-galactan from *G. crenularis* expands the possibility to determine the event at a further molecular detail.

Investigation of the acrosome reaction using sperm from *G. crenularis* was not feasible because this sea urchin occurs in high depth and low temperature sea waters, with a short reproduction period (Hirai, 1963). Also, it was not possible to maintain the invertebrate in the laboratory. Furthermore, the acrosome in this species is too small and difficult to visualize using microscopic methods. As an alternative we used sperm from *E. lucunter*, which express in their egg jelly a sulfated galactan composed of [3-α-L-Gal*p*-2(OSO_4)-1-]$_n$ (Fig. 5*B*) (Alves *et al.,* 1997).

Sperm from *E. lucunter* were equally sensitive to homologous 2-sulfated α-galactan and to heterologous 2-sulfated α-fucan from *Strongylocentrotus franciscanus* (see structure in Fig. 5*C*) but not to the 2-sulfated β-galactan from *G. crenularis*, even when the polysaccharide was tested at high concentrations (Fig. 6*A*). This indicates that *E. lucunter* sperm receptor does not differentiate between the CH_2OH of L-galactose and CH_3 of L-fucose at position 6. These two polysaccharides present the same sulfation pattern and position of glycosilation, but differ in the sugar moieties. In a similar way, sperm from *S. franciscanus* were sensitive to the homologous sulfated α-fucan and to the heterologous *E. lucunter* sulfated α-galactan (Hirohashi *et al*., 2002c). In spite of that, *E. lucunter* sperm markedly distinct between α- and β-galactans.

Perhaps the sulfated β-galactan could increase the intracellular Ca^{2+} of *E. lucunter* sperm but not up-to-the proper high concentration required to induce the complete acrosome reaction. In fact, a low-molecular-weight sulfated α-fucan increases intracellular Ca^{2+} and pH, which is enough to induce exocytosis of the acrosome vesicle, but only at a slower kinetics, which are not able to induce the complete acrosome reaction (Hirohashi and Vacquier, 2002 a). In order to test for a similar effect of the sulfated β-galactan in *E. lucunter* sperm we measured increase in intracellular Ca^{2+} using fura-2 loaded sperm after incubation with the egg jelly polysaccharide (Fig. 6*B*). Increase of intracellular Ca^{2+} content was detected when *E. lucunter* sperm were incubated with homologous polysaccharide but not with the sulfated β-galactan from *G. crenularis* (Fig. 6*B*).

In conclusion, studies with the sulfated β-galactan from *G. crenularis* extend the characterization of the induction of sea urchin acrosome reaction to a further molecular detail. It indicates that the echinoderm sperm are sensitive only to polysaccharides with the appropriate anomeric configuration.

The scalar coupling constants $^3J_{H-H}$ and $^1J_{C-H}$ differ between sulfated β-galactans and sulfated α-galactan or α- fucan-Conformational analysis is an important route to follow for further characterization of the biological effect of the sea urchin polysaccharides at molecular levels. The differences in chemical structure may in fact determine spacing between sulfate groups required to match the interval between basic amino acid residues in the protein chain of the receptors.

We approached this aspect determining the scalar coupling constant of the 2-sulfated polysaccharides isolated from three species of sea urchins. The sulfated β-galactan from *G. crenularis* showed well-defined doublets of ^{1}H-^{1}H couplings for the anomeric signals in the 1D NMR spectra (Figs 2*A* and *B*) (Table II). This pattern of ^{1}H-^{1}H coupling is evidenced by multiplets in all cross-peaks showed in the COSY spectrum (Figure 4*A*) and by the doublets in the other homonuclear 2D experiments (TOCSY and NOESY spectra, Figure 4*B*-*E*). Interesting, similar pattern of coupled signals was also observed for another invertebrate sulfated β-galactans (Amornrut *et al*., 1999) but poorly noted in sulfated α-galactans and in a sulfated α-fucan (Alves *et al*., 1997, Pereira *et al*., 2002). These marked spin-spin couplings of the sulfated β-galactan from *G. crenularis*, together with the presence of inter-residue NOEs exclusively between protons involved in the glycosidic bond, suggest a polysaccharide with dynamic behavior and the absence of a single preponderant conformation. This proposition is confirmed by the MD simulations, as discussed below.

The scalar-coupling constants $^3J_{H-H}$ and $^1J_{C-H}$ observed for the sulfated β-galactan differ significantly compared with the values for sulfated α-galactan and α-fucan, especially $^3J_{H-H}$ (Table II). Again, these different coupling-constant values reflect distinct conformations for these polysaccharides. The 2-sulfated and non-sulfated units found in the sulfated β-galactan from *G. crenularis* showed similar $^3J_{H-H}$ and $^1J_{C-H}$ values, with only discrete difference in the $^1J_{C-H}$ values (Table II). It means that 2-sulfation does not alter significantly the glycosidic geometry of the β-galactopyransyl residues.

Molecular dynamics of α- and β-galactans-Differences in the scalar-coupling constants between sulfated β-galactan and sulfated α-galactan or α-fucan suggest distinct conformations, but this proposition requires further study. We employed conformational calculations based on molecular dynamic (MD), which is widely used to study carbohydrate conformation (Woods 1995).

Initially we simulated the conformation of the disaccharides α-L-Gal*p*-(1→3)-α-L-Gal*p*-2(SO_4), β-D-Gal*p*-(1→3)-β-D-Gal*p*, β-D-Gal*p*-2(SO_4)-(1→3)-β-D-Gal*p* and β-D-Gal*p*-(1→3)-β-D-Gal*p*-2(SO_4). The non-sulfated galactans presented more flexible conformations than their sulfated counterparts (Fig. 7*A vs B*; Fig. 7*C* vs *D* and *E*), indicating that sulfate groups increase the rigidity of the polysaccharide chain, as already suggested (Becker *et al*., 2007). But, more significant, the configuration of the glycosidic linkage is critical for the flexibility of sulfated-galactans and -fucans in aqueous solution. The β-D-galactopyranosyl residues showed an increased flexibility when compared to α-L-galactopyranosyl units (Fig. 7*A,B vs C-E*), which did not differ from α-L-fucopyranose (Becker *et al*., 2007).

In order to refine the analysis obtained by relaxed contour plots data upon addition of solvent molecules, each galactan minimum energy conformation was further submitted to a 0.1 μs MD simulation in aqueous solutions. The analysis of these simulations confirms the observations that α-L-galactopyranosyl units have a more rigid structure than β-D-galactopyranoses. Thus, the α-L-galactopyranose disaccharides, as in the sulfated α-galactan from *E. lucunter*, present unique prevalent conformation in solution (glycosidic dihedral angles of Φ/Ψ= -102°/131°, Fig. 7*B*). In contrast, β-D-galactopyranosyl disaccharides, as in the sulfated β-galactan from *G. crenularis*, present at least two main solution conformations for each dihedral angle (Figs 7*C-E*), indicating that four possible conformations co-existing simultaneously in solution. As a consequence, the glycosidic linkage around the sulfated β-galactan has no prevalent conformation in aqueous solutions, and a series of conformational sub-states occur in equilibrium. Curiously, the conformers experimented by the β-configuration do not match the preponderant conformer observed for the α-forms.

MD simulations of the desulfated derivatives from the two enantiomeric forms of the galactans (Figs 7*A vs* 7*C*) indicated that still α-galactopyranose has less dynamic molecular behavior compared to β-galactopyranose. Although sulfate groups serve as steric hindrances, which restrict the glycosidic motions, the three-dimensional order of these sulfated galactans are clearly dominated by their ring enantiomeric form.

Thus, the sulfated β-galactan from *G. crenularis* is a more dynamic and flexible polysaccharide than the sulfated α-galactan from *E. luncunter* or the sulfated α-*fucan* from *S. franciscanus*. But, more significant, the observation that only the α-polysaccharides induce the acrosome reaction in sperm from *E. lucunter* and *S. franciscanus* can arise from the observation that the preponderant conformer population experimented by the active sulfated α-polysaccharides is not observed

among populations of the β-form, besides its much more flexible structure in aqueous solution.

Major conclusions-The egg jelly of the sea urchin *G. crenularis* contains a sulfated β-galactan, which is constituted of the disaccharide repeating structure [-3-β-D-Gal*p*-2(OSO_4)-1→3-β-D-Gal*p*-1-]. This is the first report of a sulfated β-galactan with a regular and homogeneous disaccharide structure. Sulfated β-galactans have been reported in marine green algae. In these organisms the polysaccharides have complex structures, composed preponderantly of 4-sulfated, 3-linked β-D-galactopyranosyl units, but with branching and mostly highly pyruvilated at the non-reducing terminal residues, forming cyclic ketals (Bilan *et al*., 2007; Farias *et al*., 2008). Red algae contain linear sulfated galactan, made of alternating 3-linked β-D-galactopyranosyl and 4-linked α-galactopyranosyl residues, but considerable structural variation in these sulfated galactan occurs among different species, including complex sulfation pattern, substitution by methyl groups or pyruvic acid, formation of anydro sugar, etc. (Usov *et al.,* 1997).

We employed this new sulfated β-D-galactan from *G. crenularis* to investigate the acrosome reaction in a further molecular detail, using sperm from *E. lucunter*. This species expresses a 2-sulfated α-L-galactan in the egg jelly. The sperm react to the homologous sulfated α-galactan and also to a 2-sulfated α-fucan, but not to the sulfated β-galactan from *G*. c*renularis*. In a similar way, sperm from *S. franciscanus* react equally to 2-sulfated α-fucan and α-galactan (Hirohashi *et al*., 2002 c). Therefore, the anomeric configuration of the glycosidic linkage, rather than monosaccharide composition (galactose or fucose), is the main structural requirement to induce the acrosome reaction in *E. lucunter* and possibly in *S. franciscanus* sperm. Our explanation for this result is that sulfated β-galactan from *G. crenularis*, besides a more flexible structure compared to the α-polysaccharides, cannot assume the precise conformation necessary for recognition by the *E. lucunter* and *S. franciscanus* sperm. In conclusion, our results extend the observation about the structural stringency of the sea urchin polysaccharides as inducers of the sperm acrosome reaction to a conformational level.

Abbreviations

FPLC, fast protein liquid chromatography; COSY, correlation spectroscopy; NMR, nuclear magnetic resonance; NOESY, nuclear Overhausen effect spectroscopy;

TOCSY, total correlation spectroscopy; HSQC, heteronuclear single quantum coherence; MD, molecular dynamic.

Acknowledgements

We would like to thank Dr. Ana-Paula Valente for help on the NMR experiments at the Bruker 400 MHz and Adriana A. Piquet for technical assistance.

References

1) Mourão, PAS. A carbohydrate-based mechanism of species recognition in sea urchin fertilization. *Braz J Med Biol Res*. Jan;40(1):5-17. 2007.

2) Vilela-Silva AC, Hirohashi N, Mourão PA. The structure of sulfated polysaccharides ensures a carbohydrate-based mechanism for species recognition during sea urchin fertilization. *Int J Dev Biol*. 52(5-6):551-9.2008.

3) Vilela-Silva ESAC, Alves AP, Valente AP, Vacquier VD and Mourão PAS. Structure of the sulfated alfa-L-fucan from the egg jelly coat of the sea urchin *Strongylocentrotus franciscanus*: patterns of preferencial 2-O- and 4-O-sulfation determine sperm cell recognition. *Glicobiology*, 9, 927-933, 1999.

4) Vilela-Silva ESAC, Castro MO, Valente AP, Biermann CH, and Mourão PAS. Sulfated fucans from the egg jellies of the closely related sea urchins *Strongylocentrotus droebachiensis* and *Strongylocentrotus pallidus* ensure species-specific fertilization. *J Biol Chem*., 277: 379-387, 2002.

5) Biermann CH, Marks JA, Vilela-Silva AC, Castro MO, Mourão PA. Carbohydrate-based species recognition in sea urchin fertilization: another avenue for speciation? *Evol Dev*. 6(5):353-61. 2004.

6) Hirohashi N, and Vacquier VD. Egg sialoglycans increase intracellular pH and potentiate the acrosome reaction of sea urchin sperm. *J. Biol. Chem*., 277: 8041-8047, 2002b.

7) Vacquier, V.D. & Moy, G.W. Isolation of bindin: the protein responsible for adhesion of sperm to sea urchin eggs. *Proc. Natl. Acad*. *Sci*., 74, 2456-2460, 1977.

8) Berteau O, Mulloy B. Sulfated fucans, fresh perspectives: structures, functions, and biological properties of sulfated fucans and an overview of enzymes active toward this class of polysaccharide. *Glycobiology*. Jun;13(6):29R-40R. Epub 2003 Mar 6. 2003.

9) Hirai E. On the breeding seasons of invertebrates in the neighbourhood of the Marine Biological Station of Asamuzhi. *Sci. Rep. Tôhoku Univ. Ser. IV(Biol.),* 29, 369-375, 1963.

10) Vacquier VD, and Moy GW. The fucose sulfate polymer of egg jelly binds to sperm REJ and is the inducer of the sea urchin sperm acrosome reaction. *Dev. Biol*., 192(1), 125-135, 1997.

11) Albano RM, and Mourão PAS. Isolation, fractionation, and preliminary characterization of a novel class of sulfated glycans from the tunic of *Styela plicata* (Chordata tunicata). *J. Biol. Chem*., 261,758-765, 1986.

12) Dubois M; Gilles KA; Hamilton JK; Rebers PA; Smith F. Colorimetric method for determination of sugars and related substances. *Anal. Chem*., 28, 350-354, 1956.

13) Kabat EA, and Mayer MM. (1971) In: Experimental Immunochemistry, Charles C. Thomas Publisher, Springfield, IL, USA. 505-513.

14) Farndale RW, Buttle DJ and Barrett AJ. Improved quantitation and discrimination of sulphated glycosaminoglycans by use of dimethylmethylene blue. *Biochim Biophys Acta*. Sep 4;883(2):173-7, 1986.

15) Saito H, Yamagata T, and Suzuki S. Enzymatic Methods for the Determination of Small Quantities of Isomeric Chondroitin Sulfates *J. Biol. Chem*. 243, 1536-1542, 1968.

16) Kircher HW. Gas-Liquid Partition Chromatography of Methylated Sugars. *Anal. Chem*. 32, 1103-1106, 1960.

17) Gerwig GJ, Kamerling JP, Vliegenthart JF. Determination of the absolute configuration of mono-saccharides in complex carbohydrates by capillary G.L.C. *Carbohydr Res*. Dec;77:10-7. 1979.

18) Vieira RP, Mulloy B, and Mourão PAS. Structure of a fucose- branched chondroitin sulfate from sea cucumber. Evidence for the presence of 3 - O - sulfo - beta - glucuronosyl residues. *J. Biol. Chem*., 266,13530- 13536, 1991.

19) Alves AP, Mulloy B, Diniz JA and Mourão PAS. Sulfated polysaccharides from the egg jelly layer are species specific inducers of acrosomal reaction in sperms of sea urchins. *J. Biol. Chem*., 272, 6965-6971, 1997.

20) Pomin VH, Pereira MS, Valente AP, Tollefsen DM, Pavão MS, Mourão PAS. Selective cleavage and anticoagulant activity of a sulfated fucan: stereospecific removal of a 2-sulfate ester from the polysaccharide by mild acid hydrolysis, preparation of oligosaccharides, and heparin cofactor II-dependent anticoagulant activity. *Glycobiology*. 2005 Apr;15(4):369-81. Epub 2004 Dec 8. Erratum in: *Glycobiology*. May;15(5):13G, 2005a.

21) Mourão, PA, Perlin, AS. Structural features of sulfated glycans from the tunic of Styela plicata (Chordata-Tunicata). A unique occurrence of L-galactose in sulfated polysaccharides. *Eur. J. Biochem.* 1987.

22) Van Der Spoel D, Lindahl E, Hess B, Groenhof G, Mark AE, Berendsen HJ. GROMACS: fast, flexible, and free. *J Comput Chem*. Dec;26(16):1701-18. 2005.

23) Van Gunsteren WF; Billeter SR; Eising AA; Hunenberger PH; Kruger P; Mark AE; Scott WRP; Tironi IG: Biomolecular Simulation: The GROMOS96 Manual and User Guide (University of Groningen, Groningen, The Netherlands and ETH, Zurich, Switzerland), 1996.

24) Schuettelkopf AW; van Aalten DMF: PRODRG: a tool for high-throughput crystallography of protein-ligand complexes. *Acta Cryst.*, *D60*, 1355-1363, 2004.

25) Verli H and Guimarães JA: Molecular dynamics simulation of a decasaccharide fragment of heparin in aqueous solution. *Carbohydr. Res.*,*339*, 281-290, 2004.

26) Becker CF, Guimarães J. A., and Verli H. Molecular dynamics and atomic charge calculations in the study of heparin conformation in aqueous solution. *Carbohydrate. Res.* 340, 1499-1507, 2005.

27) Pol-Fachin L, and Verli H. Depiction of the forces participating in the 2-O-sulfo-alpha-L-iduronic acid conformational preference in heparin sequences in aqueous solutions.*Carbohydr. Res.* 343, 1435-1445, 2008.

28) Berendsen HJC, Grigera JR, Straatsma TP. The Missing Term in Effective Pair Potentials. *J. Phys. Chem.* 91, 6269–6271,1987.

29) Verli H and Guimarães JA. Structural and functional behavior of biologically active monomeric melittin. *J. Mol. Graph. Model.* 24, 203-212, 2005.

30) Hess B; Bekker H, Berendsen HJC, Fraaije JGE. Molecular dynamics simulations of the hydration of poly(vinyl methyl ether): Hydrogen bonds and quasi-hydrogen bonds M. *J. Comput. Chem.* 18, 1463–1472, 1997.

31) Darden T, York D, Pedersen L. Particle mesh ewald-an N.log(N) method for ewald sums in large systems. *J. Chem. Phys.* 98, 10089-10092,1993.

No texto tinha citação de Berendsen 1984

32) Su YH, Vacquier VD. Cyclic GMP-specific phosphodiesterase-5 regulates motility of sea urchin spermatozoa. *Mol Biol Cell*. Jan;17(1):114-21. Epub 2005 Oct 19. 2006.

33) Hirohashi, N. & Vacquier, V.D. High molecular mass egg fucose sulfate polymer is required for opening both Ca2+ channels involved in triggering the sea urchin sperm acrosome reaction. *J. Biol. Chem.*, 277, 1182-1189, 2002a.

34) Alves AP, Mulloy B, Moy GW, Vacquier VD and Mourão PAS. Females of the sea urchin *Strongylocentrotus purpuratus* differ in the structures of their egg jelly sulfated fucans. *Glycobiology*. 8, 939- 946, 1998.

35) Ravenscroft N, Gamian A, Romanowska E. 3-Deoxy-Octulosonic-Acid-Containing Hexasaccharide Fragment of Unusual Core Type Isolated from *Hafnia alvei* 2 Lipopolysaccharide. *Eur. J Bio*, Volume 227 Issue 3, Pages 889 – 896. 2005.

36) Amornrut C.; Toida T.; Imanari T.; Woo ER.; Park H; Linhardt R; Wu YS. A new sulfated beta-galactan from clams with anti-HIV activity. *Carbohydr Res*. Sep 15; 321(1-2):121-7,1999.

37) Pereira MS, Melo FR, Mourão PAS. Is there a correlation between structure and anticoagulant action of sulfated galactans and sulfated fucans? *Glycobiology*. Oct;12(10):573-80, 2002.

38) Woods, RJ. Three-dimensional structures of oligosaccharides. Current Opinion in Structural Biology. 5:591-598, 1995.

39) Becker CF; Mourão PAS; Guimarães JA; Verli H: Study of galactan and fucan conformations in aqueous solution: structural implications to biological activities. *J. Mol. Graph. Model.*, *26*, 391-399, 2007.

40) Bilan MI, Vinogradova EV, Shashkov AS, Usov AI. Structure of a highly pyruvylated galactan sulfate from the Pacific green alga *Codium yezoense* (Bryopsidales, Chlorophyta). *Carbohydr Res*. 342:586-596. 2007.

41) Farias EH. Pomin VH, Valente A-P, Nader HB, Rocha HA, Mourão PA. A preponderantly 4-sulfated, 3-linked galactan from the green alga *Codium isthmocladum*. *Glycobiology*. 18:250-259. 2008.

42) Usov AI, Bilan MI, Shashkov AS. Structure of a sulfated xylogalactan from the calcareous red alga Corallina pilulifera P. et R. (Rhodophyta, Corallinaceae). *Carbohydr Res*. Aug 25;303(1):93-102. 1997.

Table I. ^{1}H and ^{13}C chemical shifts (ppm) of the sulfated and desulfated β-D-galactan from *G. crenularis* and standard compounds

Polysaccharide	Structrure	^{1}H and ^{13}C chemical shift[a] (ppm)					
		H-1 C-1	H-2 C-2	H-3 C-3	H-4 C-4	H-5 C-5	H-6 C-6
Sulfated β-D-galactan from *G. crenularis*	1) 3-β-D-Gal*p*-2(SO_3^-)-1 (unit A)	4.94	**4.52**	*4.11*	4.37	4.02	3.82
		104.1	**80.2**	*81.8*	70.5	74.3	62.5
	2) 3-β-D-Gal*p*-1 (unit B)	4.73	3.87	*3.90*	4.24	3.75	3.82
		107.2	72.0	*83.5*	69.1	77.0	62.5
Desulfated β-D-galactan from *G. crenularis*	3) 3-β-D-Gal*p*-1 (unit B)	4.79	3.90	*3.93*	4.29	3.82	3.87
		103.5	69.9	*81.9*	68.3	74.8	60.5
Desulfated β-D-galactan from *C. isthmocladum*[b]	4) 3-β-D-Gal*p*-1	4.81	3.64	*3.92*	4.39	3.86	3.94-3.85
		102.6	73.8	*82.9*	67.1	75.2	60.3
	5) 6-β-D-Gal*p*-1	4.62	3.82	3.89	4.38	4.09	*4.36-4.01*
		103.1	70.1	70.2	67.0	73.9	*69.9*
Sulfated β-D-galactan from *Meretrix petechialis*[c]	6) 3-β-D-Gal*p*-2(SO_3^-)-1	4.83	**4.45**	*3.97*	ND	ND	ND
Sulfated α-L-galactan from *E. lucunter*[d]	7) 3-α-L-Gal*p*-2(SO_3^-)-1	5.47	**4.66**	*4.23*	4.33	4.35	3.82
		97.2	**76.2**	*75.9*	72.5	69.5	63.8
Desulfated α-L-galactan from *E. lucunter*	8) 3-α-L-Gal*p*-1	5.26	4.08	*4.14*	4.32	4.24	3.82
		98.1	73.5	*77.2*	69.5	68.5	63.9

[a] Chemical shifts are relative to external trimethylsilylpropionic acid at 0 ppm for ^{1}H and methanol for ^{13}C. Values in boldface indicate sulfate position and in italic indicate glycosilated positions.

[b] Reference values from Farias *et al*., 2008.

[c] Data from Amornrut *et al*., 1999.

[d] Reference values from Alves *et al*., 1997.

ND, not determined.

Table II. $^{3}J_{H\text{-}H}$ and $^{1}J_{C\text{-}H}$ (Hz) in the NMR spectra of sulfated α- or β-galactans and α-fucans

Polysaccharide	Structrure	$^{3}J_{H\text{-}H}$ (Hz)				
		H1-H2	H2-H3	H3-H4	H4-H5	H5-H6
Sulfated β-D-galactan from *G. crenularis*	3-β-D-Gal*p*-2(SO_3^-)-1 (unit A)	7.4	7.9	2.7	ND	ND
	3-β-D-Gal*p*-1 (unit B)	7.01	ND	ND	ND	ND
Desulfated β-D-galactan from *G. crenularis*	3-β-D-Gal*p*-1 (unit B)	7.29	ND	2.83	ND	ND
Sulfated β-D-galactan from *Meretrix petechialis*[a]	3-β-D-Gal*p*-2(SO_3^-)-1	7.6-7.8	7.8-8.2	<1.5	ND	ND
Sulfated α-L-galactan from *E. lucunter*[b]	3-α-L-Gal*p*-2(SO_3^-)-1	3.0	10.5	ND	ND	4.5
Sulfated α-L-fucan from *S. franciscanus*[b]	3-α-L-Fuc*p*-2(SO_3^-)-1	3.1	9.5	ND	ND	4.9
Sulfated α-L-fucan from *L. grisea*[c]	3-α-L-Fuc*p*-2(SO_3^-)-1	3.5-4.0	~10.0	<3.0	<3.0	6.7-7.0
		$^{1}J_{C\text{-}H}$ (Hz)				
		C1-H1	C2-H2	C3-H3	C4-H4	C5-H5	C6-H6
Sulfated β-D-galactan from *G. crenularis*	3-β-D-Gal*p*-2(SO_3^-)-1 (unit A)	164.7	156.8	143.4	151.4	143.0	143.9
	3-β-D-Gal*p*-1 (unit B)	163.5	141.2	143.1	150.5	139.9	143.9
Sulfated α-L-galactan from *E. lucunter*[b]	3-α-L-Gal*p*-2(SO_3^-)-1	177.5	151.3	146.2	146.5	146.8	143.3
Sulfated α-L-fucan from *S. franciscanus*[b]	3-α-L-Fuc*p*-2(SO_3^-)-1	177.2	148.7	144.6	140.9	147.1	125.3

[a] Data from Amornnut *et al*., 1999.

[b] See also Pereira *et al*., 2002.

[c] Data from Mulloy *et al*., 1994.

ND, not determined.

Figures legends

Fig. 1 - Purification and electrophoretic mobility of the sulfated galactan from the egg jelly of *G. crenularis*. (*A*) Total sulfated polysaccharide from the egg jelly (20 mg) was applied to a Mono Q FPLC column (HR5/5), equilibrated with 20 mM Tris-HCl (pH 8.0). The column was developed by a linear gradient of 0 - 3.0 M NaCl in the same solution. Fractions were assayed by metachromasia using 1,9-dimethylmethylene blue (O), the Dubois reaction for hexose (●), and the Ehrlich assay for sialic acid (▲). The NaCl concentration was estimated by conductivity (– – –). Fractions containing the sulfated galactan (indicated by the *horizontal bar*) were pooled, dialyzed against distilled water, and lyophilized. (*B*) Total polysaccharides from the egg jelly and the purified sulfated galactan (15 μg of each) were applied to a 0.5% agarose gel, and electrophoresis was carried out for 1 h at 110 V in 0.05 M 1,3-diaminopropane:acetate (pH 9.0). Gels were fixed with 0.1% *N*-cetyl-*N*,*N*,*N*-trimethylammonium bromide solution. After 12 h, the gel was dried and stained with 0.1% toluidine blue in acetic acid/ethanol/water (0.1:1:5, v/v). (*C*) The purified sulfated galactan (10 μg) were run on 6% polyacrylamide gels in 0.2 M sodium barbital (pH 8.6) and stained with 0.1% toluidine blue in 1% acetic acid. Molecular mass markers used were dextran sulfate (St-1; average molecular mass ≥ 500 kDa), chondroitin 6-sulfate (St-2; average molecular mass ~60 kDa), chondroitin 4-sulfate (St-3; average molecular weight ~40 kDa) and heparin (St-1; average molecular mass ~10 kDa).

Fig. 2 **-** 1D ^{1}H-NMR spectra at 400 MHz of the native sulfated galactan from *G. crenularis* (*A*) and its desulfated derivative (*B*). About 5 mg of each polysaccharide were dissolved in 0.5 mL of D_2O and the 1D NMR spectra were recorded at 50°C. The residual water signal was suppressed by presaturation. ^{1}H chemical shifts are relative to external trimethylsilylpropionic acid at 0 ppm. The signals designated with A, B correspond to the 2-sulfated and non-sulfated β-D-galactopyranosyl units, respectively, and numbers correspond to each hydrogen of the hexose ring. Numbers in *Panel A* below the spectrum indicate integrals of A1 and B1 signals. The peak marked by the asterisk corresponds to a contaminant.

Fig. 3 **-** ^{1}H/^{13}C HSQC spectra of the sulfated galactan from *G. crenularis* (*A*) and its desulfated derivative (*B*). Chemical shifts are relative to external trimethylsilylpropionic acid at 0 ppm for ^{1}H and methanol for ^{13}C. The spin systems were denoted as A and B

for 2-sulfated and non-sulfated β-galactopyranosyl units, respectively. Spectra were recorded at 50°C.

Fig. 4 **-** Strips of the anomeric regions (expansions from 4.4 to 5.1 ppm) from the COSY (*A* and *D*), TOCSY (*B* and *E*) and NOESY (*C*) spectra of the sulfated galactan (*A*-*C*) from *G. crenularis* and its desulfated derivative (*D* and *E*). About 5 mg of each polysaccharide were dissolved in 0.5 mL of D_2O and the 2D NMR spectra were recorded at 50°C at 400 MHz. Chemical shifts are relative to external trimethylsilylpropionic acid at 0 ppm for ^1H. The spin systems were denoted as A and B for 2-sulfated and non-sulfated β-galactopyranosyl units, respectively. The peak marked by the asterisk corresponds to a contaminant.

Fig. 5 - Structures of 2-sulfated polysaccharides obtained from the egg jelly of different species of sea urchins. (*A*) The sulfated β-D-galactan from *G. crenularis* is composed of the following disaccharide repeating unit: [-3-β-D-Gal*p*-2(SO_4)-(1→3)-β-D-Gal*p*-1-]$_n$. The polysaccharides from *E. lucunter* (*B*) and *S. franciscanus* (*C*) are composed of α-L-galactopyranosyl or α-L-fucopyranosyl residues, respectively, both 2-sulfated and 3-linked.

Fig. 6 **-** Effects of 2-sulfated α-L-galactan, α-L-fucan and β-D-galactan from the egg jellies of *E. lucunter*, *S. franciscanus* and *G. crenularis*, respectively, as inducers of acrosome reaction (*A*) and on increases intracellular Ca^{2+} (*B*) of *E. lucunter* sperm. These polysaccharides have identical positions of glycosilation and of sulfation but differ in their monosaccharides and/or anomeric configuration. The sulfated galactan from *G. crenularis* has an extra non-sulfated residue. See structures in *Panel A*. (*A*) Acrosome reaction: sulfated polysaccharides were dissolved in sea water, incubated with sperm from *E. lucunter* and the acrosome reaction was detected using fluorescence phalloidin (see Experimental Procedures). Negative control was done with artificial sea water. Approximately 100-150 sperm were scored per data point. The concentrations of polysaccharides were normalized by hexose content. (*B*) Increases in intracellular Ca^{2+}: each sulfated polysaccharide was added to a fura-2 loaded *E. lucunter* sperm suspension (see *arrow*), at a final concentration of 100 μg/mL. The fluorescence was registered for 100 sec.

Fig. 7 **-** Molecular dynamic (MD) of galactans composed of the following disaccharide units: (*A*) α-L-Gal*p*-(1→3)-α-L-Gal*p*, (*B*) α-L-Gal*p*-2(SO_4)-(1→3)-α-L-Gal*p*-2(SO_4), (*C*)

β-D-Gal*p*-(1→3)-β-D-Gal*p*, (*D*) β-D-Gal*p*-2(SO_4)-(1→3)-β-D-Gal*p* and (*E*) β-D-Gal*p*-(1→3)-β-D-Gal*p*-2(SO_4). The contour plots are shown at every 10 kJ.mol^{-1} from 10 to 50 kJ.mol^{-1}. Asterisks (*) indicate the input minimum energy conformations for MD refinement. The fluctuation and distribution of the ϕ (black) and (red) dihedral angles are also presented, together with average and prevalence values (%) for each conformer population. The standard deviation for all average values lies in ~20º.

Figure 1

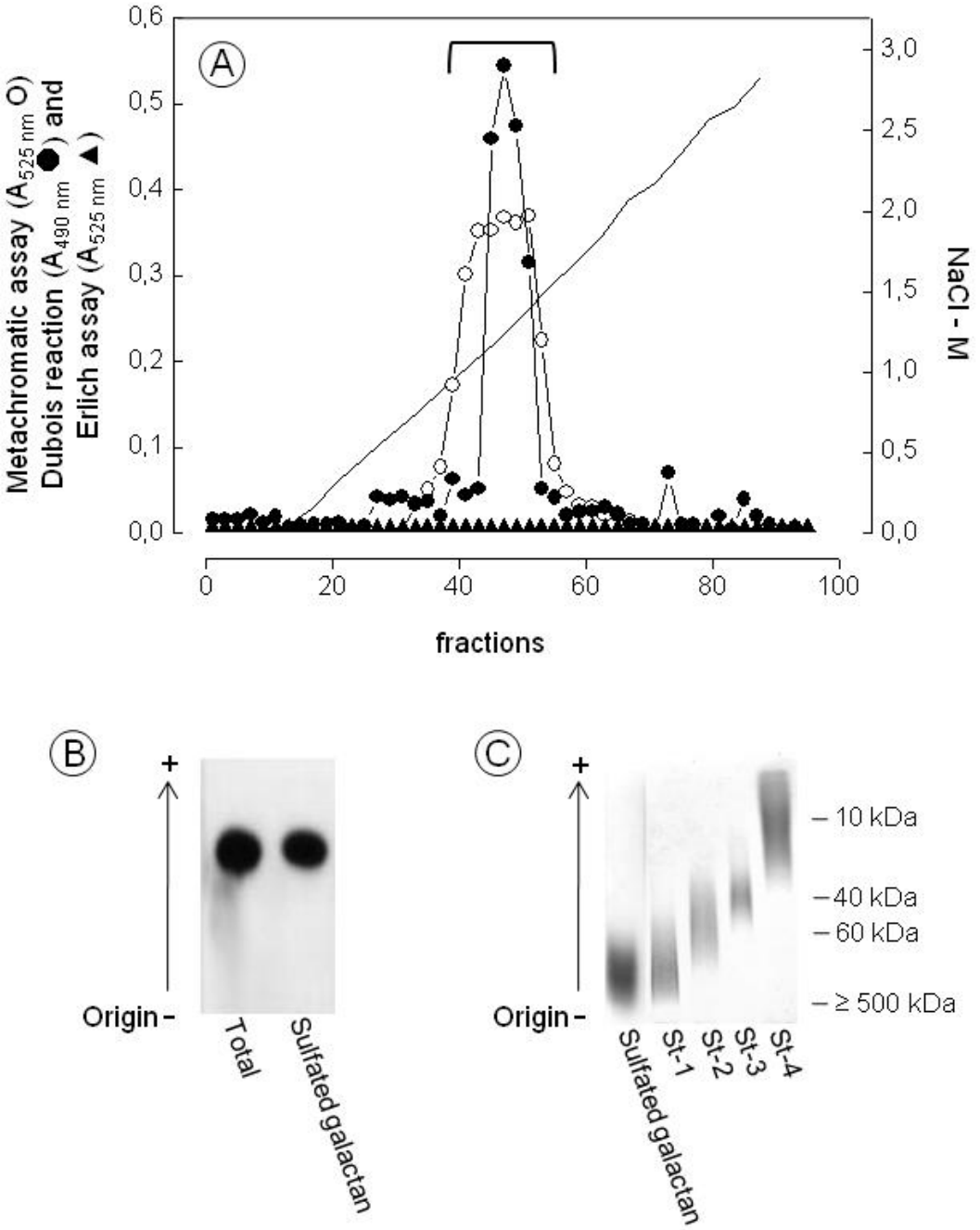
A
Metachromatic assay ($A_{525\ nm}$ O)
Dubois reaction ($A_{490\ nm}$ ●) and
Erlich assay ($A_{525\ nm}$ ▲)
NaCl - M
fractions
B
+
Origin -
Total
Sulfated galactan
C
+
Origin -
– 10 kDa
– 40 kDa
– 60 kDa
– ≥ 500 kDa
Sulfated galactan
St-1
St-2
St-3
St-4

Figure 2

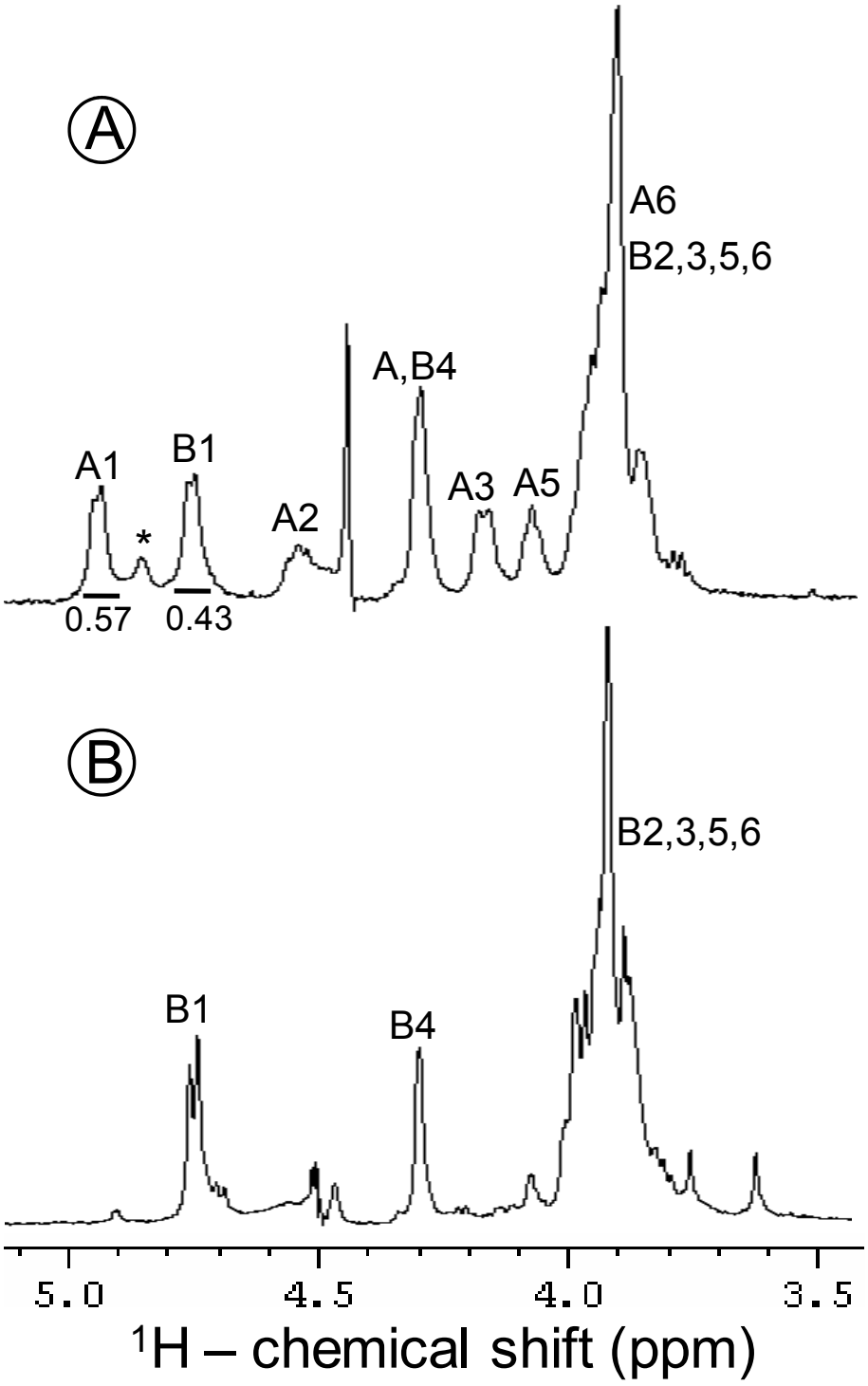
A
A6
B2,3,5,6
A,B4
A1
B1
A2
A3
A5
*
0.57
0.43
B
B2,3,5,6
B1
B4
5.0
4.5
4.0
3.5
1H – chemical shift (ppm)

Figure 3

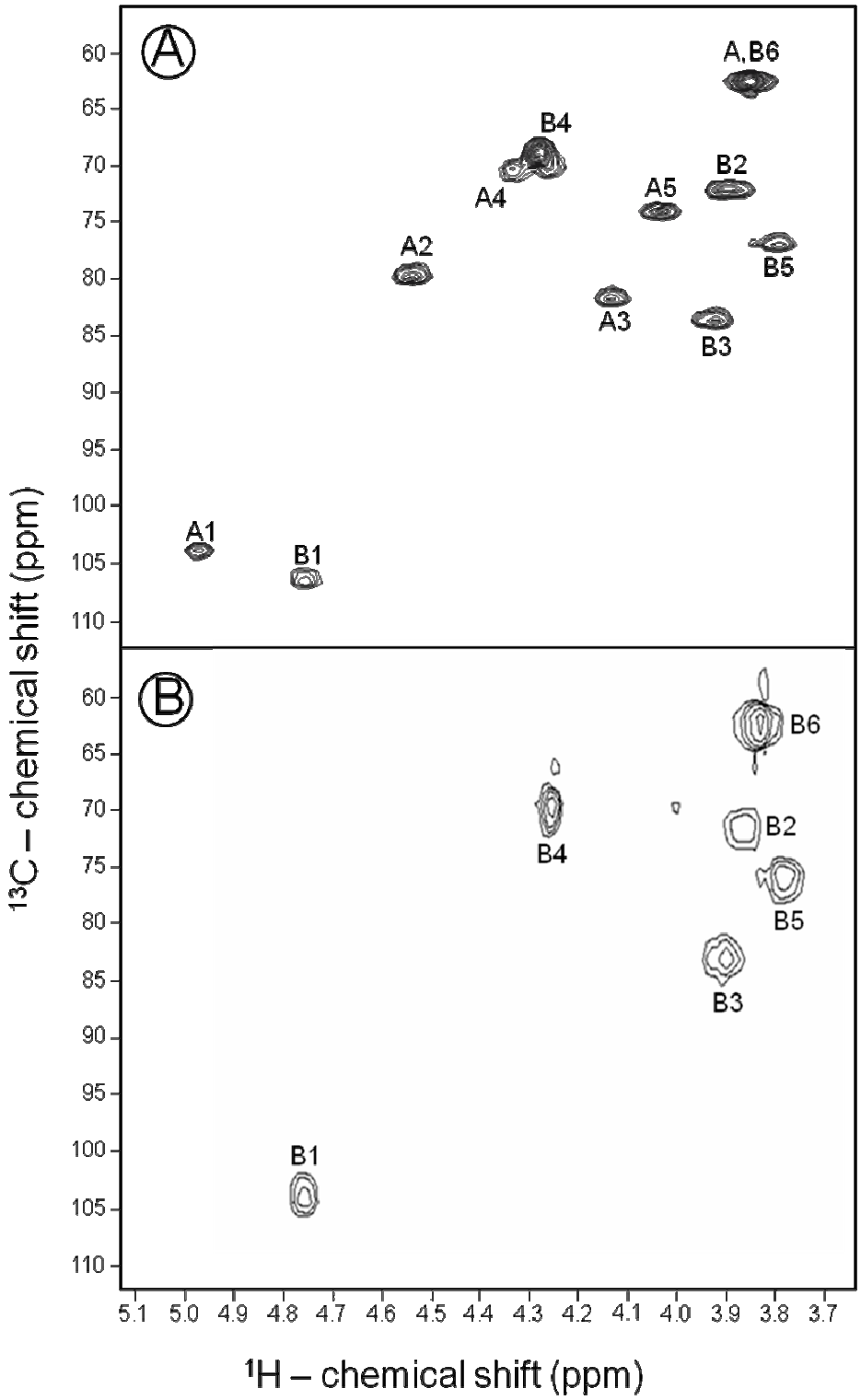
A
A,B6
B4
A4
B2
A5
A2
B5
A3
B3
A1
B1
B
B6
B4
B2
B5
B3
B1
60
65
70
75
80
85
90
95
100
105
110
5.1 5.0 4.9 4.8 4.7 4.6 4.5 4.4 4.3 4.2 4.1 4.0 3.9 3.8 3.7
13C – chemical shift (ppm)
1H – chemical shift (ppm)

Figure 4

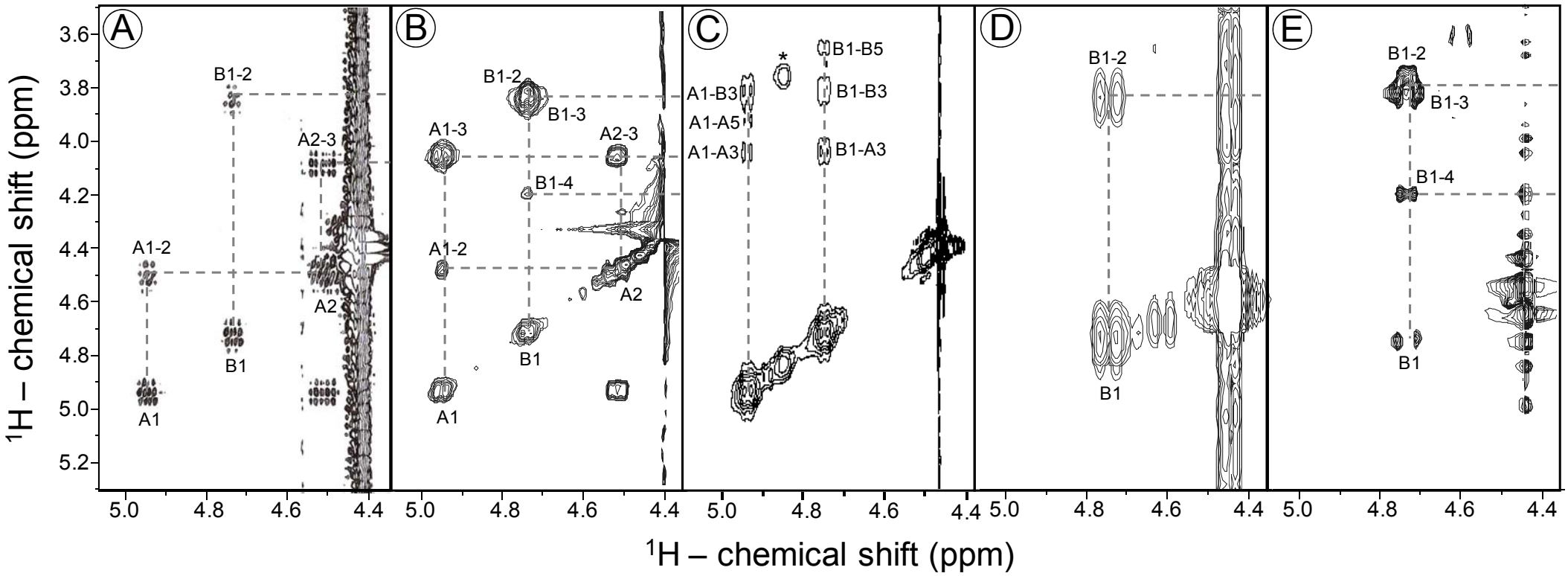
A
B
C
D
E
A1-2
B1-2
A2-3
A1
B1
A2
A1-3
B1-3
B1-4
A1-B3
A1-A5
A1-A3
B1-B5
B1-B3
B1-A3
*
^{1}H – chemical shift (ppm)
^{1}H – chemical shift (ppm)

Figure 5

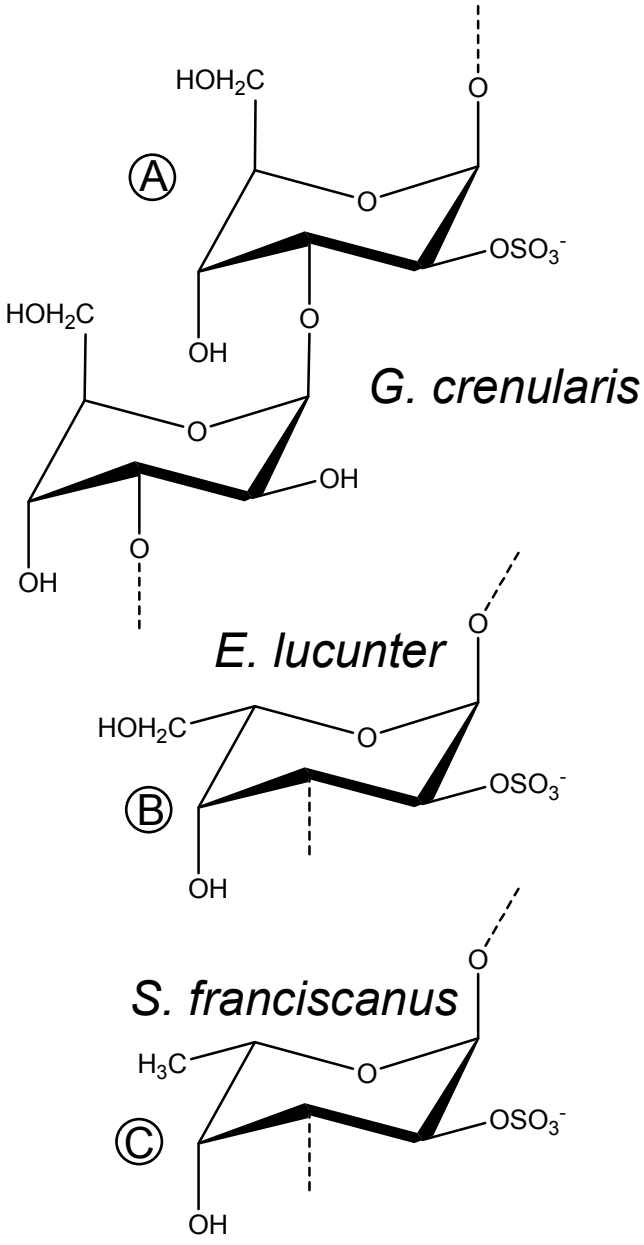
HOH2C
O
A
O
OSO3-
HOH2C
O
OH
G. crenularis
O
OH
OH
O
E. lucunter
O
HOH2C
O
OSO3-
B
OH
S. franciscanus
O
H3C
O
OSO3-
C
OH

Figure 6

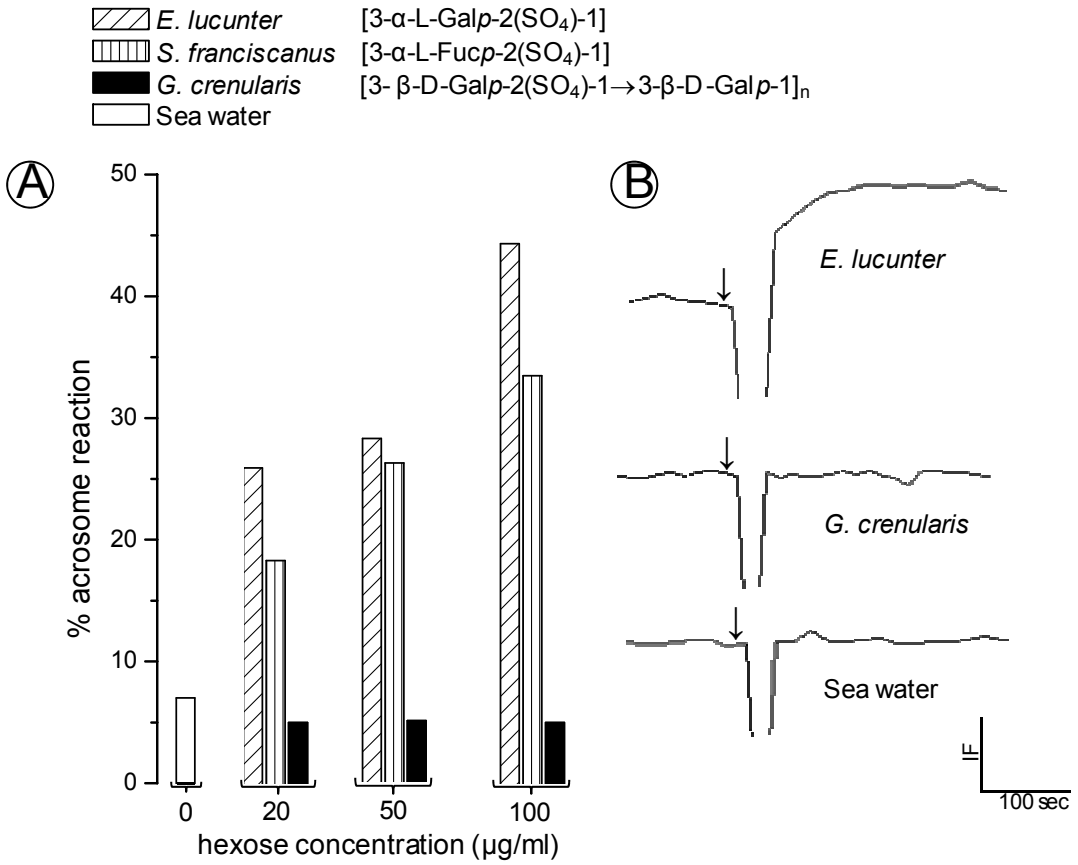
E. lucunter [3-α-L-Galp-2(SO4)-1]
S. franciscanus [3-α-L-Fucp-2(SO4)-1]
G. crenularis [3- β-D-Galp-2(SO4)-1→3-β-D-Galp-1]n
Sea water
A
B
% acrosome reaction
hexose concentration (µg/ml)
E. lucunter
G. crenularis
Sea water
IF
100 sec

Figure 7 A,B

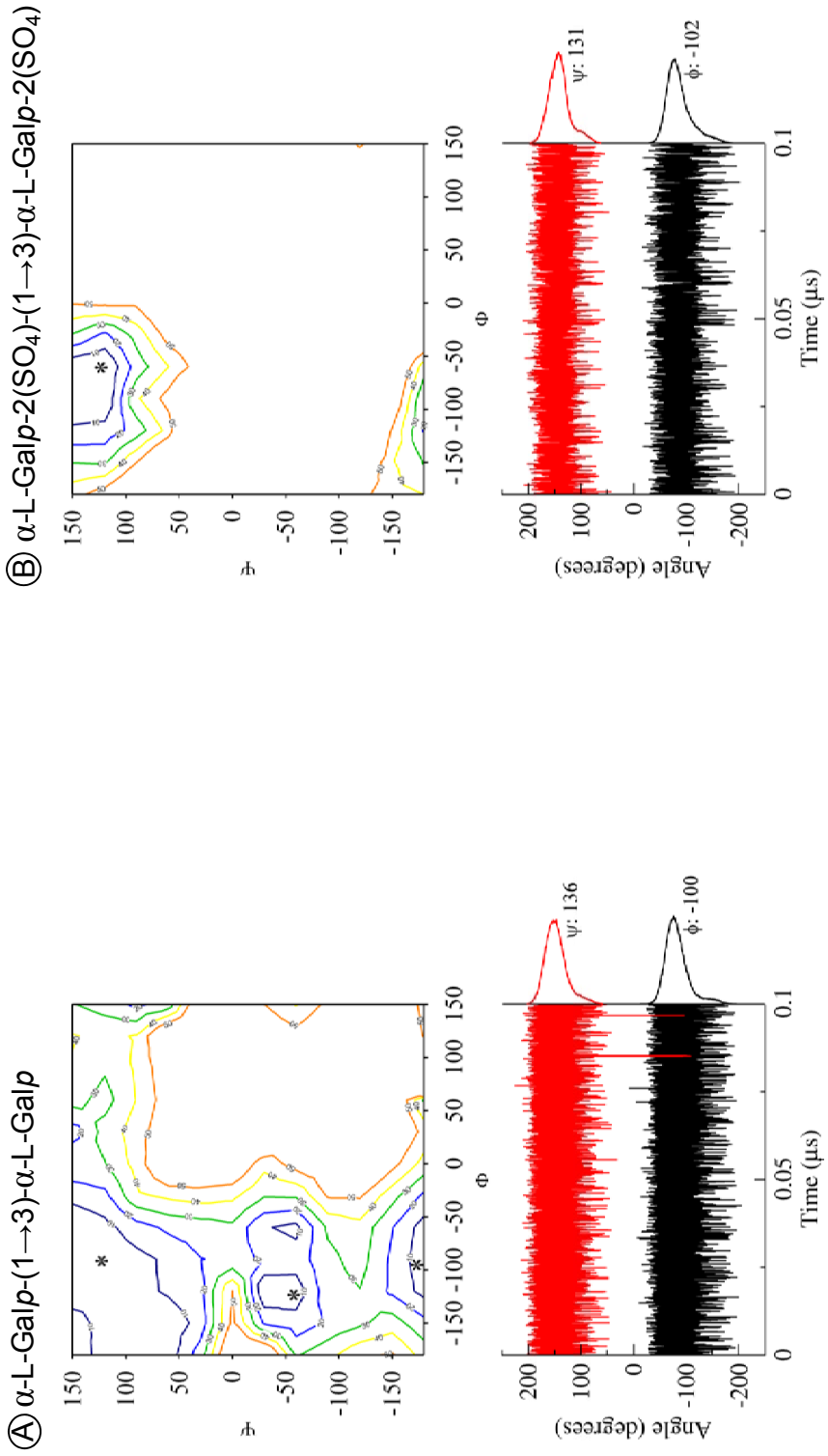
Ⓑ α-L-Galp-2(SO4)-(1→3)-α-L-Galp-2(SO4)
Ⓐ α-L-Galp-(1→3)-α-L-Galp
ψ
Φ
Angle (degrees)
Time (μs)
ψ: 131
ϕ: -102
ψ: 136
ϕ: -100

Figure 7 C-D

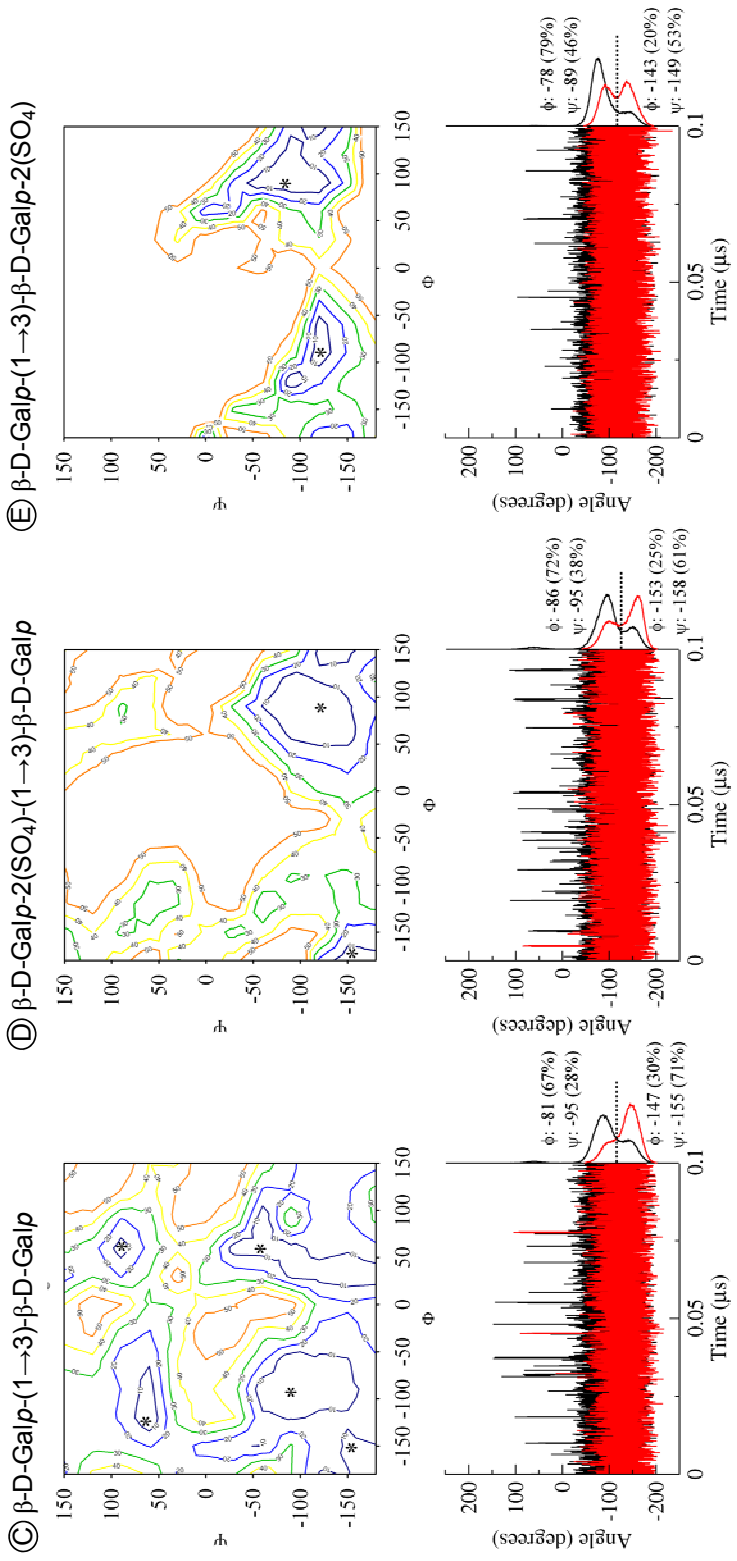
Ⓒ β-D-Galp-(1→3)-β-D-Galp
Ⓓ β-D-Galp-2(SO4)-(1→3)-β-D-Galp
Ⓔ β-D-Galp-(1→3)-β-D-Galp-2(SO4)
ϕ: -81 (67%)
ψ: -95 (28%)
ϕ: -147 (30%)
ψ: -155 (71%)
ϕ: -86 (72%)
ψ: -95 (38%)
ϕ: -153 (25%)
ψ: -158 (61%)
ϕ: -78 (79%)
ψ: -89 (46%)
ϕ: -143 (20%)
ψ: -149 (53%)
Angle (degrees)
Time (μs)
Φ
Ψ

CAPÍTULO 5: OCORRÊNCIA DE UNIDADE 3-β-D-Gal*p*-1 NOS ORGANISMOS MARINHOS ATRAVÉS DA EVOLUÇÃO

A ocorrência intrigante de unidades 3-β-D-Gal*p*-1 nas galactanas sulfatadas do ouriço-do-mar *G. crenularis* (Figure 20) e na alga verde *C. isthmocladum* (Figura 15), assim como na alga verde *C. yezonense* (Bilan *et al*., 2007) e na angiosperma marinha *R. maritima* (Figure 2B, Aquino *et al*., 2005), nos estimulou a pesquisar a distribuição deste tipo de unidade nos polissacarídeos de outros organismos marinhos dos reinos animais e vegetais (Whittaker, 1969). Assim, pudemos observar realmente uma relação filogenética entre os organismos que sintetizam galactanas sulfatadas, particularmente com unidades 3-β-D-Gal*p*-1.

Análises do cladograma hipotético ilustrado na Figura 22, mostra que a unidade 3-β-D-Gal*p*-1 é preservada nas espécies de filos que co-habitam o ambiente marinho. Essas espécies pertencem aos filos de algas marrons (Phaephyta), algas verdes (Chlorophyta), algas vermelhas (Rhodophyta), grama-marinhas (Angiospermae, Spermatophyta), animais invertebrados [ouriços-do-mar (Echinodermata, Echinoidea), bivalves (Mollusca, Bivalvia), ascídias (Urochordata, Ascidiacea)] e animais vertebrados como peixes (Teleostei, Chordata) que expressam o GAG queratam sulfato, embora a 6-sulfatação seja incomum.

A unidade 3-β-D-Gal*p*-1 é claramente preservada na maioria dos filos durante a evolução, mas o sítio preferencial de sulfatação é variável: 4-sulfatação em algas e angiosperma marinha, e a 2- ou 6-sulfatação em galactanas de invertebrados e, raramente, em queratam sulfato (e angiosperma marinha). Analisando essa relação filogenética, há uma tendência significativa de 2-sulfatação em animais, 4-sulfatação em autótrofos (alga e angiosperma marinha), e uma distribuição dispersa da 6-sulfatação (Figura 22).

Essas observações levantam a hipótese de que a galactosiltransferase responsável pela incorporação da unidade 3-β-D-Gal*p*-1 é mantida durante a evolução em uma região específica da árvore filogenética (em filos específicos).

Entretanto, há uma notória variação na ocorrência dos tipos de sulfotransferases. Dados, que apóiam a hipótese de que as cadeias de galactose são preservadas nos diferentes filos ao longo da evolução, mas há um nível variável nos sítios de sulfatação que diferem de espécie para espécie e de tecido para tecido. De certa forma estes resultados são análogos à biossíntese dos GAGs de vertebrados, onde as cadeias glicosídicas variam muito pouco. Porém, as diferenças fundamentais dos glicosaminoglicanos aparecem após a biossíntesse de suas cadeias, onde a modificação principal está relacionada à sulfatação em diferentes sítios do polissacarídeo.

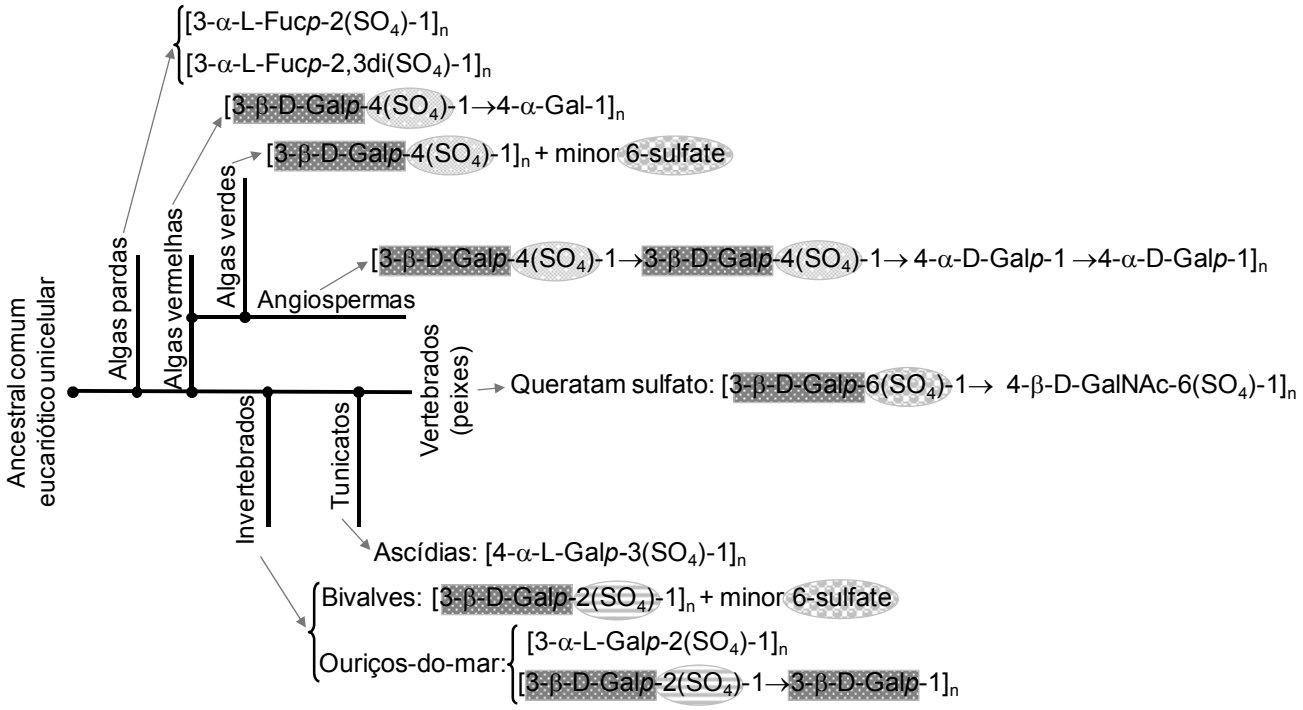

Figura 22. Árvore filogenética esquemática mostrando a relação entre polissacarídeos sulfatados de organismos marinhos pertencentes a diferentes filos taxonômicos. A unidade 3-β-D-Gal*p*-1 está iluminada pelas caixas cinza escuras e as posições 2-, 4- e 6-sulfatadas estão iluminadas pelas elipses listradas, cheias e circulares. As algas marrons (Phaeophyta) expressam polímeros de α-L-fucose ligados (1→3) e (1→4) e com diferentes padrões de sulfatação (Berteau e Mulloy, 2003; Pereira *et al*., 1999). As algas vermelhas (Rhodophyta) expressam galactanas sulfatadas compostas principalmente por seqüências [3-β-D-Gal*p*-1→4-α-D-Gal*p*-1]$_n$ (Farias *et al*., 2000; Pereira *et al*., 2005). Muitas delas são compostas por residues de 4-α-D-3,6-AnGal*p*-1 (resídues de 3,6 anidrogalactose) e 3-β-D-Gal*p*-4(SO_4)-1, comumete encontradas nos principais polissacarídeos de algas vermelhas, as carragenanas. A unidade 3-β-D-Gal*p*-4(SO_4)-1 é predominante nas galactanas sulfatadas de algas verdes (Clorophyta) (Farias *et al*., 2008; Bilan *et al*., 2007). A angiosperma marinha *R. maritma* sintetiza uma galactana sulfatada constituída pela unidade tetrassacarídica repetitive [3-β-D-Gal*p*-4(SO_4)-1→3-β-D-Gal*p*-4(SO_4)-1→4-α-D-Gal*p*-1→4-α-D-Gal*p*-1]$_n$, contendo caracterísi-cas estruturais de polissacarídeos sulfatados de invertebrados e algas (Aquino *et al*., 2005). Em invertebrados, os polissacarídeos das duas species de ouriços-do-mar (Equinodermata) *E. lucunter* (Alves *et al*., 1997) e *G. crenularis* são constituídos respectivamente por unidades repetitivas [3-β-D-Gal*p*-2(SO_4)-1]$_n$ e [3-β-D-Gal*p*-2(SO_4)-1→3-β-D-Gal*p*-1]$_n$. O bivalve *Meretrix petechialis* (Mollusca) sintetiza um polissacarídeo constituído pela unidade 3-β-D-Gal*p*-1, majoritariamente 2-sulfatada e poucas 6-sulfatadas (Amornrut *et al*., 1999). Algumas species de ascídias (Urochordata) *Ascidia nigra*, *Clavelina oblonga*, *S. plicata* e *H. monus* (Pavão *et al.,*1989; Pavão *et al*., 1990; Santos *et al.,* 1992; Albano *et al*., 1990) possuem polissacarídeos com cadeias de [4-α-L-Gal*p*-3(SO_4)-1]$_n$. O glicosaminoglicano queratam sulfato pode ser encontrado com unidades [3-β-D-Gal*p*-6(SO_4)-1→4-β-D-Gal*N*Ac-6(SO_4)-1]$_n$ (Scudder *et al*., 1986).

REFERÊNCIAS BIBLIOGRÁFICAS

-Albano, R. M., and Mourão, P. A. S. (1986). Isolation, fractionation and preliminary characterization of a novel class of sulfated glycans from the tunic of *Styela plicata* (Chordata-Tunicata). ***J. Biol. Chem.***, 261, 758–765.

-Albano, R.M., Pavão, M.S.G., Mourão, P.A.S., Mulloy, B. (1990). Structural studies of a sulfated L-galactan from *Styela plicata* (Tunicate): Analysis of the Smithdegraded polysaccharide. ***Carbohydr. Res.***, 208,163–174.

-Alves, A.P., Mulloy, B., Diniz, J.A. e Mourão, P.A.S. (1997). Sulfated polysaccharides from the egg jelly layer are species-specific inducers of acrosomal reaction in sperms of sea urchin. ***J. Biol. Chem.***, 272 (11), 6965-6971.

-Alves, A.P., Mulloy, B., Moy, G.W., Vacquier, V.D. e Mourão, P.A.S. (1998). Females of the sea urchin *Strongylocentrotus purpuratus* differ in the structures of their egg jelly sulfated fucans. ***Glycobiology***, 8 (9), 939-946.

-Amornrut, C., Toida, T., Imanari, T., Woo, E.-R., Park, H., Linhardt, R., Wu, S.J., Kim, Y.S. (1999). A new sulfated beta-galactan from clams with anti-HIV activity. ***Carbohydr. Res.***, 321,121–127.

-Andrade, L.R., Salgado, L.T., Farina, M., Pereira, M.S., Mourão, P.A.S. e Amado-Filho, G.M. (2004). Ultrastructure of acidic polysaccharides from the cell wall of brown algae. ***J. Struc. Biol.***, 145, 216-225.

-Aquino, R.S., Landeira-Fernandez, A.M., Valente, A.P., Andrade, L.R. e Mourão, P.A.S. (2005). Occurrence of sulfated galactans in marine angiosperms: evolutionary implications. ***Glycobiology***, 15 (1), 11-20.

-Becker, C.F., Guimarães, J.A. e Verli, H. (2005) Molecular dynamics and atomic charge calculations in the study of heparin conformation in aqueous solution. ***Carbohydrate. Res.***, 340,1499-1507.

-Berendsen, H.J.C., Grigera, J.R., Straatsma, T.P. (1987) The Missing Term in Effective Pair Potentials. ***J. Phys. Chem.***, 91,6269–6271.

-Berteau, O. e Mulloy, B. (2003). Sulfated fucans, fresh perspectives: structures, functions, and biological properties of sulfated fucans and an overview of enzymes active toward this class of polysaccharide. ***Glycobiology***, 13 (6), 29R-40R.

-Bilan, M.I., Vinogradova, E.V., Shashkov, A.S., Usov, A.I. (2007). Structure of a highly pyruvylated galactan sulfate from the Pacific green alga *Codium yezoense* (Bryopsidales, Chlorophyta). ***Carbohydr. Res.***, 342,586–596.

-Biermann, C.H., Marks, J.A., Vilela-Silva, A.-C.E.S., Castro, M.O., Mourão, P.A. (2004). Carbohydrate-based species recognition in sea urchin fertilization: another avenue for speciation? ***Evolution & Development.*** 6:353–61.

-Bonnell, B.S., Keller, S.H., Vacquier, V.D. e Chandler, D.E. (1994). The sea urchin egg jelly coar consists of globular glycoproteins bound to a fibrous fucan superstructure. ***Dev. Biol.***, 162, 313-330.

-Cavalcante, M.C., Mourão, P.A.S. e Pavão, M.S. (1999). Isolation and characterization of a highly sulfated heparan sulfate from ascidian test cells. ***Biochim. Biophys. Acta***, 1428(1), 77-87.

-Cavalcante, M.C., de Andrande L.R., Du Bocage Santos-Pinto, C., Straus, A.H., Takahashi, H.K., Allodi, S. e Pavão, M.S. (2002). Colocalization of heparin and histamine in the intracellualar granules of test cells from the invertebrates *Styela plicata* (Chordata-Tunicata). ***J. Struct. Biol.***, 137(3), 313-321.

-Chevolot L., Foucault, A., Kervarec, N., Sinquin, C., Fisher, A.M., Boisson-Vidal, C. (1999). Further data on the structure of brown seaweed fucans: relationships with anticoagulant activity. ***Carbohydr Res.*** 319:154-165.

-Chizhov, A.O., Dell, A., Morris, H.R., Haslam, S.M., McDowell, R.A., Shashkov, A.S. (1999). A study of fucoidan from the brown seaweed *Chorda filum*. ***Carbohydr Res.*** 320:108-119.

-Ciucanu, I. e Kerek, F. (1984). Rapid and simultaneous methylation of fatty and hydroxy fatty acids for gas chromatographic analysis. ***J. Chromatogr.,*** 286,179–185.

-Cumashi, A., Ushakova, N.A., Preobrazhenskaya, M.E., D'Incecco, A., Piccoli, A., Totani, L., Tinari, N., Morozevich, G.E., Berman, A.E., Bilan, M.I., Usov, A.I., Ustyuzhanina, N.E., Grachev, A.A., Sanderson, C.J., Kelly, M., Rabinovich, G.A., Iacobelli, S., Nifantiev, N.E., Consorzio Interuniversitario Nazionale per la Bio-Oncologia, Italy. (2007). A comparative study of the anti-inflammatory, anticoagulant, antiangiogenic, and antiadhesive activities of nine different fucoidans from brown seaweeds. ***Glycobiology.*** 17:541-552.

-Dan, J.C. (1952). Studies on the acrosome. I. Reaction to egg water and other stimuli. ***Biol. Bull.***, 107, 203-218.

-Darden, T., York, D., Pedersen, L. (1993) Particle mesh Ewald-an N.log(N) method for Ewald sums in large systems. ***J. Chem. Phys.***, 98, 10089-10092.

-Dietrich, C.P. e Dietrich, S.M.C. (1977). Electrophoretic behaviour of acidic mucopolysaccharides by agarose gel electrophoresis. ***J. Chromatogr.***, 130,299–304.

-Dubois, M., Gilles, K.A., Hamilton, J.K., Rebers, P.A., Smith, F. (1956). Colorimetric method for determination of sugars and related substances. ***Anal. Chem.***, 28, 350–354.

-Farndale, R.W., Buttle, D.J. e Barrett, A.J. Improved quantitation and discrimination of sulphated glycosaminoglycans by use of dimethylmethylene blue. ***Biochim. Biophys. Acta*****.** 883, 173-7, 1986.

-Farias, R.L., Valente, A.P., Pereira, M.S., e Mourão, P.A.S. (2000). Structure and anticoagulant activity of sulfated galactans. Isolation of a unique sulfated galactan from the red algae *Botryocladia occidentalis* and comparision of its anticoagulant action with that of sulfated galactanas from invertebrates. ***J. Biol. Chem.***, 275 (38), 29299-29307.

-Farias, E.H., Pomin, V.H., Valente, A.-P., Nader, H.B., Rocha, H.A., Mourão, P.A. (2008). A preponderantly 4-sulfated, 3-linked galactan from the green alga *Codium isthmocladum*. ***Glycobiology***, 18,250-259.

-Foltz, K.R. e Lennarz, W.J. (1993). The molecular basis of the sea urchin gamete interactions at the egg plasma membrane. ***Dev. Biol.*** 158, 46-61.

-Fonseca, R.J.C, Oliveira, S.-N.M.C.G., Melo, F.R., Pereira, M.G., Benevides, N.M.B., Mourão, P.A.S. (2008). Slight differences in sulfation of algal galactans account for differences in their anticoagulant and venous antithrombotic activities. ***Thromb. Haemost.***, 99, 539–545.

-González-Martínez, M.T., Galindo, B.E., De la Torre, L., Zapata, O., Rodríguez, E., Florman, H.M. e Darszon, A. (2001). A sustained increase in intracellular Ca^{+2} is required for the acrosome reaction in sea urchin sperm. ***Dev. Biol.***, 236, 220-229.

-Guerrero, A. E Darszon, A. (1989). Evidence for the activation of two differnt Ca^{+2} channels during the egg jelly-induced acrosome reaction of sea urchin sperm. ***J. Biol. Chem.***, 264 (33), 19593-19599.

-Harrop, H.A., Rider, C.C., Coombe, D.R. (1992). Sulphated polysaccharides exert anti-HIV activity at differing sites. Biochem Soc Trans. 20:163S.

-Hess, B., Bekker, H., Berendsen, H.J.C., Fraaije, J.G.E. (1997) Molecular dynamics simulations of the hydration of poly(vinyl methyl ether): Hydrogen bonds and quasi-hydrogen bonds M. ***J. Comput. Chem.***, 18,1463–1472.

-Hirohashi, N. e Vacquier, V.D. (2002a). Egg sialoglycans increase intracellular pH and potentiate the acrosome reaction of the sea urchin sperm. ***J. Biol. Chem.*** 277:8041-8047.

-Hirohashi, N. e Vacquier, V.D. (2002b). High molecular mass egg fucose sulfate polymer is required for opening both Ca2+ channels involved in triggering the sea urchin sperm acrosome reaction. ***J. Biol. Chem.*** 277:1182-1189.

-Hirohashi, N., Vilela-Silva, A.C.E.S., Mourão, P.A.S. e Vacquier, V.D. (2002). Structural requirements for species-specific induction of the sperm acrosome reaction by sea urchin egg sulfated fucan. ***Bioc. And Bioph. Res. Comm.***, 298, 403-407.

-Kabat, E.A., e Mayer, M.M. (1971) ***Experimental Immunochemistry***, Charles C. Thomas Publisher, Springfield, IL, USA. 505-513.

-Karlsson, A. e Singh, S.K. (1999). Acid hydrolysis of sulphated polysaccharides. Desulphation and the effect on molecular mass. ***Carb. Res.***, 38, 7-15.

-Kakkar, V.V., e Hedges, A.R. (1989). Use of heparin as a profilatic agent against venous thromboembolism. In: Lane, D.A., e Lindahl, U. (eds), ***Heparin: chemical and biological properties, clinical applications.*** Edward Arnold, London, 455-473.

-Kelton, J.G. e Hirsh, J. (1980) Bleeding associated with antithrombotic therapy. ***Semin. Hematol.***, 17, 259-379.

-Kircher, H.W. (1960). Gas–liquid partition chromatography of methylated sugars. ***Anal. Chem.***, 32,1103–1106.

-Lahaye, M. (2001). Development on gelling algal galactans, their structure and physico-chemistry. ***J. Appl. Phycol.***, 13,173–184.

-Levine, A.E., Walsh, K.A. e Fodor, E.J.B. (1978). Evidence of na acrosin-like enzyme in sea urchin sperm. ***Dev. Biol.***, 63, 299-306.

-Love, J. e Percival, E. (1964). The polysaccharides of green seaweed *Codium fragile*: Part III. A β-1,4-linked mannan. ***J. Chem. Soc.***, 3345–3350.

-Maimone, M.M. e Tollefsen, D.M. (1990). Structure of dermatan sulfate hexasaccharide that binds to heparin cofactor II with high affinity. ***J. Biol. Chem.***, 265, 18263-18271.

-Mathews, M.B. (1975). Polyanionic proteoglycans. ***Connective tissue: macromolecular structure and evolution.***, Kleinzeller, A., Springer, G.F. e Witman, H.G., eds. Springer-Velaq, Berlim, pp. 93-125.

-Matsubara, K., Matsuura, Y., Bacic, A., Liao, M.-L., Hori, K., Miyazawa, K. (2001). Anticoagulant properties of a sulfated galactan preparation from a marine green alga *Codium cylindricum*. ***Biol Macromol.***, 28,395–399.

-Melo, F.R., Pereira, M.S., Foguel, D. e Mourão, P.A.S. (2004). Antithrombin-mediated anticoagulant activity of sulfated polysaccharides: differnt mechanism for heparin and sulfated galactanas. ***J. Biol. Chem.***, 279, 20824-20835.

-Miller, D.J. e Ax, R.L. (1990). Carbohydrate and fertilization in animals. ***Mol. Rep. Dev.***, 187, 23-34.

-Mourão, P.A.S. (2004). Use of sulfated fucans as anticoagulant and antithrombotic agents: future perspectives. ***Curr. Pharm. Des.***, 10, 967-981.

-Mourão, P.A.S. (2007). A carbohydrate-based mechanism of species recognition in sea urchin fertilization. ***Braz. J. Med. Biol. Res.***, 40,5–17.

-Mourão, P.A.S. e Bastos, I.G. (1987). Highly acidic glycans from sea cucumber. ***Eur. J. Biochem.***, 166, 639-645.

-Mourão, P.A. e Pereira, M.S. (1999). Searching for alternatives to heparin: sulfated fucans from marine invertebrates. ***Trends Cardiovasc. Med.*** 9:225-232.

-Mourão, P.A. e Perlin, A.S. (1987). Structural features of sulfated glycans from the tunic of *Styela plicata* (Chordata-Tunicata). A unique occurrence of L-galactose in sulfated polysaccharides. ***Eur. J. Biochem.***, 166,431–436.

-Moy, G.W., Mendoza, L.M., Schulz, J.R., Swanson, W.J., Glabe, C.G. e Vacquier, V.D. (1996). The sea urchin sperm receptor for egg jelly is a modular protein with extensive homology to the human polycystic kidney disease protein PKD1. ***J. Biol. Chem.***, 133 (4), 809-817.

-Mulloy, B., Ribeiro, A.C., Alves, A.P., Vieira, R.P. e Mourão, P.A.S. (1994). Sulfated fucans from echinoderms have a regular tetrasaccharide repeating unit defined by specific patterns of sulfation at the O-2 and O-4 positions. ***J. Biol. Chem.***, 269 (35), 22113-22123.

-Nader, H.B. e Dietrich, C.P. (1977). Determination of sulfate after chromatography and toluidine blue complexation. ***Anal. Biochem.***, 78,112–118.

-Nelson, D.L. e Cox, M.M. (2004). ***Lehninger principles of biochemistry*****.** Worth, 4th edition, pg 253.

-Pavão, M.S.G., Albano R.M., Lawsom, A.M., Mourão, P.A.S. (1989). Structural heterogeneity among unique sulfated L-galactans from different species of ascidians (tunicates). ***J. Biol. Chem.***, 264,9972–9979.

-Pavão, M.S.G., Mourão, P.A., Mulloy, B. (1990). Structure of a unique sulfated alpha-L-galactofucan from the tunicate Clavelina. ***Carbohydr Res.***, 208,153–161.

-Pavão, M.S.G., Aiello, K.R.M., Werneck, C.C., Silva, L.C.F., Valente, A.,P., Mulloy, B., Colwell, N.S., Tollefsen, D.M. e Mourão, P.A.S. (1998). Highly sulfated dermatan sulfate from Ascidians: structure versus anticoagulant activity of these glycosaminoglycans. ***J. Biol. Chem.***, 273, 27848-27857.

-Percival, E. e Ross, A.G. (1950). The isolation and purification of fucoidin from brown seaweeds. ***J. Chem. Soc.*** 717-720.

-Pereira, M.S., Mulloy, B., e Mourão, P.A.S. (1999). Structure and anticoagulant activity of sulfated fucans. Comparision between the regular, repetitive and linear fucans from echinoderms with the more heterogeneous and branched polymers from brow algae. ***J. Biol. Chem.***, 274, 7656-7667.

-Pereira, M.S., Melo, F.R., e Mourão, P.A.S. (2002). Is there a correlation between structure and anticoagulant action of sulfated galactanas and sulfated fucans? ***Glycobiology***, 12, 573-580.

-Pereira, M.G., Benevides, N.M.B., Melo, M.R.S., Valente, A.-P., Melo, F.R., Mourão, P.A. (2005). Structure and anticoagulant activity of a sulfated galactan from the red alga, *Gelidium crinale*. Is there a specific structural requirement for the anticoagulant action? ***Carbohydr. Res.***, 340,2015–2023.

-Pol-Fachin, L. e Verli, H. (2008) Depiction of the forces participating in the 2-O-sulfo-alpha-L-iduronic acid conformational preference in heparin sequences in aqueous solutions.***Carbohydr. Res.***, 343,1435-1445.

-Pomin, V.H., Pereira, M.S., Valente, A.-P., Tollefsen, D.M., Pavão, M.S.G., Mourão, P.A. (2005a). Selective cleavage and anticoagulant activity of a sulfated fucan: Stereospecific removal of a 2-sulfated ester from the polysaccharide by mild acid hydrolysis, preparation of oligosaccharides, and heparin cofactor II-dependent anticoagulant activity. ***Glycobiology.***, 15,369–381.

-Pomin, V.H., Valente, A.-P., Pereira, M.S., Mourão, P.A. (2005b). Mild acid hydrolysis of sulfated fucans: A selective 2-desulfation reaction and an alternative approach for preparing tailored sulfated oligosaccharides. ***Glycobiology.*** 15,1376–1385.

-Ravenscroft, N., Gamian, A., Romanowska, E. (2005) 3-Deoxy-Octulosonic-Acid-Containing Hexasaccharide Fragment of Unusual Core Type Isolated from *Hafnia alvei* 2 Lipopolysaccharide. ***Eur. J. Bio.***, 227, 889–896.

-Ribeiro, A.-C.,Vieira, R.P., Mourão, P.A.S., Mulloy, B. (1994). A sulfated alpha-L-fucan from sea cucumber. ***Carbohydr. Res.***, 255,225–240.

-Rocha, H.A., Moraes, F.A., Trindade, E.S., Franco, C.R., Torquato, R.J.,Veiga, S.S.,Valente, A-P, Mourão, P.A., Leite, E.L., Nader, H.B. (2005). Structural and hemostatic activities of a sulfated galactofucan from the Brown alga *Spatoglossum schroederi.* An ideal antithrombotic agent? ***J. Biol. Chem.***, 280,41278–41288.

-Santos, J.A., Mulloy, B., Mourão, P.A.S. (1992) Structural diversity among sulfated alpha-L-galactans from ascidians (tunicates). Studies on the species *Ciona intestinalis* and *Herdmania monus*. ***Eur. J. Biochem.***, 204, 669-677.

-Schuettelkopf, A.W., van Aalten, D.M.F., (2004) PRODRG: a tool for high-throughput crystallography of protein-ligand complexes. ***Acta Cryst.,*** 60, 1355-1363.

-Scudder, P., Tanq, P.W., Hounsell, E.F., Lawson, A.M., Mehmet, H., Feizi, T. (1986). Isolation and characterization of sulphated oligosaccharides released from bovine corneal keratin sulphate by the action of endo-beta-galactosidase. ***Eur. J. Biochem.,*** 157, 365–373.

-SeGall, G.K. e Lennarz, W.J. (1979). Chemical characterization of the component of the jelly coat from sea urchin eggs responsible for induction of the acrosome reaction. ***Dev. Biol.***, 71, 33-48.

-SeGall, G.K. e Lennarz, W.J. (1981). Jelly coat and induction of the acrosome reaction in echinoid sperm. ***Dev. Biol.***, 86, 87-93.

-Shashkov, A.S., Senchenkova, S.N., Vinogradov, E.V., Zatonsky, G.V., Knirel, Y.A., Literacka, E., Kaca, W. (2000). Full structure of the *O*-specific polysaccharide of *Proteus mirabilis* O24 containing 3,4-*O*-[(S)-1-carboxyethylidene]-Dgalactose. ***Carbohydr Res.***, 329, 453–457.

-Suzuki, N. (1990). Structure and function of sea urchin egg jelly molecules. ***Zool. Sci.***, 7, 355-370.

-Thomas, F.I.M., Bolton, T.F., e Sastry, A. (2001). Mechanical forces imposed on echinoid eggs during spawning: mitigation of forces by fibrous networks within egg extracellular layers. ***J. Exp. Biol.***, 204, 815-821.

-Tilney, L.G., Hatano, S., Ishikawa, H. Mooseker, M. (1973). The polymerization of actin: its role in the generation of the acrosomal process of certain echinoderm sperm. ***J. Cell Biol.***, 59, 109-126.

-Trimmer, J.S. e Vacquier, V.D. (1986). Activation of sea urchin gamentes. ***Annu. Rev. Cell Biol.***, 2, 1-26.

-Vacquier, V.D. e Moy, G.W. (1997). The fucose sulfate polymer of egg jelly binds to spermREJ and is the inducer of the sea urchin sperm acrosome reaction. ***Dev. Biol.***, 192 (1), 125-135.

-van de Velde, F., Pereira, L., Rollema, H.S. (2004). The revised NMR chemical shift data of carrageenans. ***Carbohydr Res.***, 339, 2309–2313.

-van Der Spoel, D., Lindahl, E., Hess, B., Groenhof, G., Mark, A.E., Berendsen, H.J. (2005) GROMACS: fast, flexible, and free. ***J. Comput. Chem.***, 26, 1701-18.

-van Gunsteren, W.F., Billeter, S.R., Eising, A.A., Hunenberger, P.H., Kruger, P., Mark, A.E., Scott, W.R.P., Tironi, I.G., (1996) Biomolecular Simulation: The GROMOS96 Manual and User Guide (University of Groningen, Groningen, The Netherlands and ETH, Zurich, Switzerland).

-Usov, A.I. (1998) Structural analysis of red seaweed galactans of agar and carrageenan groups. ***Food Hydrocolloids***, 12,301–308.

-Verli, H. e Guimarães, J.A. (2004) Molecular dynamics simulation of a decasaccharide fragment of heparin in aqueous solution. ***Carbohydr. Res.***, *339*, 281-290.

-Verli, H. e Guimarães, J.A. (2005) Structural and functional behavior of biologically active monomeric melittin. ***J. Mol. Graph. Model.***, 24,203-212.

-Vieira, R.P. e Mourão, P.A.S. (1988). Occurrence of a unique fucose-branched chondroitin sulfate in the body wall of sea cucumber. ***J. Biol. Chem.***, 263, 18176-18183.

-Vieira, R.P., Mulloy, B., Mourão, P.A. (1991). Structure of a fucose-branched chondroitin sulfate from sea cucumber. Evidence for the presence of 3-*O*-sulfobeta-D-glucuronosyl residues. ***J. Biol. Chem.***, 266,13530–13536.

-Vilela-Silva, A.-C.E.S., Alves, A.P., Valente, A.-P., Vacquier, V.D. e Mourão, P.A. (1999). Structure of the sulfated α-L-fucan from the egg jelly coat of the sea urchin *Strongylocentrotus franciscanus*: patterns of preferential 2-O- and 4-O-sulfation determine sperm cell recognition. ***Glycobiology***. 9:927-233.

-Vilela-Silva, A.-C., E.S.; Werneck, C.C.; Valente, A.-P.; Vacquier, V.D.; Mourão, P.A.S. (2001). Embryos of sea urchin *Strongylocentrotus purpuratus* synthetize a dermatam sulfate enriched 4-*O*- and 6-*O*-disulfated galactosamine untis. ***Glycobiology***, 11, 433-40.

-Vilela-Silva, A.-C.E.S., Castro, M.O., Valente, A.-P., Biermann, C.H., Mourão, P.A. (2002). Sulfated fucans from the egg jellies of the closely related sea urchins *Strongylocentrotus droebachiensis* and *Strongylocentrotus pallidus* ensure species-specific fertilization. ***J. Biol. Chem.*** 277:379-387.

-Visentin, G.P. (1999). Heparin induced thrombocytopenia: Molecular pathogenesis. ***Tromb. Haemost.***, 82, 448-456.

-Warkentin, T.E. (1999). Heparin-induced trombocytopenia: A clinicopathologic syndrome. *Tromb. Haemost.*, 82, 439-447.

-Whittaker, R.H. (1969). New concepts of kingdoms of organisms. ***Science***, 163, 150–160.

ANEXOS

ANEXO I

Ciência Hoje
Vol. 39, pp 24-31, 2006

"Carboidratos: de adoçantes a medicamentos"

Vitor H. Pomin e Paulo A.S. Mourão.

CARBOIDRATOS

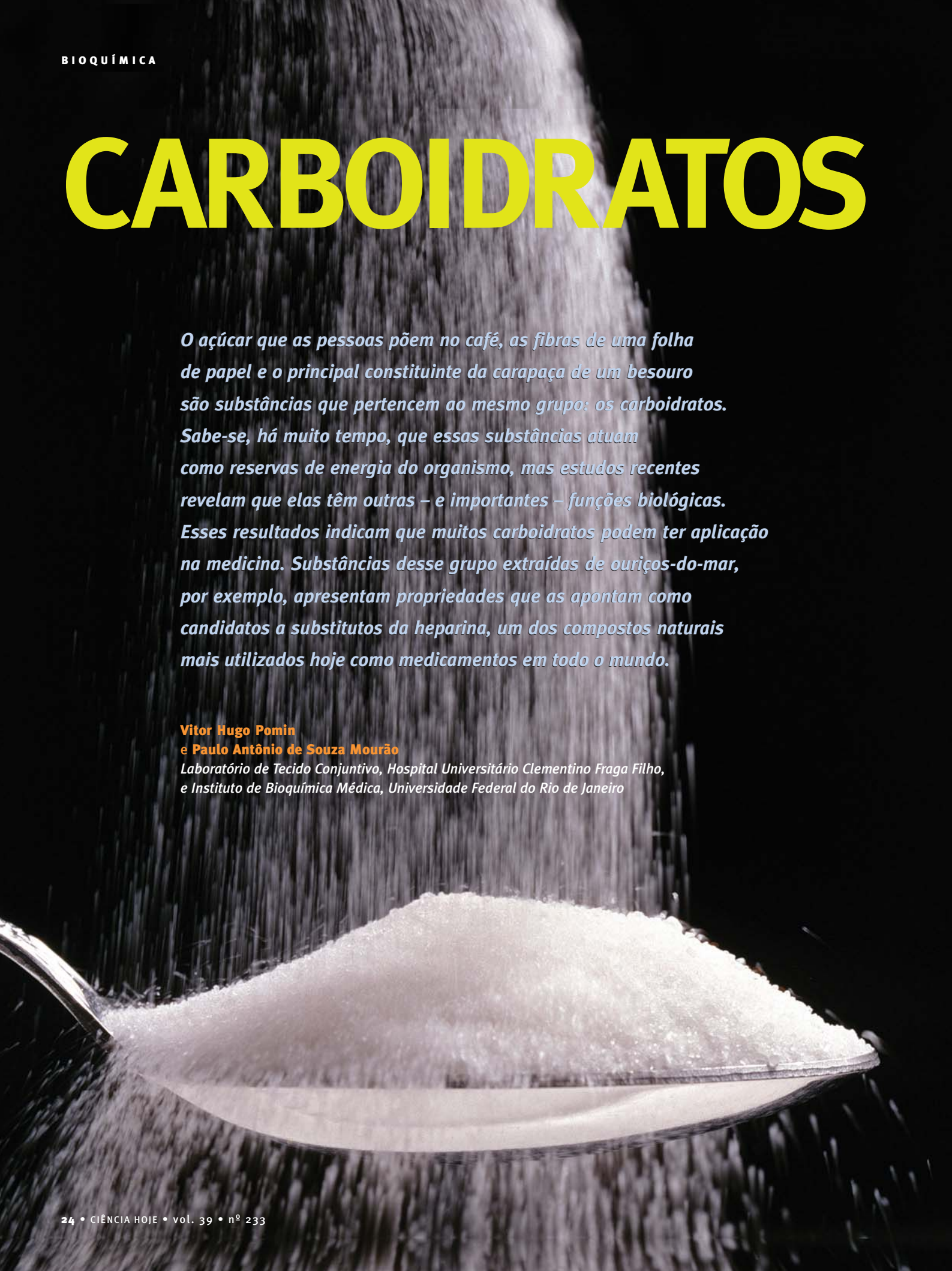

O açúcar que as pessoas põem no café, as fibras de uma folha de papel e o principal constituinte da carapaça de um besouro são substâncias que pertencem ao mesmo grupo: os carboidratos. Sabe-se, há muito tempo, que essas substâncias atuam como reservas de energia do organismo, mas estudos recentes revelam que elas têm outras – e importantes – funções biológicas. Esses resultados indicam que muitos carboidratos podem ter aplicação na medicina. Substâncias desse grupo extraídas de ouriços-do-mar, por exemplo, apresentam propriedades que as apontam como candidatos a substitutos da heparina, um dos compostos naturais mais utilizados hoje como medicamentos em todo o mundo.

Vitor Hugo Pomin
e **Paulo Antônio de Souza Mourão**
Laboratório de Tecido Conjuntivo, Hospital Universitário Clementino Fraga Filho, e Instituto de Bioquímica Médica, Universidade Federal do Rio de Janeiro

De adoçantes a medicamentos

Os carboidratos são as macromoléculas mais abundantes na natureza. Suas propriedades já eram estudadas pelos alquimistas, no século 12. Durante muito tempo acreditou-se que essas moléculas tinham função apenas energética no organismo humano. A glicose, por exemplo, é o principal carboidrato utilizado nas células como fonte de energia. O avanço do estudo desses compostos, porém, permitiu descobrir outros eventos biológicos relacionados aos carboidratos, como o reconhecimento e a sinalização celular, e tornou possível entender os mecanismos moleculares envolvidos em algumas doenças causadas por deficiência ou excesso dessas moléculas.

O avanço científico permitiu conhecer de modo mais detalhado as propriedades físico-químicas dos carboidratos, resultando na exploração dessas características em diversos processos industriais, como nas áreas alimentar e farmacêutica. Um dos carboidratos com maior utilização médica é a heparina, composto de estrutura complexa, com ação anticoagulante e antitrombótica (reduz a formação de coágulos fixos – trombos – no interior dos vasos sangüíneos), obtido de tecidos animais, onde ocorre em baixa concentração. A necessidade de maior produção de medicamentos desse tipo, devido ao aumento da incidência de doenças cardiovasculares, e os efeitos colaterais associados à heparina vêm aumentando, nos últimos tempos, o interesse pela busca de substitutos para esse composto.

Recentemente, no Laboratório de Tecido Conjuntivo, do Instituto de Bioquímica Médica da Universidade Federal do Rio de Janeiro, extraímos de ouriços-do-mar e de algas marinhas novos compostos, conhecidos como fucanas sulfatadas e galactanas sulfatadas, com propriedades semelhantes às da heparina. Experimentos mostraram que tais compostos agem como anticoagulantes e antitrombóticos em camundongos, ratos e coelhos, embora não tenham, nos organismos de origem, funções biológicas relacionadas à coagulação. Com isso, abrem perspectivas promissoras para o desenvolvimento de substitutos da heparina.

Um grupo distinto de moléculas

Os carboidratos, também conhecidos como glicídios ou açúcares, são moléculas constituintes dos seres vivos, assim como proteínas, lipídios e ácidos nucléicos (figura 1). A combinação das diferentes funções bioquímicas de cada uma dessas moléculas permite a integridade da célula e de todos os processos metabólicos, fisiológicos e genéticos dos organismos vivos. Antigamente, acreditava-se que os carboidratos estavam envolvidos apenas com funções estruturais e energéticas. Isso decorria da dificuldade técnica no estudo químico e biológico desses compostos.

A partir da década de 1970, o surgimento de técnicas avançadas de cromatografia, eletroforese e espectrometria permitiu ampliar a compreensão das funções dos carboidratos. Hoje existe um novo ramo da ciência – a glicobiologia – voltado apenas para o estudo desses compostos. Sabe-se agora que eles participam da sinalização entre células e da interação entre outras moléculas, ações biológicas essenciais para a vida. Além disso, sua estrutura química se revelou mais variável e diversificada que a das proteínas e dos ácidos nucléicos.

Os primórdios do estudo de carboidratos estão ligados ao seu uso como agentes adoçantes (mel) ou no preparo do vinho a partir da uva. Nos escritos dos alquimistas mouros, no século 12, há referências ao açúcar da uva, conhecido hoje como glicose. Os relatos iniciais sobre açúcares na história vêm dos árabes e persas. Na Europa, o primeiro agente adoçante foi sem dúvida o mel, cuja composição inclui frutose, glicose, água, vitaminas e muitas outras substâncias.

Há indícios de que Alexandre, o Grande – o imperador Alexandre III da Macedônia (356-323 a.C.) – introduziu na Europa o açúcar obtido da cana-de-açúcar, conhecido hoje como sacarose (e o primeiro açúcar a ser cristalizado). A dificuldade do cultivo da cana-de-açúcar no clima europeu levou ao uso, como alternativa, do açúcar obtido da beterraba (glicose), cristalizado em 1747 pelo farmacêutico alemão Andreas Marggraf (1709-1782). A história dos carboidratos está associada a seu efeito adoçante, mas hoje sabemos que a maioria desses compostos não apresenta essa propriedade.

A análise da glicose revelou sua fórmula química básica – CH_2O, que apresenta a proporção de um átomo de carbono para uma molécula de água. Daí vem o nome carboidrato (ou hidrato de carbono). Tal proporção mantém-se em todos os compostos desse grupo. Os mais simples, chamados de monossacarídeos, podem ter de três a sete átomos de carbono, e os mais conhecidos – glicose, frutose e galactose – têm seis. A fórmula desses três açúcares é a mesma, $C_6H_{12}O_6$, mas eles diferem no arranjo dos átomos de carbono, hidrogênio e oxigênio em suas moléculas.

Os monossacarídeos, principalmente as hexoses, podem se unir em cadeia, formando desde dissacarídeos (com duas unidades, como a sacarose, que une uma frutose e uma glicose) até polissacarídeos (com grande número de unidades, como o amido, que tem cerca de 1.400 moléculas de glicose, e a celulose, formada por entre 10 mil e 15 mil moléculas de glicose). Embora muitos polissacarídeos sejam formados pela mesma unidade

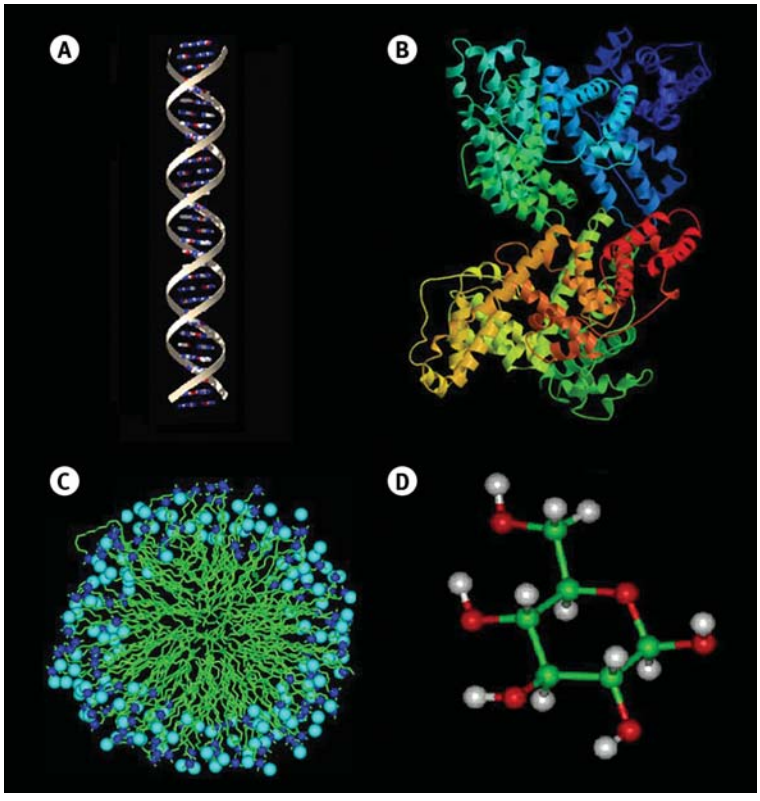

Figura 1. Estruturas representativas de algumas macromoléculas biológicas: em A, ácido desoxirribonucléico, ou DNA (as fitas laterais representam os carboidratos ligados a grupos fosfatos e as 'hastes' do interior, em azul, vermelho e branco, são as bases nitrogenadas que formam o código genético); em B, albumina, proteína mais abundante do plasma, com 585 aminoácidos e rica em estruturas espirais conhecidas como 'hélices' (cada cor representa uma região da proteína); em C, micela, uma estrutura formada por várias moléculas de lipídio em solução aquosa (as linhas verdes representam a 'cauda' hidrofóbica e as esferas azuis a 'cabeça' hidrofílica); em D, a glicose, principal monossacarídeo da natureza, formada por átomos de hidrogênio (em cinza), oxigênio (em vermelho) e carbono (em verde)

(glicose, no caso do amido e da celulose), as diferenças em suas estruturas, como presença ou não de ramificações e variedade nas ligações entre as unidades, conferem a eles propriedades físico-químicas muito diversas.

Outro polissacarídeo importante é a quitina, que constitui o exoesqueleto – a carapaça – dos artrópodes (insetos e crustáceos). A estrutura molecular da celulose e da quitina impede que sejam digeridos pelas enzimas do nosso trato gastrintestinal. A celulose, presente na madeira, é o composto orgânico mais abundante no planeta. Como o filo dos artrópodes tem o maior número de espécies e indivíduos na natureza, a quitina é outro polissacarídeo abundante. Além disso, os ácidos nucléicos (DNA e RNA), moléculas responsáveis pela hereditariedade e encontradas em todos os seres vivos, têm açúcares (ribose e desoxirribose) em suas estruturas. Os carboidratos, portanto, são os compostos biológicos predominantes na natureza (figura 2).

GRUPO KEYSTONE

Figura 2. A celulose, principal componente da madeira, e a quitina, que forma a carapaça externa dos artrópodes (como besouros e outros insetos, aracnídeos e crustáceos), são os polissacarídeos mais abundantes na natureza

De combustíveis a reguladores

Os carboidratos são os 'combustíveis da vida'. Eles armazenam a energia nos seres vivos, na forma de amido e glicogênio (outro polissacarídeo), e a liberam para as reações metabólicas quando são degradados (em especial a glicose). Atuam ainda como doadores de carbono para a síntese de outros constituintes das células. São os principais produtos da fotossíntese, processo em que a energia solar é transformada em energia química pelas plantas e depois transferida, através da cadeia alimentar, para os animais. Estima-se que sejam formados mais de 100 bilhões de toneladas de carboidratos na Terra, a cada ano, pela fotossíntese – nesse processo, as plantas captam a luz solar e usam sua energia para promover reações, envolvendo moléculas de gás carbônico (CO_2) e de água (H_2O), que produzem glicose, armazenada depois como amido nos tecidos vegetais.

Entretanto, os carboidratos não têm apenas função energética. Estão presentes também na superfície externa da membrana das células. Nesse caso, podem ser glicoproteínas (quando ligados a uma proteína), glicolipídios (se unidos a um lipídio) ou proteoglicanos (quando estão na forma de cadeias de glicosaminoglicanos – um tipo de polissacarídeo – unidas a uma proteína). Essas formas conjugadas presentes nas membranas atuam como receptores e sinalizadores, interagindo com moléculas e outras células.

A remoção de hemácias envelhecidas do sangue foi um dos primeiros eventos biológicos estudados que revelou a participação da estrutura dos carboidratos (em glicoproteínas) em um processo de 'sinalização'. Hemácias jovens têm, em sua superfície, glicoproteínas cuja extremidade é rica em ácido siálico. Quando tais células envelhecem, suas glicoproteínas perdem esse ácido e passam a expressar, em sua extremidade, a galactose. Esse monossacarídeo é reconhecido por receptores do fígado, que então capturam e removem da circulação as hemácias 'velhas'.

Os grupos sangüíneos A, B, O e AB são outro exemplo típico de um sistema de sinalização controlado pela estrutura de carboidratos em glicoproteínas. Os grupos A e B diferem em apenas um tipo de monossacarídeo nos glicolipídios ou glicoproteínas das hemácias. No A está presente a *N*-acetilgalactosamina (uma galactose ligada a grupos químicos amino e acetil) e o B tem a galactose – a diferença entre esses dois carboidratos está em apenas alguns átomos, mas isso pode levar a um resultado fatal, se o indivíduo receber o tipo sangüíneo incompatível em uma transfusão.

Os carboidratos encontrados nesses compostos mistos também funcionam como receptores na membrana celular. A ação de diversas toxinas de

plantas e bactérias (da cólera, da difteria, do tétano e do botulismo, entre outras) depende da interação com gangliosídios (glicolipídios ácidos) específicos de suas células-alvo. Por isso, estudos nessa área pretendem projetar agentes terapêuticos capazes de inibir essa interação, evitando os efeitos nocivos das toxinas.

Em 2005, o glicocientista Lior Horonchik e seus colaboradores, do Departamento de Biologia Molecular da Escola de Medicina de Jerusalém (em Israel), mostraram que a degeneração dos neurônios causada por infecção pelo príon (proteína responsável pelo chamado 'mal da vaca louca') depende da presença, na superfície das células nervosas, de receptores (proteoglicanos) que contêm glicosaminoglicanos. O príon precisa interagir com esses polissacarídeos para entrar no neurônio – isso significa que o papel deles no reconhecimento celular é fundamental para o desenvolvimento dessa infecção.

Algumas moléculas reguladoras da proliferação de tipos celulares – como o fator de crescimento para fibroblastos (FGF) e o fator de transformação do crescimento β (TGF-β) – também atuam interagindo com os carboidratos dos proteoglicanos. Essas informações permitem que os glicocientistas desenvolvam moléculas com o objetivo de regular esses processos biológicos.

Doenças relacionadas

O fato de que muitas doenças, genéticas ou adquiridas, decorrem de defeitos no metabolismo de carboidratos é outro forte estímulo para o estudo desses compostos. A galactosemia, por exemplo, é uma doença hereditária rara, caracterizada pela deficiência em enzimas que processam a galactose. Nos portadores, esse carboidrato, normalmente convertido em glicose, é acumulado na forma de galactose-fosfato, o que leva a retardo mental severo e, com freqüência, à morte. Recém-nascidos e crianças com galactosemia não podem ingerir substâncias com galactose, em particular o leite (a lactose, presente no leite, é um dissacarídeo formado por glicose e galactose).

Já a intolerância à lactose, também causada por deficiência enzimática, pode ter três origens: defeito genético raro na capacidade de sintetizar a lactase intestinal, redução da produção da enzima devido a doenças intestinais ou deficiência adquirida com o avanço da idade. Tanto na galactosemia quanto na intolerância à lactose, é essencial uma dieta livre de lactose. Outros exemplos de doenças ligadas a desordens no metabolismo dos carboidratos são as mucopolissacaridoses, como as síndromes

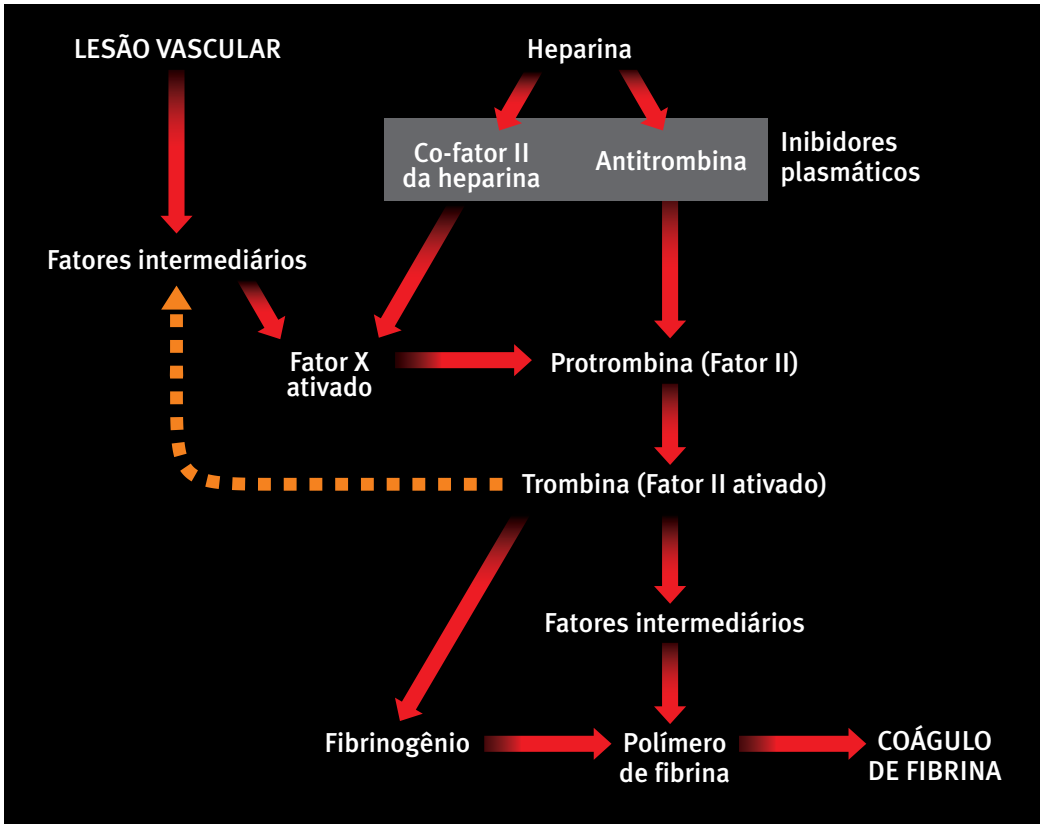

Figura 3. Esquema simplificado da coagulação sangüínea. Após a lesão vascular, são ativadas enzimas (fatores plasmáticos) que iniciam a 'cascata' de coagulação, até a ativação do fator X e do fator II (protrombina), responsáveis pela ativação da trombina, enzima que induzirá a transformação de fibrinogênio em fibrina (proteína filamentosa que forma os coágulos, interrompendo a perda de sangue). O controle da ação da trombina é essencial para regular a 'cascata', pois ela participa das etapas finais de formação do coágulo e também 'reforça' o processo ativando os fatores intermediários envolvidos. O co-fator II da heparina e a antitrombina inibem a ação da trombina e têm sua atuação acelerada pela heparina

de Hurler e de Hunter, que levam a retardo mental e à morte prematura.

A doença mais conhecida relacionada aos carboidratos é o diabetes, decorrente de fatores hereditários e ambientais, que levam a uma deficiência na produção ou a uma incapacidade de ação da insulina (hormônio cuja função principal é controlar a entrada de glicose nas células). Nos portadores, a quantidade de glicose no sangue aumenta, comprometendo vários órgãos e os sistemas renal, nervoso e circulatório. A doença pode ser regulada pelo consumo controlado de carboidratos e, em casos mais severos, pela administração de insulina.

Além do diabetes, uma dieta exagerada em carboidratos pode acarretar outros problemas, como obesidade, doenças cardiovasculares, tromboses e avanço da aterosclerose (depósito de substâncias nas paredes dos vasos sangüíneos, obstruindo a circulação). O excesso na ingestão desses compostos também intensifica a síntese e o armazenamento de gordura, além de desestimular os receptores de insulina nas células, gerando a forma mais grave do diabetes. Esse quadro piora com um estilo de vida sedentário, que reduz a metabolização dos glicídios. Em contrapartida, dietas com poucos carboidratos também podem prejudicar a saúde, já que eles são a fonte principal de energia para as células.

Uso industrial dos carboidratos

Além da importância biológica dos carboidratos, esses compostos são matérias-primas para indústrias importantes, como as de madeira, papel, fibras têxteis, produtos farmacêuticos e alimentícios. A celulose é o principal carboidrato industrial, com um consumo mundial estimado em quase 1 bilhão de toneladas por ano.

Alguns polissacarídeos, como ágar, pectinas e carragenanas, extraídos de algas marinhas, são utilizados – graças a suas propriedades gelatinosas – em cosméticos, remédios e alimentos. A carragenana é empregada para revestir cápsulas (drágeas) de medicamentos, para que o fármaco seja liberado apenas no intestino, aumentando a sua absorção. O ágar serve ainda para a cultura de microorganismos, em laboratórios. Tanto o ágar como a carragenana são também usados, como espessantes, na produção de sorvetes.

A sacarose (extraída da cana-de-açúcar) é o principal adoçante empregado na culinária e na indústria de doces. O açúcar 'invertido' (obtido pela 'quebra' da sacarose, que resulta em uma mistura de glicose e frutose) é menos cristalizável, mas muito usado na fabricação de balas e biscoitos. A quitosana, um polissacarídeo derivado da quitina, tem sido utilizada no tratamento da água (para absorver as gorduras), na alimentação e na saúde. Por sua atuação na redução da gordura e do colesterol, a quitosana pode ajudar no combate à obesidade, e estudos farmacológicos recentes comprovaram que ela apresenta efeitos antimicrobianos e antioxidantes.

Outro exemplo de polissacarídeo usado na indústria farmacêutica é o condroitim-sulfato, um tipo de glicosaminoglicano. Os colírios oftalmológicos, em sua maioria, são soluções de condroitim-sulfato, já que esse composto é o constituinte predominante da matriz extracelular do globo ocular e tem grande afinidade por água, o que permite melhor lubrificação. Também vem sendo utilizado na prevenção e tratamento da osteoartrose, talvez porque seja abundante em proteoglicanos do tecido cartilaginoso.

Benefícios e riscos da heparina

Os avanços no estudo das funções dos carboidratos ajudaram a entender doenças associadas a essas moléculas, a conhecer a ação farmacológica de alguns polissacarídeos e a desenvolver novos compostos desse tipo com ação terapêutica. Um bom exemplo é a heparina, um glicosaminoglicano com atuação anticoagulante e antitrombótica, hoje o segundo composto natural mais usado na medicina, perdendo apenas para a insulina. Sua utilização é freqüente por causa da incidência de doenças cardiovasculares. Estas, segundo a Organização Mundial de Saúde, são responsáveis por cerca de 30% das mortes em todo o mundo (mais de 16,5 milhões de pessoas em 2004). No Brasil, cerca de 70% das mortes estão associadas a essas doenças, índice similar ao dos países desenvolvidos.

A heparina tem uma potente atividade anticoagulante porque amplifica a ação de dois compostos presentes no plasma, antitrombina e co-fator II da heparina, capazes de inibir a ação da trombina (enzima que promove a coagulação) e do fator X ativado (proteína que acelera a formação da trombina) (figura 3). A heparina interage simultaneamente com esses compostos e com a trombina ou o fator X ativado. Essa interação ocorre principalmente entre as cargas negativas da heparina e as regiões positivas dos inibidores plasmáticos e da trombina. A formação desses complexos inibe a ação da trom-

bina, interrompendo o processo de coagulação do sangue.

O uso clínico desse glicosaminoglicano, no entanto, apresenta efeitos colaterais, como redução da quantidade de plaquetas (trombocitopenia) e propensão a hemorragias. Além disso, a dose necessária para obter o resultado adequado varia de paciente para paciente e a heparina precisa ser extraída de tecidos de mamíferos (como intestino de porco e pulmão bovino), onde ocorre em baixa concentração e ainda apresenta risco de contaminação por vírus e príons. Os efeitos indesejados desse composto, associados ao aumento da incidência de doenças tromboembólicas no mundo, motivam a pesquisa de novos agentes anticoagulantes e antitrombóticos.

Esperança nos ouriços-do-mar

Muitos compostos têm sido testados, em todo o mundo, em busca de novas drogas que evitem ou combatam a trombose. Em nosso laboratório, substâncias extraídas de ouriços-do-mar e de algumas espécies de algas marinhas revelaram-se fontes promissoras de moléculas anticoagulantes e antitrombóticas.

Nos ouriços-do-mar, os carboidratos que estudamos estão situados na superfície dos óvulos e participam do processo de fertilização. Quando o espermatozóide desses animais entra em contato com o gel que recobre os óvulos, polissacarídeos presentes nesse gel induzem, no espermatozóide, a chamada reação acrossômica. Nessa reação são liberadas enzimas que 'dissolvem' o gel, facilitando a penetração do espermatozóide, e uma proteína deste, a actina, é polimerizada, formando filamentos que ajudam a expor outra proteína, a bindina, em sua superfície. A bindina liga-se ao seu receptor na superfície do óvulo, desencadeando a fusão das membranas dos dois gametas, a liberação do material genético do espermatozóide dentro do óvulo e a fusão dos dois núcleos, formando o zigoto, que dará origem ao embrião.

Dois mecanismos diferentes são fundamentais para que gametas da mesma espécie de ouriço-do-mar se reconheçam (figura 4). Um é baseado na especificidade da proteína bindina (reconhecimento com base na bindina), e o outro depende da indução da reação acrossômica pelo polissacarídeo que recobre o gel do óvulo (reconhecimento com base no carboidrato). Se a reação acrossômica não é induzida, a bindina não é exposta e, portanto, não há fertilização. Esse último mecanismo foi descrito em nosso laboratório, e demonstramos principalmente que cada espécie de ouriço-do-mar tem um polissacarídeo de estrutura particular recobrindo seu óvulo.

As análises desses polissacarídeos revelaram que são polímeros constituídos exclusivamente por monossacarídeos de fucose ou galactose. Esses compostos têm ainda, ligados à estrutura básica de carboidrato (CH_2O), grupamentos sulfatos idênticos aos encontrados nos glicosaminoglicanos, que conferem carga negativa ao polímero. Por isso, são conhecidos como fucanas sulfatadas e galactanas sulfatadas. Outra observação curiosa é que esses compostos exibem grande variedade estrutural, em função do tipo de ligação entre os monossacarídeos e do padrão de sulfatação.

O reconhecimento de moléculas específicas de cada espécie de ouriço-do-mar, durante a fertilização, tem grande importância biológica, pois várias espécies podem conviver no mesmo ambiente e seus gametas são liberados na água do mar, onde ocorre a fertilização. Esse reconhecimento, portanto, impede a formação de híbridos.

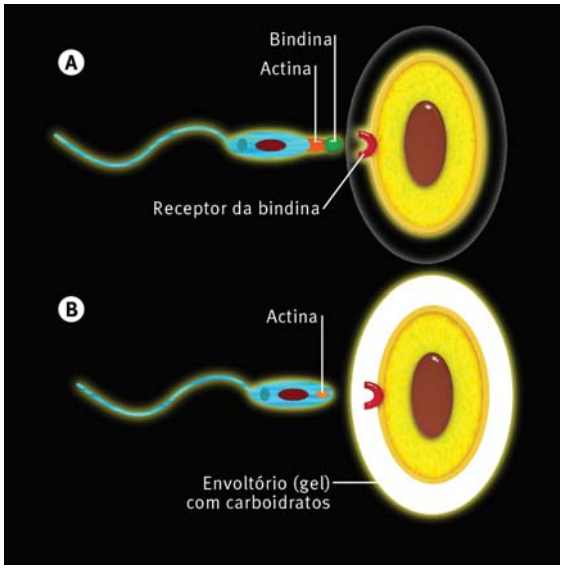

Figura 4. Mecanismos de reconhecimento entre espermatozóide e óvulo em ouriços-do-mar. Em A, reconhecimento baseado na estrutura, distinta em cada espécie, da proteína bindina – na reação acrossômica, ocorre a 'dissolução' do envoltório gelatinoso do óvulo e a actina (em laranja) é polimerizada no espermatozóide. Após esses eventos, a bindina (em verde) é exposta, podendo ligar-se ao receptor de membrana (em vermelho) do óvulo da mesma espécie. Em B, reconhecimento baseado na estrutura, distinta em cada espécie, do carboidrato – para que a reação acrossômica ocorra, o espermatozóide deve ser reconhecido pelos polissacarídeos sulfatados presentes no envoltório gelatinoso (em branco) do óvulo da mesma espécie

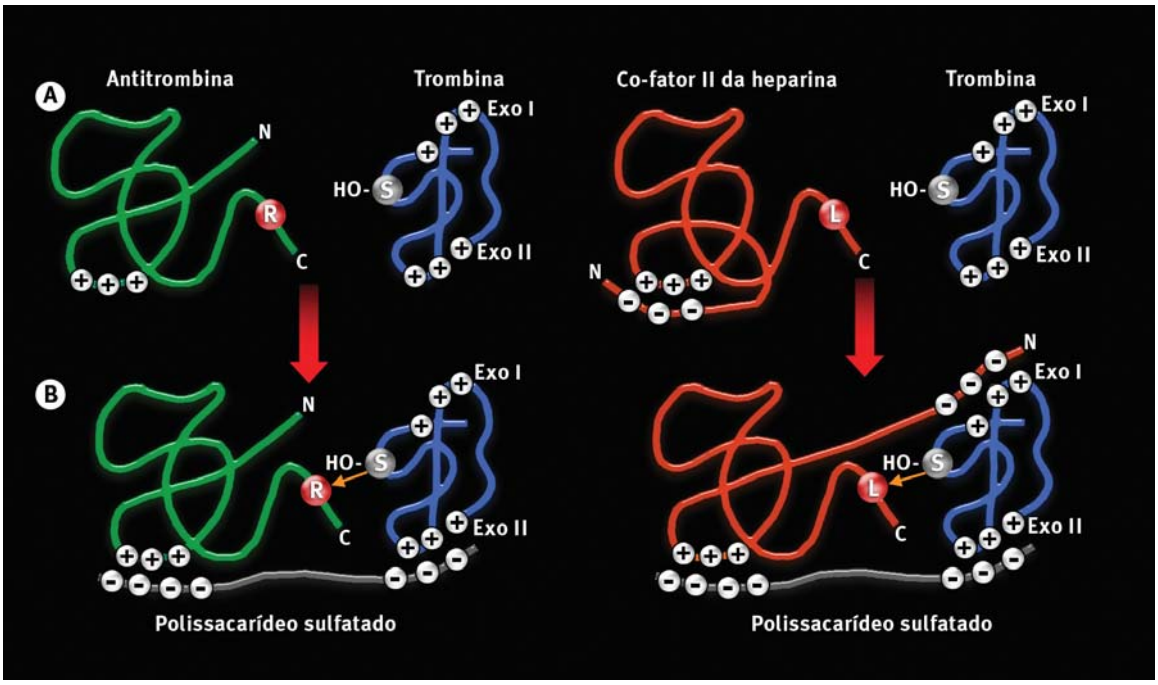

Figura 5. Representação molecular da ação anticoagulante dos polissacarídeos sulfatados. A trombina (em azul) é inibida pela ação da antitrombina (em verde) e do co-fator II da heparina (em laranja). Em ambos os casos, o polissacarídeo sulfatado (em cinza) aproxima o inibidor e a trombina, através da interação de suas cargas negativas com as cargas positivas dessas moléculas (na trombina, a interação ocorre no sítio denominado EXO II). Em seguida, o grupo hidroxila (-OH) do aminoácido serina (S), presente na trombina, liga-se a aminoácidos situados na extremidade 'C' dos inibidores – a arginina (R), na antitrombina, e a lisina (L), no co-fator II de heparina. No entanto, o polissacarídeo sulfatado altera o mecanismo anticoagulante do co-fator II da heparina, induzindo nesse inibidor uma modificação estrutural que permite a interação de sua extremidade 'N' com o sítio EXO I da trombina

Nossos estudos com fucanas e galactanas sulfatadas, de ouriços-do-mar e de algas marinhas, demonstraram que sua ação anticoagulante é similar à da heparina – elas também amplificam a inibição da antitrombina e do co-fator II da heparina sobre a trombina. Ao contrário da heparina, obtida de mamífero, essas fucanas e galactanas (sulfatadas) apresentam menores riscos de contaminação por partículas virais e príons nocivos ao homem, já que são isoladas de organismos marinhos.

A estrutura química dos polissacarídeos sulfatados de ouriços-do-mar, como as análises revelaram, é mais simples que a dos compostos obtidos de algas marinhas e que a da heparina. Isso permitiu estabelecer uma relação entre as estruturas químicas das fucanas sulfatadas e galactanas sulfatadas de invertebrados marinhos e sua ação anticoagulante (figura 5). Os testes desses compostos em diferentes modelos de trombose em animais experimentais mostraram uma potente atividade preventiva contra a trombose, tanto venosa quanto arterial. Portanto, esses novos polissacarídeos sulfatados podem ajudar no desenho estrutural de novas drogas com ações específicas sobre cada tipo de trombose e com poucos efeitos adversos.

Resultados recentes indicaram outras ações terapêuticas – anticâncer, antiviral e antiinflamatória – das fucanas sulfatadas de organismos marinhos. No entanto, ainda não foram elucidados os mecanismos de ação desses polissacarídeos nessas outras ações biológicas, assim como a influência de suas características estruturais.

A contribuição da glicobiologia

Em síntese, o estudo dos carboidratos e glicoconjugados é vasto dentro da biociência. Inúmeras funções podem ser desempenhadas por essas macromoléculas, em nível molecular, celular, tecidual ou fisiológico e até na produção industrial. Sem dúvida, as descobertas recentes com o estudo de carboidratos contribuíram para a compreensão de inúmeros eventos biológicos e para a obtenção de novos compostos com ações terapêuticas em diversas patologias. Assim como as demais áreas da pesquisa bioquímica, a glicobiologia ainda pode colaborar muito para ajudar a desvendar os processos biológicos da natureza. ■

SUGESTÕES PARA LEITURA

LEHNINGER, A. L.; NELSON, D. & COX, M. M. *Princípios de bioquímica.* São Paulo, Sarvier, 2002.

MOURÃO, P. A. S. 'Use of sulfated fucans as anticoagulant and antithrombotic agents: future perspectives', in *Current Pharmaceutical Design, v.* 10 (9), p. 967, 2004.

VOET, D.; VOET, J. G. & PRATT, C. *Fundamentos de bioquímica.* Porto Alegre, Artmed, 2000.

ANEXO II

Clinica Chimica Acta
Vol. 383, pp 116-125, 2007

"The renal clearance of dextran sulfate decreases in puromycin aminonucleoside-induced glomerulosclerosis: A puzzle observation."

Ana-Maria R. dos Santos, Vitor H. Pomin, Mariana P. Stelling, Marco A.M. Guimarães, Lucio R. Cardoso e Paulo A.S. Mourão.

Available online at www.sciencedirect.com
ScienceDirect
Clinica Chimica Acta 383 (2007) 116–125
www.elsevier.com/locate/clinchim

The renal clearance of dextran sulfate decreases in puromycin aminonucleoside-induced glomerulosclerosis: A puzzle observation

Ana M.R. Santos [a,c], Vitor H. Pomin [a,c], Mariana P. Stelling [a,c], Marco A.M. Guimarães [d], Lucio R. Cardoso [b], Paulo A.S. Mourão [a,c,*]

[a] *Laboratório de Tecido Conjuntivo, Hospital Universitário Clementino Fraga Filho, Universidade Federal do Rio de Janeiro, Caixa Postal 68041, Rio de Janeiro, RJ, 21941-590, Brazil*
[b] *Serviço de Nefrologia, Hospital Universitário Clementino Fraga Filho, Universidade Federal do Rio de Janeiro, Rio de Janeiro, RJ, Brazil*
[c] *Programa de Glicobiologia, Instituto de Bioquímica Médica, Universidade Federal do Rio de Janeiro, Rio de Janeiro, RJ, Brazil*
[d] *Departamento de Patologia e Laboratórios, Universidade do Estado do Rio de Janeiro, Rio de Janeiro, RJ, Brazil*

Received 22 November 2006; received in revised form 8 May 2007; accepted 9 May 2007
Available online 26 May 2007

Abstract

Background: Puromycin aminonucleoside-induced nephrosis is characterized by increased renal excretion of plasma proteins. We employed this experimental model to study the urinary clearance of dextran sulfate.
Methods: The dextran sulfate eliminated by the urine was determined using a metachromatic assay. Polysaccharide fragments were analyzed by chromatographic and electrophoretic procedures. Disaccharide composition of the glomerular heparan sulfate was assessed using digestion with specific lyases.
Results: In normal rats dextran sulfate is partially degraded to lower molecular weight fragments and only then eliminated by the urine. Surprisingly, in puromycin aminonucleoside-induced glomerulosclerosis the molecular size of the fragments of dextran sulfate found in the urine is the same or even lower than in control animals in spite of the marked proteinuria. Furthermore, urinary excretion of dextran sulfate decreases in the experimentally induced nephrosis. This observation cannot be totally attributed to a reduced number of physiologically active nephrons since the glomerular filtration rate decreases ~32% after puromycin aminonucleoside administration while the urinary excretion of 8 kDa-dextran sulfate decreases 3-fold. The glomerular heparan sulfate shows reduced sulfation when compared with normal animals. Possibly puromycin aminonucleoside decreases the activity of kidney endoglycosidases, which reduce the molecular size of the sulfated polysaccharide, leading to a decrease in its renal clearance. Reduced sulfation of the glomerular heparan sulfate in the puromycin aminonucleoside-induced nephrosis does not alter the size of the dextran sulfate eliminated by the kidney, as suggested for protein.
Conclusions: Each pathological process induces a particular modification in the kidney, which in turn can affect the renal selectivity to specific macromolecules in different ways.
© 2007 Elsevier B.V. All rights reserved.

Keywords: Sulfated polysaccharide; Heparan sulfate; Renal selectivity to macromolecules; Glomerular heparin sulfate

1. Introduction

The kidney glomerular membrane is considered a classical example of a biological barrier selective to the size and charge of macromolecules [1,2]. However, glomerular selectivity is altered in several diseases such as diabetes [3], chronic renal failure [4], focal and/or segmental glomerulosclerosis and in minimal change nephrotic syndrome [5]. All these pathological conditions are characterized by a marked increase in the urinary excretion of macromolecules (mostly albumin and other plasma proteins).

Different experimental models can mimic, in animals, conditions similar to those observed in human renal diseases. One of these models is the puromycin aminonucleoside-induced nephrosis. Depending on the dose of puromycin aminonucleoside used and the time of exposure to the drug, it is possible to observe

* Corresponding author. Programa de Glicobiologia, Instituto de Bioquímica Médica, Universidade Federal do Rio de Janeiro, Caixa Postal 68041, Rio de Janeiro, RJ, 21941-590, Brazil. Tel./fax: +55 21 2562 2090.
E-mail address: pmourao@hucff.ufrj.br (P.A.S. Mourão).

0009-8981/$ - see front matter © 2007 Elsevier B.V. All rights reserved.
doi:10.1016/j.cca.2007.05.013

Author's personal copy

either a minimal change nephrotic syndrome or a focal and segmental glomerulosclerosis. This glomerulosclerosis is characterized by podocyte lesion, mesangial expansion, endothelial swelling obliterating the capillary lumen and increased glomerular volume [6]. Puromycin aminonucleoside-induced nephrosis is also characterized by an increased renal excretion of plasma protein, as observed in human diseases, therefore widely used to evaluate glomerular selectivity to macromolecules. The increased renal excretion of plasma protein in puromycin aminonucleoside-induced nephrosis is a consequence of a change in the selectivity of the glomerular basement membrane to macromolecules [7–9].

However, recent studies have questioned the classic concept concerning the size and charge selectivity of the glomerular barrier to macromolecules. Conventional studies, based mainly on micropuncture, pointed to a small value of the sieving coefficient for albumin [10], which is one or two orders of magnitude lower than the sieving coefficient for an uncharged Ficoll of equivalent size. Although this difference could be explained by the influence of the charge selective glomerular barrier [11,12], a recent view is that the sieving coefficient for Ficoll and albumin is the same but large amounts of filtered albumin are retrieved intact by the tubule [13]. This mechanism avoids the elimination of albumin by the urine under physiological conditions.

In contrast with these observations, other authors concluded that the high sieving coefficient for albumin, as proposed by the retrieval hypothesis, cannot be reconciled with the direct experimental estimations based on *in vivo* micropuncture. This discrepancy, combined with the consistency of micropuncture data from several laboratories, supports the conventional view that normal glomerular capillary maintains extremely low values of the sieving coefficient for albumin [14]. In a further development, the authors of the retrieval hypothesis proposed that albumin, filtered by the kidney, is modified by lysosomal enzymes. As a result of this process, albumin is excreted mostly as fragments of < 10 kDa [15–17]. In several renal diseases, the activity of these enzymes could be altered and contribute for the increased renal excretion of protein [16,18].

In addition to albumin, several authors have also studied the renal excretion of dextran sulfate under normal and pathological conditions. Dextran sulfate is a highly negatively charged polysaccharide obtained by chemical sulfation of neutral, natural dextran. It has been frequently used to evaluate glomerular filtration [1,2]. Dextran sulfate is not reabsorbed by post glomerular tubules. Therefore, its clearance reflects an event which occurs exclusively at the glomerular level [15]. It has been proposed that dextran sulfate undergoes endothelial cell-mediated uptake, followed by desulfation but not depolymerization by lysosomal enzymes and then exocytosis [19–23].

Renal excretion of dextran sulfate has also been studied in pathological conditions. Diabetic and hypertensive states led to a reduced desulfation of dextran sulfate by lysosomal enzymes [24,25]. Furthermore, a reduced clearance of dextran sulfate in diabetic rats has been observed while the fractional clearance of neutral dextran was not affected when compared with control animals [15,26].

We have now investigated the renal filtration of dextran sulfates with different molecular sizes by normal rats and by animals with puromycin aminonucleoside-induced nephrosis. This polysaccharide fulfills several requirements for an appropriate compound for studies concerning renal selectivity to macromolecules. First, dextran sulfate is not re-absorbed by post glomerular tubules and its clearance is an event which occurs exclusively at the level of glomerular filtration [15]. Second, this polysaccharide is easily detected in the urine based on a simple assay and its molecular size and charge density can be estimated with standard electrophoretic and chromatographic procedures. Third, we already observed that renal filtration of dextran sulfate by normal rats has a well-defined molecular size cut-off [27]. Finally, commercially available dextran sulfate is composed of a mixture of oligosaccharides with well-defined molecular masses, which are appropriate to determine size selectivity of renal filtration under normal and pathological conditions. Surprisingly, we observed that renal selectivity to dextran sulfate is not markedly modified in the puromycin aminonucleoside-induced glomerulosclerosis. In fact, the urinary excretion of dextran sulfate decreases in experimental nephrosis. These observations raise interesting questions concerning the renal filtration of macromolecules, as will be discussed.

2. Materials and methods

2.1. Puromycin aminonucleoside-induced glomerulosclerosis in rats

Segmental and focal glomerulosclerosis was induced in rats by subcutaneous administration of puromycin aminonucleoside, as described [5]. We followed the institutional guidelines for animal care and experimentation. The animals were divided into two groups, 12 animals each. One group received 7 subcutaneous doses of 20 mg/kg body weight of puromycin aminonucleoside (3′-amino-3′-deoxy-*N*,*N*-dimethyl-adenosine, from Sigma), dissolved in saline, on the first, 7th, 14th, 28th, 42nd, 56th and 90th days. Another group received control saline. The animals were fed standard laboratory chow and drinking water *ad libitum*. Body weight was measured weekly. At days 29, 59 and 89, the rats were transferred to metabolic cages in order to collect 24-h urine samples. Urine was collected in flasks containing crystals of thymol and stored at −5 °C until analysis. At the 90th day, blood was collected by heart puncture and the plasma separated by centrifugation. Thereafter, the animals were sacrificed, the kidneys carefully removed and used for the extraction of glycosaminoglycans (see below).

2.2. Administration of dextran sulfate

We employed dextran sulfates with modal molecular masses of 8 or 50 kDa (Sigma). Both preparations of dextran sulfate are highly sulfated polysaccharides. The manufacture indicates 2.3 sulfate esters/glucose unit. This was confirmed by chemical analysis performed in our laboratory, which showed 2.5 sulfate esters/glucose units [28,29]. For some experiments dextran sulfates with high (fraction F5) and low molecular size (fractions F1–F3) were prepared by gel filtration chromatography on Bio-Gel P10 (see below). The various preparations of dextran sulfates were dissolved in saline and injected at a dose of 10 mg/kg body weight into the tail vein of puromycin aminonucleoside-treated rats and of saline control animals at the 30th, 60th and 90th days after the start of the experimental protocol, described in the preceding item. The animals were then put in metabolic cages immediately after the administration of dextran sulfate or saline in order to collect 24-h urine samples.

2.3. Quantification of dextran sulfate in urine

Dextran sulfate content in urine was determined using 1,9-dimethylmethylene blue [30]. Briefly, the dye solution was prepared by dissolving 16 mg of 1,9-dimethylmethylene blue, 3.04 g of glycine, 2.37 g of sodium chloride and 0.5 ml of 0.1 mol/l hydrochloride acid in 1 l of distilled water. The pH of the solution

Author's personal copy

was adjusted to 3. For each assay, appropriated volumes of urine (10–100 μl) were mixed with 1.0 ml of the dye solution at room temperature, and absorbance was immediately measured at 525 nm. Standard curves were prepared for each sulfated polysaccharide. The two preparations of dextran sulfates used in this study have a similar sensitivity to 1,9-dimethylmethylene blue.

2.4. Polyacrylamide gel electrophoresis (PAGE)

The molecular masses of dextran sulfate were estimated by PAGE [31]. Appropriate volumes of urine (1–10 μl) and of standard dextran sulfate (~5 μg) were applied to a 1-mm-thick 6% polyacrylamide slab gel and after electrophoresis (100 V for ~1 h in 0.06 mol/l sodium barbital buffer), the gel was stained with 0.1% toluidine blue in 1% acetic acid. After staining, the gel was washed in 1% acetic acid for 24 h and quantified by densitometry with a model GS-690 imaging densitometer (Bio-Rad laboratories).

2.5. Gel-filtration chromatography of dextran sulfate

For analysis on gel filtration the urine samples were previously incubated with papain in order to reduce the concentration of protein. In these experiments, 2.5 ml of the urine sample were mixed with the same volume of 0.1 mol/l sodium acetate solution (pH 6.0), containing 5 mM EDTA, 5 mM cysteine and 0.5 mg papain. After incubation for 12 h at 60 °C, the mixture was lyophilized and dissolved in 5 ml of 1.0 mol/l NaCl. This solution of dextran sulfate obtained from rat urine or the standard dextran sulfate with a modal molecular mass of 8 kDa (5 mg of each) was fractionated on a Bio-Gel P10 (Bio-Rad Laboratories, Hercules, CA) column (200×0.9 cm), equilibrated with aqueous 10% ethanol, containing 1.0 mol/l NaCl, as described previously [32]. The fractions (1 ml) were eluted with the same solution at a flow rate of ~3 ml/h and assayed by their metachromatic property using 1,9-dimethylmethylene blue [30], by the phenol-sulfuric acid reaction for total hexose [33] and by the carbazole reaction for hexuronic acid [34].

2.6. Anion-exchange chromatography of dextran sulfate

A similar solution of urinary dextran sulfate, obtained after incubation with papain (see above), was used for anion-exchange chromatography. However, for this experiment, the dextran sulfate was submitted to a further step of purification, which involves ethanol precipitation. The solution of dextran sulfate obtained after incubation with papain was mixed with 2 vol of ethanol, maintained at 4 °C for 24 h, the precipitate was collected by centrifugation and dried at 60 °C overnight. This sample was dissolved in 10 ml of sodium acetate (pH 6.0) and applied to a DEAE-cellulose column (25 ml bed volume), equilibrated with the same solution. The column was developed by a gradient of 0 → 2.0 mol/l NaCl. The flow rate of the column was 0.5 ml/min, fractions of 0.5 ml were collected and assayed for sulfated polysaccharide using the metachromatic assay with 1,9-dimethylmethylene blue [30], by the phenol-sulfuric acid reaction for total hexose [33] and by the carbazole reaction for hexuronic acid [34]. The range of NaCl concentrations used to develop the column does not interfere in the metachromatic assay. The fractions were pooled, mixed with 3 vol of methanol and after standing for 24 h at 4 °C, the precipitate formed was collected by centrifugation, washed twice with 80% ethanol and dried at room temperature.

2.7. Isolation of sulfated polysaccharide from the renal glomerulous

A glomerulous preparation was obtained from the kidney after the organ was macerated and sieved with a 0.15 mol/l NaCl solution. This preparation was submitted to consecutive extractions with 10 vol of acetone and of a mixture of methanol:chloroform (1:1,v/v). The final insoluble material was dried at room temperature and the glycosaminoglycans were extracted by papain digestion, as described above for the urine sample. The solution of glomerular glycosaminoglycans was then incubated with DNAse (5 mg/ml in phosphate buffered saline at 37 °C for 12 h), in order to remove contaminant nucleic acid. Finally, a 10% cetylpyridinium chloride solution was added to the clear supernatant of the DNAse incubation to a final concentration of 0.5%. After 24 h at room temperature the solution was centrifuged, the pellet was washed with 0.05% cetylpyridinium chloride and dissolved in 2 mol/l NaCl/absolute ethanol (100:15, v/v). The polysaccharides were precipitated with the addition of 2 vol of ethanol, washed 2 times with a solution of 80% ethanol and finally with absolute ethanol. After centrifugation the supernatant was discarded, the precipitated polysaccharides were dried under vacuum and dissolved in distilled water.

2.8. Disaccharide composition of the glomerular heparan sulfate

The disaccharide composition of the glomerular heparan sulfate was determined as previously described [35]. In these experiments, heparan sulfate (~100 μg) was exhaustively digested with three additions of a mixture of heparin lyase (EC 4.2.2.7) and heparan sulfate lyase (EC 4.2.2.8), both from *Flavobacterium heparinum* (Seikagku American Inc., Rockville, MD) (1 mU of each) in 100 μl of 100 mmol/l sodium acetate and 10 mM calcium acetate (pH 7.0), over a 36 h-period at 37 °C. The solution was then applied to a Superdex peptide column (from Amersham Biotech) linked to a HPLC system from Shimadzu (Japan) and the fractions corresponding to disaccharides, as indicated by the UV absorbance at 232 nm, were pooled and freeze dried. The lyase derived disaccharides and standard compounds were then subjected to a SAX-HPLC analytical column (250×4.6 mm from Sigma), as follows: after equilibration in the mobile phase (distilled water adjusted to pH 3.5 with HCl) at 0.5 ml/min, samples were injected and disaccharides eluted with a linear gradient of NaCl, from 0 to 1.5 mol/l over 45 min in the same mobile phase. Fractions of 0.5 ml were collected and monitored for UV absorbance at 232 nm. Disaccharides were identified by comparison with the elution positions of known disaccharide standards.

2.9. Other methods

Protein in the urine was determined by the sulfosalicylic method [36]. Creatinine in rat plasma and urine was determined using the picric acid based assay with a commercial kit from Merckognost Harnsteinanalyse, Merck. Glomerular filtration rate (GFR) was determined based on the clearance of creatinine using the formula

$$\mathrm{GFR} = \frac{C_U \times V_U}{C_P} \times \frac{1}{144} \times \frac{1}{100\mathrm{mg\ body\ weight}}$$

where C_U and C_P represent the urine and plasma concentrations of creatinine (both as mg/dL) and V_U the urinary volume (as ml) in a 24 h-period.

2.10. Statistical analysis

Data were expressed as mean±SD. One-way analysis of variance was used to compare the means and the Duncan test was used to analyze parametric data. Statistical significance was considered when $p < 0.05$.

3. Results

3.1. Rats with puromycin aminonucleoside-induced nephrosis show an intense proteinuria

Rats receiving subcutaneous doses of 20 mg/kg body weight of puromycin aminonucleoside developed an intense proteinuria (Fig. 1A) and a ~32% decrease in their glomerular filtration rates (Fig. 1B) after 7 doses of puromycin aminonucleoside over a period of 90 days. The kidney weight of rats receiving puromycin aminonucleoside increased significantly (Fig. 1C) compared to control, saline-treated animals, while the increase in body weight is less evident (Fig. 1D). Histological analysis of the kidneys after puromycin aminonucleoside administration showed podocyte lesions, mesangial expansion,

Author's personal copy

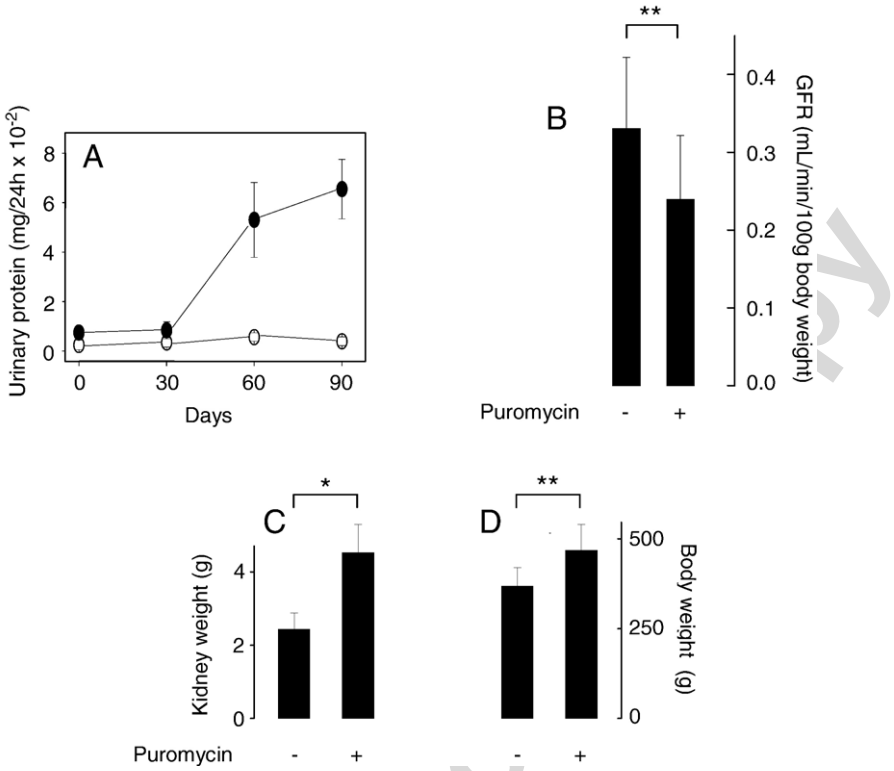

Fig. 1. Effects of puromycin aminonucleoside administration to rats on urinary protein excretion (A), glomerular filtration rates (GFR) (B) and on kidney (C) and body weights (D) compared to control animals. Panel A shows temporal curves of urinary elimination of proteins in the course of either puromycin aminonucleoside (●) or saline (○) administration by subcutaneous route. Panels B–D show changes in the GFR (B) and on kidney (C) and body (D) weights after 90 days of the protocol of puromycin aminonucleoside administration (+) compared with control animals receiving saline (−). Values are expressed as mean±SEM, $n=12$. * and ** indicate significant differences of $p<0.005$ and $p<0.05$, respectively, based on the Kruskal–Wallis test.

endothelial swelling, obliteration of the capillary lumen, and increased glomerular volume (focal glomerular sclerosis — data not shown).

3.2. Dextran sulfate itself does not induce proteinuria or modification of renal function

Rats receiving intravascular doses of 10 mg/kg body weight of either 8 or 50 kDa-dextran sulfate did not develop proteinuria (Fig. 2A), their glomerular filtration rates were not altered significantly (Fig. 2B) and no modification occurred in their kidney weights (Fig. 2C) when compared to control animals. Curiously, dextran sulfate with an average molecular mass of 50 kDa showed a slight protective effect on the puromycin aminonucleoside-induced proteinuria when compared to the 8 kDa-dextran sulfate (open squares in Fig. 2A). No modification of body weight was observed in any experimental condition (Fig. 2D).

3.3. Renal clearance of dextran sulfate decreases in puromycin aminonucleoside-treated rats

Once having established an experimental model of nephrotic syndrome in rats, characterized by an intense proteinuria (Fig. 1) and shown that dextran sulfate itself is not toxic to the kidney (Fig. 2), we then proceeded to compare the elimination of the sulfated polysaccharide by the kidneys of normal and puromycin aminonucleoside-treated animals. Two types of dextran sulfates were administered to the rats intravascularly. Approximately 60% of the total amount of dextran sulfate with a modal molecular size of 8 kDa was eliminated by the urine of normal, control animals, in a 24 h-period whereas only minor amounts (< 10%) of dextran sulfate with a modal molecular size of 50 kDa were found in the urine in the same period of time (Fig. 3A). These observations clearly indicate that renal selective filtration of dextran sulfate is based on the molecular size of the polymer.

Unexpectedly, as the nephrotic syndrome proceeded, no significant increase in the renal excretion of dextran sulfate with a modal molecular size of 50 kDa was observed (closed squares in Fig. 3). But, even more surprising, the renal elimination of dextran sulfate with a modal molecular size of 8 kDa decreased to ~25% of the total amount administered to the animals in the 60th day of puromycin aminonucleoside administration and then showed a slight increase in the 90th day but without recovering the same level of renal excretion observed in normal animals (Fig. 3A). Even when the excretion of 8 kDa-dextran sulfate was referred to the urine levels of creatinine (Fig. 3B) we still observe a marked decreased in the polysaccharide clearance.

3.4. The size of the dextran sulfates eliminated to the urine is not markedly modified in puromycin aminonucleoside-induced nephrosis

Dextran sulfate with a modal molecular mass of 8 kDa is in fact a mixture of chains with different molecular sizes, as can be

Author's perso

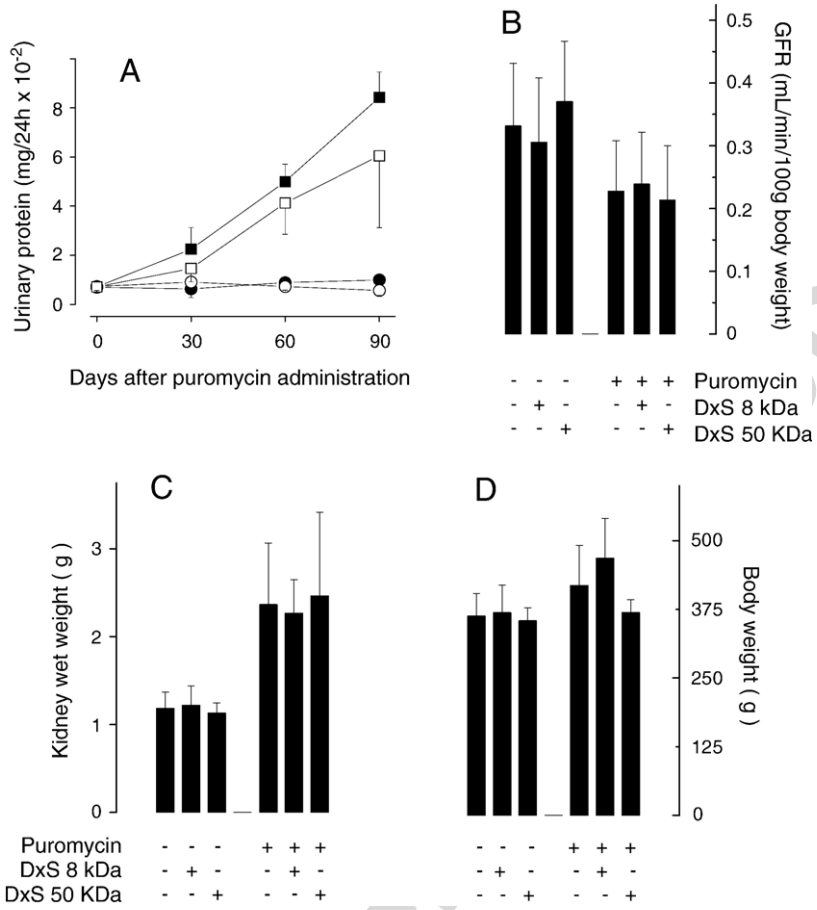

Fig. 2. Effects of dextran sulfate (DxS) alone or combined with puromycin aminonucleoside on urinary protein excretion (A), glomerular filtration rates (GFR) (B) and on kidney (C) and body (D) weights, compared with control animals receiving saline. Panel A shows temporal curves of urinary elimination of proteins in the course of administration of dextran sulfates with either an modal molecular mass of 8 kDa (●,■) or 50 kDa (○,□), alone (●,○) or combined with puromycin aminonucleoside (■,□). Panels B–C show changes in the GFR (B) and on kidney (C) and body (D) weights after 90 days of the protocol of puromycin aminonucleoside and/or dextran sulfate administration.

seen by gel filtration chromatography (Fig. 4A). Clearly, well-defined fractions (retained in the column more than the bulk of the dextran sulfate) were obtained by gel filtration on Bio-Gel P-10. These fractions, denominated as F1 to F4 in Fig. 4A, denote more homogeneous molecular sizes. In contrast, fractions less retained on the column, eluted between 60 and 105 ml (F5 in Fig. 4A), showed a wide-dispersion, denoting a mixture of chains with a variety of molecular sizes.

This mixture of dextran sulfate is appropriate to evaluate molecular size dependent filtration of sulfated polysaccharide by the kidney. In fact, when we analyzed the rat urine after intravenous administration of dextran sulfate with modal molecular mass of 8kDa, we found exclusively fractions F1, F2 and F3 (Fig. 4B).[1] Therefore, the kidney showed a permselectivity to dextran sulfate and only the molecules with lower molecular size were filtrated. No oligosaccharides were identified by the phenol-sulfuric acid reaction (for hexose) besides those already shown in the panels of Fig. 4, excluding the existence of possible desulfated oligosaccharides not assayed because of the absence of metachromatic property.

When similar experiments were performed in rats with puromycin aminonucleoside-induced nephrosis, again only fractions with low molecular masses were found in the urine (Fig. 4C). No increase (or even a decrease) in the size of fragments of dextran sulfate eliminated to the urine was observed.

When a mixture of fractions F1–F3 was administered to the rats we observed that dextran sulfate was totally eliminated to the urine. Instead, when dextran sulfate with higher molecular size (fraction F5) was used, we observed that only ~60% is found in the urine but with a reduced molecular size, almost similar to fractions F1–F3, as revealed by PAGE. It was not possible to analyze the oligosaccharides found in the urine by gel chromatography due to scarce material.

Glycosaminoglycans normally found in the urine, with an average molecular size of 10kDa, were eluted from the Bio-Gel P-10 column as the high molecular weight components of

[1] It is not possible to estimate the molecular masses of the oligosaccharides in Fig. 4 due to the absence of appropriated standards. We cannot calibrate the column using neutral dextrans or mammalian glycosaminoglycans as standards because the elution of polysaccharides on gel chromatography also depends on the structure of the sugar units. We attempted to determine the molecular mass of the dextran sulfate oligosaccharides found in the urine using mass spectrometry. Unfortunately we were not successful possibly due to the high molecular size and complex structure of these oligosaccharides.

Author's personal copy

dextran sulfate, as indicated by the hexuronic acid positive fractions in Fig. 4B and C (open circles). This observation indicates that the renal permselectivity to sulfated polysaccharides also depends on the chemical structure of these polymers since glycosaminoglycan chains with significantly higher molecular sizes than dextran sulfate were found in the urine, as shown previously [27].

3.5. The charge density of the dextran sulfate is not modified during its renal elimination

A further aspect that remains to be clarified is whether dextran sulfate is significantly desulfated during its renal elimination. Chemical determination of the sulfate content of dextran sulfate is not a simple procedure, especially in samples obtained with low amounts from the urine. As an alternative approach we used anion-exchange chromatography on DEAE-cellulose in order to evaluate the charge density of dextran sulfate. As already reported for the size of its chains, 8kDa-dextran sulfate also showed heterogeneity of its charge density. Two fractions were obtained on an anion exchange chromatography (P1 and P2 in Fig. 5A).[2] On PAGE these two components showed only slight difference in their mobility (Fig. 6), suggesting that in fact they differ mostly in their charge density. However, chemical analyses of these two fractions did not show difference in their sulfate contents (not shown). It may be that their differences in sulfate content cannot be distinguished by the chemical methods used. We cannot exclude that minor structural features, such as branching

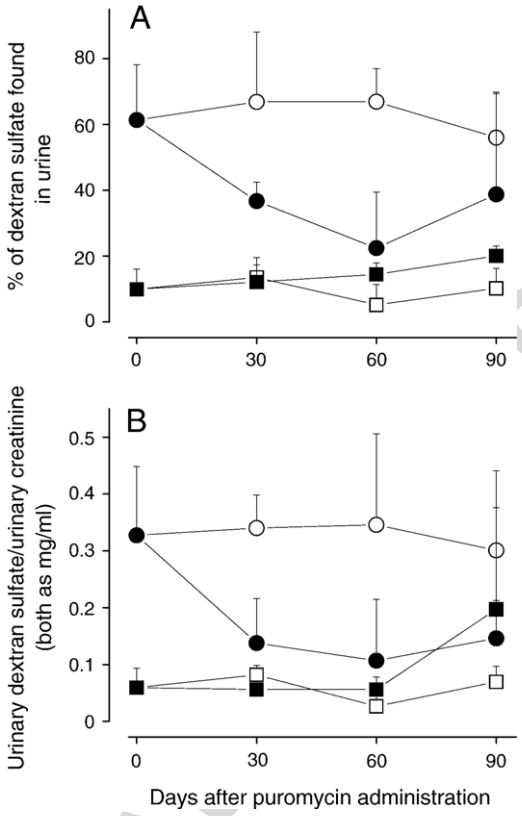

Fig. 3. Urinary excretion of dextran sulfates in the course of a nephrosis induced by puromycin aminonucleoside. Dextran sulfates with modal molecular masses of 8 kDa (●,○) and 50 kDa (■,□) were administered to saline-(○,□) or puromycin aminonucleoside-treated (●,■) rats by intravascular route, before and after nephrosis induced by puromycin aminonucleoside. 24-urine samples were collected and the dextran sulfate concentration was estimated based on standard curves obtained by a metachromatic assay using 1,9-dimethylmethylene blue. The results (mean±SEM, $n=12$) are expressed as percentage of dextran sulfate found in the urine compared with the total dose administered to the rat (*A*) or as concentration of dextran sulfate referred to urinary creatinine, both as mg/ml (B). For clarity only one SEM bar is presented. Values are expressed as mean±SEM, $n=12$.

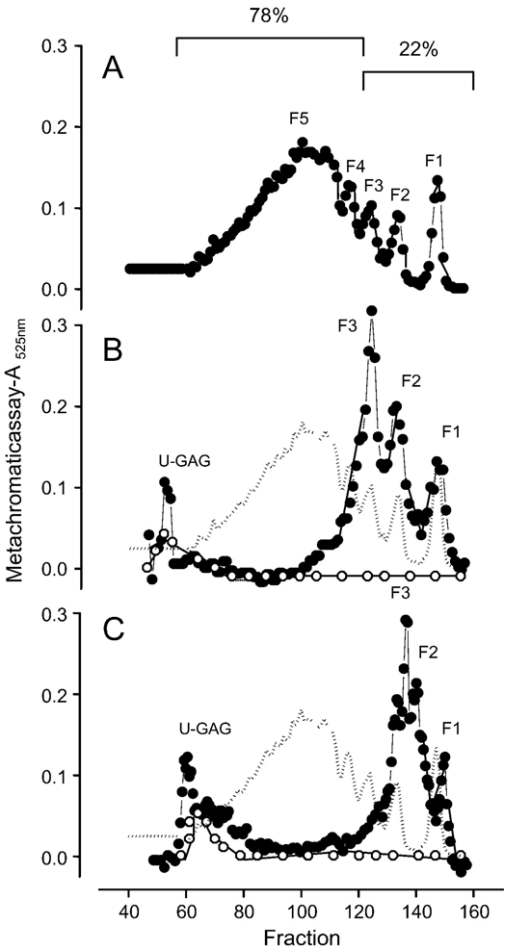

Fig. 4. Gel filtration on Bio-Gel P10 of dextran sulfate with a modal molecular mass of 8 kDa before (A) and after renal filtration in normal (B) and puromycin aminonucleoside-treated (C) rats. Dextran sulfate (~5 mg) was applied to a Bio-Gel P10 column (200×0.9 cm), equilibrated with aqueous 10% ethanol, containing 1.0 mol/l NaCl. The column was eluted with the same solution at a flow rate of ~3 ml/h, fractions of 1 ml were collected and assayed by the metachromatic assay (●) and the carbazole reaction (○). When the fractions were assayed by the phenol-sulfuric acid reaction a similar profile was obtained as that of the metachromatic assay (not shown in the panels). In Panel A, the proportions of fractions F1→F3 compared with the total dextran sulfate was determined based on their respective integrals. For comparison, data from the total dextran sulfate mixture were included in Panels B and C (dotted lines). U-GAG, urinary glycosaminoglycan.

[2] Dextran sulfate with a modal molecular mass of 50 kDa was eluted from the anion-exchange column as a single fraction with ~1.0 mol/l NaCl.

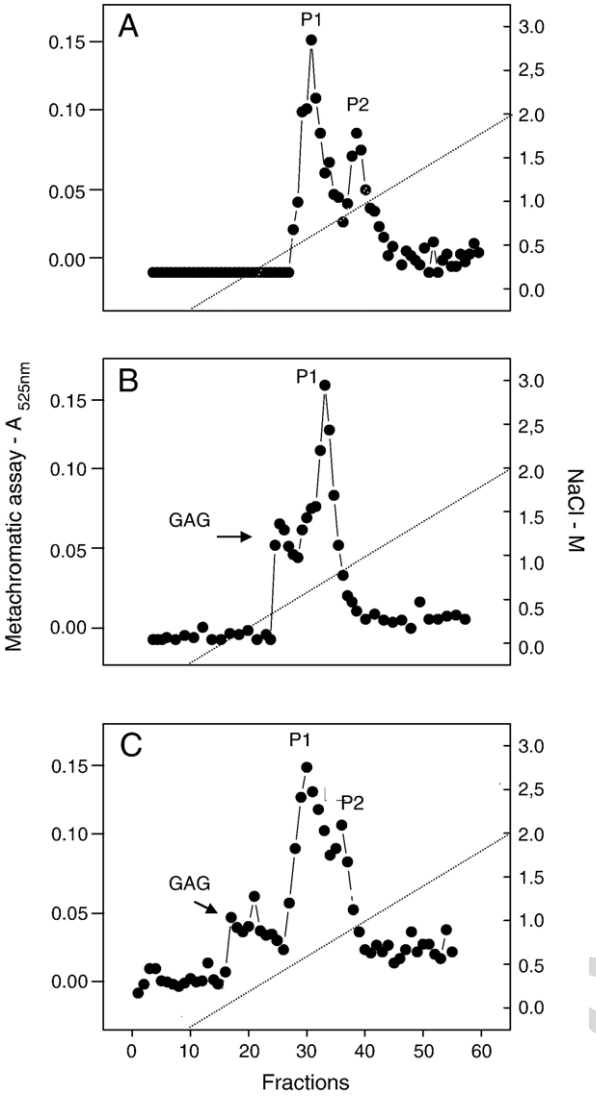

Fig. 5. Anion-exchange chromatography on DEAE cellulose of dextran sulfate before (A) and after renal filtration by normal (B) and puromycin aminonucleoside-treated (C) rats. Dextran sulfate with a modal molecular size of 8 kDa (0.25 mg) was applied to a DEAE-cellulose column (28 ml bed volume) in a 0.1 mol/l sodium acetate solution. The column was then washed with 5 ml of the same solution and eluted with a linear gradient of 0→2.0 mol/l NaCl. The polysaccharide in the fractions was monitored by the metachromatic assay. When the fractions were assayed by the phenol-sulfuric acid reaction a similar profile was obtained as that of the metachromatic assay (not shown in the panels). The fractions were pooled, mixed with 3 volumes of methanol and after standing for 24 h at 4 °C, the precipitate was collected by centrifugation, dried at room temperature and dissolved in distilled water.

units, may change the elution of these two fractions on anion-exchange column See Refs. [28] and [29] for examples of the effects of the stereochemistry of polysaccharides on their separations on anion-exchange chromatography.

Anion-exchange chromatography of dextran sulfate found in the urine of normal rat showed that only fraction P1 was filtrated by the kidney (Fig. 5B). In addition, a left shoulder was also observed on fraction P1. PAGE clearly indicated that this component corresponds to the urinary glycosaminaglycans, characterized by a higher molecular weight than the dextran sulfate administered to the rats (Fig. 6). These results suggest that in addition to the size permselectivity, the kidney may also show some charge selectivity to filtration of dextran sulfate or, alternatively, distinguish dextran sulfate with minor structural differences. But, more important, anion-exchange chromatography does not show any significant desulfation of dextran sulfate during its renal clearance. No dextran sulfate was identified, besides P1 and P2, when the fractions from the anion exchange column were assayed by the phenol sulfuric acid reaction, excluding the existence of possible desulfated product, not assayed because of the absence of metachromatic property.

Analysis of the dextran sulfate eliminated by the urine by rats with puromycin aminonucleoside-induced nephrosis shows no drastic modification when compared to normal animals. However, a slight increase in the content of fraction P2 was observed after puromycin administration, suggesting less selectivity to the charge density of dextran sulfate. More significant though, was that no evidence for desulfation of dextran sulfate was observed in rats with puromycin-induced nephrosis.

3.6. Is dextran sulfate accumulated in the renal glomerulous?

The observation that dextran sulfate is only partially eliminated to the urine after its intravascular administration suggests that this sulfated polysaccharide may accumulate in the glomerulous. In order to analyze this proposition we extracted sulfated polysaccharides from glomerulous preparations of control and puromycin aminonucleoside-treated rats, receiving dextran sulfates with high and low molecular weights. In all animals we found exclusively the standard heparan sulfate. No detectable amounts of dextran sulfate were found in these kidneys using polyacrylamide gel electrophoresis. Also no alteration in the molecular size of

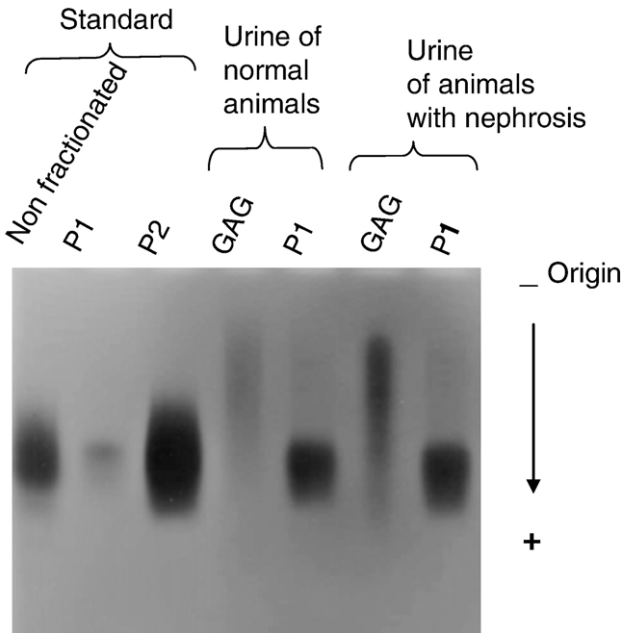

Fig. 6. Polyacrylamide gel electrophoresis of the dextran sulfate fractions obtained by chromatography on DEAE-cellulose. Fractions of 5 μg each were analyzed as described under the Materials and methods section.

Author's personal copy

glomerular heparan sufate was observed in puromycin aminonucleoside-induced nephrosis (Fig. 7). Other studies reported accumulation of dextran sulfate in the kidney [27,37], but these authors used the whole organ instead of the glomerulous preparation. We also did not detect accumulation of dextran sulfate in the liver, as suggested previously [27].

3.7. The disaccharide composition of the glomerular heparan sulfate is modified in puromycin-induced nephrosis

We further investigated the structure of the glomerular heparan sulfate using digestion with a mixture of heparin + heparan sulfate lyases, in order to determine the disaccharide composition of the glycosaminoglycan (Table 1). Animals with puromycin-induced nephrosis showed a decrease in the proportion of sulfated disaccharides, mostly due to a lower content of *O*-sulfated units (a decrease of 10% compared with control animals).

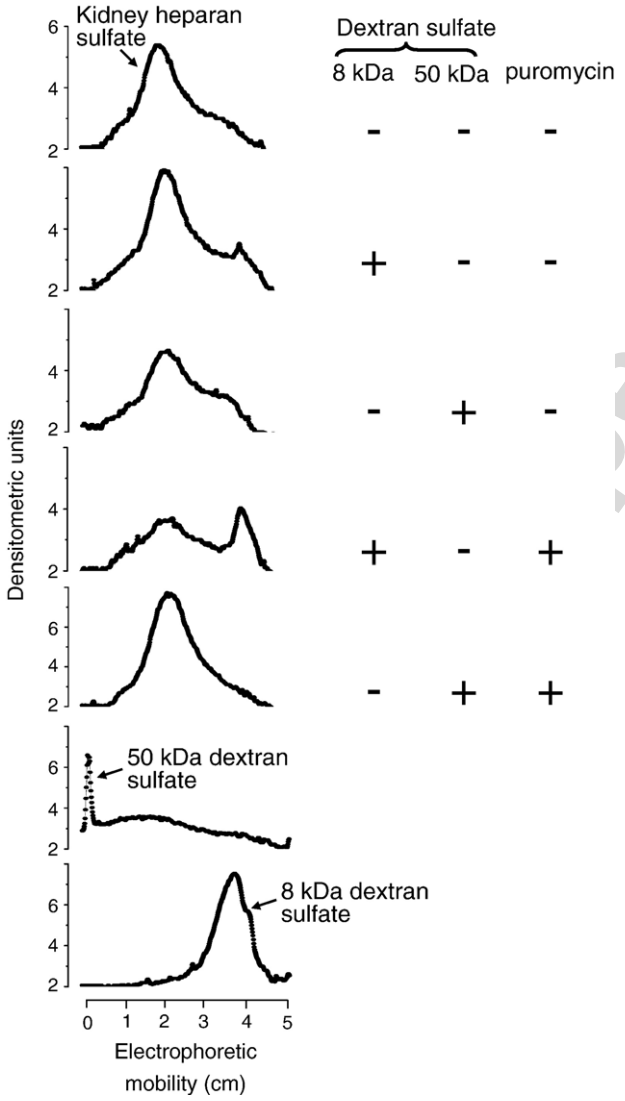

Fig. 7. Densitometry of the polyacrylamide gel electrophoresis of the heparan sulfate extracted from the renal glomerulous of rats treated with either dextran sulfate with modal molecular mass of 8 kDa or 50 kDa alone or combined with puromycin aminonucleoside. Some of the low-molecular weight bands found in the samples from renal glomerulous are from nucleic acid, as indicated by the blue staining instead of the typical pink color obtained with sulfated polysaccharides.

Table 1
Disaccharide composition of the heparan sulfate from the renal glomerulous of normal and puromycin aminonucleoside-treated rats [a]

Disaccharide units [b]	Tr (min) [c]	% of total disaccharides	
		Normal	Puromycin-treated rats
α-ΔU-1→4-GlcNAc	18.6	57.0	68.8
α-ΔU-1→4-GlcNSO$_4$	21.8	17.4	16.3
α-ΔU-1→4-GlcNAc(6SO$_4$)	23.9	12.7	5.6
α-ΔU-1→4-GlcNSO$_4$(6SO$_4$)	27.5	5.4	6.0
α-ΔU(2SO4)-1→4-GlcNSO$_4$	30.1	7.3	2.4
α-ΔU(2SO$_4$)-1→4-GlcNSO$_4$ (6SO$_4$)	35.5	0.2	0.9
Total sulfation/100 disaccharides		56.1	41.4
N-sulfation		30.3	25.6
O-sulfation		25.8	15.8
6-*O*-sulfation		18.3	12.5
2-*O*-sulfation		7.5	3.3
N-acetylation		69.7	74.4

[a] The composition of the glomerular heparan sulfate was determined based on the analysis of the disaccharides formed upon exhaustive digestion with a mixture of heparin + heparan sulfate lyases.
[b] α-ΔU, α-$\Delta^{4,5}$-unsaturated hexuronic acid; α-ΔU(2SO$_4$), α-$\Delta^{4,5}$-unsaturated hexuronic acid 2-sufate; GlcNAc, *N*-acetylated glucosamine; GlcNSO$_4$(6SO$_4$), *N*-sulfated glucosamine 6-*O*-sulfated.
[c] Retention time of the disaccharide in a SAX-HPLC column.

4. Discussion

Urinary elimination of dextran sulfate administered to normal and puromycin aminonucleoside-treated rats was evaluated. Our results allowed three major observations, described below.

First, the kidney of normal animals showed a permselectivity to dextran sulfate and only the molecules with lower molecular size were filtrated. Even more significant, fractions F1 to F3, which are eliminated to the urine (Fig. 4B), account for ~22% of the total dextran sulfate. However, based on the metachromatic assay, we estimated that ~60% of the total dextran sulfate administered to normal rats is eliminated to the urine (Fig. 3). The only way to reconcile these two observations is to consider that dextran sulfate is partially degraded to lower molecular weight fragments and only then eliminated to the urine.

Second, the molecular size of the fragments of dextran sulfate found in the urine is not modified or even decreased in puromycin aminonucleoside-induced glomerulosclerosis although a marked proteinuria is observed in these animals (Fig. 4C).

Third, as the nephrotic syndrome proceeded, renal elimination of dextran sulfate with an modal molecular size of 8 kDa decreased to lower amounts than those of normal control (~25% in rats treated for 60 days with puromycin aminonucleoside as compared to ~60% in control animals; see Fig. 3A). Part of this result may be attributed to a reduced number of physiologically active nephrons, since the GFR decreases ~32% after 90 days of puromycin aminonucleoside administration. However, the decrease in the urinary excretion of the 8 kDa-dextran sulfate was even more intense, being 3-fold after 60 days of puromycin administration. An explanation for this result is that puromycin aminonucleoside also

Personal copy

decreases the degradation of dextran sulfate to low molecular size fragments. A further support for this proposition is that if the amount of dextran sulfate found in the urine is referred to the urinary creatinine (Fig. 3B) we still observe the same decrease in excretion of dextran sulfate. Change in the charge selectivity of the glomerular membrane to dextran sulfate during puromycin aminonucleoside administration seems unlikely since we have no marked difference of charge density of the dextran sulfate eliminated to the urine by normal and nephrotic animals (Fig. 5).

A more detailed analysis of the elution profiles in Fig. 4 showed that the relative proportions of fractions F1 → F3 found in the urine (Fig. 4B and C) were markedly distinct from the proportions in the native dextran sulfate (Fig. 4A). Furthermore, the elution of these fractions obtained from urine was not exactly the same as in the standard dextran sulfate. These observations support our proposition that fractions F1 → F3 did not originate from a single renal filtration of the dextran sulfate but from a metabolic degradation of high molecular size components of the dextran sulfate mixture.

Dextran sulfate has been frequently used to evaluate glomerular filtration [1,2]. This polysaccharide is not reabsorbed by the post glomerular tubule and, therefore, its clearance reflects an event at the glomerular level [15]. A decrease in the fractional clearance of dextran sulfate was observed in rats with diabetes-induced nephrosis. As an explanation for this unexpected result, it was proposed that the renal selectivity based on charge was not very significant [38]. Possibly, dextran sulfate was uptaken by the renal endothelial cells, desulfated and finally eliminated to the urine [2,15,21,22]. In animals with experimentally induced diabetes, the sulfatase activity decreased. Therefore, the molecules of dextran sulfate captured by the endothelial cells were eliminated to the tubules without removal of their sulfate esters. At this stage, the polysaccharide was re-captured by the cells of the tubule and returned to circulation, yielding a decreased fractional clearance of the molecule.

Our results suggest that we cannot extend to the nephrosis induced by puromycin aminonucleoside the same observation reported previously for animals with renal lesion induced by diabetes. Each pathological process may have its particularity in renal lesion. In our case we have no evidence for significant desulfation of dextran sulfate during its urinary clearance. In our experiments, a plausible explanation for the decreased urinary clearance of dextran sulfate in the puromycin aminonucleoside-induced nephrosis is a decrease in the activity of the endoglycosidase of the renal endothelial cells. As a consequence of the reduced activity of this enzyme, the population of dextran sulfate molecules that achieve the minimal size for its renal elimination in the puromycin aminonucleoside-induced nephrosis, decreases significantly. Of course, this proposition requires future attempts to identify lysosomal endoglycosidases in the renal endothelial cells, able to cleave dextran sulfate molecules. But, even more significant, our results cannot be explained by the classical concepts concerning the glomerular filtration of macromolecules, which propose that the increased urinary clearance of these molecules in renal lesions is based exclusively in a decreased selectivity of the glomerular membrane.

Interestingly, in a previous study using rats with nephropathy induced by diabetes, the authors administered to the animals high doses of low-molecular-weight dextran sulfate (as in our experiments) and also observed that diabetic rats excrete less dextran sulfate than control animals [37]. These authors also reported that only fragments of dextran sulfate with lower size were eliminated to the urine.

It is difficult to compare our results with those reported for experimental diabetes-induced nephrosis [15]. These different pathological processes may induce distinct modifications in the kidney. Thus, it is possible that puromycin aminonucleoside affects mostly the endoglycosidase activity while in the diabetes-induced nephrosis an inhibition of the sulfatases is the predominant event. Furthermore, the experimental conditions used to follow renal clearance of dextran sulfate were markedly distinct in the puromycin aminonucleoside and in the diabetes-induced nephrosis. We used high amounts of dextran sulfate in order to detect its urinary elimination by biochemical methods. In the case of animals with diabetes-induced nephrosis, the kidneys were perfused with dextran sulfate at a significantly lower concentration than in our experiments. It is possible that the preponderant action of either a sulfatase or an endoglycosidase depends on the concentrations of dextran sulfate, due to different affinity constants of these two enzymes toward the polysaccharide.

The glycosaminoglycans found on the surface of renal endothelial cells have been implicated as regulatory molecules which define the glomerular selectivity to macromolecules. In the case of nephrosis induced by administration of low doses of puromycin aminonucleoside, the decrease in the selectivity to charge of the glomerular membrane (and the consequent proteinuria) was attributed to the removal of heparan sulfate molecules due to overexpression of a heparanase [39]. Under the experimental protocol we used to induce nephrosis with puromycin aminonucleoside, there is no modification in the size of the heparan sulfate chains (Fig. 7). However, analysis of the disaccharide composition of the glomerular heparan sulfate showed a decreased sulfation of the glycosaminoglycan in the puromycin aminonucleoside-treated rats compared with control animals, mostly due to a reduced *O*-sulfation of the disaccharide units (Table 1). However, our results show clearly that this modification of the glomerular heparan sulfate did not change the size of dextran sulfate filtered by the kidney in the course of the puromycin aminonucleoside-induced nephrosis.

Finally, we may consider a practical relevance of our results, besides the obvious concepts on renal filtration of macromolecules. Dextran sulfate is obtained by chemical sulfation of natural dextran. This polysaccharide does not occur in mammals and has no present therapeutic use. However, dextran sulfate may be considered as a "model molecule" for studies on renal elimination of sulfated polysaccharides. Heparin, a sulfated polysaccharide, is widely used as an antithrombotic agent. Renal elimination is considered the preponderant route for its removal from circulation. Therefore, studies on renal elimination of sulfated polysaccharides may help to further understand the pharmacokinetics of heparin and other sulfated polysaccharides with therapeutic use.

In conclusion, we showed clear evidence that dextran sulfate undergoes a decrease of its molecular size before elimination by the kidney. Unexpectedly, in a puromycin aminonucleoside-induced nephrosis, the urinary clearance of dextran sulfate

Author's personal copy

decreases and the size of the fragments found in the urine remain unaffected when compared with control animals. These results cannot be explained by the classical concepts of renal filtration of macromolecules. Each pathological condition may induce a particular modification in the kidney and affect the renal elimination of specific macromolecules in different ways.

Acknowledgments

This work was supported by grants from Conselho Nacional de Desenvolvimento Científico e Tecnológico (CNPq) and Fundação de Amparo à Pesquisa do Estado do Rio de Janeiro (FAPERJ). The authors are grateful to Adriana A. Piquet for technical assistance. We are grateful to Dr. Maria Christina Mello for revision on the manuscript.

Appendix A. Supplementary data

Supplementary data associated with this article can be found, in the online version, at doi:10.1016/j.cca.2007.05.013.

References

[1] Brenner BM, Bohrer MP, Baylis Ch, Deen WM. Determinants of glomerular permselectivity: insights derived from observations in vivo. Kidney Int 1977;12:229–37.
[2] Chang RL, Deen WM, Robertson CR, Brenner BM. Permselectivity of the glomerular capillary wall: III. Restricted transport of polyanions. Kidney Int 1975;8:212–8.
[3] Marshall SM, Hansen KW, Osterby R, Frystyk J, Orskov H, Flyvbjerg A. Effects of heparin on renal morphology and albuminuria in experimental diabetes. Am J Physiol 1996;271:E326–32.
[4] Barsotti G, Cupisti A, Gervasi GB, et al. Effects of oral administration of heparan sulphate in the remnant kidney model. Nephron 1999;81:310–6.
[5] Cahill MM, Ryan GB, Bertram JF. Biphasic glomerular hypertrophy in rats administered puromycin aminonucleoside. Kidney Int 1996;50:768–75.
[6] Diamond JR, Karnovsky MJ. Focal and segmental glomeruloesclerosis following a single intravenous dose of puromycin aminonucleoside. Am J Pathol 1986;122:481–7.
[7] Hjalmarsson C, Ohlson M, Haraldsson B. Puromycin aminonucleoside damages the glomerular size barrier with minimal effects on charge density. Am J Physiol 2001;281:F503–12.
[8] Levidiotis V, Kanellis J, Ierino FL, Power DA. Increased expression of heparanase in puromycin aminonucleoside nephrosis. Kidney Int 2001;60: 1287–96.
[9] Olson JL, Rennke HG, Venkatachalam MA. Alteration in the charge and size selectivity barrier of the glomerular filter in aminonucleoside nephrosis in rats. Lab Invest 1981;44:271–9.
[10] Tojo A, Endou H. Intrarenal handling of proteins in rats using fractional micropuncture technique. Am J Physiol 1992;263:F601–6.
[11] Deen WM, Lazzara MJ, Myers BD. Structural determinants of glomerular permeability. Am J Physiol 2001;281:F579–96.
[12] Haraldsson B, Sorensson J. Why do we not all have proteinuria? An update of our current understanding of the glomerular barrier. News Physiol Sci 2004;19:7–10.
[13] Russo LM, Bakris GL, Comper WD. Renal handling of albumin: a critical review of basic concepts and perspective. Am J Kidney Dis 2002;39: 899–919.
[14] Deen WM, Lazzara MJ. Glomerular filtration for albumin: how small is the sieving coefficient? Kidney Int 2004;66:S63–4.
[15] Burne MJ, Panagiotopoulos S, Jerums G, Comper WD. Alterations in renal degradation of albumin in early experimental diabetes in the rat: a new factor in the mechanism of albuminuria. Clin Sci 1988;95:67–72.
[16] Greive KA, Balazs ND, Comper WD. Protein fragments in urine have been considerably underestimated by various protein assays. Clin Chem 2001;47: 1717–9.
[17] Osicka TM, Houlihan CA, Chan JG, Jerums G, Comper WD. Albuminuria in patients with type 1 diabetes is directly linked to changes in the lysosome-mediated degradation of albumin during renal passage. Diabetes 2000;49:1579–84.
[18] Comper WD, Osicka TM, Jerums G. High prevalence of immuno-unreactive intact albumin in the urine of diabetic patients. Am J Kidney Dis 2003;41:336–42.
[19] Burne MJ, Vyas SV, Smit MF, Pratt LM, Comper WD. Competition between polyanions in glomerular binding and renal clearance. Arch Biochem Biophys 1997;340:257–64.
[20] Comper WD, Tay M, Wells X, Dawes J. Desulphation of dextran sulphate during kidney ultrafiltration. Biochem J 1994;297:31–4.
[21] Tay M, Comper WD, Singh AK. Charge selectivity in kidney ultrafiltration is associated with glomomerular uptake of transport probes. Am J Physiol 1991;260:F549–54.
[22] Vyas SV, Comper WD. Dextran sulfate binding to isolated rat glomeruli and glomerular basement membrane. Biochim Biophys Acta 1994;15: 367–72.
[23] Vyas SV, Burne MJ, Pratt LM, Comper WD. Glomerular processing of dextran sulfate during transcapillary transport. Arch Biochem Biophys 1996;332:205–12.
[24] Russo LM, Osicka TM, Bonnet F, Jerums G, Comper WD. Albuminuria in hypertension is linked to altered lysosomal activity and TGF-beta1 expression. Hypertension 2002;39:281–6.
[25] Russo LM, Osicka TM, Brammar GC, Candido R, Jerums G, Comper WD. Renal processing of albumin in diabetes and hypertension in rats: possible role of TGF-beta1. Am J Nephrol 2003;23:61–70.
[26] Michels LD, Davidman M, Keane WF. Glomerular permeability to neutral and anionic dextrans in experimental diabetes. Kidney Int 1982;21: 699–705.
[27] Guimarães MA, Mourao PA. Urinary excretion of sulfated polysaccharides adminstered to Wistar rats suggests a renal permselectivity to these polymers based on molecular size. Biochim Biophys Acta 1997;1335: 161–72.
[28] Vieira RP, Mourão PAS. Occurrence of a unique fucose-branched chondroitin sulfate in the body wall of a sea cucumber. J Biol Chem 1988;263:18176–83.
[29] Alves AP, Mulloy B, Moy GW, Vacquier VD, Mourão PAS. Females of the sea urchin *Strongylocentrotus purpuratus* differ in the structures oftheir egg jelly sulfated fucans. Glycobiology 1998;8:939–46.
[30] Farndale RW, Buttle DJ, Barret AJ. Improved quantitation and discrimination of sulphated glycosaminoglycans by use of dimethylmethylene blue. Biochim Biophys Acta 1986;883:173–7.
[31] Hilborn JC, Anastassiadis PA. Acrylamide gel electrophoresis of acidic mucopolysaccharides. Anal Biochem 1969;31:51–8.
[32] Pomin VH, Valente AP, Pereira MS, Mourao PA. Mild acid hydrolysis of sulfated fucans: a selective 2-desulfation reaction and an alternative approach for preparing tailored sulfated oligosaccharides. Glycobiology 2005;15:1376–85.
[33] Dubois M, Gilles KA, Hamilton JK, Rebers PA, Smith F. Colorimetric method for determination of sugars and related substances. Anal Chem 1956;28:350–4.
[34] Bitter T, Muir HM. A modified uronic acid carbazole reaction. Anal Biochem 1962;4:330–4.
[35] Werneck CC, Cruz MS, Silva LC, Villa-Verde DM, Savino, Mourao PA. Is there a glycosaminoglycan-related heterogeneity of the thymic epithelium? J Cell Physiol 2000;185:68–79.
[36] Saunders WB, editor. Clinical Diagnosis by Laboratory Methods. Philadelphia: Davidson JR and Henry JB, Inc.; 1969. 48 pp.
[37] de Lima CR, Aguiar JA, Michelacci YM. Reduced urinary excretion of sulfated polysaccharides in diabetic rats. Biochim Biophys Acta 2005;1741:30–41.
[38] Comper WD, Glasgow EF. Charge selectivity in kidney ultrafiltration. Kidney Int 1995;47:1242–51.
[39] Tryggvason K, Wartiovaara J. Molecular basis of glomerular permselectivity. Curr Opin Nephrol Hypertens 2001;10:543–9.

Author's personal copy

ANEXO III

The Journal of Biological Chemistry
Vol. 282, pp 1615-1626, 2007

"The Hemolymph of the ascidian Styela plicata (Chordata-Tunicata) contains heparin inside basophil-like cells and a unique sulfated galactoglucan in the plasma."

Cintia M. de Barros, Leonardo R. Andrade, Silvana Allodi, Christian Viskov, Pierre A. Mourier, Moisés C.M. Cavalcante, Anita H. Straus, Helio K. Takahashi, Vitor H. Pomin, Vinicius F. Carvalho, Marco A. Martins e Mauro S.G. Pavão

Supplemental Material can be found at:
http://www.jbc.org/cgi/content/full/M604056200/DC1

THE JOURNAL OF BIOLOGICAL CHEMISTRY VOL. 282, NO. 3, pp. 1615–1626, January 19, 2007
© 2007 by The American Society for Biochemistry and Molecular Biology, Inc. Printed in the U.S.A.

The Hemolymph of the Ascidian *Styela plicata* (Chordata-Tunicata) Contains Heparin inside Basophil-like Cells and a Unique Sulfated Galactoglucan in the Plasma*[S]

Received for publication, April 27, 2006, and in revised form, November 16, 2006 Published, JBC Papers in Press, November 17, 2006, DOI 10.1074/jbc.M604056200

Cintia M. de Barros[‡§], Leonardo R. Andrade[§¶], Silvana Allodi[§¶], Christian Viskov[‖], Pierre A. Mourier[‖], Moisés C. M. Cavalcante[‡], Anita H. Straus[1], Helio K. Takahashi[**1], Vitor H. Pomin[‡], Vinicius F. Carvalho[‡‡], Marco A. Martins[‡‡1], and Mauro S. G. Pavão[‡1,2]**

*From the [‡]Laboratório de Tecido Conjuntivo, Hospital Universitário Clementino Fraga Filho and Instituto de Bioquímica Médica, [§]Programa de Pós-Graduação em Ciências Morfológicas, Instituto de Ciências Biomédicas, and [¶]Departamento de Histologia e Embriologia, Instituto de Ciências Biomédicas, Universidade Federal do Rio de Janeiro, Cidade Universitária, Rio de Janeiro, RJ, CEP 21941-590, Brasil, [‖]Sanofi-aventis, Centre de Recherche de Paris, Unité de Glycochimie, Batiment Lavoisier 13, Quai Jules Guesde 94400 Vitry-sur Seine, France, **Departamento de Bioquímica, Escola Paulista de Medicina, Universidade Federal de São Paulo, São Paulo, 04023-900 SP, Brasil, and [‡‡]Laboratório de Inflamação, Instituto Oswaldo Cruz, Fundação Oswaldo Cruz (FIOCRUZ), Rio de Janeiro, RJ, CEP 21045-900, Brasil*

The hemolymph of ascidians (Chordata-Tunicata) contains different types of hemocytes embedded in a liquid plasma. In the present study, heparin and a sulfated heteropolysaccharide were purified from the hemolymph of the ascidian *Styela plicata*. The heteropolysaccharide occurs free in the plasma, is composed of glucose (~60%) and galactose (~40%), and is highly sulfated. Heparin, on the other hand, occurs in the hemocytes, and high performance liquid chromatography of the products formed by degradation with specific lyases revealed that it is composed mainly by the disaccharides ΔUA(2SO$_4$)-1→4-β-D-GlcN(SO$_4$) (39.7%) and ΔUA(2SO$_4$)-1→4-β-D-GlcN(SO$_4$)(6SO$_4$) (38.2%). Small amounts of the 3-*O*-sulfated disaccharides ΔUA(2SO$_4$)-1→4-β-D-GlcN(SO$_4$)(3SO$_4$) (9.8%) and ΔUA(2SO$_4$)-1→4-β-D-GlcN(SO$_4$)(3SO$_4$)(6SO$_4$) (3.8%) were also detected. These 3-*O*-sulfated disaccharides were demonstrated to be essential for the binding of the hemocyte heparin to antithrombin III. Electron microscopy techniques were used to characterize the ultrastructure of the hemocytes and to localize heparin and histamine in these cells. At least five cell types were recognized and classified as univacuolated and multivacuolated cells, amebocytes, hemoblasts, and granulocytes. Immunocytochemistry showed that heparin and histamine co-localize in intracellular granules of only one type of hemocyte, the granulocyte. These results show for the first time that in ascidians, a sulfated galactoglucan circulates free in the plasma, and heparin occurs as an intracellular product of a circulating basophil-like cell.

Heparin is a highly sulfated glycosaminoglycan (GAG)[3] made up of a mixture of polymers with a similar backbone of repeating hexuronic acid (α-L-iduronic acid or β-D-glucuronic acid) linked 1,4 to α-D-glucosamine units. The heparin molecules possess a high heterogeneity, which results from different substitutions on the D-glucosamine (*N*-acetylated, *N*-sulfated, *O*-sulfated at C6 and/or C3) and on the uronic (glucuronic or iduronic) acid residue (*O*-sulfated at C2) (for reviews, see Refs. 1–4).

In mammals, heparin is synthesized on to a specific protein core, forming the serglycin proteoglycans (PGs) (5–9). These PGs occur in secretory granules of some immunologic cells, such as mast cells and basophils (10–12). In basophils, different from mast cells, the serglycin core protein is substituted exclusively with oversulfated chondroitin sulfate chains (13). Mature mast cells are not found in blood but reside in peripheral mucosa or connective tissue interstice. Basophils, on the other hand, circulate in the blood (14, 15).

In invertebrates, heparin has been reported to occur in different species of mollusks (16–22), crustaceans (23–27), and ascidians (28–30). In the ascidian *Styela plicata* (Chordata-Tunicata), a heparin composed mainly by the disaccharide α-L-iduronic acid 2-sulfate-1→4β-D-GlcN(SO$_4$)(6SO$_4$), with a minor contribution (~25%) of the disaccharide α-L-iduronic acid-1→4β-D-GlcN(SO$_4$)(6SO$_4$) was detected in intracellular granules of accessory cells, named test cells, that reside in the periviteline space of oocytes (28). Because of the morphological and biochemical similarities between ascidian test cells and mammalian mast cells, we have hypothesized that these cells could be evolutively related. Other cell types in this ascidian,

* This work was supported by grants from Conselho Nacional de Desenvolvimento Cientifico e Tecnológico (CNPq) and Fundação de Amparo a Pesquisa do Rio de Janeiro and by National Institutes of Health Fogarty International Center Grant R03 TW05775 (to M. S. G. P.). The costs of publication of this article were defrayed in part by the payment of page charges. This article must therefore be hereby marked "*advertisement*" in accordance with 18 U.S.C. Section 1734 solely to indicate this fact.

[S] The on-line version of this article (available at http://www.jbc.org) contains supplemental Fig. 3*C*.

[1] Research fellows of CNPq.

[2] To whom correspondence should be addressed: Instituto de Bioquímica Médica, Centro de Ciências da Saúde, Cidade Universitária, Universidade Federal do Rio de Janeiro, Caixa Postal 68041, Rio de Janeiro, RJ, 21941-590, Brasil. Tel.: 55-21-2562-2093; Fax: 55-21-2562-2090; E-mail: mpavao@hucff.ufrj.br.

[3] The abbreviations used are: GAG, glycosaminoglycan; ΔUA, α-Δ^{4,5}-unsaturated hexuronic acid; ΔUA(2SO$_4$), α-Δ^{4,5}-unsaturated hexuronic acid 2-sulfate; GlcN(SO$_4$), GlcN(SO$_4$)(6SO$_4$), and GlcN(SO$_4$)(3SO$_4$)(6SO$_4$), derivatives of D-glucosamine, bearing a sulfate ester at position N, at both positions N and 6, and at positions N, 3, and 6, respectively; GlcNAc(6SO$_4$), *N*-acetyl-D-glucosamine 6-sulfate; HPLC, high performance liquid chromatography; FPLC, fast protein liquid chromatography; PG, proteoglycan; PBS, phosphate-buffered saline; CTA, cetyltrimethylammonium; SAX, strong anion exchange; GlcA, gluconic acid.

Downloaded from www.jbc.org at CAPES Usage on June 30, 2007

located at the lumen of pharynx and intestine, have also been shown to contain intracellular heparin (28).

The hemolymph of ascidians contains different types of circulating blood cells (31–34). Some of these cells migrate from hemolymph to tissues, where they carry out several immunologic actions, such as phagocytosis of self and non-self molecules, expression of cytotoxic agents, encapsulation of antigens, and also reparation of damaged tissues (35). In the ascidian *S. plicata*, the hemocytes have been classified by light microscopy by Radford *et al.* (32). The authors described eight individual cell types: hemoblast, lymphocyte-like cell, signet ring cell, refractile vacuolated cell, nonrefractile vacuolated cell, pigment cell, fried egg cell, and fine granular cell.

As mentioned earlier, in evolved chordates, intracellular GAGs are restricted to immunologic cells that either reside in the tissues (mast cells) or circulate in the blood (basophils) (15). Considering the phylogenetic position of ascidians and taking into account that a heparin-containing cell, similar to a mammalian mast cell, was detected in the tissues of *S. plicata*, it is possible that a basophil-like cell containing intracellular GAGs circulates in the hemolymph of this invertebrate chordate. To investigate this hypothesis, we submitted the hemolymph of *S. plicata* to proteolytic digestion before and after separation of plasma and hemocytes and analyzed the extracted and purified sulfated glycans. In addition, ultrastructural and immunocytochemical studies were carried out to characterize and determine which hemocytes express these glycans. Our results reveal the occurrence of two sulfated glycans in the hemolymph of this ascidian: heparin, which is present in intracellular granules of a circulating basophil-like cell, and a sulfated galactoglucan, which occurs free in the plasma. These results show for the first time the presence of heparin in a circulating basophil-like cell in an invertebrate chordate and may contribute toward the understanding of the evolution of the immune system in this phylum.

EXPERIMENTAL PROCEDURES

Materials

Heparan sulfate from human aorta was extracted and purified as described previously (36). Chondroitin 4-sulfate from whale cartilage, dermatan sulfate and heparin from porcine intestinal mucosa (140 units/mg), twice-crystallized papain (15 units/mg protein), and the standard disaccharides α-ΔUA-1→4-GlcN(SO_4), α-ΔUA-1→4-GlcNAc(6SO_4), α-ΔUA(2SO_4)-1→4-GlcNAc, α-ΔUA(2SO_4)-1→4-GlcN-(SO_4), α-ΔUA(2SO_4)-1→4-GlcNAc(6SO_4), α-ΔUA-1→4-GlcN(SO_4)(6SO_4), and α-ΔUA(2SO_4)-1→4-GlcN(SO_4)(6SO_4) were purchased from Sigma; chondroitin AC lyase (EC 4.2.2.5) from *Arthrobacter aurescens*, chondroitin ABC lyase (EC 4.2.2.4) from *Proteus vulgaris*, and heparan sulfate lyase (EC 4.2.2.8) and heparin lyase (EC 4.2.2.7) from *Flavobacterium heparinum* were from Seikagaku America Inc. (Rockville, MD). For HPLC-SAX experiments, the enzymes from *F. heparinum* heparinase I (EC 4.2.2.7), heparinase II (no EC number), and heparinase III (EC 4.2.2.8) were obtained from Grampian Enzymes (Aberdeen). Agarose (standard low M_r) was obtained from Bio-Rad; toluidine blue was from Fisher; 1,9-dimethylmethylene blue was from Serva Feinbiochimica (Heidelberg, Germany); human antithrombin and thrombin were from Hematologic Technologies Inc. or from Hyphen Biomed; and thrombin chromogenic substrate tosyl-Gly-Pro-Arg-*p*-nitroanilide acetate (Chromozyn TH) was from Roche Applied Science. Histamine *N*-methyltransferase was partially purified from guinea pig brain according to Brown *et al.* (37), and aliquots were stored at −20 °C. *S*-Adenosyl[*methyl*-^{3}H]methionine was purchased from PerkinElmer Life Sciences and neutralized with an equal volume of 0.1 M NaOH immediately before use. Unlabeled telemethylhistamine (Sigma) was diluted in 1 mM acetic acid and stored at 4 °C. Chloroform (Merck) was used fresh for the organic extraction procedure.

Collection of Tunicates

Adult individuals of *S. plicata* were collected at Praia da Urca (Guanabara Bay), Rio de Janeiro, Brazil, and maintained in an aerated aquarium containing filtered sea water at 20 °C until use.

Isolation of the Hemocytes

The hemolymph was harvested from the heart by direct punction and collected into plastic tubes containing an equal volume of marine anticoagulant, containing 0.45 M sodium chloride, 0.1 M glucose, 0.01 M trisodium citrate, 0.01 M citric acid, and 0.001 M EDTA (pH 7.0) (38). After harvesting, the hemocytes were separated from plasma by centrifugation (130 × *g* for 10 min at room temperature).

Extraction of the Sulfated Polysaccharides

The hemocytes were immersed in acetone and kept for 24 h at 4 °C. The dried hemocytes (1 g) were suspended in 20 ml of 0.1 M sodium acetate buffer (pH 5.5), containing 100 mg of papain, 5 mM EDTA, and 5 mM cysteine and incubated at 60 °C for 24 h. The incubation mixture was then centrifuged (2000 × *g* for 10 min at room temperature), the supernatant was separated, and the precipitate was incubated with papain two more times, as described above. The clear supernatants from the three extractions were combined, and the polysaccharides were precipitated with 2 volumes of 95% ethanol and maintained at 4 °C for 24 h. The precipitate formed was collected by centrifugation (2000 × *g* for 10 min at room temperature) and freeze-dried. For the extraction of the plasma polysaccharides, after the removal of the hemocytes, the plasma was dialyzed against distilled water, lyophilized, and incubated with papain, as described above.

Purification of the Polysaccharides

The glycans obtained from plasma (~8 mg) were applied to a Q Sepharose-FPLC column, equilibrated with 20 mM Tris/HCl buffer (pH 8.0). The glycans were eluted by a linear gradient of 0–2.0 M NaCl (150 ml) at a flow rate of 2.0 ml/min. Fractions of 1.5 ml were collected and checked by a metachromatic assay using 1,9-dimethyl-methylene blue (39). Fractions eluted with different NaCl concentrations were pooled as indicated in Fig. 2*A*, dialyzed against distilled water, and lyophilized.

The glycans (~2 mg) obtained from hemocytes or porcine heparin (~1 mg) were applied to a Mono Q-FPLC column, equilibrated with 20 mM Tris/HCl buffer (pH 8.0). The glycans

Downloaded from www.jbc.org at CAPES Usage on June 30, 2007

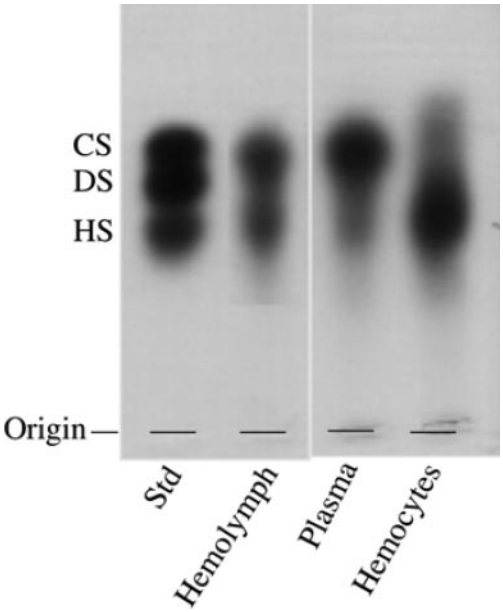

FIGURE 1. **Agarose gel electrophoresis of the crude glycans isolated from total hemolymph, plasma, and hemocytes.** The hemolymph of *S. plicata* was collected and fractionated into plasma and hemocytes by centrifugation, as described under "Experimental Procedures." The hemolymph, plasma, or hemocytes were submitted to proteolytic digestion, and the extracted glycans (~1.5 μg, as uronic acid) were applied to a 0.5% agarose gel in 0.05 M 1,3-diaminopropane/acetate (pH 9.0), along with a mixture of standard (*Std*) glycosaminoglycans, containing chondroitin sulfate (*CS*), dermatan sulfate (*DS*), and heparan sulfate (*HS*).

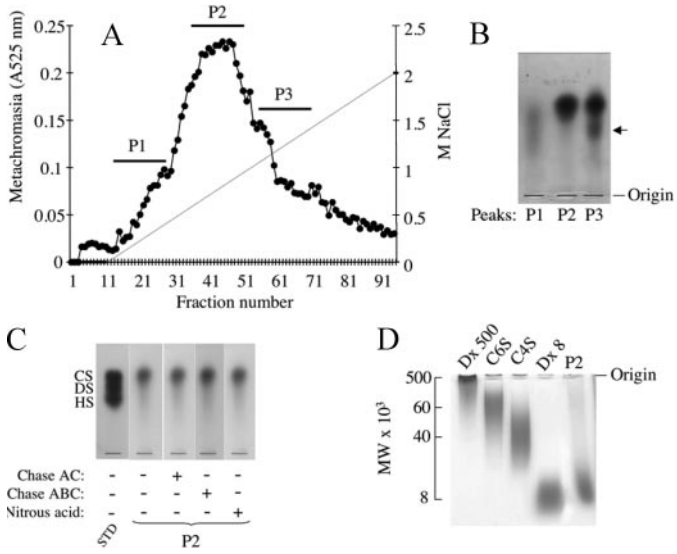

FIGURE 2. **Isolation and characterization of the sulfated polysaccharide from plasma.** *A*, about 8 mg of the sulfated polysaccharide from plasma were applied to a Q Sepharose-FPLC column as described under "Experimental Procedures." Fractions were assayed for metachromasia (●) and NaCl (- - - - -) concentration. *B*, fractions under the peaks denominated P1, P2, and P3 were pooled, dialyzed against distilled water, lyophilized, and analyzed by agarose gel electrophoresis, as described in the legend to Fig. 1. *C*, the purified sulfated polysaccharide from plasma (P2) (~10 μg dry weight) was analyzed by agarose gel electrophoresis, before (−) or after (+) incubation with chondroitin AC (*Chase AC*) or ABC (*Chase ABC*) lyases or deaminative cleavage with nitrous acid, as described under "Experimental Procedures." *D*, P2 and the molecular weight markers dextran 500, chondroitin 4-sulfate, chondroitin 6-sulfate, and dextran 8 (~10 μg as dry weight of each) were applied to a 1-mm-thick 6% polyacrylamide slab gel, as described under "Experimental Procedures."

were eluted by a linear gradient of 0–2.0 M NaCl (45 ml) at a flow rate of 0.5 ml/min. Fractions of 0.5 ml were collected and checked by metachromatic assay using 1,9-dimethyl-methylene blue. Fractions eluted with different NaCl concentrations were pooled as indicated in Fig. 4*A*, dialyzed against distilled water, and lyophilized.

Electrophoretic Analysis

Agarose Gel—The crude or purified glycans from plasma (~10 μg dry weight) or hemocytes (1.5 μg as uronic acid), before or after incubation with specific GAG lyases or deaminative cleavage with nitrous acid were analyzed by agarose gel electrophoresis, as described previously (40). Briefly, the glycans and a mixture of standard GAGs, containing chondroitin sulfate, dermatan sulfate, and heparan sulfate (1.5 μg as uronic acid of each), were applied to a 0.5% agarose gel in 0.05 M 1,3-diaminopropane/acetate (pH 9.0) and run for 1 h at 110 mV. After electrophoresis, the glycans were fixed with aqueous 0.1% cetylmethylammonium bromide solution and stained with 0.1% toluidine blue in acetic acid/ethanol/water (0.1:5:5, v/v/v).

Polyacrylamide Gel—The molecular masses of the purified glycans from plasma and hemocytes were estimated by polyacrylamide gel electrophoresis. Samples (~10 μg) were applied to a 1-mm-thick 6% polyacrylamide slab gel, and after electrophoresis at 100 V for ~1 h in 0.06 M sodium barbital (pH 8.6), the gel was stained with 0.1% toluidine blue in 1% acetic acid. After staining, the gel was washed overnight in 1% acetic acid. The molecular mass markers used were dextran 500 (average M_r 500,000), chondroitin 6-sulfate from shark cartilage (average M_r 60,000), chondroitin 4-sulfate from whale cartilage (average M_r 40,000), porcine intestinal mucosa heparin (average M_r 18,000), and dextran 8 (average M_r 8,000).

CTA-SAX Chromatography of Heparin Digests—To prepare the digests, exhaustive digestion of heparin (0.1 mg) was performed at room temperature for 48 h with a mixture of 2.5 mIU of heparinase I, 2.5 mIU of heparinase II, and 2.5 mIU of heparinase III in a total volume of 30 μl of 100 mM sodium acetate buffer, pH 7.0, containing 2 mM $Ca(OAc)_2$ and 2 mg/ml bovine serum albumin. The columns used for the chromatography of the heparin digests were dynamically coated with CTA, as described earlier (41). The eluting salt was ammonium methane sulfonate, prepared by neutralization until pH 2.5 of methane sulfonic acid by aqueous ammonia solutions. The solvent B of CTA-SAX was 2 M ammonium methane sulfonate at pH 2.5. The solvent A was water (quality Milli-Q) brought to pH 3 by the addition of methane sulfonic acid. A linear gradient starting from 1% B to 100% B within 74 min was used at a flow rate of 0.22 ml/min. After 74 min, the percentage of B remained at 100%. After each run, a reconditioning step of 18 min was used. Column temperature was 40 °C.

Enzymatic Treatments

Chondroitin Lyases—The ascidian glycans (~100 μg) were incubated with 0.01 units of chondroitin AC or ABC lyase in 0.1 ml of 50 mM Tris-HCl buffer (pH 8.0), containing 5 mM EDTA and 15 mM sodium acetate. After incubation at 37 °C for 12 h, another 0.01 units of enzyme was added to the mixture, and the reaction continued for an additional 12-h period.

Downloaded from www.jbc.org at CAPES Usage on June 30, 2007

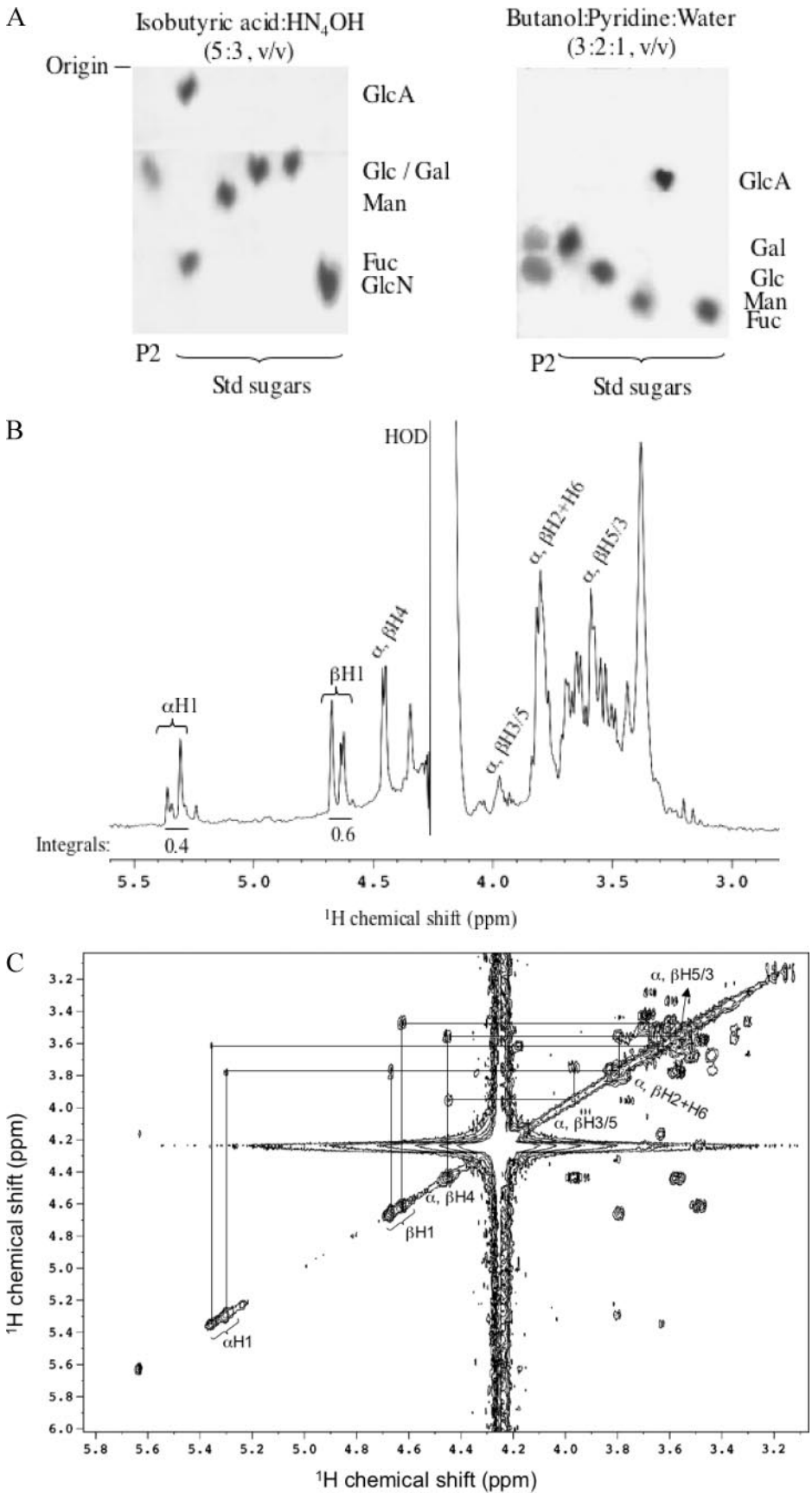

Downloaded from www.jbc.org at CAPES Usage on June 30, 2007

Heparan Sulfate and Heparin Lyases—About 50 μg (as dry weight of each) of the glycans extracted from the ascidian tissues were incubated with 0.005 units of either heparan sulfate lyase or heparin lyase in 100 μl of 100 mM sodium acetate buffer (pH 7.0), containing 10 mM calcium acetate for 17 h at 37 °C. At the end of the incubation period, the mixtures were analyzed by agarose gel electrophoresis, as described earlier.

Hexuronic Acid—The hexuronic acid content of the glycans from the various tissues was estimated by the carbazole reaction (42).

Deaminative Cleavage with Nitrous Acid—Deaminative cleavage with nitrous acid of the sulfated glycans was performed as described by Shievely and Conrad (43).

Chemical Analyses—Total hexose was measured by the phenol-sulfuric acid method of DuBois *et al.* (44). After acid hydrolysis (6.0 N trifluoroacetic acid, 100 °C for 5 h), total sulfate was determined by the $BaCl_2$-gelatin method (45). The proportions of the different hexoses in the acid hydrolysates were determined by paper chromatography in butanol/piridine/water (3:2:1, v/v/v) for 36 h or in isobutyric acid, 1.0 NH_4OH (5:3, v/v). The sugars were detected on the chromatogram by silver nitrate staining.

NMR Spectroscopy—^1H spectra were recorded using a Bruker DRX 600 with a triple resonance probe. About 3 mg of the purified plasma polysaccharide was dissolved in 0.5 ml of 99.9% D_2O (CIL). All spectra were recorded at 60 °C with hydrogen oxygen deuterium suppression by presaturation. The correlation spectroscopy (COSY) spectrum was recorded using states-TPPI (states-time proportion phase incrementation) for quadrature detection in the indirect dimension. All chemical shifts were relative to external trimethylsilylpropionic acid for ^1H.

Antithrombin III Affinity Chromatography—The polysaccharide (10 mg) was chromatographed on an ATIII-Sepharose column (15 × 2.6 cm). The column was prepared by bounding 100 mg of human ATIII (Hyphen Biomed) on cyanogen bromide-activated Sepharose 4B (Sigma). The polysaccharide fraction was eluted by NaCl solution. The low affinity fraction was eluted out of the column at 0.25 M NaCl solution buffered at pH 7.4 with Tris (10 mM) and desalted on Sephadex G10. The high affinity fraction was eluted with 3 M NaCl, 10 mM Tris and desalted on Sephadex G10.

Inhibition of Thrombin by Antithrombin in the Presence of Mammalian or Hemocyte Heparins—These effects were evaluated by the assay of amydolytic activity of thrombin, using chromogenic substrate, as described (28). Incubations were performed in disposable UV semimicrocuvettes. The final concentrations of reactants included 50 nM antithrombin, 15 nM thrombin, and 0–10 μg/ml heparin in 100 μl of 0.02 M Tris/HCl, 0.15 M NaCl, and 1.0 mg/ml polyethylene glycol (pH 7.4) (TS/PEG buffer). Thrombin was added last to initiate the reaction. After a 60-s incubation at room temperature, 500 μl of 100 μM chromogenic substrate Chromogenix TH in TS/PEG buffer was added, and the absorbance at 405 nm was recorded for 100 s. The rate of change of absorbance was proportional to the thrombin activity remaining in the incubation. No inhibition occurred in control experiments in which thrombin was incubated with antithrombin in the absence of heparin; nor did inhibition occur when thrombin was incubated with heparin alone over the range of concentrations tested.

Conventional Transmission Electron Microscopy—The hemocytes were fixed in 2.5% glutaraldehyde EM grade, 4% formaldehyde freshly prepared from paraformaldehyde in 0.1 M sodium cacodylate buffer (pH 7.2) under microwaves (Laboratory Microwaves Processor, Pelco model RFS59MP; 2.45 GHz) for 10 s twice at 45 °C and rinsed twice in cacodylate buffer for 15 min at room temperature. The samples were postfixed in 1% osmium tetroxide in 0.1 M sodium cacodylate buffer (pH 7.2) in a microwave oven for 10 s, dehydrated through a graded series of acetone, and embedded in epoxy resin Poly/Bed 812 (Polyscience, Inc.). Ultrathin sections (80 nm) were obtained (LKB ultramicrotome) and collected on copper grids (300 mesh). The sections were stained with 2% uranyl acetate for 20 min and 1% lead citrate for 5 min. The samples were observed in a Zeiss 900 EM electron microscope, operated at 80 kV.

Immunocytochemistry—Circulating hemocytes were slightly centrifuged from hemolymph and fixed overnight in 4% formaldehyde, 0.1% glutaraldehyde in 0.1 M sodium phosphate buffer (pH 7.2) and 4% 1-ethyl-3-(3-dimethylaminopropyl)carbodiimide (Sigma) at 4 °C. The samples were washed with 0.05% sodium borohydride in 0.1 M sodium phosphate buffer (pH 7.2), dehydrated in a graded series of methanol until 95%, and embedded in LR Gold acrylic resin at room temperature. Ultrathin sections (90 nm) were obtained and collected on nickel grids (300 mesh).

The sections were hydrated in phosphate-buffered saline (PBS) (1%) for 10 min, and nonspecific sites were blocked with 1% bovine serum albumin in 1% PBS containing 50 mM ammonium chloride for 10 min. The samples were incubated overnight in a humid chamber with anti-heparin monoclonal antibody (46) or anti-histamine polyclonal antibodies (Chemicon) diluted in 1% PBS. After washing with 1% PBS, the sections were incubated with secondary goat anti-mouse or anti-rabbit 10-nm gold-conjugated IgM antibody (Sigma) for 3 h and washed in 1% PBS containing 1% bovine serum albumin and finally with distilled water. The sections were stained with 1% uranyl acetate for 20 min. The controls were done omitting the incubation with the primary antibody.

Histamine N-Methyltransferase Activity—Tissues of *S. plicata* (intestine, hemolymph, and pharynx) as well as a preparation of rat peritoneal mast cells were homogenized with PBS (1%, v/v), subjected to three consecutive cycles of freeze and thaw, and then centrifuged at 1,500 × *g* for 10

FIGURE 3. **Chemical analysis of the sulfated polysaccharide from plasma.** *A*, paper chromatography. The purified sulfated polysaccharide from plasma was hydrolyzed with 6.0 N trifluoroacetic acid at 100 °C for 5 h. The hexoses formed were spotted on Whatman No. 1 paper and subjected to chromatography in butanol/piridine/water (3:2:1, v/v/v) or isobutyric acid, 1 N NH_4OH (5:3, v/v) for 36 h. The sugars were detected on the chromatogram by silver nitrate staining. The following monosaccharides were used as standards: GlcA, Glc, Gal, Man, fucose (*Fuc*), and GlcN. *B*, NMR spectroscopy. ^1H spectra were recorded using a Bruker DRX 600 with a triple resonance probe. About 3 mg of the purified plasma polysaccharide was dissolved in 0.5 ml of 99.9% D_2O (CIL). *HOD*, hydrogen oxygen deuterium. The integrals listed under the region of anomeric protons were normalized to the total hexose-H1 intensity.

Downloaded from www.jbc.org at CAPES Usage on June 30, 2007

min. Supernatants were then stored at −20 °C until total protein and histamine quantification. Total protein content was spectrophotometrically quantified (540 nm) in the supernatant by means of the Biuret technique (47). Histamine content was estimated in the supernatant by the radioenzymatic technique of Snyder *et al.* (48), modified by Côrrea and Saavedra (49). Briefly, the assay was carried out in a final volume of 60 μl, consisting of 10 μl of standard histamine solution or tissue extract and 50 μl of a freshly prepared mixture containing histamine *N*-methyltransferase preparation, 0.125 μCi of *S*-adenosyl[*methyl*-^{3}H]methionine, and 0.05 M sodium phosphate buffer, pH 7.9. Measurements were made in duplicate, and the blanks were prepared by replacing the sample test with 0.05 M sodium phosphate buffer, pH 7.9. After sample incubation overnight at 4 °C, the enzymatic reaction was stopped by the addition of 0.5 ml of 1 M NaOH containing 10 μl of the unlabeled methylhistamine carrier. The [^{3}H]methylhistamine formed was then extracted into 3 ml of chloroform. After evaporation of the organic phase, the radioactivity was counted with a Beckman LS-100 Scintilograph.

RESULTS

The Hemolymph of S. plicata Contains Different Sulfated Polysaccharides—Ascidian hemolymph contains different types of cells, named hemocytes, embedded in liquid plasma. In order to investigate the presence of sulfated polysaccharides, the hemolymph was subjected to proteolytic treatment with papain, and the extracted material was analyzed by agarose gel electrophoresis (Fig. 1). Two main metachromatic bands with different electrophoretic motilities, corresponding to two different sulfated polysaccharides, were observed in the gel. The low mobility band possesses the same migration as standard heparan sulfate, whereas the band with the higher electrophoretic mobility migrates as standard chondroitin sulfate. To investigate the origin of these sulfated polysaccharides, the hemolymph was separated into plasma and hemocytes by centrifugation, and the glycans were extracted separately by protease digestion and analyzed by agarose gel electrophoresis. As shown in Fig. 1, the sulfated polysaccharides from the hemolymph have different origins. The material migrating as chondroitin sulfate originates from the plasma, whereas that migrating as heparan sulfate comes from the hemocytes.

The Polysaccharide from the Plasma Is a Sulfated Galactoglucan—The sulfated polysaccharide from plasma was fractionated on an ion exchange column, as described under "Experimental Procedures." Three peaks, denominated P1, P2, and P3, were eluted from the column with different NaCl concentrations (Fig. 2*A*). P2, which eluted from the column at ~0.8 M NaCl, displayed a homogeneous metachromatic band, migrating as chondroitin sulfate, when analyzed by agarose gel electrophoresis (Fig. 2*B*). P3, which eluted from the column with ~1.2 M NaCl, showed two metachromatic bands (Fig. 2*B*). The higher mobility band in P3 represents the chondroitin sulfate-migrating material from P2, which is contaminated with a lower mobility band, corresponding to the heparan sulfate-migrating material from hemocytes.

TABLE 1
Chemical composition of the sulfated polysaccharide from *S. plicata* hemolymph

Fraction	Molar ratio		
	Glc	Gal	Sulfate/total sugar
P2	0.61	0.39	1.0

TABLE 2
Proton chemical shifts (ppm) of the sulfated galactoglycan

	Proton chemical shifts[a]					
	H1	H2	H3	H4	H5	H6
α-Anomeric	5.31	3.79	3.97/3.56	4.46	3.56/3.97	3.78
β-Anomeric	4.62	3.79	3.97/3.56	4.46	3.56/3.97	3.78

[a] Data obtained from one- and two-dimensional spectra described in Fig. 3, *B* and *C* (supplemental material).

In order to obtain information about the plasma polysaccharide, the purified polymer obtained from the ion exchange column (P2) was incubated with chondroitinase AC- and ABC-lyase or treated with nitrous acid, and the products were analyzed by agarose gel electrophoresis (Fig. 2*C*). The plasma polysaccharide resisted the incubations with chondroitin sulfate lyases and the nitrous acid treatment, indicating that it is not chondroitin/dermatan sulfate or heparan sulfate/heparin.

To estimate the size of the plasma polysaccharide, P2 was analyzed by polyacrylamide gel electrophoresis, where its migration was compared with those of known molecular weight standard glycans. As shown in Fig. 2*D*, P2 migrated slightly behind dextran 8,000 (average M_r 8,000), which suggests an average molecular weight of ~10,000.

The chemical analysis of the plasma polysaccharide was carried out by paper chromatography on two different buffer systems after acid hydrolysis of the purified polymer (P2). As indicated by the chromatographic analysis on butanol/pyridine/water, the polymer is composed mainly by glucose (60%), followed by galactose (40%). No amino sugar or hexuronic acid was detected (Fig. 3, Table 1) as indicated by the chromatographic analysis on isobutyric acid/NH_4. High amounts of sulfate ester, in equimolecular proportions with hexoses, were also detected (Table 1). Structural analysis by one-dimensional (Fig. 3*B*) and two-dimensional (supplemental Fig. 3*C*) NMR supports the chromatographic data. Clearly, the one-dimensional ^{1}H NMR spectrum revealed intensity signals of anomeric protons in a proportion of 4:6 for α- and β-forms, respectively (Fig. 3*B*). This proportion is coincident to the galactose/glucose ratio shown in Table 1 and indicates that the sulfated galactoglucan is composed mainly by α-galactopyranose and β-glucopyranose residues. The COSY spectrum revealed the presence of six connected protons through scalar coupling (cross-peaks), confirming that this compound is a hexose polymer (supplemental Fig. 3*C*). No evidence of amino or other complex sugars were detected, discarding the possibility of a minor glycosaminoglycan contaminant. Both α- and β-H1 revealed cross-peaks with H2 at ~3.8 ppm, suggesting the same assignment (Table 2). This similarity derives from the equal proton chemical shift of galactose and glucose, which are just C4 epimers. Moreover, the H2 high field resonance certainly indicates that there is no

Downloaded from www.jbc.org at CAPES Usage on June 30, 2007

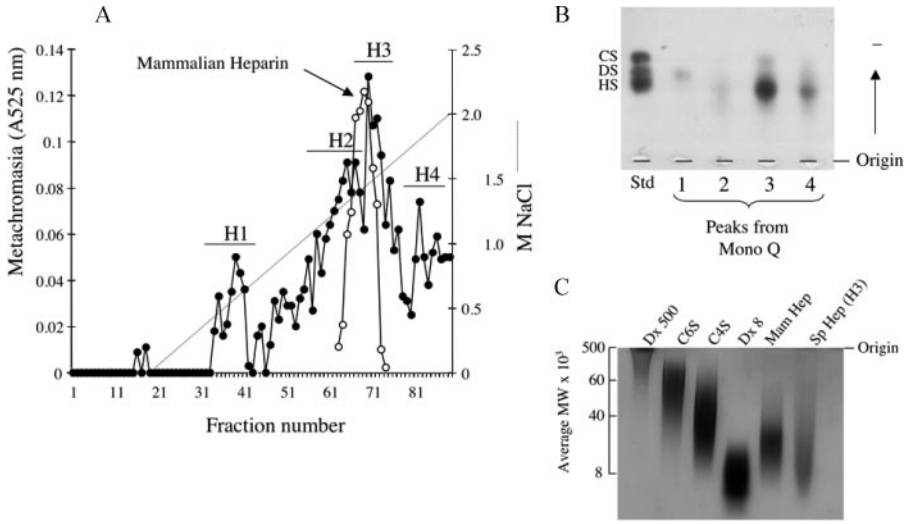

FIGURE 4. **Isolation and characterization of the sulfated glycan from hemocytes.** *A*, about 2 mg of the sulfated glycan from hemocyte (●) or mammalian heparin (○) (~1 mg) were applied to a Mono Q-FPLC column as described under "Experimental Procedures." Fractions were assayed for metachromasia and NaCl (- - - - -) concentration. *B*, fractions under the peaks denominated H1, H2, H3, and H4 were pooled, dialyzed against distilled water, lyophilized, and analyzed by agarose gel electrophoresis, as described in the legend to Fig. 1. *C*, the purified glycan from hemocyte (*Sp Hep (H3)*; ~10 μg dry weight) and the molecular weight markers dextran 500 (*Dx 500*), chondroitin 4-sulfate (*C4S*), chondroitin 6-sulfate (*C6S*), dextran 8 (*Dx 8*), and mammalian heparin (*Man Hep*) (~10 μg as dry weight of each) were applied to a 1-mm-thick 6% polyacrylamide slab gel, as described under "Experimental Procedures." *Std*, standard.

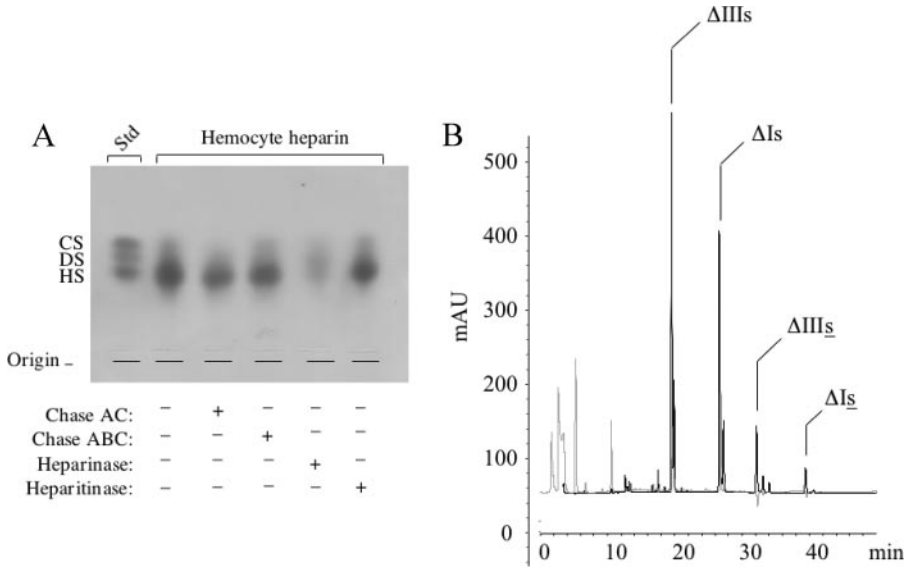

FIGURE 5. **Characterization of the hemocyte heparin.** *A*, the purified hemocyte heparin (~1.5 μg as uronic acid) and a mixture of standard (*Std*) chondroitin sulfate (*CS*), dermatan sulfate (*DS*), and heparan sulfate (*HS*) were analyzed by agarose gel electrophoresis, before (−) or after (+) incubation with chondroitin AC (*Chase AC*) or ABC (*Chase ABC*) lyases or heparin or heparan sulfate lyases, as described under "Experimental Procedures." *B*, the disaccharides formed by exhaustive action of heparinase I, II, and III) on the hemocyte heparin were applied to a CTA-SAX HPLC column. The column was eluted with a gradient of NaCl as described under "Experimental Procedures." The eluant was monitored for UV absorbance at 232 (*black line*) and 202–247 (*gray line*) nm. The assigned peaks correspond to the disaccharides: Δ*IIIs*, ΔUA(2SO$_4$)-1→4-β-D-GlcN(SO$_4$); Δ*Is*, ΔUA(2SO$_4$)-1→4-β-D-GlcN(SO$_4$)(6SO$_4$); Δ*Is* ΔUA(2SO$_4$)-1→4-β-D-GlcN(SO$_4$)(3SO$_4$)(6SO$_4$); Δ*IIIs*, ΔUA(2SO$_4$)-1→4-β-D-GlcN(SO$_4$)(3SO$_4$).

2-sulfation in this compound. The low field resonance at 4.45 ppm for H4 suggests 4-sulfated and/or 4-linked units.

The Hemocytes of S. plicata Contain a Heparin-like Glycosaminoglycan—The sulfated glycans extracted from hemocytes were fractionated on an ion exchange column, as described under "Experimental Procedures." The glycans were eluted in four metachromatic peaks, denominated H1, H2, H3, and H4, at different NaCl concentrations (Fig. 4*A*). H1 and H2 contain very little material (Fig. 4*B*) and were discarded. H3, eluted at approximately the same NaCl concentration required to elute porcine intestinal mucosa heparin (~1.5 M) (Fig. 4*A*). When analyzed by agarose gel electrophoresis, H3 shows a single metachromatic band migrating as heparan sulfate standard (Fig. 4*B*). A small amount of this material was eluted at a higher NaCl concentration (H4 in Fig. 4, *A* and *B*).

An estimate of the molecular weight of the purified hemocyte glycan (H3) was carried out by polyacrylamide gel electrophoresis, where its migration was compared with those of known molecular weight standard GAGs. As shown in Fig. 4*C*, H3 migrated slightly ahead of porcine intestinal mucosa heparin, which suggests an average molecular weight of ~12,000 (Fig. 2*D*).

In order to obtain information about the nature of the hemocyte glycan, the purified polymer from the ion exchange column (H3) was incubated with condroitinase AC-/ABC-lyase and heparin-/heparan sulfate-lyase, and the products were analyzed by agarose gel electrophoresis (Fig. 5*A*). The hemocyte glycan was resistant to the action of chondroitin AC/ABC lyases as well as heparan sulfate lyase but was almost totally degraded by heparin lyase, indicating that this is a heparin-like GAG. CTA-SAX HPLC analysis of the products formed by the action of heparin-lyase (I, II, and III) on H3 revealed that the hemocyte heparin is formed mainly by the disaccharides ΔUA(2SO$_4$)-1→4-β-D-GlcN-(SO$_4$) (39.7%) and ΔUA(2SO$_4$)-1→4-β-D-GlcN(SO$_4$)(6SO$_4$) (38.2%). Smaller amounts of the disaccharides ΔUA(2SO$_4$)-1→4-β-D-GlcN(SO$_4$)-(3SO$_4$)(6SO$_4$) (3.8%) and ΔUA(2SO$_4$)-1→4-β-D-GlcN(SO$_4$)(3SO$_4$) (9.8%) were also present (Fig. 5*B*, Table 3).

The disaccharide ΔUA(2SO$_4$)-1→4-β-D-GlcN(SO$_4$)-(3SO$_4$)(6SO$_4$) was already identified in depolymerized porcine mucosa heparin (41). The ΔUA(2SO$_4$)-1→4-β-D-GlcN(SO$_4$)-(3SO$_4$) tentative structure was attributed according to several analytical indications; the UV maximum at 232 nm is charac-

Downloaded from www.jbc.org at CAPES Usage on June 30, 2007

teristic of the hexuronic acid bearing 2-*O*-sulfate, and the selective detection signal at 202–247 nm shows an absence of *N*-acetyl and a characteristic minimum of absorbance due to the presence of 3-*O*-sulfated moiety (for a complete method description, see also Ref. 41). The liquid chromatography-mass spectrometry experiment assigns a molecular mass of 577 Da (data not shown). Thus, the chromatographic retention is clearly not compatible with the only other possible alternative structure, $\Delta UA(2SO_4)$-1→4-β-D-$GlcN(SO_4)(6SO_4)$. Therefore, the disaccharide structure is unequivocally attributed to $\Delta UA(2SO_4)$-1→4-β-D-$GlcN(SO_4)(3SO_4)$. The presence of high levels of 3-*O*-sulfation on the glucosamine may explain the partial resistance of the hemocyte heparin to heparinase digestion observed in Fig. 3*A*.

TABLE 3
Disaccharide composition of ascidian and mammalian heparins

Disaccharide	Percentage of the disaccharides		
	Test cell[a]	Granule cell[b]	PIH[a,c]
	%	%	%
ΔUA-1→4-β-D-GlcN($6SO_4$)	<1	1.4	<5
ΔUA-1→4-β-D-GlcN(SO_4)($6SO_4$)	25	2	9–11
$\Delta UA(2SO_4)$-1→4-β-D-GlcN(SO_4)	<1	39.7	6–8
$\Delta UA(2SO_4)$-1→4-β-D-GlcN(SO_4)($6SO_4$)	75	38.2	60–70
$\Delta UA(2SO_4)$-1→4-β-D-GlcN(SO_4)($3SO_4$)	<1	9.8	<1
$\Delta UA(2SO_4)$-1→4-β-D-GlcN(SO_4)($3SO_4$)($6SO_4$)	<1	3.8	<1

[a] Cavalcante *et al.* (28).
[b] This work.
[c] Porcine intestinal heparin (C. M. de Barros, L. R. Andrade, S. Allodi, C. Viskov, P. A. Mourier, M. C. M. Cavalcante, A. H. Straus, H. K. Takahashi, V. H. Pomin, V. F. Carvalho, M. A. Martins, and M. S. G. Pavão, unpublished data).

The affinity chromatography of the hemocyte glycan demonstrates that both disaccharide $\Delta UA(2SO_4)$-1→4-β-D-$GlcN(SO_4)(3SO_4)$ and $\Delta UA(2SO_4)$-1→4-β-D-$GlcN(SO_4)$-$(3SO_4)(6SO_4)$ are responsible for the affinity of the polymer for ATIII. 10 mg of hemocyte heparin were chromatographed on ATIII-Sepharose (see "Experimental Procedures"), and the low affinity fraction, which represents about 60% of the heparin chains, was eluted out of the column at 0.25 M NaCl and was desalted on Sephadex G10. This polysaccharide fraction was digested with heparin-lyases (I, II, and III) and analyzed by CTA-SAX HPLC (Fig. 6*B*).

The high affinity fraction, which accounts for 40% of the heparin chains, was eluted out of the ATIII-Sepharose at 3 M NaCl and was desalted on Sephadex G10. This fraction of the hemocyte glycan was digested with heparin-lyases (I, II, III) and analyzed by CTA-SAX HPLC (Fig. 6*C*).

In the chromatogram shown in Fig. 6*B*, it appears clearly that the low affinity fraction of the polysaccharide is basically composed by the disaccharides $\Delta UA(2SO_4)$-1→4-β-D-$GlcN(SO_4)$ and $\Delta UA(2SO_4)$-1→4-β-D-$GlcN(SO_4)(6SO_4)$. The two 3-*O*-sulfated disaccharides are nearly absent in this part of the hemocyte heparin. On the contrary, the presence of the 3-*O*-sulfated disaccharides is greatly enhanced in the high affinity fraction of the polymer with respect to hemocyte heparin prior to fractionation (Fig. 6*C*). Table 4 summarizes these results, and the data clearly demonstrate the key involvement of $\Delta UA(2SO_4)$-1→4-β-D-$GlcN(SO_4)(3SO_4)(6SO_4)$ and $\Delta UA(2SO_4)$-1→4-β-D-$GlcN(SO_4)$-$(3SO_4)$ in the ATIII affinity of the polymer. However, the presence of a high affinity pentasaccharide-like binding sequence in the hemocyte heparin remains to be identified and demonstrated in further work.

Hemocyte Heparin Contains Antithrombin Activity—Antithrombin-mediated anticoagulant activity is a specific pharmacological characteristic of heparins. In order to investigate if the hemocyte heparin also

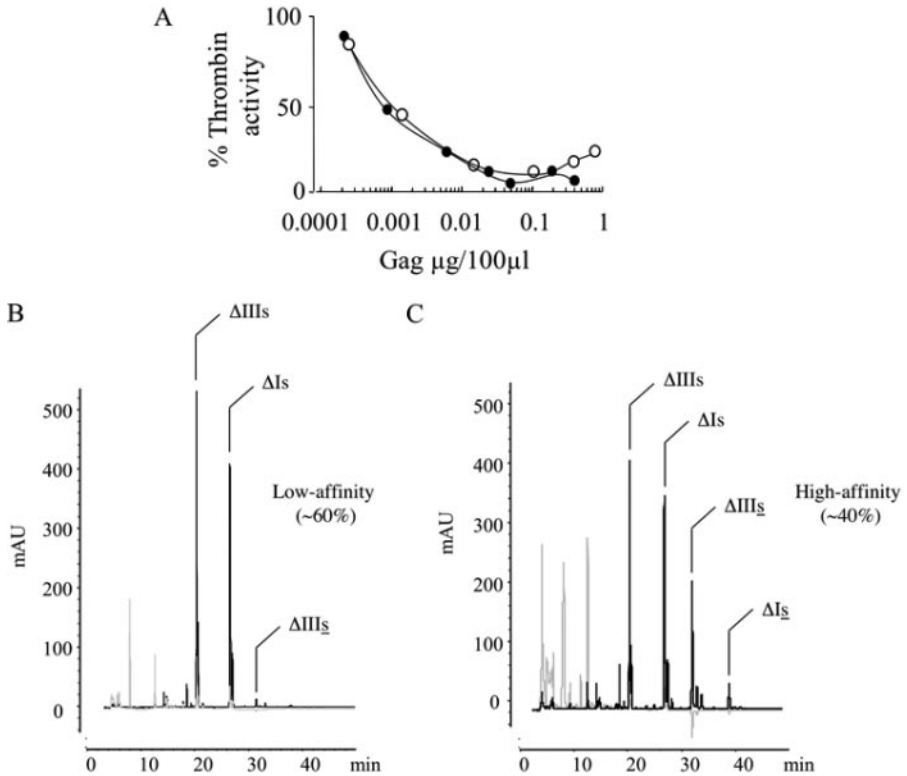

FIGURE 6. **Antithrombin activity of the hemocyte heparin and disaccharide analysis of low and high affinity antithrombin fractions.** *A*, antithrombin activity. Shown is inhibition of thrombin activity in the presence of hemocyte (●) or mammalian (○) heparin. Antithrombin (50 nM) was incubated with thrombin (15 nM) in the presence of various concentrations of heparins. After 60 s, the remaining thrombin activity was determined with a chromogenic substrate as described under "Experimental Procedures." *B* and *C*, disaccharide composition. The purified hemocyte heparin (10 mg) was chromatographed on an ATIII-Sepharose column (40 × 5 cm). The polysaccharide fraction was eluted by NaCl solution as described under "Experimental Procedures." Low affinity (*B*) and high affinity (*C*) fractions were eluted with 0.25 and 3 M NaCl, respectively. These fractions were exhaustively digested with a mixture of heparinase I, II, and III and applied to a CTA-SAX HPLC column as described under "Experimental Procedures." The eluant was monitored for UV absorbance at 232 (*black line*) and 202–247 nm (*gray line*). Δ*IIIs*, $\Delta UA(2SO_4)$-1→4-β-D-GlcN(SO4); Δ*Is*, $\Delta UA(2SO_4)$-1→4-β-D-$GlcN(SO_4)$ ($6SO_4$); ΔIs, $\Delta UA(2SO_4)$-1→4-β-D-$GlcN(SO_4)(3SO_4)(6SO_4)$; ΔIIIs, $\Delta UA(2SO_4)$-1→4-β-D-$GlcN(SO_4)(3SO_4)$.

Downloaded from www.jbc.org at CAPES Usage on June 30, 2007

TABLE 4
Disaccharide composition of the low and high antithrombin III affinity fractions of the hemocyte heparin

Disaccharide	Percentage of the disaccharides		
	Hemocyte heparin	Low affinity fraction	High affinity fraction
	%	%	%
$\Delta UA(2SO_4)$-1→4-β-D-$GlcN(SO_4)$	39.7	42.5	33
$\Delta UA(2SO_4)$-1→4-β-D-$GlcN(SO_4)(6SO_4)$	38.2	45.1	33.5
$\Delta UA(2SO_4)$-1→4-β-D-$GlcN(SO_4)(3SO_4)(6SO_4)$	3.8	0.6	4.2
$\Delta UA(2SO_4)$-1→4-β-D-$GlcN(SO_4)(3SO_4)$	9.8	1.4	21.2
Sum of other minor saccharides	8.5	10.4	9.1

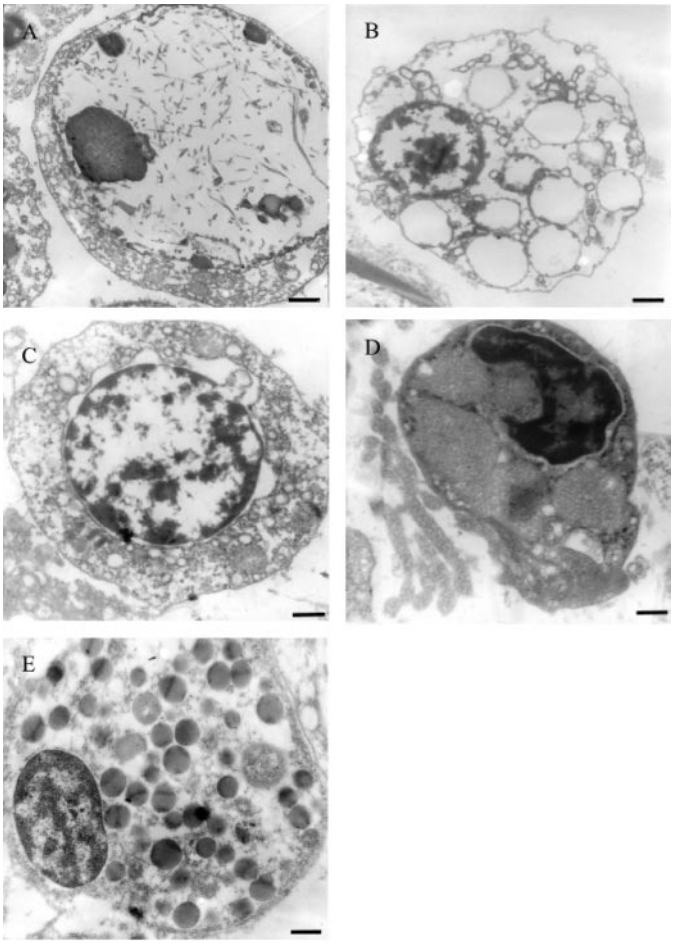

FIGURE 7. **Conventional transmission electron micrographs showing the ultrastructural features of *S. plicata* hemocytes.** *A*, univacuolated cell (*bar*, 0.68 μm). *B*, multivacuolated cell (*bar*, 0.66 μm). *C*, hemoblast or lymphocyte-like cell (*bar*, 0.66 μm). *D*, amebocyte (*bar*, 0.36 μm). *E*, granulocyte cell (*bar*, 0.50 μm).

possesses this activity, we measured the inhibition of thrombin by antithrombin in the presence of increasing concentrations of invertebrate or mammalian GAG (Fig. 6*A*). The rate of thrombin inhibition by antithrombin induced by the hemocyte heparin was similar to that induced by porcine intestinal mucosa heparin, indicating that both mammalian and invertebrate heparins have the same anticoagulant activity.

S. plicata Hemolymph Contains Different Types of Hemocytes—Different types of cells occur in *S. plicata* hemocyte population. Transmission electron microscopy observations revealed that the hemolymph of this ascidian has at least five recognizable cell types. Fig. 7*A* shows an univacuolated cell type (5.5–9.5 μm in diameter) containing a huge vacuole that occupies almost the whole volume of the cytoplasm. Dispersed fibrilar material and electron-lucent round vesicles are present within the vacuole. Some of the smaller electron-dense vesicles are seen close to the membrane that surrounds the vacuole with an aspect that suggests a sprouting from the membranes.

A multivacuolated cell type is shown in Fig. 7*B*. This 6.5–8.0-μm cell has a spherical shape and contains 2–20 regularly sized electron-lucent vacuoles close to small vesicles. Its nucleus is very evident, including the chromatin arrangement.

Another cell type is shown in Fig. 7*C*. It resembles hemoblasts or lymphocyte-like cells described by others in ascidians (31, 32, 34). This 4.0–5.5-μm cell has small vesicles, sometimes continuous with the nuclear envelope and mitochondria profiles.

Fig. 7*D* shows the smallest cell type (2.5–5.0-μm diameter). It has a dense cytoplasm with small vesicles, large mitochondria profiles, and a nucleus that occupies most of the cell. This cell has similar characteristics to the cell type named amebocyte by Fuke and Fukumoto (50).

Finally, Fig. 7*E* shows the granulocyte cell with a 3.5–6.0-μm diameter. Many granules or vesicles containing a material with varying electron densities can be observed intracellularly. The granules are uniform in the sense that most of them are spherical and with comparable sizes (~0.4 μm).

Heparin Is Restricted to Only One Type of Hemocyte—In order to identify which cells contain heparin, a preparation of the hemocytes was immunogold-labeled with anti-heparin antibody. As shown in Fig. 8, 10-nm gold particles were observed in only one type of cell, named the granulocyte cell. The gold particles associated with the anti-heparin (Fig. 8*B*) antibody were localized inside electron-dense granules.

In mammals, histamine is associated with heparin in the granules of mast cells and basophils. In the present work, 10-nm gold particles were observed within intracellular granules of ascidian granulocytes (Fig. 8*C*) and rat peritoneal mast cells (Fig. 8, *D* and *E*) after immunogold labeling with anti-histamine antibody. The pattern of gold labeling is very similar to that observed when anti-heparin antibody was used. No significant labeling was observed in other regions of the granulocytes or in other hemocytes or in rat peritoneal mast cell when primary antibody was omitted.

In a previous study (20), histamine was detected in the intestine and pharynx of *S. plicata*, using immunolabeling with anti-histamine antibody. To confirm the presence of histamine in these tissues and also the results of the immunogold labeling described in the present work, the activity of the enzyme histamine *N*-methyltransferase was measured in homogenates of intestine, pharynx, and hemolymph of *S. plicata* as well as in

Downloaded from www.jbc.org at CAPES Usage on June 30, 2007

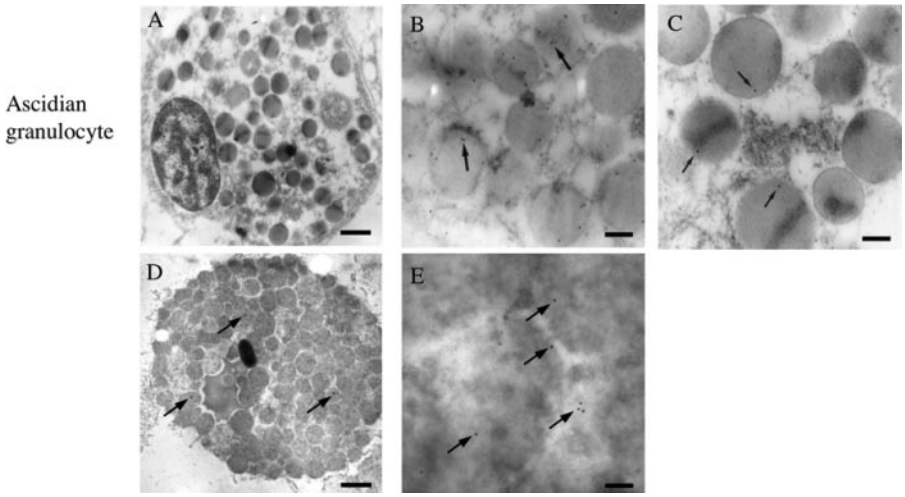

FIGURE 8. **Immunolocalization of heparin and histamine in the granulocyte cell.** Electron micrograph showing the pattern of gold labeling associated with anti-heparin (*mAb ST-1*) and anti-histamine antibodies in the ascidian granulocyte (*B* and *C*) and rat peritoneal mast cell (*D* and *E*). *A*, granule cell (*bar*, 0.50 μm). *B*, gold labeling associated with anti-heparin antibody (*bar*, 0.22 μm). *C*, gold labeling associated with anti-histamine antibody (*bar*, 0.22 μm). *D* and *E*, gold labeling associated with anti-histamine antibody. *Bar*, 0.73 μm (*D*) and 0.083 μm (*E*). *Arrows*, gold particles.

TABLE 5

Histamine content in the hemolymph and in different tissues of *S. plicata*

Tissue	Histamine content[a]
	ng/mg protein
Hemolymph	7.18 ± 0.75
Pharynx	56.02 ± 3.43
Intestine	48.43 ± 5.45

[a] Histamine content was estimated by measuring the activity of the enzyme histamine-*N*-methyltransferase, as described under "Experimental Procedures."

homogenates of rat peritoneal mast cells. As shown in Table 5, significant levels of histamine, estimated by the activity of histidine *N*-methyltransferase, were detected in all of the samples analyzed. Histamine content was higher in intestine and pharynx. This result provides a biochemical evidence of the presence of histamine in the granulocyte and in the intestine and pharynx of the ascidian.

DISCUSSION

In the present paper, we described the purification and characterization of two sulfated glycans from the hemolymph of *S. plicata*: a sulfated galactoglucan and a heparin glycosaminoglycan. In addition, electron microscopy techniques were used to characterize the ultrastructure of the hemocytes and to localize heparin and histamine in these cells.

The hemolymph of ascidians is composed of different types of cells, named hemocytes, and a liquid plasma. Several proteins have been described as occurring in the plasma hemolymph, such as serine protease inhibitors (51), serine proteases (52), metalloproteinases (53), phenoloxidase (54), trypsin inhibitors (55), trypsin (56), hemocyte aggregation factor (57), and different types of lectins (58–60). Although other sulfated polysaccharides have been described in the tunic of different species of ascidians, including *S. plicata* (61, 62), according to our knowledge, the occurrence of a free sulfated polysaccharide in the plasma is reported here for the first time.

It is interesting to note that the chemical composition of the sulfated glycans in ascidians varies according to the tissue and stage of development. For example, in adult tunic, the main polysaccharide is a high molecular weight sulfated galactan, composed by α-L-galactopyranose residues sulfated at position 3 and linked through positions 1→4 (62, 63). This polymer is synthesized by epidermal cells that epimerize D-glucose, possibly from a trehalose precursor, into L-galactose (64, 65). The larval tunic, on the other hand, possesses a heteropolysaccharide composed mainly of glucose and sulfated fucose, with minor amounts of L-galactose (66). The hemolymph polysaccharide reported in the present study is a low molecular weight sulfated galactoglucan, which has a higher sulfate content (1.0 mol of sulfate/mol of hexose) when compared with adult (0.7 mol of sulfate/mol of hexose) (62) and larval (0.4 mol of sulfate/mol of hexose) tunic (66) glycans. The enantiomeric form of galactose and the position of sulfation of the hemolymph polysaccharide are under investigation. Sulfated GAGs do not occur in the tunic but abound in different organs of ascidians (64, 67). An oversulfated dermatan sulfate composed of IdoA($2SO_4$)-GalNAc($4SO_4$) disaccharide units and a low sulfated heparin have been reported in the intestine, heart, pharynx, and mantle of the ascidian *S. plicata* (68, 69). Moreover, a dermatan sulfate with the unique disaccharide unit IdoA($2SO_4$)-GalNAc($6SO_4$) was isolated from the body of the ascidian *Phallusia nigra* (70, 71).

Previously, we reported the occurrence of heparin, composed of the disaccharides ΔUA($2SO_4$)-GlcN(SO_4)($6SO_4$) (75%) and ΔUA-4-GlcN(SO_4)($6SO_4$) (25%), in intracellular granules of test cells of *S. plicata* (28). Now we report in the hemolymph of this ascidian a heparin with a different composition, formed by approximately equal amounts of the disulfated disaccharide ΔUA($2SO_4$)-GlcN(SO_4) and the trisulfated disaccharide ΔUA($2SO_4$)-GlcN(SO_4)($6SO_4$). Smaller quantities of tri- and tetrasulfated disaccharides, containing 3-*O*-sulfated glucosamine, which is required for binding to antithrombin, were also found (72, 73). Overall, these results suggest that the enzymes of the synthesis of heparin in *S. plicata* are either differently regulated or differ in the test cells and hemocytes.

Because of heparin's unique binding to antithrombin, involving the specific pentasaccharide sequence GlcNAc($6SO_4$)-GlcA-GlcNS($3SO_4$)-IdoA($2SO_4$)-GlcNS($6SO_4$), which contains a unique 3-*O*-sulfated glucosamine, mammalian heparin is endowed with a potent anticoagulant activity (74, 75). Analysis of the anticoagulant action of the hemocyte heparin revealed an antithrombin activity 10-fold higher than that of test cell heparin and similar to that observed in mammalian heparin (porcine intestinal mucosa). These results are in agree-

Downloaded from www.jbc.org at CAPES Usage on June 30, 2007

ment with the presence of significant amounts of 3-*O*-sulfated glucosamine residues in the hemocyte heparin, not detected in test cell heparin (28), that could form a pentasaccharide-like sequence with high affinity to antithrombin.

Important data about the morphology of *S. plicata* hemocytes were revealed by conventional transmission electron microscopy. According to our observations, five types of circulating hemocytes were described: univacuolated and multivacuolated cells, amebocytes, hemoblasts, and granulocytes. Different from our results, Radford *et al.* (32) described eight individual hemocyte types in the ascidian *S. plicata*. This may be due to the different methodology employed in that work, which was based mainly on bright field optical microscopy and cell sorting performed on immunofluorescently stained hemocytes.

The identification of a granulocyte in the hemolymph of *S. plicata*, morphologically related to vertebrate basophils, was of notice. In the granules of the ascidan granulocyte, a central electron-dense region can be observed. Granules with an electron-dense core are present mainly in granulocytes of higher vertebrates, such as reptiles and mammals (76–78), whereas granules with no electron-dense core have been reported in more primitive vertebrate granulocytes, such as fish and bufonid.

In addition to morphological similarities, *S. plicata* granulocyte also contains biochemical characteristics common to vertebrate basophils, such as intracellular GAG, in this case heparin and histamine. Mammalian heparin is synthesized onto a specific protein core, forming the serglycin PGs (5–9). These PGs are resistant to proteolytic degradation (5, 79). In the present work, peptide-free heparin chains were obtained after proteolytic degradation of the hemocytes, suggesting that the granulocyte heparin is probably linked to a core protein different from that of serglycin PGs.

Histamine was unequivocally detected in the intestine and pharynx of *S. plicata* and in the hemolymph by measuring the activity of the enzyme histidine *N*-metyltransferase, which is involved in the catabolism of histamine. We also estimated the content of histamine in rat peritoneal mast cells using this method (~13 pg/cell). It should be emphasized that the histamine assay we have employed for tissues from *S. plicata* is a sensitive and highly specific method. Its specificity is achieved by employing an enzyme, histamine *N*-methyltransferase, isolated from guinea pig brains, whereas the sensitivity is accounted for by the use of the *S*-adenosyl[*methyl*-^{3}H]methionine as the radioactive cofactor. As far as we know, it is quite unlikely that histidine *N*-metyltransferase could be using serotonin or dopamine as substrate. The major false positives for histamine found in mammalian tissue samples, mainly concerning fluorimetric assays, are spermine, spermidine, and putrescine. Prior studies have demonstrated that the radioenzymic method for histamine did not mistake the latter for the former as reported (80). This is interesting when analyzing within the context of the ascidian *Ciona intestinalis* genome, which does not show the presence of a histidine decarboxylase-like gene in the organism. The histidine decarboxylase-like gene codifies an enzyme involved in the biosynthesis of histamine. This raises the possibility that histidine decarboxylase-like genes reside at nonsequenced sites in the organism's genome.

The results presented in the present study suggest that the hemolymph granulocyte may be a primitive counterpart of mammalian basophil, involved in immunological mechanisms, especially when migrating from the blood vessels to perform activities such as encapsulation, phagocytosis, liberation of microbial peptides, triggering of the complement system, and regeneration of tissues.

Acknowledgment—We thank Claudia Du Bocage Santos-Pinto for technical assistance.

REFERENCES

1. Rodén, L. (1980) in *Biochemistry of Glycoproteins and Proteoglycans* (Lennarz, W. J., ed) pp. 267–371, Plennum Press, New York
2. Conrad, H. E. (1998) *Heparin-binding Proteins*, Academic Press, Inc., San Diego
3. Casu, B., and Lindahl, U. (2001) *Adv. Carbohydr. Chem. Biochem.* **57,** 159–206
4. Powell, A. K., Yates, E. A., Fernig, D. G., and Turnbull, J. E. (2004) *Glycobiology* **14,** 17R–30R
5. Yurt, R. W., Leid, R. W., Jr., and Austen, K. F. (1977) *J. Biol. Chem.* **252,** 518–521
6. Robinson, H. C., Horner, A. A., Hook, M., Ogren, S., and Lindahl, U. (1978) *J. Biol. Chem.* **253,** 6687–6693
7. Metcalfe, D. D., Lewis, R. A., Silbert, J. E., Rosenberg, R. D., Wasserman, S. I., and Austen, K. F. J. (1979) *J. Clin. Invest.* **64,** 1537–1543
8. Metcalfe, D. D., Smith, J. A., Austen, K. F., and Silbert, J. E. (1980) *J. Biol. Chem.* **255,** 11753–11758
9. Bland, C. E., Ginsburg, H., Silbert, J. E., and Metcalfe, D. D. (1982) *J. Biol. Chem.* **257,** 8661–8666
10. Yurt, R. W., Leid, R. W., Jr., Spragg, J., and Austen, K. F. (1977) *J. Immunol.* **118,** 1201–1207
11. Schwartz, L. B., Riedel, C., Caulfield, J. P., Wasserman, S. I., and Austen, K. F. (1981) *J. Immunol.* **126,** 2071–2078
12. MacDermott, R. P., Schmidt, R. E., Caulfield, J. P., Hein, A., Bartley, G. T., Ritz, J., Schlossman, S. F., Austen, K. F., and Stevens, R. L. (1985) *J. Exp. Med.* **162,** 1771–1787
13. Razin, E., Stevens, R. L., Akiyama, F., Schmid, K., and Austen, K. F. (1982) *J. Biol. Chem.* **257,** 7229–7236
14. Nakano, T., Sonoda, T., Hayashi, C., Yamatodani, A., Kanayama, Y., Yamamura, T., Asai, H., Yonezawa, T., Kitamura, Y., and Galli, S. J. (1985) *J. Exp. Med.* **162,** 1025–1043
15. Wedemeyer, J., Tsai, M., and Galli, S. J. (2000) *Curr. Opin. Immunol.* **12,** 624–631
16. Dietrich, C. P., de Paiva, J. F., Moraes, C. T., Takahashi, H. K., Porcionatto, M. A., and Nader, H. B. (1985) *Biochim. Biophys. Acta.* **843,** 1–7
17. Pejler, G., Danielsson, A., Bjork, I., Lindahl, U., Nader, H. B., and Dietrich, C. P. (1987) *J. Biol. Chem.* **262,** 11413–11421
18. Dietrich, C. P., Nader, H. B., de Paiva, J. F., Santos, E. A., Holme, K. R., and Perlin, A. S. (1989) *Int. J. Biol. Macromol.* **11,** 361–366
19. Nader, H. B., Chavante, S. F., dos-Santos, E. A., Oliveira, T. W., de-Paiva, J. F., Jeronimo, S. M., Medeiros, G. F., de-Abreu, L. R., Leite, E. L., de-Sousa-Filho, J. F., Castro, R, A., Toma, L., Tersariol, I. L., Porcionatto, M. A., and Dietrich, C. P. (1999) *Braz. J. Med. Biol. Res.* **32,** 529–538
20. Arumugam, M., and Shanmugam, A. (2004) *Indian J. Exp. Biol.* **42,** 529–532
21. Cesaretti, M., Luppi, E., Maccari, F., and Volpi, N. (2004) *Glycobiology* **14,** 1275–1284
22. Luppi, E., Cesaretti, M., and Volpi, N. (2005) *Biomacromolecules* **6,** 1672–1678
23. Hovingh, P., and Linker, A. (1982) *J. Biol. Chem.* **257,** 9840–9844
24. Dietrich, C. P., Paiva, J. F., Castro, R. A., Chavante, S. F., Jeske, W., Fareed, J., Gorin, P. A., Mendes, A., and Nader, H. B. (1999) *Biochim. Biophys. Acta*

Downloaded from www.jbc.org at CAPES Usage on June 30, 2007

1428, 273–283
25. Chavante, S. F., Santos, E. A., Oliveira, F. W., Guerrini, M., Torri, G., Casu, B., Dietrich, C. P., and Nader, H. B. (2000) *Int. J. Biol. Macromol.* **27,** 49–57
26. Tirumalai, R., and Subramoniam, T. (2001) *Mol. Reprod. Dev.* **58,** 54–62
27. Demir, M., Iqbal, O., Dietrich, C. P., Hoppensteadt, D. A., Ahmad, S., Daud, A. N., and Fareed, J. (2001) *Clin. Appl. Thromb. Hemost.* **7,** 44–52
28. Cavalcante, M. C., Allodi, S., Valente, A. P., Straus, A. H., Takahashi, H. K., Mourão, P. A., and Pavão, M. S. (2000) *J. Biol. Chem.* **275,** 36189–36196
29. Cavalcante, M. C., Andrade, L. R., Du Bocage Santos-Pinto, C., Straus, A. H., Takahashi, H. K., Allodi, S., and Pavão, M. S. (2002) *J. Struct. Biol.* **137,** 313–321
30. Pavão, M. S. (2002) *An. Acad. Bras. Cienc.* **74,** 105–112
31. Sawada, T., Zhang, J., and Cooper, E. L. (1993) *Biol. Bull.* **184,** 87–96
32. Radford, J. L., Hutchinson, A. E., Burandt, M., and Raftos, D. A. (1998) *Acta Zool.* **79,** 44–49
33. Menzel, L. P., Lee, I. H., Sjostrand, B., and Lehrer, R. I. (2002) *Dev. Comp. Immunol.* **26,** 505–515
34. Hirose, E., Shirae, M., and Saito, Y. (2003) *Zoolog. Sci.* **20,** 647–656
35. Hirose, E. (2003) *Zoolog. Sci.* **20,** 387–394
36. Cardoso, L. E., and Mourão, P. A. (1994) *Braz. J. Med. Biol. Res.* **27,** 509–514
37. Brown, D. D., Tomchick, R., and Axelrod, J. (1959) *J. Biol. Chem.* **234,** 2948–2950
38. Peddie, C. M., and Smith, V. J. (1994) *Ann. N. Y. Acad. Sci.* **712,** 332–334
39. Farndale, R. W., Buttle, D. J., and Barrett, A. J. (1986) *Biochim. Biophys. Acta* **883,** 173–177
40. Dietrich, C. P., and Dietrich, S. M. (1976) *Anal. Biochem.* **70,** 645–647
41. Mourier, P., and Viskov, C. (2004) *Anal. Biochem.* **332,** 299–313
42. Bitter, T., and Muir, H. M. (1962) *Anal. Biochem.* **4,** 330–334
43. Shively, J. E., and Conrad, H. E. (1976) *Biochemistry* **15,** 3932–3942
44. Dubois, M., Gilles, K. A., Hamilton, J. K., Rebers, P. A., and Smith, F. (1956) *Anal. Chem.* **28,** 350–354
45. Saito, H., Yamagata, T., and Suzuki, S. (1968) *J. Biol. Chem.* **243,** 1536–1542
46. Straus, A. H., Travassos, L. R., and Takahashi, H. K. (1992) *Anal. Biochem.* **201,** 1–8
47. Fleury, P., and Eberhard, R. (1951) *Ann. Biol. Clin.* **9,** 453–466
48. Snyder, S. H., Baldessarini, R. J., and Axelrod, J. (1966) *J. Pharmacol. Exp. Ther.* **153,** 544–549
49. Correa, F. M. A., and Saavedra, J. M. (1981) *Brain Res.* **205,** 445–451
50. Fuke, M., and Fukumoto, M. (1993) *Acta Zool.* **74,** 61–71
51. Shishikura, F., Abe, T., Ohtake, S., and Tanaka, K. (1996) *Comp. Biochem. Physiol. B Biochem. Mol. Biol.* **114,** 1–9
52. Shishikura, F., Abe, T., Ohtake, S., and Tanaka, K. (1997) *Comp. Biochem. Physiol. B Biochem. Mol. Biol.* **118,** 131–141
53. Azumi, K., and Yokosawa, H. (1996) *Zool. Sci.* **13,** 365–370
54. Akita, N., and Hoshi, M. (1995) *Cell Struct. Funct.* **20,** 81–87
55. Kumazaki, T., Hoshiba, N., Yokosawa, H., and Ishii, S. (1990) *J. Biochem.* (*Tokyo*) **107,** 409–413
56. Yokosawa, H., Odajima, R., and Ishii, S. (1985) *J. Biochem.* (*Tokyo*) **97,** 1621–1630
57. Takahashi, H., Azumi, K., and Yokosawa, H. (1995) *Eur. J. Biochem.* **233,** 778–783
58. Green, P. L., Nair, S. V., and Raftos, D. A. (2003) *Dev. Comp. Immunol.* **27,** 3–9
59. Pearce, S., Newton, R. A., Nair, S. V., and Raftos, D. A. (2001) *Dev. Comp. Immunol.* **25,** 377–385
60. Kenjo, A., Takahashi, M., Matsushita, M., Endo, Y., Nakata, M., Mizuochi, T., and Fujita, T. (2001) *J. Bio.l Chem.* **276,** 19959–19965
61. Pavão, M. S., Albano, R. M., and Mourão, P. A. S. (1989) *Carbohydr. Res.* **189,** 374–379
62. Pavão, M. S., Albano, R. M., Lawson, A. M., and Mourão, P. A. (1989) *J. Biol. Chem.* **264,** 9972–9979
63. Pavão, M. S., Mourão, P. A., and Mulloy, B. (1990) *Carbohydr. Res.* **208,** 153–161
64. Pavão, M. S., Rodrigues, M. A., and Mourão, P. A. (1994) *Biochim. Biophys. Acta* **1199,** 229–237
65. Mourão, P. A., and Assreuy, A. M. (1995) *J. Biol. Chem.* **270,** 3132–3140
66. Pavão, M. S. G., Lambert, C. C., Lambert, G., and Mourão, P. A. S. (1994) *J. Exp. Zool.* **269,** 89–94
67. Pavão, M. S. (1996) *Braz. J. Med. Biol. Res.* **29,** 1227–1233
68. Pavão, M. S., Aiello, K. R., Werneck, C. C., Silva, L. C., Valente, A. P., Mulloy, B., Colwell, N. S., Tollefsen, D. M., and Mourão, P. A. (1998) *J. Biol. Chem.* **273,** 27848–27857
69. Gandra, M., Cavalcante, M., and Pavão, M. S. (2000) *Glycobiology* **10,** 1333–1340
70. Pavão, M. S., Mourão, P. A., Mulloy, B., and Tollefsen, D. M. (1995) *J. Biol. Chem.* **270,** 31027–31036
71. Mourão, P. A., Pavão, M. S., Mulloy, B., and Wait, R. (1997) *Carbohydr. Res.* **300,** 315–321
72. Lindahl, U., Backstrom, G., Thunberg, L., and Leder, I. G. (1980) *Proc. Natl. Acad. Sci. U. S. A.* **77,** 6551–6555
73. Petitou, M., Casu, B., and Lindahl, U. (2003) *Biochimie* (*Paris*) **85,** 83–89
74. Lane, D. A., and Lindahl, U. (1989) *Heparin: Chemical and Biological Properties, Clinical Applications*, CRC Press, Inc., Boca Raton, FL
75. Lindahl, U., Lidholt, K., Spillmann, D., and Kjellen, L. (1994) *Thromb. Res.* **75,** 1–32
76. Martinez-Silvestre, A., Rodriguez-Dominguez, M. A., Mateo, J. A., Pastor, J., Marco, I., Lavin, S., and Cuenca, R. (2004) *Vet. Rec.* **155,** 266–269
77. Martinez-Silvestre, A., Marco, I., Rodriguez-Dominguez, M. A., Lavin, S., and Cuenca, R. (2005) *Res. Vet. Sci.* **78,** 127–134
78. Zucker-Franklin, D., and Hirsch, J. G. (1964) *J. Exp. Med.* **120,** 569–756
79. Horner, A. A. (1971) *J. Biol. Chem.* **246,** 231–239
80. Kobayashi, Y., and Maudsley, D. V. (1972) *Anal. Biochem.* **46,** 85–90

Downloaded from www.jbc.org at CAPES Usage on June 30, 2007

Curriculum vitae

Vitor Hugo Pomin

Data de Nascimento: 04 de Janeiro de 1980.
Naturalidade: Petrópolis, Rio de Janeiro.

Formação acadêmica:

- Licenciado em Ciências Biológicas pelo Instituto de Biologia da UFRJ, Abril de1999 a Dezembro de 2003.

- Mestrado em Química Biológica pelo Instituto de Bioquímica Médica da UFRJ, de Março de 2004 a Setembro de 2005.

- Doutorado em Química Biológica pelo Instituto de Bioquímica Médica da UFRJ, de Setembro de 2005 a Setembro de 2008.

Experiência profissional:

1. Bolsista de Doutorado-sanduíche do CNPq de Novembro de 2007 a Maio de 2008, laboratório do Professor James H. Prestegard, localizado no Complex Carbohydrate Research Center, UGA, USA.

-Publicações:

1. **Pomin, V.H.** & Mourão, P.A.S. 2008. Structure, biology, evolution and medical importance of sulfated -fucans and –galactans. 2008. *Glycobiology*, (in press).
2. Farias, E.H.C.; **Pomin, V.H.**; Valente, A.-P.; Rocha, H.A.O.; Nader, H.B. & Mourão, P.A.S. 2008. A preponderantly 4-sulfated, 3-linked galactan from the green alga *Codium isthmocladum*. *Glycobiology*, v. 18, p. 250-259.
3. Barros, C.M.; Andrade, L.R.; Allodi, S.; Viskov, C.; Mourier, P.A.; Cavalcante, M.C.; Straus, A.H.; Takahashi, H.K.; Carvalho, V.F.; **Pomin, V. H.**; Martins, M.A. & Pavão, M.S. 2007. The Hemolymph of the ascidian Styela plicata (Chordata-Tunicata) contains heparin inside basophil-like cells and a unique sulfated galactoglucan in the plasma. *The Journal of Biological Chemistry*, v. 282, p. 1615-1626.
4. Santos, A.M.R.; **Pomin, V.H.**; Stelling, M.P; Guimaraes, M.A.M.; Cardoso, L.R. & Mourão, P.A.S. 2007. The renal clearance of dextran sulfate decreases in puromycin aminonucleoside-induced glomerulosclerosis: A puzzle observation. *Clinica Chimica Acta*, v. 383, p. 116-125.
5. **Pomin, V.H.** ; Valente, A.-P. ; Pereira, M.S. & Mourão, P.A.S. 2005. Mild acid hydrolysis of sulfated fucans: a selective 2-desulfation reaction and an alternative approach for preparing tailored sulfated oligosaccharides. *Glycobiology*, v. 15, p. 1376-1385.
6. **Pomin, V.H.**; Pereira, M.S.; Valente, A.-P.; Tollefsen, D.M.; Pavão, M.S.; Mourão, P.A.S. 2005. Selective cleavage and anticoagulant activity of a sulfated fucan: stereospecific removal of a 2-sulfate ester from the polysaccharide by mild acid hydrolysis, preparation of oligosaccharides, and heparin cofactor II-dependent anticoagulant activity. *Glycobiology*, v. 15, p. 369-381.
7. **Vitor H. Pomin** e Paulo A.S. Mourão. 2006. Carboidratos: de adoçantes a medicamentos. Ciência Hoje, 39:24-31.

Orientações de estudantes:
1. Bruno Cunha Vairo – iniciação científica de novembro de 2005/ atualmente.
2. Carla Sagradas – iniciação científica de junho de 2007/ atualmente.

Comunicação em congressos:
- 21 comunicações em congressos internacionais e 4 em congressos nacionais.

Livros Grátis

(http://www.livrosgratis.com.br)

Milhares de Livros para Download:

Baixar livros de Administração
Baixar livros de Agronomia
Baixar livros de Arquitetura
Baixar livros de Artes
Baixar livros de Astronomia
Baixar livros de Biologia Geral
Baixar livros de Ciência da Computação
Baixar livros de Ciência da Informação
Baixar livros de Ciência Política
Baixar livros de Ciências da Saúde
Baixar livros de Comunicação
Baixar livros do Conselho Nacional de Educação - CNE
Baixar livros de Defesa civil
Baixar livros de Direito
Baixar livros de Direitos humanos
Baixar livros de Economia
Baixar livros de Economia Doméstica
Baixar livros de Educação
Baixar livros de Educação - Trânsito
Baixar livros de Educação Física
Baixar livros de Engenharia Aeroespacial
Baixar livros de Farmácia
Baixar livros de Filosofia
Baixar livros de Física
Baixar livros de Geociências
Baixar livros de Geografia
Baixar livros de História
Baixar livros de Línguas

Baixar livros de Literatura
Baixar livros de Literatura de Cordel
Baixar livros de Literatura Infantil
Baixar livros de Matemática
Baixar livros de Medicina
Baixar livros de Medicina Veterinária
Baixar livros de Meio Ambiente
Baixar livros de Meteorologia
Baixar Monografias e TCC
Baixar livros Multidisciplinar
Baixar livros de Música
Baixar livros de Psicologia
Baixar livros de Química
Baixar livros de Saúde Coletiva
Baixar livros de Serviço Social
Baixar livros de Sociologia
Baixar livros de Teologia
Baixar livros de Trabalho
Baixar livros de Turismo